

**Development of Electrochemical Sensors for Analytical
and Biomedical Applications**

A DISSERTATION
SUBMITTED TO THE FACULTY OF THE GRADUATE
SCHOOL OF UNIVERSITY OF MINNESOTA
BY

Xin V. Chen

IN PARTIAL FULFILLMENT OF THE REQUIREMENTS FOR
THE DEGREE OF DOCTOR OF PHILOSOPHY

Dr. Philippe Bühlmann, Advisor

August 2019

© **Xin V. Chen 2019**

ACKNOWLEDGEMENT

I want to first greatly appreciate the guidance over the years from my advisor Philippe Bühlmann. Phil is not only an excellent scientist with his wealth of knowledge, but also an effective communicator of science. I learned a lot on the rigor of research and scientific thinking from him. Equally important, Phil is also a great mentor and a great Director of Graduate Studies. He is responsible, caring, uplifting, and emphasizes on student success and wellbeing. He is also known for his very notable initiatives on understating and improving student mental health, especially in graduate school.

I also want to give special thanks to Dr. Maral. P.S. Mousavi and Mr. Adam Dittmer for helping me get started on my research. I also appreciate all the help, support, and caring from all Bühlmann group members: Dr. Jesse Carey, Dr. Jinbo Hu, Dr. Xue Zhen, Dr. Evan Anderson, Brian Spindler, Ellie Raethke, Blair Troudt, Celeste Rousseau, Kwangrok Choi, Casey Charging, and Eliza Herrero,

With regard to research work, I would like to thank the following people:

Dr. Maral Mousavi for her contribution to the development of fluorophilic ionophore.

Brian Spindler for his help in calibrations of silicone-based ISEs.

Kwangrok Choi for his help in the work of poly(methacrylate)-based ISEs.

I also greatly appreciate the kind help and advice from Professors Renee Frontiera, Nicholas Frost, Sang-Hyun Oh, Mike Bowser, Kyle Bantz, Chris Hogan, and Andreas Stein. Many thanks for serving on my preliminary exam committee and thesis defense committee.

I would also like to thank Department of Chemistry and University of Minnesota for the quality of education, an inclusive environment, and a sense of community. I also want to thank Council of Graduate Students—the officially recognized graduate student government at University of Minnesota—for connecting graduate students, championing important issues, and advancing the life and education for graduate students. I also want to thank University of Minnesota Alumni Association for their great service to alumni and students.

DEDICATION

This thesis is dedicated to my parents,

Mr. Mingzhe Chen and Mrs. Liqiong Xing

for their lifelong support, inspiration, and unconditional love.

ABSTRACT

The focus of this dissertation is on two main topics: the development of chemical sensors with reduced biofouling for applications in biological samples (Chapter I–II), and the development of chemical sensors with improved biocompatibility (Chapter III–V).

Conventional polymeric membrane-based ion-selective electrodes (ISEs) rely on plasticized poly(vinyl chloride) (PVC) as sensor membranes. The plasticizers that solubilize PVC backbone—a prerequisite for PVC-phase ISEs—leach out gradually, resulting in a limited sensor lifetime. Polar groups in the plasticizer may also lower the sensor selectivity. To improve selectivity and expand working ranges, fluoros-phase ISEs relying on nonpolar perfluorinated compounds as sensing membrane were developed. A novel fluorophilic ionophore was synthesized and used to make ionophore-doped fluoros-phase ISEs with Nernstian responses and an optimal working range centered around neutral pH—suitable for most biological samples. The reproducibility of fluoros-phase ISEs was enhanced by a new electrode body design. Importantly, fluoros-phase ISEs maintained their excellent selectivity after prolonged exposure in serum whereas PVC-phase ISEs lost selectivity considerably. Insights were also obtained on the optimal ionophore-to-ionic site ratio.

To improve biocompatibility, silicone-based reference and ion-selective electrodes were developed to eliminate plasticizers. Reference electrodes doped with several ionic liquids showed sample-independent and long-term stable potentials in artificial blood

electrolytes and serum samples. Potassium-selective silicone-based ISEs developed with two ionophores and two silicones showed Nernstian responses and good selectivities. In an attempt to prevent leaching of ionophores from ISE membrane into samples, a well-known potassium ionophore was covalently attached to silicone membranes. Miniaturized microelectrodes suitable for implantable devices were also developed based on this platform.

In a similar effort, plasticizer-free polymethacrylate-based ISEs exhibited Nernstian responses to pH and selectivities comparable to PVC-phase ISEs. To further improve biocompatibility for applications in the pharmaceutical and food industries, either an ionophore or ionic site or both were covalently attached to sensor membranes. Sensors with either ionophore or ionic site attached provided similar good characteristics whereas when both were attached, Nernstian responses were not found consistently. Furthermore, heating experiments showed that sensors exposed to 90 °C heating maintained good selectivity.

Table of Content

ACKNOWLEDGEMENT	i
DEDICATION	iii
ABSTRACT	iv
LIST OF FIGURES	x
LIST OF TABLES	xxi
LIST OF ABBREVIATION.....	xxii
I. INTRODUCTION OF ELECTROCHEMICAL SENSORS AND BIOCOMPTABILITY OF SENSORS	1
1.1.2 Components of an ISE membrane	6
1.1.2.1 Polymeric Matrix	6
1.1.2.2 Plasticizer	7
1.1.2.3 Ionophore.....	7
1.1.2.3 Ionic Site.....	9
1.1.3 Selectivity	9
1.2 Fluorous-Phase Ion-Selective Electrodes	13
1.2.1 Perfluorinated Compounds	13
1.3.2 Fluorous-Phase ISEs.....	13
1.3 ISEs for pH Measurements.....	16
1.3.1. pH Glass Electrodes	16
1.3.2 The Working Range of Ionophore-Doped Polymeric Membrane-Based pH ISEs.....	17
1.4 Biocompatibility and Anti-Biofouling Aspects of ISEs	21
1.4.1 Biocompatibility of Materials and Devices	21
1.4.2 Leaching of Plasticizer and Plasticizer-Free ISE Membranes.....	22
1.4.2.1. ISEs with Polysiloxane-Based Membranes.....	22
1.4.2.2 Polyacrylate and Polymethacrylate-Based ISEs.....	31

1.4.2.3 Polyurethane (PU)-Based ISEs.....	36
1.4.3 Leaching of Ionophores and Ionic Site and Covalent Attachment.....	38
1.4.3.1 Model of Leaching	38
1.4.3.2 Covalent Attachment Strategy.....	40
1.4.3.3 Verification of Covalent Attachment	47
1.4.4 Biocompatibility Studies of ISEs	48
II. Fluorous-Phase Ion-Selective pH Electrodes for Measurements in Biological Samples	
.....	49
2.1 Introduction	50
2.2 Experimental Section.....	53
2.3 Results and Discussion	60
2.3.1 Response Range of ISEs with the New Ionophore.....	60
2.3.2 Potentiometric Selectivity	64
2.3.3 Basicity of Fluorophilic H ⁺ Ionophores.....	67
2.3.4 Improved Resistance of Fluorous-Phase Ion-Selective Electrodes to Biofouling	
.....	70
2.4 Conclusions	73
2.5 Supporting Information	74
2.5.1. Characterization of the Fluorophilic Ionophore N[CH ₂ CH ₂ CH ₂ CH ₂ R _{f8}] ₃ (2)	74
2.5.2. Design of Electrode Body	76
2.5.3. Selectivity Measurements.....	81
2.5.4. Working Range of pH ISEs Based on Ionophore 2.....	83
III. Reference Electrodes Based on Ionic Liquid Doped Reference Membranes with	
Biocompatible Silicone Matrixes	84
3.1 Introduction	85
3.2 Experimental Section.....	88
3.3 Results and Discussion	92

3.3.1 Silicone Materials and Sensor Membrane Fabrication.....	92
3.3.2 Responses to KCl of Reference Electrode Membranes Doped with [C ₈ mim ⁺][NTf ₂ ⁻]	96
3.3.3 Functionality of Reference Electrodes and Miscibility of Ionic Liquids with Silicone Materials	99
3.3.4 Effect of Sample Concentration on Solid-Contact Reference Electrodes with Fluorosilicone 1 Membranes	101
3.3.5 Long-term Stability in Artificial Blood Electrolyte Solution.....	103
3.3.6 Comparison of Reference Membranes doped with Different Ionic Liquids ..	105
3.4 Conclusions	109
3.5 Supporting Information	110
3.5.1. Characteristic of Reference Electrode Membranes	110
3.5.2. Sample Dependence of the Potential of Reference Electrodes Based on Different Silicone Materials.	111
3.5.3 Water Layer Test	112
3.5.4 Differential Scanning Calorimetry Original Traces	115
IV. DEVELOPMENT OF BIOCOMPATIBLE ELECTROCHEMICAL SENSORS FOR POTASSIUM MEASUREMENTS.....	131
4.1 Introduction	132
4.2 Experimental.....	135
4.2.1 Materials	135
4.2.2 Silicone Electrode Fabrication	135
4.2.4 Electrochemical Measurement.	138
4.2.5 Synthesis of Covalently Attachable Triethoxysilyl-Modified-BME-44	138
4.3 Results and Discussion	142
4.3.1 K ⁺ -Selective ISEs based on Silicone/Fluorosilicone Membranes and Mobile Ionophores	142
4.3.2 Planar Electrodes and Micro-Electrodes	148

4.3.3 Leaching of Sensor Components and Covalent Attachment of Ionophore. ...	150
4.3.4 Evaluation of Covalent Attachment	157
4.3.5 Performances ISEs Based on Covalently Attached Ionophore	159
4.4 Conclusions	162
4.5 Supporting Information	163
V. DEVELOPMENT OF POLY(METHACRYLATE)-BASED PH SENSORS WITH ALL SENSOR COMPONENTS COVALENTLY ATTACHED	169
5.1 Introduction	170
5.2 Experimental.....	173
5.2.1 Materials	173
5.2.2 Purification of pH Ionophore Tridodecylamine	174
5.2.3 PVC Membrane Preparation.....	174
5.3.8 ISEs with Crosslinked Poly(Decyl Methacrylate) Membranes and Covalently Attached Ionic Sites.....	204
5.3.9 ISEs with Crosslinked Poly(Decyl Methacrylate) Membranes and Both Ionic Site and Ionophore Covalently Attached.....	210
VI. CONCLUSIONS AND OUTLOOK.....	224
6.1 Summary of Results	225
6.2 Future Work.....	228
VII. REFERENCES	231

LIST OF FIGURES

Figure 1.1 A schematic of a potentiometric electrochemical sensor setup with an ion-selective electrode (left) and a reference electrode (right). Reprinted from Ref. 1.....	2
Figure 1.2. Schematic comparison of the free energy of transfer of monovalent cations between an ionophore-free membrane and a K^+ ionophore-doped membrane.	8
Figure 1.3. Illustration of the separate solution method (SSM) and fixed interference method (FIM) under ideal conditions.	12
Figure 1.4. Examples of previously reported fluorophilic salts	14
Figure 1.5. Schematic of the first ion-selective electrode based on a fluoruous liquid phase supported by an inert porous support. Reprinted from Ref. 46.	15
Figure 1.5. Diagram of a typical glass electrode, reprinted from Ref. 51	16
Figure 1.6. Upper and lower detection limits of an ISE; reprinted from Ref. 2	18
Figure 1.7. Common commercially available poly(dimethylsiloxanes), i.e., “silicones” (left), poly[(3,3,3-trifluoropropyl)methylsiloxanes], i.e., “fluorosilicones” (middle), and reported commercially not available poly(dimethylsiloxane- <i>co</i> -cynanopropylmethysiloxanes) (right).....	23
Figure 1.8. Examples of polyacrylate- and polymethacrylate-based membranes reported for use in ISEs. Left: poly(methyl methacrylate- <i>co</i> -glycidyl methacrylate- <i>co</i> - <i>n</i> -butyl acrylate); right: hexanediol-diacrylate-crosslinked poly(<i>n</i> -butyl acrylate).	33
Figure 1.9. Polyurethanes used as ISE membranes. Top: commercially available aliphatic polyurethane Tecoflex; right: non-commercially available aromatic polyurethane with varying (60 – 80 wt%) “soft segment”.	37
Figure 1.9. Phase boundary model developed to calculate leaching of components in ISE membranes.....	40

Figure 2.1. Structure formulas of the fluorophilic H ⁺ ionophores 1 to 3 . R _{f8} = -(CF ₂) ₇ CF ₃	52
Figure 2.2. Structure formulas of the fluorophilic ionic site (4) and the fluororous matrix (5) of the fluororous-phase sensing membranes.....	53
Figure 2.3. Design of an electrode body that avoids exertion of twisting forces on the sensing membrane during electrode assembly.	58
Figure 2.4. Working range of pH ISEs based on ionophore 2 : EMF measurements were started at pH 7.4 (970 mM KCl, 10 mM K ₂ HPO ₄ and 10 mM KH ₂ PO ₄ solution). The pH was increased by adding small aliquots of 10 M KOH solution. Subsequently, starting again at pH 7.4, the pH was decreased by adding aliquots of 1 M HCl solution. See Figure S2.9 of the Supporting Information for a graph with data for three individual electrodes.....	61
Figure 2.5. EMF response to pH with a constant metal ion concentration, demonstrating the high selectivity of ISEs based on ionophore 2 for H ⁺ with respect to K ⁺ , Na ⁺ , and Ca ²⁺ . Selectivities with respect to K ⁺ and Na ⁺ were measured in a constant 1 M K ⁺ and 1 M Na ⁺ background, respectively (K ⁺ or Na ⁺ salts of 10 mM HPO ₄ ²⁻ , 10 mM H ₂ PO ₄ ⁻ , and 970 mM Cl ⁻). The pH was gradually increased by addition of 10 M KOH or NaOH aliquots. The response to Ca ²⁺ was measured with a constant 10 mM Ca ²⁺ background; measurements were started with 10 mM Ca(OH) ₂ , and the pH was gradually decreased by adding aliquots of a solution that contained 3 M HCl and 10 mM CaCl ₂	66
Figure 2.6. Calibration of fluororous-phase pH electrodes with the 4 to 1 ionophore-to-ionic- site ratio and PVC-phase pH electrodes with the 2 to 1 ionophore-to-ionic site ratio, each before and after serum exposure. EMF measurements were started at pH 7.4 (970 mM KCl, 10 mM K ₂ HPO ₄ and 10 mM KH ₂ PO ₄ solution). The pH was increased by adding small aliquots of 10 M KOH solution.	72
Figure S2.1. ¹ H NMR spectrum of the fluorophilic ionophore N[CH ₂ CH ₂ CH ₂ CH ₂ R _{f8}] ₃ (2).	74

Figure S2.2. Electrospray mass spectrum of fluorophilic ionophore $N[CH_2CH_2CH_2CH_2R_{f8}]_3$ (2).	75
Figure S2.3. 3D view of outer electrode body piece (upper end shown in front). Four locking slots (at 90° to each other) securely hold the lugs of the inner electrode body piece (see Figures S2.2 and S2.3), preventing the inner body piece from rotating within the outer electrode body piece when the screw cap is mounted.	76
Figure S2.4. 3D view of inner electrode body piece (upper end in front). Two lugs (at 180° to each other) securely fit into locking slots of the inner electrode body piece (see Figures S2.1 and S2.3).....	77
Figure S2.5. 3D view of screw cap (left) and the inner electrode body piece mounted inside the outer electrode body piece (right). The two lugs of the inner electrode body piece fit into the locking slots of the outer body piece. When the cap is screwed onto the outer body piece, it exerts pressure onto the inner body piece, pushing it onto the sensing membrane (located between the inner and outer body pieces) without causing any rotating motion of the membrane. This ensures a tight and smooth mechanical seal of the membrane.	78
Figure S2.6. 3D views of cross-sections of the outer electrode body piece (top), inner electrode body piece (center), and the whole assembly with the screw cap (bottom).	79
Figure S2.7. 3D view of a cross-section of the inner and outer electrode body pieces, illustrating where the membrane is located.	80
Figure S2.8. Detailed dimensions of the electrode body (unit: mm).....	81
Figure S2.9. Working range of pH ISEs based on ionophore 2 : EMF measurements were started at pH 7.4 (970 mM KCl, 10 mM K_2HPO_4 and 10 mM KH_2PO_4 solution). The pH was increased by adding small aliquots of 10 M KOH solution. Subsequently, starting again at pH 7.4, the pH was decreased by adding aliquots of 1 M HCl solution. Three identical electrodes (labeled as 1, 2, and 3) were made and tested together. Linear range: pH 2.2 to 11.2 (Slope: 54.7 ± 0.7 mV/decade; $n = 3$).	83

Scheme 3.1. Curing chemistries of representative fluorosilicones and silicones studied in this work (see also **Table 3.1**).93

Figure 3.1. Effect of KCl (1.0 to 16 mM) on the potential of reference electrodes with [C₈mim⁺][NTf₂⁻]-doped silicone membranes (conventional electrode setup with a 1.0 mM KCl inner filling solution), as measured against a free-flow double-junction reference electrode. The average slopes and standard deviations of the linear regressions of each of the five types of membranes are given in **Table S3.2**.98

Figure 3.3. Potential responses of [C₈mim⁺][NTf₂⁻]-doped **Fluorosilicone 1** reference electrodes to artificial blood electrolyte solutions of high and low concentrations (see **Table 3.3** for the composition of test solutions). Solid contact electrodes were prepared with CIM carbon as transducer layer, and conventional electrode bodies contained 1.0 mM KCl inner filling solution. Potentials were measured against a free-flow double-junction reference electrode. The average slopes of conventional electrodes and solid-contact electrodes are -0.01 ± 0.002 mV/decade (n=3) and -0.1 ± 0.2 mV/decade (n=3), respectively.103

Figure 3.4. Long term emf as observed with a [C₈mim⁺][NTf₂⁻]-doped **Fluorosilicone 1** solid-contact reference electrode immersed into artificial blood electrolyte solutions (a 1:1 mixture of the HIGH and LOW solutions described by **Table 3.3**) against a free-flow double-junction reference electrode at 37 °C. (The data highlighted in red was used for the linear fit shown in black.)104

Figure 3.5. Potential responses of reference electrodes with **Fluorosilicone 1** membranes doped with [C₈mim⁺][NTf₂⁻], [C₁₀mim⁺][NTf₂⁻], [C₁₂mim⁺][NTf₂⁻], or [NBu₃Me⁺][NTf₂⁻] in the 1.0 to 16 mM KCl range. Average slopes and standard deviations of linear regressions are shown in **Table 3.4**.106

Figure S3.1. Potential stability of **Fluorosilicone 1** solid-contact reference electrodes in the range of 1.0 to 16 mM KCl. Membranes were doped with [C₈mim⁺][NTf₂⁻], and CIM carbon was used as solid contact between the silicone membrane and conducting substrate. Measurements started in 1.0 mM KCl, and aliquots of concentrated KCl solution were

added to sequentially double the KCl concentration. Potentials were measured against a free-flow double-junction reference electrode.	112
Figure S3.2. Water layer test of a Fluorosilicone 1 solid-contact electrode. The electrode was conditioned in 0.1 M KCl solution for 48 h prior to measurements. At t = 0.4 h, the solution was exchanged for a 0.1 M NaCl solution, and at t = 2.5 h, the solution was switched back to 0.1 M KCl.	114
Figure S3.3. DSC trace of ionic liquid [C ₈ mim ⁺][NTf ₂ ⁻].	115
Figure S3.4. DSC trace of neat polymer Fluorosilicone 1	116
Figure S3.5. DSC trace of Fluorosilicone 1 membrane doped with 10 wt% [C ₈ mim ⁺][NTf ₂ ⁻].	117
Figure S3.6. DSC trace of Fluorosilicone 1 membrane doped with 20 wt% [C ₈ mim ⁺][NTf ₂ ⁻].	118
Figure S3.7. DSC trace of neat polymer Fluorosilicone 2	119
Figure S3.8. DSC trace of Fluorosilicone 2 membrane doped with 10 wt% [C ₈ mim ⁺][NTf ₂ ⁻].	120
Figure S3.9. DSC trace of Fluorosilicone 2 membrane doped with 20 wt% [C ₈ mim ⁺][NTf ₂ ⁻].	121
Figure S3.10. DSC trace of neat polymer Silicone 1	122
Figure S3.11. DSC trace of Silicone 1 membrane doped with 10 wt% [C ₈ mim ⁺][NTf ₂ ⁻].	123
Figure S3.12. DSC trace of Silicone 1 membrane doped with 20 wt% [C ₈ mim ⁺][NTf ₂ ⁻].	124
Figure S3.13. DSC trace of neat polymer Silicone 2	125
Figure S3.14. DSC trace of Silicone 2 membrane doped with 10 wt% [C ₈ mim ⁺][NTf ₂ ⁻].	126

Figure S3.15. DSC trace of Silicone 2 membrane doped with 20 wt% [C ₈ mim ⁺][NTf ₂ ⁻].	127
Figure S3.16. DSC trace of neat polymer Silicone 3	128
Figure S3.17. DSC trace of Silicone 3 membrane doped with 10 wt% [C ₈ mim ⁺][NTf ₂ ⁻].	129
Figure 4.1 Potassium ionophores with good selectivity against sodium. ^{86, 213-215}	142
Figure 4.2 KCl response of K ⁺ -selective ISEs based on mobile valinomycin-doped fluorosilicone matrixes. Measurements were started at 1× 10 ^{-6.3} M KCl, and the KCl concentration was gradually increased by adding aliquots of concentrated KCl. Average slopes (mV/decade; n=3): pristine Fluorosilicone 1 with a conventional ISE setup (51.5 ± 1.5); centrifuged Fluorosilicone 1 with a conventional ISE setup (51.4 ± 0.9); pristine Fluorosilicone 1 with a solid-contact ISE setup (57.5 ± 2.4); centrifuged Fluorosilicone 1 with a solid-contact ISE setup (56.8 ± 2.3; n=2).	144
Figure 4.3 Suspected acetate binding to fluorosilicone backbone assisted by electro-withdrawing trifluoropropyl groups.	145
Figure 4.4 KCl response of K ⁺ -selective ISEs based on mobile BME-44-doped silicone matrixes. Measurements were started at 1× 10 ^{-6.3} M KCl, and the KCl concentration was gradually increased by adding aliquots of concentrated KCl. Average slopes (mV/decade; n=3): Fluorosilicone 2 with a conventional ISE setup (27.4 ± 9.4); Silicone 2 with a conventional ISE setup (51.6 ± 4.8); pristine Fluorosilicone 1 with a conventional ISE setup (42.3 ± 1.5); centrifuged Fluorosilicone 1 with a solid-contact ISE setup (53.1 ± 3.8); centrifuged Fluorosilicone 1 with a conventional ISE setup (40.4 ± 6.0). Calibrations curves were shifted vertically for clarity.	147
Figure 4.5 (a) Top and (b) side views of thick membranes (200 μm thickness) with a CIM carbon solid contact (left) and spin-coated thin-layer membranes (30 μm thickness, translucent yellow) without CIM carbon solid contact (right); (c) dip-coated membrane on a microelectrode, along with microscope views.....	149

Figure 4.6 KCl response of K ⁺ -selective ISEs based on dip-coated thin-layer microelectrodes and spin-coated thin-layer electrodes. Measurements of spin-coated thin-layer membranes were started at 1× 10 ⁻⁷ M KCl. Measurements of dip-coated microelectrodes were started at 1 mM KCl. The KCl concentration was gradually increased by adding aliquots of concentrated KCl. Average slopes (mV/decade; n=3): spin-coated BME-44/centrifuged Fluorosilicone 1 (55.9 ± 0.3); dip-coated valinomycin/pristine Fluorosilicone 1 (55.9 ± 0.3); dip-coated BME-44/ Silicone 1 (56.9, n=1).....	150
Figure 4.7 Synthesis Route 1 and Route 2 with CDI as reagent.	154
Figure 4.8 Synthesis Route 3 with phosgene as the key reagent.	157
Figure 4.9 Soxhlet extraction of Fluorosilicone 1 membranes: (a) before extraction; (b) after 16 h extraction with hexane of Fluorosilicone 1 membranes doped with mobile BME-44; (c) after 20 h extraction with dichloromethane of Fluorosilicone 1 membranes doped with mobile BME-44; (b) after 21 h extraction with dichloromethane of Fluorosilicone 1 membranes modified with triethoxysilyl-modified-BME-44.....	159
Figure 4.10 KCl response of ISEs based on Fluorosilicone 1 membrane doped with the covalently attached ionophore triethoxysilyl-modified BME-44. Measurements were started at 1× 10 ⁻⁹ M KCl and the KCl concentration was gradually increased by adding aliquots of concentrated KCl. Average slopes: Fluorosilicone 1 doped with 13 mmol/kg triethoxysilyl-modified-BME-44 (44.7 ± 1 mV/decade; n = 9); Fluorosilicone 1 doped with 106 mmol/kg (10 wt%) triethoxysilyl-modified BME-44 (44.6 ± 2.1 mV/decade; n = 4).....	161
Figure S4.1 ¹ H NMR (CDCl ₂) spectrum of 4'-isocyanato-5'-nitrobenzo-15-crown-5. ...	163
Figure S4.2 ESI-MS spectrum of purified 4'-isocyanato-5'-nitrobenzo-15-crown-5.	164
Figure S4.3 ¹ H-NMR (CDCl ₂) spectrum of vinyl-modified-BME-44.	165
Figure S4.4 ESI-MS spectrum of vinyl-modified-BME-44.	166
Figure S4.5 ¹ H-NMR (CDCl ₂) spectrum of covalently attachable triethoxysilyl-modified BME-44.	167

Figure S4.6 ESI-MS spectrum of covalently attachable triethoxysilyl-modified-BME-44.	168
Figure 5.1 Structure of tridodecylamine.....	181
Figure 5.2 pH response of PVC-phase pH-selective electrodes with two different ionophore-to-ionic site ratios (3 to 1 and 1.5 to 1). EMF measurements were started at pH 7.4 (10 mM NaCl, 10 mM Na ₂ HPO ₄ , and 10 mM NaH ₂ PO ₄ solution). The pH was increased by adding small aliquots of 6 M NaOH solution. Subsequently, starting again at pH 7.4, the pH was decreased by adding aliquots of 1 M HCl solution. Linear range: pH 4.1 to 12.0. Slope: -57.7 ± 0.5 mV/decade for the 3 to 1 ionophore-to-ionic site ratio (n = 7) and -51.6 ± 1.1 mV/decade for the 1.5 to 1 ionophore-to-ionic site ratio (n = 7).	182
Figure 5.3 Formation of poly(MMA- <i>co</i> -LMA) by copolymerization.....	185
Figure 5.4 Type II poly(MMA- <i>co</i> -LMA) copolymer membrane.....	185
Figure 5.5 pH response of a solid-contact Type I poly(MMA- <i>co</i> -LMA) copolymer membrane. EMF measurements were started at pH 7.4 (10 mM NaCl, Na ₂ HPO ₄ , and 10 mM NaH ₂ PO ₄ solution). The pH was increased by adding small aliquots of 6 M NaOH solution. Subsequently, starting again at pH 7.4, the pH was decreased by adding aliquots of 1 M HCl solution. Linear range: pH 4.1 to 12.4 (slope: -54.8 ± 1.1 mV/decade; n = 5).	186
Figure 5.6 pH response of a Type II poly(MMA- <i>co</i> -LMA) copolymer membrane mounted in a conventional electrode body with inner filling solution (10 mM NaCl, Na ₂ HPO ₄ , and 10 mM NaH ₂ PO ₄ solution). EMF measurements were started at pH 7.4 (10 mM NaCl, Na ₂ HPO ₄ , and 10 mM NaH ₂ PO ₄ solution) solution. The pH was increased by adding small aliquots of 6 M NaOH solution. Subsequently, starting again at pH 7.4, the pH was decreased by adding aliquots of 1 M HCl solution. Linear range: pH 4.1 to 12.4 (Slope: -53.8 ± 1.8 mV/decade; n = 3).	187
Figure 5.7 Reaction scheme for the preparation of crosslinked poly(decyl methacrylate) membranes.....	189

Figure 5.8 Physical appearance of poly(decyl methacrylate) membranes with different weight percentages of crosslinker. 190

Figure 5.9 pH response of crosslinked poly(decyl methacrylate) membranes mounted in conventional ISE bodies with an inner filling solution (10 mM NaCl, Na₂HPO₄, and 10 mM NaH₂PO₄ solution). EMF measurements were started at pH 7.4 (10 mM NaCl, Na₂HPO₄, and 10 mM NaH₂PO₄ solution) solution. The pH was increased by adding small aliquots of 6 M NaOH solution. Subsequently, starting again at pH 7.4, the pH was decreased by adding aliquots of 1 M HCl solution. Linear range: pH 4.1 to 12.4 (slope: – 54.9 mV/decade; n = 1). 191

Figure 5.10 pH response of a crosslinked poly(decyl methacrylate) membrane in a conventional electrode setup with an inner filling solution (10 mM NaCl, Na₂HPO₄, and 10 mM NaH₂PO₄ solution). EMF measurements were started at pH 7.4 (10 mM NaCl, Na₂HPO₄, and 10 mM NaH₂PO₄ solution) solution. The pH was increased by adding small aliquots of 6 M NaOH solution. 193

Figure 5.11 Time profile of the pH response of a crosslinked poly(decyl methacrylate) membrane in a conventional electrode setup with an inner filling solution (10 mM NaCl, Na₂HPO₄, and 10 mM NaH₂PO₄ solution). EMF measurements were started at pH 7.4 (10 mM NaCl, Na₂HPO₄, and 10 mM NaH₂PO₄ solution). The pH was increased by adding small aliquots of 6 M NaOH solution. 194

Figure 5.12 Crosslinked polymethacrylate membrane UV-polymerized on top of nanographite carbon as solid-contact material. With the improved setup and oxygen- and water-free conditions, membranes can be efficiently and reliably polymerized without any cracks in the carbon solid contact. 196

Figure 5.13 pH response and reversibility of crosslinked poly(decyl methacrylate) membranes in a solid-contact electrode set up. Top left and right: 1.5 wt% and 4 wt% crosslinked poly(methacrylate) membranes with nanographite as solid contact. Bottom left and right: 1.5 wt% and 4 wt% crosslinked poly(methacrylate) membranes with a graphite rod as solid contact. EMF measurements were started at pH 4.7 (10 mM NaCl and 10 mM

NaH₂PO₄ solution) solution. The pH was increased by adding small aliquots of 6 M NaOH solution. Subsequently the pH was lowered by adding small aliquots of 1 M HCl solution.

.....198

Figure 5.14 Illustration of common electrode body design that can lead to water bypassing the sensing membrane and shorting problems (left), and a design with polymeric membranes covalently attached to the external electrode body, avoiding such shorting (right).....201

Figure 5.15 Reaction scheme for the preparation of crosslinked poly(methacrylate) membranes doped with a covalently attached pH ionophore.....202

Figure 5.16 pH response and reversibility of crosslinked poly(decyl methacrylate) membranes in a solid contact ISE set up with a covalently attached ionophore. EMF measurements were started at pH 4.7 (10 mM NaCl and 10 mM NaH₂PO₄ solution) solution. The pH was increased by adding small aliquots of 6 M NaOH solution. Subsequently the pH was lowered by adding small aliquots of 1 M HCl solution. Average slope: -55.7 ± 1.0 mV/decade (n=3).204

Figure 5.17 Reaction scheme for crosslinked poly(methacrylate) membranes doped with covalently attached ionic site.....207

Figure 5.18 pH response of crosslinked poly(decyl methacrylate) membranes in a solid contact ISE set up with a covalently attached ionic site (4 or 10 wt%). EMF measurements were started at pH 12.0 (10 mM NaCl and 10 mM NaH₂PO₄ solution adjusted to pH 12). The pH was lowered by adding small aliquots of 1 M HCl solution. Average slope (mV/decade): 4 wt%, -56.0 (n=1); 10 wt%, -51.9 ± 2.1 (n=5).209

Figure 5.19 Reaction scheme for the preparation of crosslinked poly(decyl methacrylate) membranes with both ionophore and ionic site covalently attached to the polymer backbone.211

Figure 5.20 pH response of crosslinked poly(decyl methacrylate) membranes in a solid contact ISE set up with both ionophore and ionic sites covalently attached at two different

concentrations (5 or 10 wt%). EMF measurements were started at pH 12.0 (10 mM NaCl and 10 mM NaH ₂ PO ₄ solution adjusted to pH 12). The pH was lowered by adding small aliquots of 1 M HCl solution. Average slope (mV/decade): 10 wt%, -54.6 (n=1), 5 wt%, -10.5 ± 12.3 (n=6).	215
Figure S5.1 ¹ H-NMR (CDCl ₃) spectrum of purified tridodecylamine.	217
Figure S5.2 ¹ H-NMR (CDCl ₃) spectrum of unpurified tridodecylamine.	218
Figure S5.4 ESI-MS spectrum of unpurified tridodecylamine.	220
Figure S5.5 ¹ H-NMR (CDCl ₃) spectrum of 75 mol% 3-sulfonylpropyl methacrylate tridodecylammonium salt and 25% tridodecylamine.	221
Figure S5.6 ¹ H-NMR (D ₂ O) spectrum of 3-sulfonylpropyl methacrylate potassium salt.	222
Figure S5.7 ¹ H-NMR (CDCl ₃) spectrum of 3-sulfonylpropyl methacrylate <i>N</i> -isopropyl- <i>N</i> -(2-(methacryloyloxy)ethyl)propan-2-ammonium.	223

LIST OF TABLES

Table 1.1. Covalently Attachable Ionophores Minimally Modified from Existing Mobile Ionophores.	41
Table 1.2. Covalently Attachable Ionic Sites	46
Table 2.1. Selectivities and Working Ranges of ISEs based on Ionophores 1, 2, and 3...65	
Table 3.1. Characteristics of Reference Electrode Membranes.....	95
Table 3.2. Glass Transition Temperatures of the Ionic Liquid [C ₈ mim ⁺][NTf ₂ ⁻], Neat Polymers, and [C ₈ mim ⁺][NTf ₂ ⁻]-Doped Polymers.	99
Table 3.3. Composition of Artificial Blood Electrolyte Solutions and Potential Stability Characteristics of Reference Electrodes with [C ₈ mim ⁺][NTf ₂ ⁻]-doped Fluorosilicone 1 Membranes Tested in Artificial Blood Electrolyte Solutions.	102
Table 3.4. Effect of KCl on EMF of Reference Electrodes with Fluorosilicone 1 Membranes Doped with Different Ionic Liquids.	105
Table S3.1. Characteristics of Reference Electrode Membranes.	110
Table S3.2. Sample Dependence of the Potential of Reference Electrodes Based on Different Silicone Materials.	111
Table 5.1. pH Response and Reversibility of Solid-Contact ISEs with Crosslinked Poly(methacrylate) Membranes.....	199

LIST OF ABBREVIATION

ACD	Advanced Chemistry Development
AIBN	2,2'-azoisobutyronitrile
aq.	aqueous
BME-44	Potassium Ionphore III; 2-Dodecyl-2-methyl-1,3-propanediyl bis[<i>N</i> -[5'-nitro(benzo-15-crown-5)-4'-yl]carbamate
[C ₈ mim ⁺][NTf ₂ ⁻]	1-methyl-3-octylimidazolium bis(trifluoromethylsulfonyl)imide
[C ₁₀ mim ⁺][NTf ₂ ⁻]	1-methyl-3-decylimidazolium
[C ₁₂ mim ⁺][NTf ₂ ⁻]	1-methyl-3-dodecylimidazolium
CDI	1,1'-carbonyldiimidazole
CIM	colloid-imprinted mesoporous
d	day
DCM	dichloromethane
DMA	decyl methacrylate
DMPP	2,2-dimethoxy-2-phenylacetophenone
DOS	bis(20ethylhexyl) sebacate
DSC	differential scanning calorimetry
emf	electromotive force

eq	equivalent
ETH 1001	Calcium Ionophore I; diethyl <i>N,N'</i> -[(4 <i>R</i> ,5 <i>R</i>)-4,5-dimethyl-1,8-dioxo-3,6-dioxaoctamethylene]bis(12-methylaminododecanoate)
ETH 1062	Cadmium Ionophore I; <i>N,N,N',N'</i> -tetrabutyl-3,6-dioxaoctanedi(thioamide)
ETH 129	Calcium Ionophore II; <i>N,N,N',N'</i> -tetra[cyclohexyl]diglycolic acid diamide
ETH 157	Sodium Ionophore II; <i>N,N'</i> -dibenzyl- <i>N,N'</i> -diphenyl-1,2-phenylenedioxydiacetamide
ETH 1778	octadecyl isonicotinate
ETH 1907	4-nonadecylpyridine
ETH 2120	Sodium Ionophore III; <i>N,N,N',N'</i> -tetracyclohexyl-1,2-phenylenedioxydiacetamide
ETH 227	Sodium Ionophore I; <i>N,N',N''</i> -triheptyl- <i>N,N',N''</i> -trimethyl-4,4',4''-propylidynetris(3-oxabutylamide)
ETH 2418	octadecyl 2-(4-dipropylaminophenylazo)benzoate
ETH 4030	Magnesium ionophore III; <i>N,N''</i> -Octamethylene-bis(<i>N'</i> -heptyl- <i>N'</i> -methylmalonamide)
ETH500	tetradodecylammonium tetrakis(4-chlorophenyl)borate

ETH 7025	Magnesium ionophore IV; <i>N,N',N''</i> -Tris[3-(heptylmethylamino)-3-oxopropionyl]-8,8'-iminodioctylamine
FIM	fixed interference method
GΩ	gigaohm
h	hour
ICDs	implantable cardioverter defibrillators
IE	ion-exchanger
IFCC	International Federation of Clinical Chemistry and Laboratory Medicine
IFS	inner filling solution
ISE	ion-selective electrode
IL	ionic liquid
IR	infrared spectroscopy
KTpCIPB	potassium tetrakis(4-chlorophenyl)borate
KTFPB	potassium tetrakis[3,5-bis(trifluoromethyl)phenyl]borate
KTPFB	potassium tetrakis(pentafluorophenyl)borate
LD ₅₀	median lethal dose
Lead ionophore IV	<i>tert</i> -Butylcalix[4]arene-tetrakis(N,N-dimethylthioacetamide)

LMA	lauryl methacrylate; dodecyl methacrylate
M	molar
mg	milligram
min	minute
mL	milliliter
MMA	methyl methacrylate
mV	millivolt
NaTFPB	sodium tetrakis[3,5-bis(trifluoromethyl)phenyl]borate
[NBu ₃ Me ⁺][NTf ₂ ⁻]	tributylmethylammonium bis(trifluoromethylsulfonyl)imide
NBu ₄ ⁺	tetrabutylammonium ion
NMR	nuclear magnetic resonance spectroscopy
<i>o</i> -NPOE	<i>o</i> -nitrophenyloctyl ether
NPr ₄ ⁺	tetrapropylammonium ion
org	organic
PET-G	glycol-modified polyethylene terephthalate
pK _a	acid constant
PMs	pacemakers
poly(MMA-co-LMA)	poly(methyl methacrylate- <i>co</i> -lauryl methacrylate)

poly(nBA)	poly(<i>n</i> -butyl acrylate)
PPh ₄ ⁺	tetraphenylphosphonium ion
ppm	parts per million
PTFE	polytetrafluoroethylene
PU	polyurethane
PVC	poly(vinyl chloride)
Sodium Ionophore X	4- <i>tert</i> -butylcalix[4]arene tetraacetic acid tetraethyl ester
Sodium Ionophore VI	bis[(12-crown-4)methyl]didodecylmalonate
SSM	separate solution method
<i>t</i> ₉₅	response time to reach 95% of final values
<i>T</i> _g	glass transition temperature
TDDA	tridodecylamine
THF	tetrahydrofuran
UV	ultraviolet
V	volt
wt%	weight percentage
π^*	scale of solvent polarity and polarizability

I. INTRODUCTION OF ELECTROCHEMICAL SENSORS AND BIOCOMPTABILITY OF SENSORS

1.1 Overview of Potentiometric Ion Sensors

1.1.1 Ion-Selective Electrode (ISEs)

1.1.1.1 The Response Mechanism

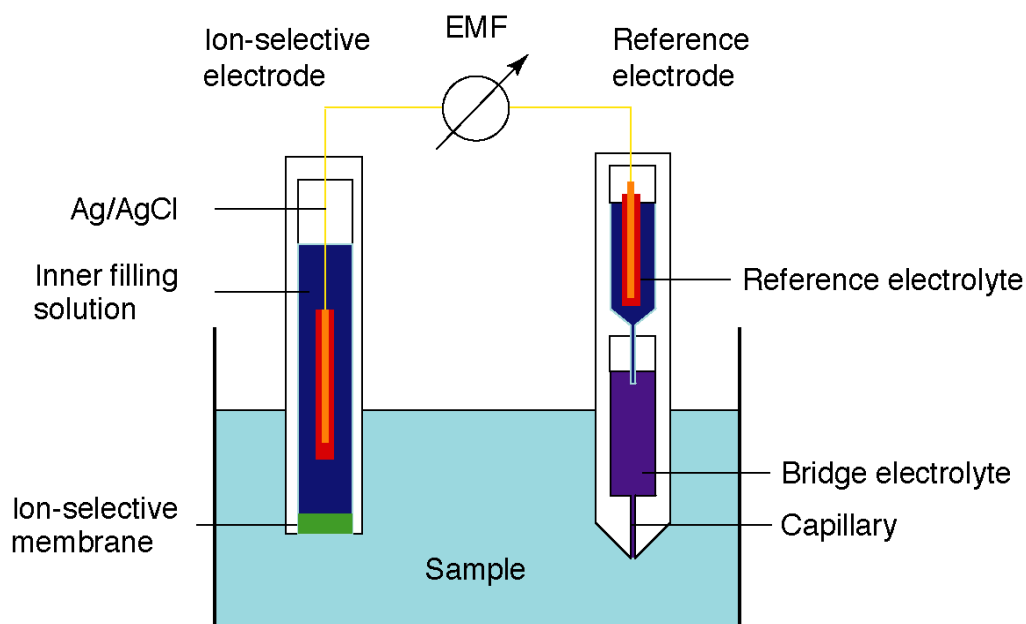


Figure 1.1 A schematic of a potentiometric electrochemical sensor setup with an ion-selective electrode (left) and a reference electrode (right). Reprinted from Ref. 1.

An ion-selective electrode (ISE) is an electrochemical sensor that selectively responds to the activities of specific ion(s) of interest in sample solutions.¹⁻⁶ An ISE in a conventional setup includes a selective sensing membrane, an inner filling solution (IFS), and an internal reference such as a Ag/AgCl wire (**Figure 1.1** left). The sensing ability of an ISE is achieved through the water-immiscible (organic phase) ion-selective membrane, hosted at the end of the electrode, between the IFS and the sample solution. The Ag/AgCl wire connects the IFS inside the ISE body with the potentiometer, providing an internal reference with a well-defined potential. The use of an external reference electrode (**Figure**

Using an appropriate bridge electrolyte, the liquid junction potential E_J at the bridge electrolyte/sample solution interface can be kept very small, independent of the sample, or it can be estimated using the Henderson formalism.⁸ In this way, the measured emf is only determined by the membrane potential E_M . With a closer look, E_M can be further divided into three contributing potentials: the phase boundary potential at the membrane/IFS interface, the membrane-internal diffusion potential, and the phase boundary potential at the membrane/sample solution interface. The membrane/IFS phase boundary potential can be assumed constant in most conditions. The membrane-internal diffusion potential can be neglected as long as concentration gradients are not present in the membrane.⁹ This shows that the membrane potential E_M only depends on the membrane/sample solution phase boundary potential, E_{PB} , which is determined by the activities of ions of interest in the sample solution. Therefore, combining all constant contributions together, equation 1 can be further simplified to:

$$emf = E_0 + E_M + E_J = E_{const} + E_{PB} \quad (2)$$

In this way, the measured emf is only determined by E_{PB} , the phase boundary potential between the membrane and sample solution. To further correlate the measured emf with the activities of ions of interest, E_{PB} is derived in the following thermodynamically.

The electrochemical potential of an ion I ($\tilde{\mu}_I$) in an aqueous phase can be expressed by:

$$\tilde{\mu}_I(aq) = \mu_I(aq) + z_I F \phi(aq) \quad (3)$$

where $\mu_I(aq)$ is the chemical potential of ion I in an aqueous phase, z_I is the charge of ion I , F is the Faraday constant, $\phi(aq)$ is the electrical potential. The chemical potential of ion I , $\mu_I(aq)$ can be further defined as:

$$\mu_I(aq) = \mu_I^\circ(aq) + RT \ln a_I(aq) \quad (4)$$

where $\mu_I^\circ(aq)$ is the chemical potential under standard conditions, R is the gas constant, T is the temperature of the aqueous solution, and $a_I(aq)$ is the activity of ion I in the aqueous solution.

Inserting equation 4 into 3 gives the expression:

$$\tilde{\mu}_I(aq) = \mu_I^\circ(aq) + RT \ln a_I(aq) + z_I F \phi(aq) \quad (5)$$

Since polymeric membranes consist of an organic material, membrane phases are often referred to as organic phases, a nomenclature that will also be used here, in consistency with much of the literature. It follows that the electrochemical potential of ion I in the membrane (organic phase) can be derived similarly as:

$$\tilde{\mu}_I(org) = \mu_I(org) + z_I F \phi(org) = \mu_I^\circ(org) + RT \ln a_I(org) + z_I F \phi(org) \quad (6)$$

When equilibrium is reached between the aqueous phase and membrane (organic phase), the electrochemical potentials of ion I in the two phases equal each other.

$$\tilde{\mu}_I(aq) = \tilde{\mu}_I(org)$$

$$\mu_I^\circ(aq) + RT \ln a_I(aq) + z_I F \phi(aq) = \mu_I^\circ(org) + RT \ln a_I(org) + z_I F \phi(org) \quad (7)$$

By definition, the phase boundary potential, E_{PB} , is the difference between the electrical potential of the membrane (organic phase) and the electrical potential of the sample solution. By reforming equation 7, E_{PB} can be expressed as:

$$E_{PB} = \phi(org) - \phi(aq) = \frac{\mu_i^{\circ}(aq) - \mu_i^{\circ}(org)}{z_1 F} + \frac{RT}{z_1 F} \ln \frac{a_i(aq)}{a_i(org)} \quad (8)$$

Combining equations 2 and 8 gives an expression for the measured emf:

$$emf = E_{const} + E_{PB} = E_{const} + \frac{\mu_i^{\circ}(aq) - \mu_i^{\circ}(org)}{z_1 F} + \frac{RT}{z_1 F} \ln a_i(aq) - \frac{RT}{z_1 F} \ln a_i(org) \quad (9)$$

The chemical potentials of ion I in both the aqueous phase and membrane (organic phase) at standard conditions, $\mu_i^{\circ}(aq)$, $\mu_i^{\circ}(org)$, and the activity of ion I in the membrane (organic phase) $a_i(org)$ can be assumed constant. Combining all the sample-independent components of equation 9 into the constant E^0 gives equation 9, which is the well-known Nernst equation:

$$emf = E^0 + \frac{RT}{z_1 F} \ln a_i(aq) = E^0 + \frac{2.303RT}{z_1 F} \log a_i(aq) \quad (10)$$

According to the Nernst equation, under ideal conditions and at $T = 293$ K (20 °C), an ISE responds to a singly charged ion I with a characteristic Nernstian slope of 58.17 mV/decade.

1.1.2 Components of an ISE membrane

1.1.2.1 Polymeric Matrix

As an essential part of every ISE that provides a response with selectivity towards an ionic analyte, the ISE membrane is typically made up of three to four components: polymer matrix, ionophore, ionic site, and—optionally—plasticizer.^{1, 2} The purpose of the polymer matrix in an ISE membrane is to provide both mechanical support and elasticity and to allow ion transport, which is key to ion sensing.² The polymer matrix employed in an ISE membrane needs to have a glass transition temperature (T_g) below room temperature

to allow sufficient movement of ionic species through the membrane,¹⁰ thus making sensing possible. The most commonly used polymer matrix in ISE membranes is polyvinylchloride (PVC) due to its excellent stability.² However, with a glass transition temperature around 80 °C, high molecular weight PVC needs a plasticizer to lower its T_g .

1.1.2.2 Plasticizer

The plasticizer used in ISE membranes plays a key role in the function of ISE membranes and thus needs to be chosen carefully. It contributes to the majority of the membrane weight and lowers the overall T_g of the polymer matrix by solubilizing the chains of the polymer.¹¹ As a result, the membrane viscosity is decreased and the mobility of ionic membrane components mobility is increased, providing a lower electrical resistance of membrane.¹² In addition to that, the plasticizer should also be miscible with the polymer to give a homogenous state to better host ionophores and ionic sites.^{13, 14} The polarity of the plasticizer needs to be given special consideration. It has been shown that the polarity of a plasticizer also has an impact on the selectivity of ISE membranes^{15, 16} and can result, e.g., in a preference for divalent ions over monovalent ones.^{17, 18}

1.1.2.3 Ionophore

Considered as a key component in the ionophore-based ISE, ionophores determine the selectivity of an ISE. This is because ionophores favor the primary ion over interfering ions by strongly and reversibly binding with the primary ion, which lowers the free energy of transfer of the primary ion from the sample into the sensing membrane (**Figure 1.2**)³. Ionophores should be very hydrophobic in order to both increase the solubility in the polymer membrane and decrease the possibility of leaching into the aqueous solution.

Strong binding of ionophores to the primary ion is preferred since this will extend the detection limit of the ISE. However, this will also affect the working range of the ISE. The stronger complexation will result in counter-ion interference, also known as Donnan failure.¹⁹⁻²¹ This is a process occurring at higher target ion concentrations at the upper detection limit of the ISE, where the primary ion and counter-ions are co-extracted into the membrane.

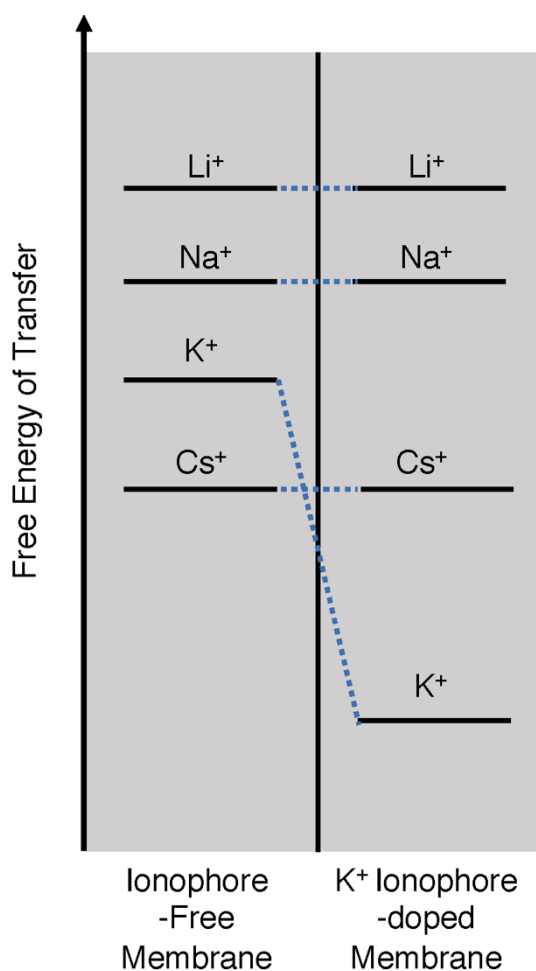


Figure 1.2. Schematic comparison of the free energy of transfer of monovalent cations between an ionophore-free membrane and a K⁺ ionophore-doped membrane.

1.1.2.3 Ionic Site

Ionic sites serve as counter-ions to the primary (target) ions in the ISE membrane phase. They need to be soluble in the polymer matrix to facilitate the ion exchange of primary ion entering into the membrane from the aqueous solution. They also prevent counter-ions in the aqueous solution from moving into the membrane matrix at the same time.^{22, 23} Electrical neutrality of both the membrane bulk and the aqueous solution is maintained during this process. Ionic sites are necessary for ISE membranes doped with electrically neutral ionophores.^{1, 23} Moreover, it has been shown that optimizing the ionic-site/ionophore ratio can enhance the selectivity of an ISE^{24, 25} (see also Chapters II and V).

1.1.3 Selectivity

Selectivity is one of the most important factors to indicate the performance of a sensor, since it describes how well a sensor can respond to the species of interest in the presence of other interfering species. It is particularly important in clinical applications where stringent criteria apply.^{26, 27} In the field of ISEs, the selectivity is defined as the preference for the primary ion I over an interfering ion J in the partition process from the aqueous phase into the membrane phase. For an ionophore-free ion-exchanger electrode, selectivity is determined by the free energy of transfer of the ions into the ionophore-free sensing membrane. It typically follows the Hofmeister series ($\text{Cs}^+ > \text{Rb}^+ > \text{K}^+ > \text{Na}^+ > \text{Li}^+$).^{7, 28-31} In the case of ionophore-based ISEs, the ionophore significantly lowers the energy of phase transfer of the target ion due to the strong binding between the ionophore and target ion.

Selectivity is quantified in the field of ISEs with the potentiometric selectivity coefficient, $K_{I,J}^{pot}$, which originates from the semi-empirical Nikolskii-Eisenman equation (equation 11).^{2, 32-34} The Nikolskii-Eisenman equation is analogous to the Nernst equation (equation 10), but with an additional selectivity-weighted activity term to represent the situation where both primary ion I and interfering ion J are present in a sample and each may influence the measure emf.

$$emf = E^0 + \frac{RT}{z_I F} \ln[a_I(IJ) + K_{I,J}^{pot} a_J(IJ)^{z_I/z_J}] \quad (11)$$

where the emf is measure electromotive force, $a_I(IJ)$ and $a_J(IJ)$ are the activities of ion I and ion J in the presence of each other, z_I and z_J are the charges of ion I and ion J . However, a serious limitation was later revealed that the semi-empirical Nikolskii-Eisenman equation does not accurately predict the mixed response of ISEs to two ions when the charges of primary ion and interfering ion are different, i.e., $z_I \neq z_J$. To address this issue, a more accurate expression for selectivity coefficient $K_{I,J}^{pot}$ was derived.³⁵⁻³⁷

According to the Nikolskii-Eisenman equation,

$$a_I(I) = a_I(IJ) + K_{I,J}^{pot} a_J(IJ)^{z_I/z_J} \quad (12)$$

An important boundary condition is reached when there is no primary ion present. Then, the term $a_I(IJ)$ becomes zero and $a_J(IJ)$ becomes $a_J(J)$. Equation 12 can thus be reformed as

$$K_{I,J}^{pot} = \frac{a_I(I)}{a_J(J)^{z_I/z_J}} \quad (13)$$

As shown before, the Nernst equation as expressed for the primary ion I is,

$$E_I = E_I^0 + \frac{RT}{z_I F} \ln a_I(I) \quad (14)$$

The Nernst equation can also be applied to the interfering ion J ,

$$E_J = E_J^0 + \frac{RT}{z_J F} \ln a_J(J) \quad (15)$$

where E_I^0 and E_J^0 are the standard potentials of ion I and ion J , respectively. By substituting equations 14 and 15 into equation 13, the selectivity coefficient, $K_{I,J}^{pot}$, can be presented in the following form:

$$K_{I,J}^{pot} = \exp \left[\frac{(E_J^0 - E_I^0) z_I F}{RT} \right] \quad (16)$$

Equation 16 and 13 become the underlying basis of the two traditional methods in the calculation of selectivity coefficient, namely the Separate Solution Method (SSM) (equation 16) and Fixed Interference Method (FIM) (equation 13).^{38, 39}

With the SSM, as the name indicates, two separate calibration curves for ion I or J are prepared independently. The Nernstian response regions of these two curves are each extrapolated to 1M activity of ion I or J . This gives the two standard potentials E_I^0 and E_J^0 , which can be used with equation 16 to calculate the selectivity coefficient (**Figure 1.3** left).

With the FIM, only solutions containing both primary ion I and interfering ion J are used. The activity of the interfering ion J is kept constant throughout the measurements, while the concentration of the primary ion I is decreased or increased incrementally (dilution is recommended to minimize the effect of sensor drifts). Either way, in the region of higher activity of the primary ion I , the ISE is responding with a Nernstian slope to ion I . However, at low ion I concentrations, the ISE will respond to the constant activity of the

interfering ion J , giving a calibration curve as shown in **Figure 1.3** (right). The selectivity coefficient can be determined by the following equation,

$$K_{I,J}^{pot} = \frac{a_I(DL)}{a_J(BG)^{z_I/z_J}} \quad (17)$$

where $a_I(DL)$ is the activity of the primary ion I at the detection limit—as defined by the intersection of the extrapolated linear (Nernstian) region and extrapolated constant emf (plateau) region—and $a_J(BG)$ is the activity of fixed interfering ion J . For pH electrodes, FIM is the only suitable method, since separate solutions containing only protons in the basic pH range, or only interfering ions in the acidic range do not exist.

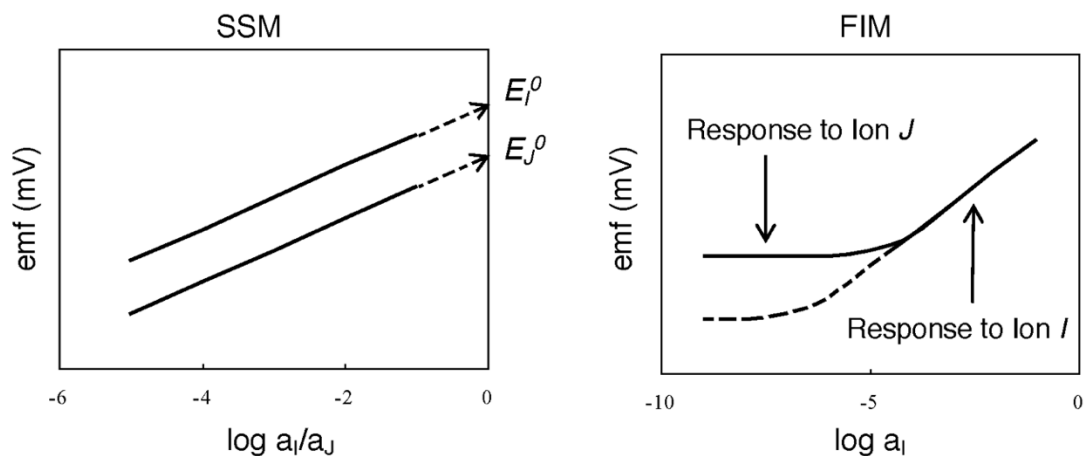


Figure 1.3. Illustration of the separate solution method (SSM) and fixed interference method (FIM) under ideal conditions.

1.2 Fluorous-Phase Ion-Selective Electrodes

1.2.1 Perfluorinated Compounds

Heavily fluorinated compounds, termed perfluorinated compounds, are a special class of organofluorine compounds that contain C-F bonds, C-C bonds as well as other heteroatoms but no hydrogen atoms.⁴⁰⁻⁴³ One of the most characteristic properties of perfluorinated compounds is their extremely low polarity and low polarizability.^{44, 45} This is due to the fact that on the Pauling scale fluorine atoms exhibit the highest electronegativity of all elements. Furthermore, perfluorinated compounds are often symmetric as well. Consequently, the polarity and polarizability of many perfluorinated compounds are so low to the degree that phase separation occurs between many perfluorinated compounds and traditional so-called “nonpolar” organic compounds, such as hydrocarbons.³⁹ The extremely low polarity of perfluorinated compounds can be quantitatively represented by using the π^* scale of solvent polarity and polarizability, where 0 is defined by cyclohexane and 1 is defined by dimethyl sulfoxide. Perfluorinated compounds are found to have extremely negative π^* values, such as -0.39 for perfluoroheptane and -0.41 for perfluorooctane.⁴⁰ The term “fluorous” is often used to contrast water- and oil-immiscible perfluorinated compounds to other organic compounds.^{40, 41}

1.3.2 Fluorous-Phase ISEs

The first-ever ISEs based on a fluorous matrix instead of conventional plasticized PVC were possible because of the synthesis of a fluorophilic tetraphenylborate salt as ionic site (**Figure 1.4** right) and doping of this salt into a filter-supported fluorous solvent as ISE

membranes (**Figure 1.5**).⁴⁶ Solvation of lipids and proteins—commonly encountered in biological samples—is drastically suppressed in the extremely low polarity fluoruous phase, which is very promising in terms of reducing biofouling. Furthermore, the selectivity, working range, and life time of ISEs are also greatly improved by using fluoruous phases.⁴⁶⁻⁴⁹ The detection limits are expanded since interfering ions have very poor solvation in the nonpolar fluoruous phase. The target ions also bind with fluorophilic ionophores more strongly due to the non-coordinating nature of the fluoruous matrix.⁴⁹ All of this results in enhanced selectivity. Similarly, the co-extraction of counter-ion into the ISE membrane, which ultimately leads to Donnan failure, is also disfavored due to the poor non-specific solvation of counter-ions in the fluoruous phase. Fluoruous membrane ISEs have been successfully developed for Cl^- , Br^- , I^- , NO_3^- , CO_3^{2-} , Ag^+ , and H^+ , as well as for perfluoroalkyl carboxylates and sulfonates.^{44, 46, 48-50} Fluorophilic ionophores and ionic sites can be designed and synthesized by adding perfluorinated chains, also known as “fluoruous ponytails”, to existing ionophores and ionic sites. Examples of such salts are shown in **Figure 1.4**.

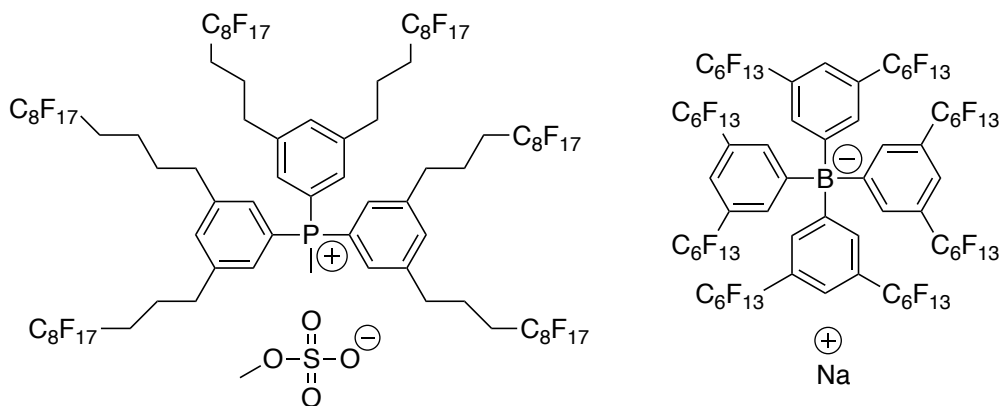


Figure 1.4. Examples of previously reported fluorophilic salts

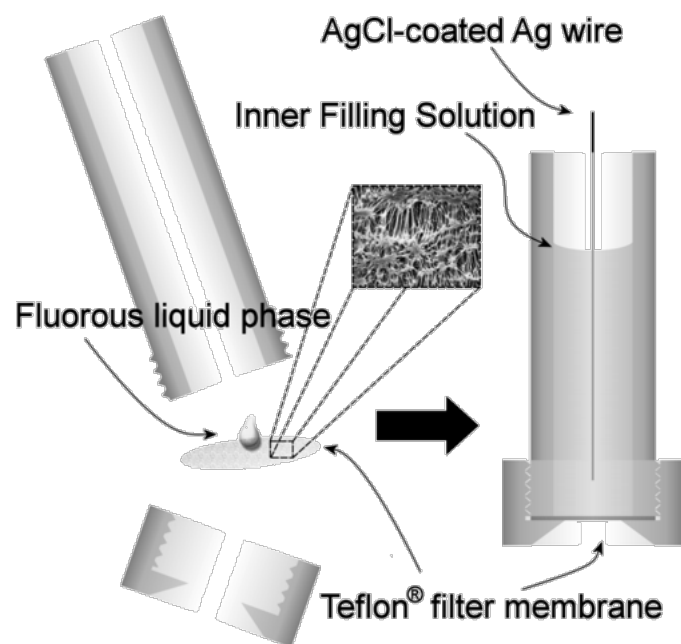


Figure 1.5. Schematic of the first ion-selective electrode based on a fluorous liquid phase supported by an inert porous support. Reprinted from Ref. 46.

1.3 ISEs for pH Measurements

1.3.1. pH Glass Electrodes

The pH glass electrode is one of the most widely used and well-established potentiometric pH sensors. It is an ion-selective electrode with a solid-state membrane made of thin glass, as shown schematically in **Figure 1.5**.⁵¹

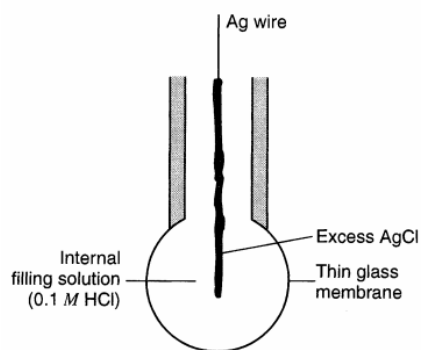
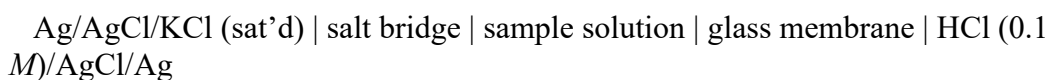


Figure 1.5. Diagram of a typical glass electrode, reprinted from Ref. 51

The underlying working mechanism is similar in general to polymeric membrane ion-selective electrodes. An overview of the relevant interfaces for a pH glass electrode/free-flow free-diffusion reference electrodes system is shown below:



Reference Electrode



Glass Electrode

The potentiometric response to the sample solution comes from two interfaces. One is the liquid junction potential at the external reference electrodes/sample solution interface, which can be considered small and constant (see above **Section 1.1.1.1**). The other one is

the interface between the glass membrane and sample solution. Potentials at all other interfaces are kept constant due to the constant composition of the respective phases. Therefore, the potentiometric response will depend on the potential at the sample solution/glass electrode interface and can be expressed as

$$emf = \frac{RT}{z_I F} \ln a_I + E^0 \quad (18)$$

where z_I and a_I are the charge and activity of ion I in the sample solution, and E^0 is a constant representing all the other phase boundary potentials in the cell.

The working mechanism of the glass membrane is rather complicated but has been detailed in the literature.⁵²⁻⁵⁶ The bulk of the membrane is dry glass. On the surface of the glass, a thin hydrated silicate layer is formed. Certain cations are adsorbed in this layer. Within the dry glass, the charge transport is performed by mobile cations, such as Na^+ or Li^+ . For a typical commercial pH glass electrode, the selectivity follows the order of $\text{H}^+ \gg \text{Na}^+ > \text{K}^+, \text{Rb}^+, \text{Cs}^+ \gg \text{Ca}^{2+}$.⁵¹

1.3.2 The Working Range of Ionophore-Doped Polymeric Membrane-Based pH ISEs.

The working range remains one of the most important characters of pH sensors. In the field of ionophore-based pH ISE, the working range is defined by both the upper detection limit and lower detection limit. These two detection limits are each determined by different mechanisms. IUPAC recommends²¹ that the detection limits of ISE be defined as the intersection of the extrapolation of two linear response ranges. **(Figure 1.6)** In the case of ISEs of limited selectivity, at lower primary ion concentrations, the interfering ion

will compete with the primary ion. Therefore, the lower detection limit is essentially determined by selectivity. The upper detection limit of an ISE is reached when the co-extraction of the primary ion and its counter ion (in the case of H^+ , its counter anion) from the sample solution into the membrane occurs. This results in the loss of membrane permselectivity, widely known as Donnan failure.^{19-21, 57}

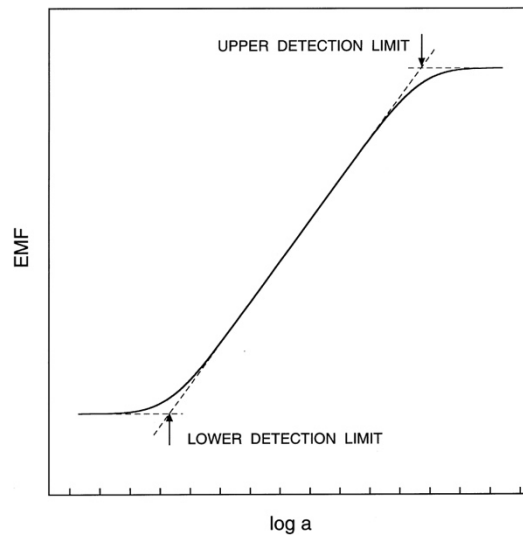


Figure 1.6. Upper and lower detection limits of an ISE; reprinted from Ref. 2

The measuring range of an ISE is defined as the ratio of the activities of the primary ion at the upper detection limit and the lower detection limit. Based on theories developed for ionophore-based pH ISEs,^{58, 59} the lower and upper detection limits can be determined as follows:

$$a_{H^+}(DL_{lower}) = \frac{a_J}{L_T - R_T} \frac{k_{J^+}}{k_{H^+}} K_a \quad (19)$$

$$a_{H^+}(DL_{upper}) = \frac{1}{k_{H^+} + k_{X^-}} \frac{R_T^-}{a_{X^-}} K_a \quad (20)$$

where K_a is the acidity constant of the protonated ionophore, L_T and R_T^- are the concentrations of ionophore and ionic sites in the membrane, respectively, and k_{H^+} , k_{J^+} and k_{X^-} are the single ion distribution coefficients of H^+ (primary ion), interfering cation, and counter anion for distribution between the aqueous solution and organic membrane phase (reflecting on the lipophilicities of these ions).

Equations 19 and 20 indicate that, for a given composition of membrane, the lower and upper detection limits are similarly determined by the acidity constant of the H^+ -ionophore complex in the ISE membrane and the lipophilicity and activity of the ionic species involved. Combining these two equations, the measuring range can be shown as

$$\frac{a_{H^+}(DL_{upper})}{a_{H^+}(DL)} = \frac{1}{k_{J^+}k_{X^-}} \frac{R_T^-(L_T - R_T^-)}{a_{X^-}a_J} \quad (21)$$

Thus, the measuring range of an ISE for pH will be

$$\begin{aligned} \Delta pH &= \log[a_{H^+}(DL_{upper})] - \log[a_{H^+}(DL)] = \log \left[\frac{a_{H^+}(DL_{upper})}{a_{H^+}(DL)} \right] \\ &= \log \left[\frac{1}{k_{J^+}k_{X^-}} \frac{R_T^-(L_T - R_T^-)}{a_{X^-}a_J} \right] = \log \left[\frac{1}{k_{J^+}k_{X^-}} \frac{0.25L_T^2 - (R_T^- - 0.5L_T)^2}{a_{X^-}a_J} \right] \end{aligned} \quad (22)$$

As can be seen from equation 22, the maximum pH working range is not affected by the acidity constant of the proton ionophore, as the upper and lower detection limits undergo the same amounts of shift. With regard to the best ionophore/ionic site ratio, assuming 1:1 complex formation between the H^+ and ionophore, the maximum range is reached when $R_T^- = 0.5L_T$. Therefore, ionic sites should be used with a concentration half of that of the ionophore. However, this theory was developed based off of a few assumptions, one of which neglects ion pair formation in the membrane phase. In fluorosulfonate phase ISEs, where strong ion pair formation was observed,^{25, 44, 46} the working range has

been shown to deviate from this theory (see Chapter II).²⁵ However, this theory can still provide some useful guidance in developing ionophore-based pH ISEs.

1.4 Biocompatibility and Anti-Biofouling Aspects of ISEs

The use of ISEs in biological samples and as implantable or wearable devices requires ISEs to be biocompatible. To be fully biocompatible, the leaching of membrane components (plasticizer, ionophore, ionic site, etc.) out of the membrane and any perturbation of the in-vivo environment should be minimized or eliminated.⁶⁰ To be fully functional in biological samples, the electrodes should also be resistant to biofouling, i.e., the ISE's response and selectivity should not be affected by the biological samples.

1.4.1 Biocompatibility of Materials and Devices

“Biocompatibility” has a wide range of definitions depending on the context and subject of focus.⁶¹ This also points to the evolving understanding of biocompatibility as new research emerges. From a polymeric material point of view, IUPAC defines biocompatibility as the ability to be in contact with a living system without imposing an adverse effect.⁶² However, several materials may be integrated into a final product. In the United States, the Food and Drug Administration (FDA) set the guideline "Biological evaluation of medical devices — Part 1: Evaluation and testing within a risk management process" to assist industry in assessing products that may be subject to regulation. This guideline is based on but extends beyond ISO 9001 from the International Organization for Standardization.⁶³ For device categories ranging from surface devices, external communicating devices, to implant devices, and contact durations ranging from limited (≤ 24 h), prolonged (> 24 h to 30 d), to permanent (> 30 d), increasing numbers of tests of biological effects are recommended.

1.4.2 Leaching of Plasticizer and Plasticizer-Free ISE Membranes.

The convectional PVC-phase ISE membranes require a plasticizer to lower the glass transition temperature of PVC below the temperature at which measurements are performed. However, plasticizers can gradually leach out of the sensing membranes over time, resulting not only in a limited sensor lifetime but possibly also inflammatory reactions.⁶⁴⁻⁶⁷ Common plasticizer-free polymeric membrane options that have a glass transition temperature below room temperature fall into three major categories: polysiloxanes (i.e. silicones), polyurethanes, and polyacrylates and polymethacrylates.

1.4.2.1. ISEs with Polysiloxane-Based Membranes

Silicone materials⁶⁸⁻⁷⁶ are widely commercially available and have been used extensively in medical application.⁷⁷⁻⁸² Most reported silicone membrane-based ISEs are based on commercially sourced silicones, with a few studies⁸³⁻⁸⁶ describing the synthesis of silicones for ISEs membranes. In terms of the polymeric backbone structure, the vast majority of silicones are hydroxy-terminated poly(dimethylsiloxanes) or poly[(3,3,3-trifluoropropyl)methylsiloxanes]—often termed “silicones” and “fluorosilicones”, respectively (**Figure 1.7**, left and middle).⁷² In terms of curing (i.e., polymerization), the condensation of condensation-type polysiloxanes is often catalyzed by a tin (Sn) catalyst, which releases a byproduct such as acetic acid, alcohol (often methanol or ethanol), oxime, or acetone, and happens at room temperature (a process termed RTV, room temperature vulcanization). Addition-type polysiloxanes often rely on a hydrosilylation curing reaction catalyzed by platinum (Pt) at elevated temperatures, releasing no side products. Inorganic

fillers such as silica are often blended into these silicones to improve mechanical properties.⁷² Improved adhesion to substrates was one of the major motivations for the introduction of polysiloxanes into the field of ISEs, in an attempt to replace poorly adhering PVC membranes.⁸⁷ Several reports claimed that the lower resistance of fluorosilicones and cyanopropyl modified silicones⁸⁶ can be explained by the presence of trifluoropropyl or cyanopropyl groups, which were assumed to result in a higher dielectric constant. However, it is likely that higher ionic impurities of the specific products were the primary cause of the lower electrical resistance. The use of commercially sourced silicones can add complexity into evaluating ISEs since the exact composition of these products is often only revealed to a certain degree and can change over the years without notice by the manufacturers.

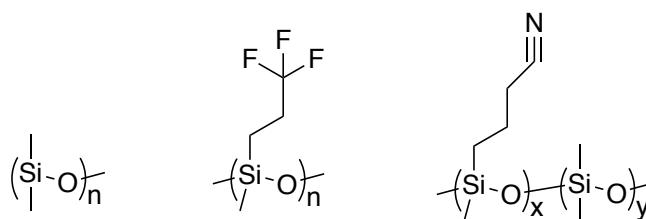


Figure 1.7. Common commercially available poly(dimethylsiloxanes), i.e., “silicones” (left), poly[(3,3,3-trifluoropropyl)methylsiloxanes], i.e., “fluorosilicones” (middle), and reported commercially not available poly(dimethylsiloxane-*co*-cyanopropylmethylsiloxanes) (right).

1.4.2.1.1 ISEs with Dow 3140 and Dow 730 Polysiloxanes as Polymer Matrix

Silicone 3140 and fluorosilicone 730 from Dow Corning are two polysiloxane materials that have been used in the field of ISEs. Both of them are one-component, room-

temperature moisture-cure (RTV) polysiloxanes, making them easier to use than multiple-component, higher-temperature-cure polysiloxanes.

A Dow 730 fluorosilicone membrane doped with the ionic site tridodecylmethylammonium nitrate showed Nernstian response to NO_3^- (an example of an ionophore-free ion-exchanger electrode) with a lifetime of 95 days (stored in 0.01 M ammonium nitrate solution; lifetime was defined as time when the response slope dropped below 50 mV/decade).⁸⁸ In a parallel test, the addition of plasticizer 2-nitrophenyl octyl ether (*o*-NPOE) to the fluorosilicone membrane gave ISEs with similar Nernstian response but reduced the sensor lifetime from 95 days to 8 days. However, in either case, insufficient selectivity with respect to sulfonate was obtained as compared to ISEs with PVC-phase membranes. When the same fluorosilicone matrix was used with nonactine as ammonium (NH_4^+) ionophore, Nernstian responses were only obtained when additional plasticizer was used.

In another study, Dow 3140 silicone was used to prepare ISE membranes with ETH 1001 [Calcium Ionophore I, diethyl *N,N'*-[(4*R*,5*R*)-4,5-dimethyl-1,8-dioxo-3,6-dioxaoctamethylene]bis(12-methylaminododecanoate)], tridodecylamine (TDDA) as pH ionophore, valinomycin as K^+ ionophore, and calix[4]arene ethyl ester derivative as Na^+ ionophore.⁸⁹ When ETH 1001 was used with potassium tetrakis(4-chloro-phenyl)borate (KTPCIPB) as ionic site, poor response slopes to Ca^{2+} were obtained. When the more lipophilic ionic site potassium tetrakis[3,5-bis(trifluoromethyl)phenyl]borate (KTFPB) was used, Nernstian slopes were obtained. The same was also true for pH-selective Dow 3140-based ISEs. Furthermore, when KTFPB was used as ionic site, the addition of a small

wt% plasticizer widened the Nernstian pH range by 2 pH units as compared to ISEs with plasticizer-free silicone membranes. In contrast, valinomycin-doped K^+ -selective silicone membranes showed good performance with or without ionic site, with KTpCIPB or KTFPB as ionic site, with or without added plasticizer. This suggests that valinomycin is compatible with Dow 3140 membrane as well as the intrinsic ionic site it contains. However, the added external ionic site was beneficial for long-term use.⁹⁰ Silicone membranes doped with calix[4]arene ethyl ester derivative as Na^+ ionophore and KTFPB as ionic site showed excellent characteristic with or without added plasticizer.

In another report, Dow 730 fluorosilicone was used as ISE membrane matrix with valinomycin as K^+ ionophore, ETH 227 (Sodium Ionophore I, *N,N,N'*-triheptyl-*N,N,N'*-trimethyl-4,4',4''-propylidynetris(3-oxabutyramide)) and ETH 2120 (Sodium Ionophore III, *N,N,N',N'*-tetracyclohexyl-1,2-phenylenedioxydiacetamide) as Na^+ ionophores, ETH 1001 and ETH 129 (Calcium Ionophore II, *N,N,N',N'*-tetra[cyclohexyl]diglycolic acid diamide) as Ca^{2+} ionophores, and *N,N*-dioctadecylmethylamine as pH ionophore.⁹¹ All were used without any added plasticizer and provided good response characteristics towards respective analytes in terms of detection limit, selectivity, and response slope, comparable to PVC-based ISEs, with the exception of pH. The difficulty of making good pH ISEs is possibly due to the acetic acid-evolving nature of Dow 730, which may result in complete protonation of the pH ionophore in the membranes; the lack of free ionophore in the membrane may explain the poor performance of the sensor, as free ionophore is a prerequisite for a selective ISE response.

Dow 730 fluorosilicone was also used as polymeric membrane matrix for ion-selective field-effect transistors (ISFETs) with valinomycin and BME-44 as K^+ ionophores, ETH 157 (Sodium Ionophore II, *N,N'*-dibenzyl-*N,N'*-diphenyl-1,2-phenylenedioxydiacetamide), Sodium Ionophore IV (12-didecalino-16-crown-5), ETH 7025 [Magnesium ionophore IV, *N,N',N''*-Tris[3-(heptylmethylamino)-3-oxopropionyl]-8,8'-iminodioctylamine], ETH 4030 [Magnesium ionophore III; *N,N''*-Octamethylene-bis(*N'*-heptyl-*N'*-methylmalonamide)] as magnesium ionophores, ETH 1062 [Cadmium Ionophore I, *N,N,N',N'*-tetrabutyl-3,6-dioxaoctanedithioamide] as Cd^{2+} ionophore, and methylene bis(diisobutyldithiocarbamate) (Lead Ionophore II or Silver Ionophore III).⁹² Fillers that are components of the commercially available Dow 730 fluorosilicone were centrifuged off prior to membrane preparation for optimal response. K^+ -selective electrodes gave a performance comparable to ISEs with PVC-based membranes. Slightly higher selectivity (ca 0.3~0.4 on logarithm scale) and a closer to Nernstian slopes were obtained when KTFPB was used as ionic site instead of KTpCIPB. The same difference between these two ionic sites also existed in Na^+ -selective electrodes. While Sodium Ionophore IV-doped membranes gave comparable selectivities as PVC-based ISEs, ETH 157 (Sodium Ionophore II)-based fluorosilicone membranes were less selective to Na^+ than PVC-based ISEs. The selectivity of silicone membranes towards heavy-metal Cd^{2+} -, Pb^{2+} -, and Ag^+ -ISEs was worse than reported values of comparable PVC membranes and their lifetime was shorter (two weeks), possibly due to instability of the ionophores in the Dow 730 fluorosilicone matrix. Ion-exchanger membranes with 50 mol% anionic site to cationic

site provided a better selectivity towards NO_3^- than comparable ISEs with PVC-based membranes.

ISEs prepared with Dow 3140 silicone membranes with polyaniline nanoparticle-based solid-contacts achieved nanomolar detection limits towards Ca^{2+} and Ag^+ and a two orders of magnitude reduction in membrane resistance.⁹³ Tridodecylamine-doped Dow 3140 membranes with a small 10 wt% content of the plasticizer bis(2-ethylhexyl) sebacate (DOS) provided Nernstian responses to pH and a comparable selectivity as ISEs with PVC-based membranes. After exposure to cheese samples, the silicone membrane were slightly less selective to pH (with respect to potassium) than ISEs with PVC-based membranes.⁹⁴

1.4.2.1.2 ISEs with Silopren Polysiloxane as Polymer Matrix

Silopren from Bayer is a two-component RTV silicone. The polymeric backbone hydroxy-terminated polysiloxane is used together with a second component that contains both crosslinkers such as tetraethoxysilane and hexamethoxydisiloxane and a catalyst (typically a tin catalyst such as dibutyltindilaurate).

A valinomycin-doped silicone membrane prepared from Silopren with 2.9 wt% crosslinking agent dibutyltindilaurate/hexamethoxydisiloxane (1:2 wt/wt) exhibited a Nernstian response towards K^+ and a very low drift of $<0.1 \text{ mV}/120 \text{ h}$ ($0.833 \text{ } \mu\text{V}/\text{h}$).⁹⁵

A catheter-based pH probe based on Silopren was used with ETH 2418 [octadecyl 2-(4-dipropylaminophenylazo)benzoate] as pH ionophore and tested in gastric juice.⁹⁶ The dynamic pH response range was from pH <1 to 9.2, which was 0.5 pH unit wider than for ISEs with plasticized-PVC membranes tested at the same time. The polysiloxane

membranes also showed no interference from Dormicum, a sedative typically given to patients when they were treated with a catheter.

Another study reported Silopren-based silicone membranes doped with valinomycin as K^+ ionophore, tridodecylamine as H^+ ionophore, nonactine as NH_4^+ ionophores, and ETH 1001 as Ca^{2+} ionophores.⁹⁷ All provided Nernstian responses and selectivities comparable to PVC-based ISEs. The silicone membranes also were found to have higher CO_2 permeabilities than plasticized PVC membranes, indicating good mobility for small molecules.

Silopren membrane with three types of hemispherand-21-based K^+ ionophores also showed Nernstian responses and excellent selectivities with respect to Na^+ .⁹⁰

1.4.2.1.3 ISEs with Shin-Etsu Polysiloxane as Polymer Matrix

KE44T, KE47T, and KE3479T are one-component RTV polysiloxanes from Shin-Etsu that are oxime-, alcohol-, and acetone-evolving, respectively.⁹⁸ In one report, one symmetrical calix[4]arene [Sodium Ionophore X, (4-tert-Butylcalix[4]arene-tetraacetic acid tetraethyl ester)] and three synthesized unsymmetrical calix[4]arene were tested as Na^+ ionophores. Two of the unsymmetrical ionophores provided excellent Nernstian responses and selectivities for all three types of Shin-Etsu silicones, whereas use of the other two ionophores resulted in poor sodium responses and could be explained by poor solubilities of the ionophores in the silicone matrix and phase separation in the silicone membranes.⁹⁸ A Na^+ -selective field effect transistor device based on a successful combination of an unsymmetrical calix[4]arene and silicone membranes maintained its

sensitivity to Na^+ for 120 days as compared to 30 – 60 days for ISEs with PVC-based membranes.

In a follow-up effort, by adding an oligosiloxane moiety to the unsymmetrical and symmetrical calix[4]arene esters to promote solubility in KE47T silicone membranes, higher stability, lower resistance, and Nernstian response to Na^+ were achieved.⁹⁹ With the highly dispersible calix[4]arene ionophore, KE47T silicone-based ion-selective field-effect transistors showed significant advantages over PVC-based ISEs. When used for sodium assays in blood serum and urine, no drifts were found for silicone membranes, whereas PVC membranes exhibited serious deviations.¹⁰⁰ Another report compared the popular Sodium Ionophore VIII (bis[(12-crown-4)methyl]didodecylmalonate) which had been previously used in PVC membranes and the oligosiloxane-modified unsymmetrical calix[4]arene, both in silicone membrane. The former did not provide sufficient responses due to the low solubility in KE47T silicone membranes, whereas the latter provided lower resistance and fast response.¹⁰¹

In an attempt to covalently attach both an ionophore and ionic sites to KE47T silicone membrane, a mono crown ether 15-crown-5 and an unsymmetrical calix[4]arene as Na^+ ionophores and a tetraphenylborate derivative as ionic site were synthesized with triethoxysilyl units. When these ionophores and ionic sites were covalently attached to silicone membranes, the resulting sensors showed Nernstian slopes, fast responses and good selectivities.¹⁰²

1.4.2.1.4 ISEs with Miscellaneous Membranes Prepared with Commercial Polysiloxane

ME-625 from Wacker is a two-component, room-temperature Pt cure (Si-H bond addition to vinyl groups) polydimethylsiloxane. However, higher temperatures considerably accelerate curing. The presence of 4 wt% valinomycin inhibited the curing, whereas at <1 wt% this ionophore did not inhibit the curing, suggesting some interaction existed between valinomycin and the Pt catalyst.⁹⁰

1.4.2.1.5 ISEs based on In-House Synthesized Polysiloxanes

ISE membranes doped with a valinomycin-doped poly(dimethylsiloxane-*co*-cyanopropylmethylsiloxane) (**Figure 1.7**, right) provided Nernstian responses. The linear backbone was synthesized from octamethylcyclotetrasiloxane and a mixture of trimer and tetramer of cyanopropyl(methyl)cyclosiloxane and was then crosslinked with a crosslinking agent similar to the one used in Silopren.⁸⁵

Another copolymer comprising dimethylsiloxane units, 2.8 or 10 wt% (cyanopropyl)methyl units, and 1.3 or 2.0 wt% (methacryloxypropyl)methylsiloxane was synthesized for the preparation of ISEs membranes.^{83, 84, 86} In this formula, the cyanopropyl group was introduced to alter the membrane polarity, and the methacryloxypropyl unit was used for crosslinking in the course of the UV polymerization and for the attachment of ionophore or ionic site. In some cases, the copolymer was crosslinked with a traditional siloxane crosslinker, and methacryloxypropyl unit was only for covalent attachment of ionophore or ionic site. Sodium Ionophore X, both in its mobile form and in its covalently

attachable form (with one of the ethyl esters converted to a methacrylate group), were tested for Na^+ sensing. Either a mobile or a covalently attachable (methacryloxyethyl-modified) tetraphenylborate was used as ionic site. All four possible combinations of mobile or attached ionophore and ionic sites provided Nernstian responses and selectivity comparable to those of ISEs with PVC-based membranes.⁷⁵ However, for the membranes with the 2.8 wt% (cyanopropyl)methyl unit, when both the ionophore and ionic site were attached, severe emf drifts were observed. For concentration of 10 wt% (cyanopropyl)methyl units, this problem was eliminated. In a parallel study with hemispherand-21 in either its mobile or covalently attached form as K^+ ionophore and with either mobile or covalently attached ionic sites, similar good characteristics were obtained as well.⁸⁶ Cyanopropyl containing silicone were also available from Petrarch Systems (Bristol, PA) and have been reported to have good potentiometric performance with valinomycin as ionophore.⁸⁷

The sol-gel process has also been used to synthesize glass membranes for ion-selective field-effect transistors with covalently attached sensing components and a selectivity comparable to that of ISEs with PVC-based membranes.^{103, 104}

1.4.2.2 Polyacrylate and Polymethacrylate-Based ISEs

Polymeric membranes prepared from methacrylate and acrylate monomers have been used for ISEs. Although no commercial sources are available, the synthesis of such membranes can be advantageous as it allows to fine-tune membrane properties such as glass transition temperature and optimal mechanical properties. Covalent attachment of

sensor components such as ionophore and ionic site also benefit from using polyacrylate- or polymethacrylate-based membranes. Copolymers with methacrylate or acrylate units are in general solvent processible, i.e., they can be purified more readily than other polymers, and they can be solvent-cast the same way as plasticized PVC membranes. Crosslinked homopolymers and copolymers of methacrylate and acrylate esters are not solvent processible but offer improved mechanical properties due to crosslinking, enabling the use of monomers that otherwise do not permit preparation of membranes that are strong enough to serve as ISE membranes. Some example structures of polyacrylate- and polymethacrylate-based membranes are shown in **Figure 1.8**.

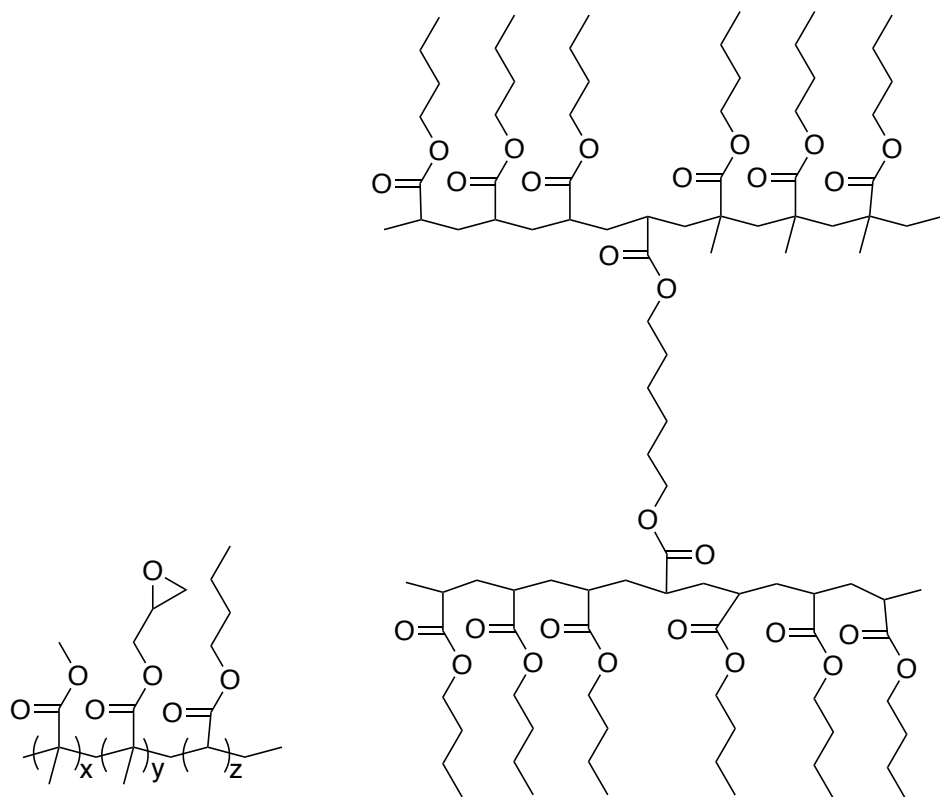


Figure 1.8. Examples of polyacrylate- and polymethacrylate-based membranes reported for use in ISEs. Left: poly(methyl methacrylate-*co*-glycidyl methacrylate-*co*-*n*-butyl acrylate); right: hexanediol-diacrylate-crosslinked poly(*n*-butyl acrylate).

A copolymer of methyl methacrylate (MMA), glycidyl methacrylate (GMA), and *n*-butyl acrylate (nBA) (**Figure 1.8** left) was synthesized via thermally initiated free radical solution polymerization.¹⁰⁵ Higher nBA contents led to lower T_g and nBA above 80 wt% did not require additional external plasticizers. In addition, a high concentration of monomer in solution during the polymerization reaction led to polymers with higher molecular weight and, therefore, mechanically more robust membranes. A weight average molecular weight (M_w) above 80,000 was observed in this study as being required for ISE

membranes. Valinomycin-doped copolymer membranes provided Nernstian responses and selectivities comparable to or better than plasticizer PVC ISEs.¹⁰⁵

Crosslinked homopolymer poly(nBA) (**Figure 1.8** right) and crosslinked copolymer poly(*n*-butyl acrylate-*co*-*n*-hexyl acrylate) via photopolymerization were also developed and shown to be compatible as ISE membranes with valinomycin (as K⁺ ionophore), Sodium Ionophore VI (bis[(12-crown-4)methyl] dodecylmethylmalonate), and TDDA (as pH ionophore).¹⁰⁶ All provided comparable results to ISEs with PVC-based membranes. A mono crown ether was also tested as mobile and covalently attached K⁺ ionophore, the latter of which showed improved response characteristic than the former. The ISE membranes doped with the mono crown ether were less selective than bis(crown ether)-based ionophore BME-44. In a similar study,¹⁰⁷ one-step thermal copolymerization with covalently attachable mono 16-crown-5 ether was performed and similar results were obtained.

Another report found poly(methyl methacrylate-*co*-isodecyl acrylate) membranes to provide the best mechanical properties with a 3:7 weight ratio of acrylate and methacrylate. ISE membranes doped with either a mobile calix[4]arene or a covalently attached calix[4]arene (modified with methacrylamide unit) exhibited similar responses to Na⁺ as PVC-based ISEs.¹⁰⁸ Another study compared the two initiators 2,2-azoisobutyronitrile (AIBN) and 2,2-dimethoxy-2-phenylacetophenone (DMPP) in polymerizing crosslinked poly(nBA). DMPP achieved full polymerization in 10 min with little ionic impurities, whereas AIBN needed 1–2 h to photopolymerize and produced much

higher concentrations of ionic impurities.¹⁰⁹ The latter probably polymerized as the result of the heat generated in the 1–2 h UV radiation since AIBN is a thermal initiator.

Copolymers of methacrylate with different alkyl substitutes have also been reported. Poly(methyl methacrylate-*co*-decyl methacrylate) doped with BME-44 as K⁺ ionophore, 6,6-dibenzyl-14-crown-4 as Li⁺ ionophore, and ETH 129 as Ca⁺²⁺ ionophore showed comparable potentiometric results to conventional PVC-phase ISEs.¹¹⁰ The same copolymer membrane with Sodium Ionophore X was superior to its PVC counterpart, whereas copolymer doped with Mg²⁺-selective ETH 1117 (*N,N'*-diheptyl-*N,N'*-dimethyl-1,4-butanediamide) showed significantly worse selectivity, likely due to the ester groups on the copolymer interfering with the ionophore.

Poly(methyl methacrylate-*co*-decyl methacrylate) doped with a covalently attachable Ca²⁺ ionophore similar to ETH 129 provided comparable selectivity to ISE with PVC membranes doped with free ETH 129. The segmented sandwich membrane technique¹¹¹⁻¹¹³ was used to evaluate the difference in Ca²⁺ binding constants of the mobile and attached ionophores and to assess diffusion coefficients. Results showed a significantly reduced mobility of the covalently attached ionophore. Ca²⁺- and Pb²⁺-selective poly(methyl methacrylate-*co*-decyl methacrylate) membrane ISEs with poly(*n*-octyl)thiophene as solid contact were reported to exhibit better (subnanomolar) detection limit.¹¹⁴ Similar low detection limits for Ag⁺, K⁺, and I⁻ were reported using the same type of membrane and setup but with different ionophores.¹¹⁵

1.4.2.3 Polyurethane (PU)-Based ISEs

Polyurethanes have been used in many biomedical applications due to their biocompatibility, which has been a focus of many studies.^{77, 116-120} Several types of polyurethanes with a T_g lower than room temperature have also been studied as ISE membranes. One study reported using a commercially available aliphatic polyurethane Tecoflex (**Figure 1.9** top) as ISE membrane matrix both with and without added plasticizers.⁸⁷ Without plasticizer, Tecoflex is soluble in solvents such as THF. Valinomycin-doped plasticizer-free Tecoflex membranes provided slightly less Nernstian response slopes of 53.6 mV/decade, and the potentiometric selectivity with respect to Na^+ ($\log K_{\text{K,Na}}^{\text{pot}}$) was -3.4. When 6.6 wt% PVC and 66 wt% plasticizer were added to the PU membrane, the slope and selectivity improved to 57.1 mV/decade and -4.3, respectively.⁸⁷ Another studied used plasticized and plasticizer-free Tecoflex membranes doped with a Ca^{2+} ionophore. Nernstian responses were obtained in both cases. Compared to plasticized Tecoflex membranes, plasticizer-free Tecoflex membranes were less selective with respect to Li^+ and NH_4^+ , and slightly less selective with respect to Na^+ and K^+ .⁶⁵

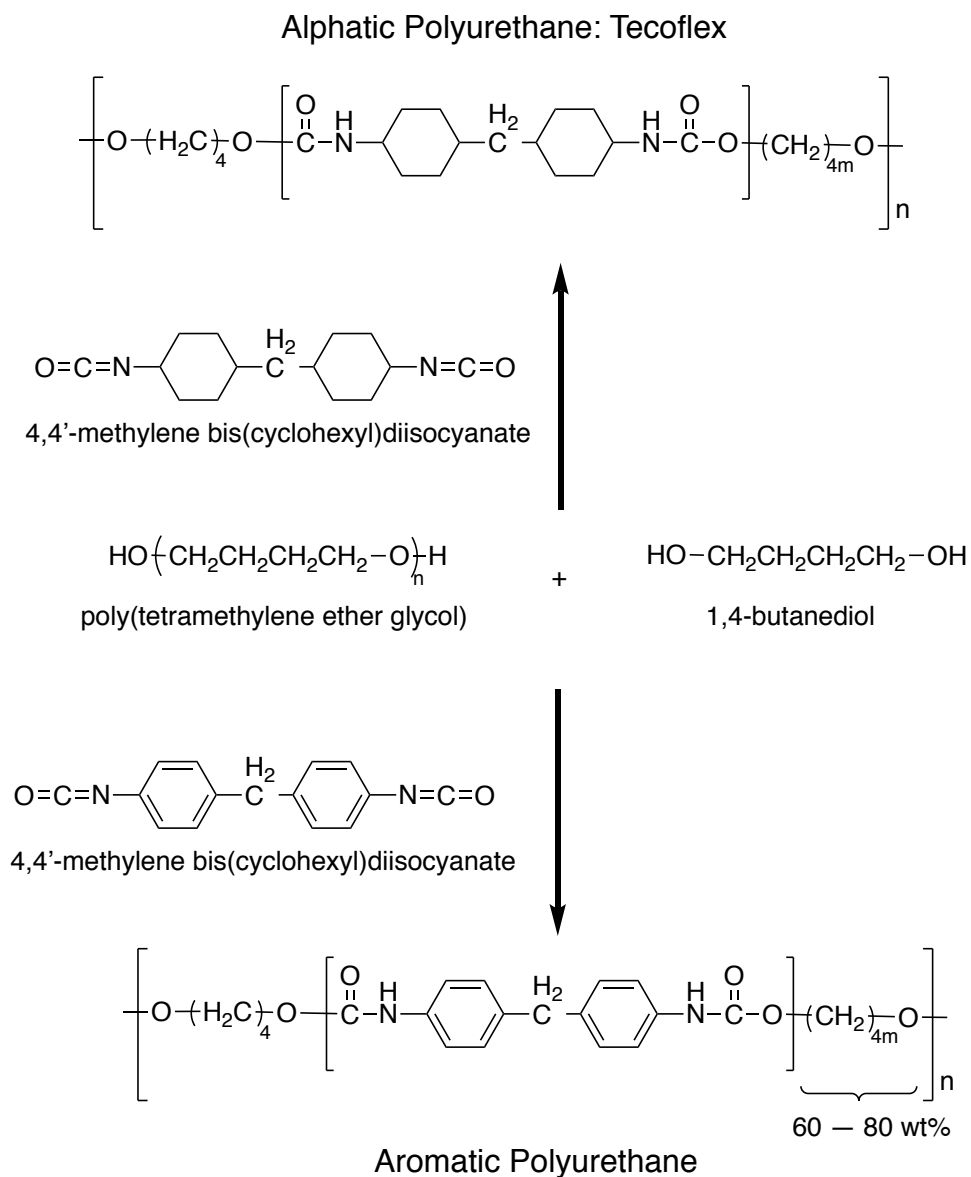


Figure 1.9. Polyurethanes used as ISE membranes. Top: commercially available aliphatic polyurethane Tecoflex; right: non-commercially available aromatic polyurethane with varying (60 – 80 wt%) “soft segment”.

Another report described the synthesis of an aromatic polyurethane with varying contents of “soft segments”, i.e., poly(tetramethylene ether glycol), as “built-in plasticizing”

units along with the stiff urethane “hard segments” (**Figure 1.9** bottom).¹²¹ Polyurethanes with 60 to 80 wt % soft segments were appropriate for ISEs membranes and were also soluble in THF. Membranes doped with the K⁺ ionophore valinomycin but without ionic sites gave negligible responses with the 60 wt% soft segment membranes and a strongly sub-Nernstian response to K⁺ with the 80 wt% soft segment membranes. This suggests a relatively “clean polymer” with little to no ionic impurities after polymerization. When ionic site was added, the electrodes showed Nernstian responses and a selectivity with respect to Na⁺ close to those for comparable ISEs with PVC membranes.

1.4.3 Leaching of Ionophores and Ionic Site and Covalent Attachment

1.4.3.1 Model of Leaching

Based on a simple and well-developed model^{12, 122, 123} (for a schematic of this model see **Figure 1.10**), the leaching of electrically neutral and electrically charged compounds out of the membrane phase into the sample phase can be calculated based on their lipophilicity p_c .

$$\ln \frac{C_{tot}(org, 0)}{C_{tot}(org, t)} = \frac{D_{aq}}{p_c d \delta} t$$

where D_{aq} is the diffusion coefficient of compound C in aqueous phase, δ is the thickness of Nernstian boundary layer, d is the thickness of membrane, and t is time. For neutral compounds, lipophilicity p_c can be conveniently calculated from the 1-octanol/water partition coefficient in the following way

$$\log p_c(\text{membrane/sample}) = a + b \log P_c(\text{octanol/water})$$

where parameters a and b are set values depending on whether the ISE is used in aqueous samples or serum samples. For charged compounds such as ionic sites, their lipophilicity also depends on the lipophilicity of the counter ions. In ISEs, the counter ion is often an ionophore-primary-ion complex \mathbf{IL} :

$$p_{\mathbf{R}^-} \approx \frac{[\mathbf{R}^-]}{c_{\mathbf{R}^-}} = K_{\mathbf{IR}} \beta_{\mathbf{IL}} \frac{c_{\mathbf{I}^+} [\mathbf{L}]}{[\mathbf{IL}]}$$

where $K_{\mathbf{IR}}$ is the distribution coefficient of the primary ion and ionic site between the membrane and aqueous phase, $\beta_{\mathbf{IL}}$ is the stability constant of the complex between ionophore and primary ion, $c_{\mathbf{I}^+}$ is the concentration of the primary ion in the sample solution, and $[\mathbf{L}]$ and $[\mathbf{IL}]$ are the total ionophore and ionophore-primary-ion complex concentrations.

With all parameters set, the concentration of a compound left in a membrane at time t can be calculated. As an example, valinomycin and BME-44—two common potassium ionophores—will leach out 100% and 99.99% into serum samples in a span of 14 days.

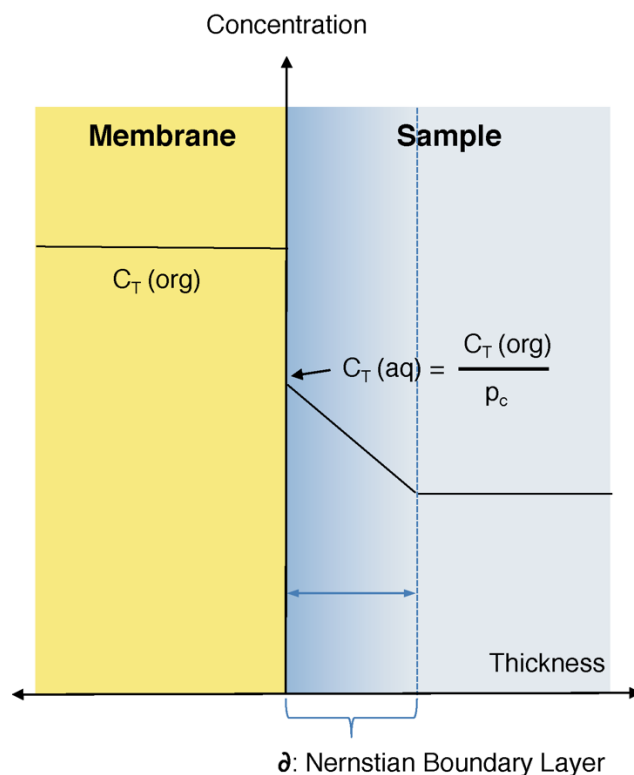
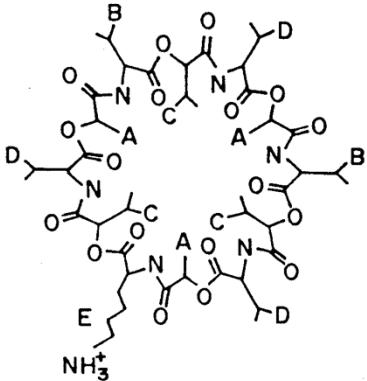
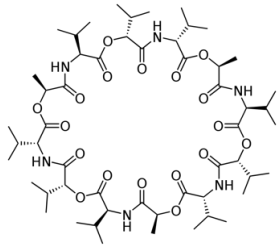
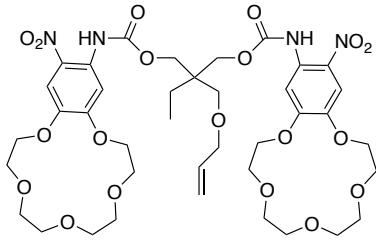
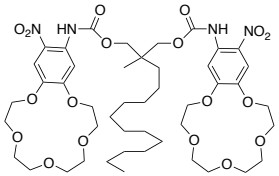


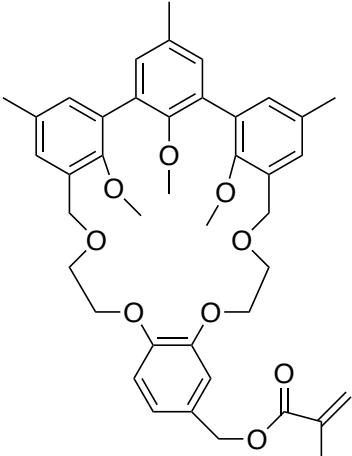
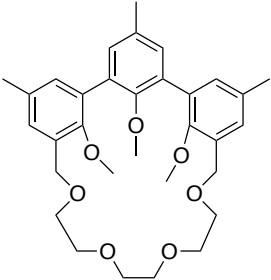
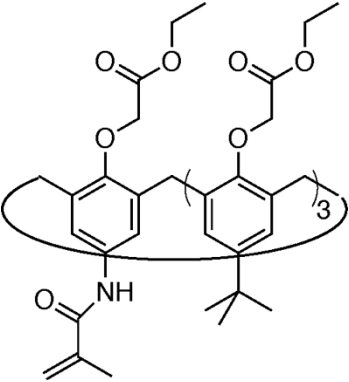
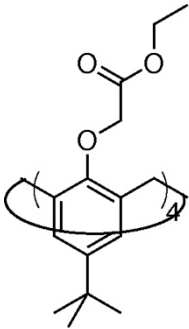
Figure 1.9. Phase boundary model developed to calculate leaching of components in ISE membranes.

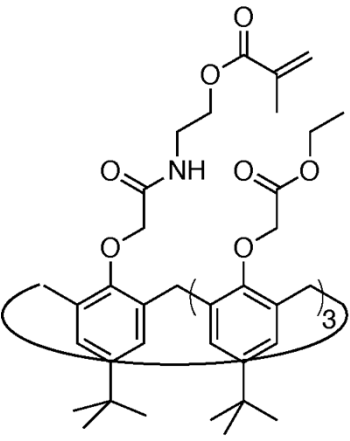
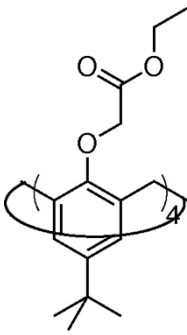
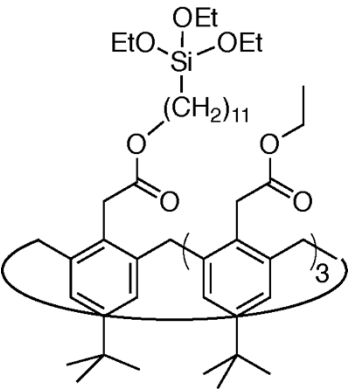
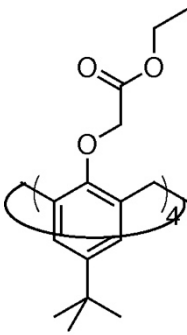
1.4.3.2 Covalent Attachment Strategy

To prevent leaching of ionophores—both in view of maintaining ISE functionality and reducing any possible toxic effect of the leached ionophores, efforts have been made to covalently attach various types of ionophores to polymeric membrane backbones. One strategy of such covalently attachment is to minimally modify existing successful mobile ionophores with a covalently attachable unit. This maintains the core structure of the ionophore and, therefore, the selectivity of the ISE. Examples of minimally modified covalently attachable ionophores are listed in **Table 1.1**.

Table 1.1. Covalently Attachable Ionophores Minimally Modified from Existing Mobile Ionophores.

Target ion	Covalently attachable ionophore	Membrane matrix	Comparable mobile ionophore
K ⁺	 <p>lysine-valinomycin, reprinted from Ref. 125,^{124, 125}</p>	carboxylic acid-, carbonyl-, and acid chloride-containing polymers ^{124, 125}	 <p>valinomycin</p>
K ⁺	 <p>vinyl-BME-44¹²⁶</p>	PVC	 <p>BME-44</p>

<p>K^+</p>	 <p>methacryloxymethyl-hemispherand-21^{84, 86}</p>	<p>poly[dimethyl-siloxane-<i>co</i>-(cyano-propyl)-methyl-siloxane-<i>co</i>-(methacryloxy-propyl)-methylsiloxane]^{84, 86}</p>	 <p>hemispherand-21</p>
<p>Na^+</p>	 <p>4'-methacrylamido-Sodium Ionophore X¹⁰⁸</p>	<p>poly(methyl methacrylate-<i>co</i>-iso-decyl acrylate)¹⁰⁸</p>	 <p>Sodium Ionophore X: 4-tert-butylcalix[4]arene tetraacetic acid tetraethyl ester</p>

<p>Na⁺</p>	 <p>methacryl-Sodium Ionophore X⁸³</p>	<p>poly[dimethylsiloxane-<i>co</i>-(cyanopropyl)-methylsiloxane-<i>co</i>-(methacryloxypropyl)-methylsiloxane]⁸³</p>	 <p>Sodium Ionophore X: 4-tert-butylcalix[4]arene tetraacetic acid tetraethyl ester</p>
<p>Na⁺</p>	 <p>triethoxysilyl-Sodium Ionophore X¹⁰²</p>	<p>polysiloxane¹⁰²</p>	 <p>Sodium Ionophore X: 4-tert-butylcalix[4]arene tetraacetic acid tetraethyl ester</p>

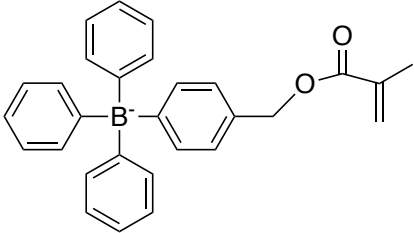
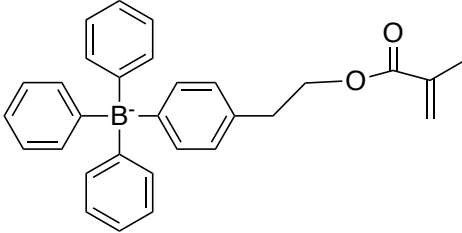
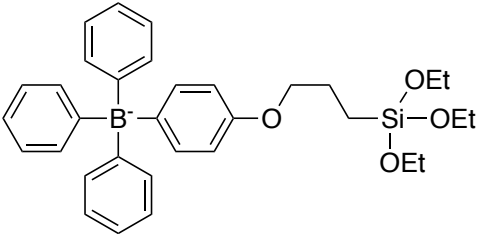
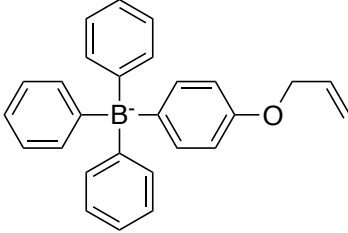
<p>Na⁺</p>	<p>triethoxysilylpropyl-Sodium Ionophore VI¹⁰⁴</p>	<p>sol-gel generated glass membrane¹⁰⁴</p>	<p>Sodium Ionophore VI: bis[(12-crown-4)methyl]didodecyl-malonate</p>
<p>Ca²⁺</p>	<p>acryloyl modified ETH 129¹²⁷</p>	<p>poly(methyl methacrylate-co-decyl methacrylate)¹²⁷</p>	<p>ETH 129</p>
<p>Pb²⁺</p>	<p>diol-Lead Ionophore IV¹²⁸</p>	<p>polyurethane¹²⁸</p>	<p>Lead Ionophore IV</p>

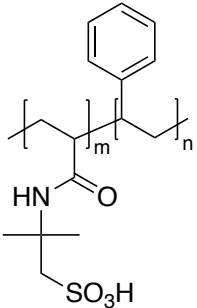
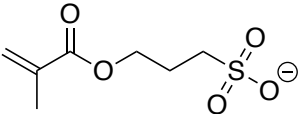
Others have developed covalently attachable ionophores that are structurally very different from previously reported mobile ionophores because of either available

commercial sources or ease of synthesis. However, due to the structural difference, these ionophores in general are less selective than those covalently attachable ionophores closely resembling existing successful mobile ionophores. In applications where high selectivity is not needed, these more readily available covalently attachable ionophores are still of value. Such examples include mono crown ethers as covalently attachable K^+ ,^{107, 109, 129, 130} Na^+ ,^{102, 104} and Pb^{2+} ionophores,¹³¹ a cyclic polyamine as covalently attachable dibasic phosphate ionophore,¹³² a derivative of Chromoionophore II as covalently attachable H^+ ionophore,¹³³ and porphyrins as In^{3+} ionophores.¹³⁴

On the other hand, ionic sites have also been covalently attached, although when used together with ionophore, ionic sites are typically very hydrophobic and do not leach out to a significant degree.^{111, 135} However covalent attachment of ionic sites is still useful for ion-exchanger electrodes and other applications such as high temperature measurements. Due to the limited options for ionic sites, only derivatives of tetraphenylborate and sulfonate have been used as covalently attached ionic sites. Reported examples are summarized in **Table 1.2**.

Table 1.2. Covalently Attachable Ionic Sites

Covalently attachable ionic site	Membrane matrix
 <p>methcryloylmethyl-tetraphenylborate⁸⁴</p>	<p>poly[dimethylsiloxane-<i>co</i>-(cyanopropyl)methylsiloxane-<i>co</i>-(methacryloxypropyl)methylsiloxane]⁸⁴</p>
 <p>methcryloylethyl-tetraphenylborate⁸³</p>	<p>poly[dimethyl-siloxane-<i>co</i>-(cyanopropyl)-methylsiloxane-<i>co</i>-(methacryloxypropyl)-methylsiloxane]⁸³</p>
 <p>triethoxysilylpropoxytetraphenylborate^{102, 104, 136}</p>	<p>polysiloxane¹⁰² sol-gel generated glass membrane¹⁰⁴</p>
 <p>allyloxytetraphenylborate^{103, 136}</p>	<p>intermediate compound not used for membranes.</p>

 <p>The structure shows a polymer chain with a backbone of carbon atoms. One carbon atom is substituted with a phenyl ring. Another carbon atom is substituted with a nitrogen atom bonded to a hydrogen atom and a carbonyl group. A third carbon atom is substituted with a tert-butyl group and a sulfonic acid group (-SO₃H).</p> <p>sulfonated-PVC¹³⁷</p>	<p>PVC-based membrane¹³⁷</p>
 <p>The structure shows a methacryloyloxy group (CH₂=C(CH₃)COO-) attached to a propyl chain, which is terminated by a sulfonate group (-SO₃⁻).</p> <p>3-(methacryloyloxy)propane-1-sulfonate (see Chapter V)</p>	<p>poly(decyl methacrylate) (see Chapter V)</p>

1.4.3.3 Verification of Covalent Attachment

A powerful test to verify covalent attachment is a Soxhlet extraction that replaces the solvent in contact with the extracted sample by a siphoning action every few minutes for an extended period of many hours or days. Mobile compounds contained in a membrane sample will be extracted out completely by an appropriate solvent in Soxhlet extraction whereas covalently attached compounds remain in the membrane phase. Notably, this test is much more stringent than any likely real-life application. Another gold standard is simply comparing the lifetime (response, selectivity, resistance, etc) of sensors with mobile and attached compounds exposed to real samples such as environmental or biological samples. Some studies have also qualitatively or quantitatively determined the concentration of a leached compound in a solution in equilibrium with a sensing membrane

to detect any leached compounds.^{107, 138} This approach can be very difficult though because the concentrations of the leached compounds in equilibrium with a membrane phase are often very low.

1.4.4 Biocompatibility Studies of ISEs

In one study, both plasticized polyurethane and plasticizer-free silicone were found to have less nonspecific (fibrinogen and albumin) protein adsorption and a favorable albumin-to-fibrinogen ratio than plasticized PVC.⁸⁷ A greater extent of fibrinogen absorption indicates a higher chance of thrombogenesis and inflammatory reactions whereas a greater amount of albumin absorption indicates the opposite.^{139, 140} PVC membranes plasticized with the less polar bis(2-ethylhexyl) adipate as plasticizer also showed better results than those plasticized with the more polar *o*-NPOE. In whole blood clotting time tests, PU-based membranes (with added PVC or with added PVC and plasticizer) performed slightly better than plasticized PVC and plasticizer-free silicone.⁸⁷ In another study using a cage implant experiment¹⁴¹ (i.e., a mesh cage enclosing the material of study and, for control, an empty mesh cage, both implanted subcutaneously in rats and left there for 14 days) revealed that an increased plasticizer content in polyurethane ISE membranes correlated with increased inflammation.⁶⁵

II. Fluorous-Phase Ion-Selective pH Electrodes for Measurements in Biological Samples

This chapter was reproduced from “Fluorous-Phase Ion-Selective Ph Electrodes for Measurements in Biological Samples. *submitted for publication.*”

Mousavi, M. P. S. contributed to this work by optimizing the synthesis of fluorophilic ionophore.

2.1 Introduction

Ionophore-based ion-selective electrodes (ISEs) have been well-established analytical tools for more than four decades and have applications in many fields, including clinical diagnostics, environmental analysis, and industry process control.^{1-3, 6, 142-146} Recent advancements have focused on improving their detection limits,^{48, 147-149} developing calibration-free ISEs,¹⁵⁰ making them suitable for new applications,¹⁵¹ and expanding sensing ranges.⁴⁶ The latter are defined by the difference between their upper and lower detection limits, which are determined by the co-extraction of counter ions (also known as Donnan failure)^{19, 20} and the interference from ions other than the target ion,³⁹ respectively. Our group previously reported the development of fluoruous-phase ISEs, i.e., ISEs with highly fluorinated sensing membrane matrixes that are both highly hydrophobic and highly lipophobic. The extremely low polarity and polarizability of fluoruous phases^{40, 41} significantly suppress the non-specific phase transfer of both counter-ions and interfering ions into such sensing membranes, thereby expanding the upper and lower detect limits. The introduction of a fluorophilic tetraphenylborate derivative enabled the very first fluoruous-phase ion exchanger electrodes.⁴⁶ The use of fluorophilic ionophores subsequently permitted the development of fluoruous-phase ISEs for Ag^+ , H^+ , and CO_3^{2-} .^{44, 48, 49} Self-supporting fluoruous membranes for ISEs were demonstrated using the amorphous perfluoropolymer Teflon AF and semifluorinated polymers,^{152, 153} and the use of fluoruous-phase ISEs was shown for biological and environmental samples¹⁵⁴⁻¹⁵⁷ and at high temperatures in highly corrosive solutions.¹⁵¹ With a view to the important role of pH in

many physiological processes, we report here on a much improved fluorous-membrane ISE for measurements of pH.

Because pH is defined as the negative logarithm of the activity of H^+ and not as the logarithm of the H^+ concentration, ISEs have the intrinsic advantage that they measure the activity of H^+ directly, which is difficult to do with other analytical techniques. However, the conventional glass electrodes have some disadvantages. Glass is a fragile material with high resistivity, which requires extra care when using glass electrodes and also limits uses of pH glass electrodes as part of miniaturized and implantable devices.¹⁵⁸ The use of pH glass electrodes in biological samples is hindered by protein adsorption onto the pH sensitive glass bulb, requiring frequent cleaning and maintenance,¹⁵⁹ and glass electrodes are not compatible with acidic samples that contain fluoride. To this end, H^+ -selective ISEs with polymeric sensing membranes have been developed. A wide range of electrically neutral ionophores with functional groups that can be protonated were successfully tested as H^+ -selective ionophores. Among them, the most successful ones are amine^{160, 161} and pyridine^{122, 162} derivatives.

Assuming the formation of 1:1 complexes between the ionophore and H^+ , the incorporation of ionophores and ionic sites at a 2:1 ratio and the use of hydrophobic matrixes with negligible cation binding properties were predicted to maximize the measuring range of such H^+ -selective ISEs.⁵⁹ The later criterion is met in an ideal manner by the fluorous matrixes of two fluorous-phase pH ISEs with the fluorophilic pH ionophores **1** and **3** (see **Figure 2.1**), as reported previously.⁴⁴ While these two ISEs covered together a wide pH range, the one based on the more weakly binding H^+ ionophore

(1) was limited to the acidic pH range, and the one based on the more strongly binding H^+ ionophore (3) was prone to Donnan failure. Herein, we report on an improved fluorous-phase pH ISE that offers a wide working range centered around pH 7. It is based on the new fluorophilic ionophore 2, which has $-(CH_2)_4-$ spacers of optimized length between the proton-binding amino center of the ionophore and the perfluorooctyl groups that make this compound fluorophilic. We also describe in detail the redesign of an electrode body that provides significant improvements in reliability and is suitable not only for fluorous membranes but also any other stiff or fragile membrane material.

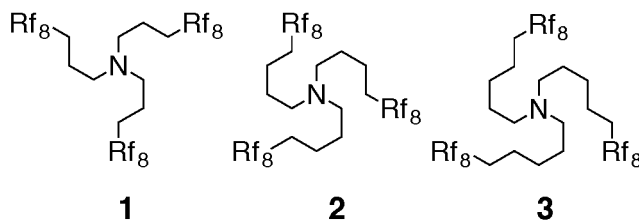


Figure 2.1. Structure formulas of the fluorophilic H^+ ionophores 1 to 3. $Rf_8 = -(CF_2)_7CF_3$.

2.2 Experimental Section

Materials. All commercial reagents were of the highest purity available and used without purification. Perfluoroperhydrophenanthrene (**5**) and 1-iodo-4-(perfluorooctyl)butane ($\text{CF}_3(\text{CF}_2)_7(\text{CH}_2)_4\text{I}$) were purchased from SynQuest Lab (Alachua, FL) and Sigma Aldrich (St. Louis, MO), respectively. Sodium tetrakis[3,5-bis(perfluorohexyl)phenyl]borate (**4**) was synthesized according to a previously published procedure.⁴⁶ EMD Millipore Fluoropore Polytetrafluoroethylene (PTFE) membrane filters (pore size $0.45\ \mu\text{m}$, filter diameter 47 mm, thickness $50\ \mu\text{m}$, 85% porosity) were purchased from Fisher Scientific (Hanover Park, IL). Viton fluoroelastomer O-rings were obtained from McMaster-Carr (Chicago, IL). Autonom freeze-dried animal serum was purchased in powder form from Sero (Billingstad, Norway). High molecular weight poly(vinyl chloride), 2-nitrophenyl octyl ether (*o*-NPOE), tridodecylamine, and potassium tetrakis(4-chlorophenyl)borate were purchased from Sigma Aldrich (St. Louis, MO). All aqueous solutions were prepared with deionized and charcoal-treated water ($0.182\ \text{M}\Omega\ \text{cm}$ specific resistance) from a Milli-Q Plus reagent-grade water system (Millipore, Bedford, MA).

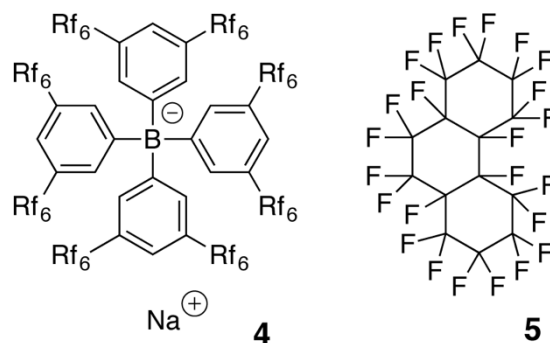


Figure 2.2. Structure formulas of the fluorophilic ionic site (**4**) and the fluorous matrix (**5**) of the fluorous-phase sensing membranes.

Synthesis of Ionophore N[(CH₂)₄R_f]₃ (2**).** The synthesis of ionophore **2** was performed using a modified literature procedure by stepwise alkylation of ammonia to a primary, secondary, and finally tertiary amine. This synthesis method was reported previously¹⁶³ for the preparation of other N[(CH₂)_nR_f]₃ compounds but has been used here for the first time for the synthesis of **2**. In view of applications in catalysis, **2** was prepared previously by oxidation of R_f(CH₂)₄OH to the aldehyde, reductive amination with benzylamine, and deprotection to give a secondary amine, and finally a second reductive amination step to yield **2**.¹⁶⁴ Based on our own experience with both synthesis methods, the stepwise alkylation of ammonia with CF₃(CF₂)₇(CH₂)₄I appears preferable for the preparation of **2** because it poses fewer challenges with the purification of intermediates.

CF₃(CF₂)₇(CH₂)₄I (2.5 g) was dissolved in 3 ml tetrahydrofuran (THF) in a thick-walled test tube, which was then sealed with a rubber septum and cooled to -78 °C in an isopropanol/dry ice bath. Another thick-walled test tube was loaded with 3 mL THF, sealed with a rubber septum, and cooled to -78 °C with an isopropanol/dry ice bath, followed by condensation of approximately 2 mL liquid ammonia from an ammonia tank into the THF. Then, the cooled liquid ammonia/THF solution was added into the cooled CF₃(CF₂)₇(CH₂)₄I/THF solution through a cannula. For safety, this tube was placed into a closed plastic bottle as a secondary container. The reaction was stirred with a magnetic stir bar and allowed to warm gradually to room temperature, where it was stirred for another 48 h. In the post-reaction work-up, the solvent was removed, and the crude reaction mixture was re-dissolved in diethyl ether and washed with 1 M Na₂CO₃ solution. After washing of the aqueous phase three times with diethyl ether, the combined organic phases were dried

over MgSO₄, and the solvent was removed. The solid obtained thereby (1.4 g) was dissolved together with 2.0 g of CF₃(CF₂)₇(CH₂)₄I and 0.2 g of Na₂CO₃ in 3 mL THF and heated under reflux for 3 days. After cooling to room temperature, the same post-reaction workup was repeated, giving 2.7 g of a solid. From this, 2.0 g were taken and dissolved together with 0.41 g of CF₃(CF₂)₇(CH₂)₄I in THF and heated under reflux for 3 days. After cooling and evaporation of the THF, diethyl ether was added to give a suspension, which was filtered. The insoluble filtrate was washed three times with diethyl ether, and the four organic phases were combined and washed with 1 M Na₂CO₃ solution. The resulting aqueous phase was washed three times with diethyl ether, followed by combining of all organic phases and washing with brine and drying over MgSO₄. After removal of the drying agent by filtration, the solvent was evaporated, and the product thus obtained was purified by column chromatography on silica gel with dichloromethane as eluent. This yielded N[CH₂CH₂CH₂CH₂R_{f8}]₃ (**2**) as a slightly yellow solid (460 mg, 23%). ¹H NMR (CDCl₃, δ): 2.39 (t, 6H, N-CH₂, ³J_{HH} = 5 Hz), 2.04–2.12 (m, 6H, CH₂R_{f8}), 1.48–1.63 (m, 12H, CH₂CH₂CH₂R_{f8}). MS: [M-H]⁺ = 1440.1. For ¹H NMR and MS spectra, see **Figures S2.1** and **S2.2** of the Supporting Information.

Fluorous-Phase Electrode Preparation. Solutions containing **2** (2 mM) and **4** (0.5 mM) in the fluorous matrix **5** were used for the fabrication of membranes for ionophore-based electrodes. Solutions of **4** (0.35 mM) in **5** were used for ionophore-free ion exchanger electrodes. In both cases, the solutions were stirred overnight with a magnetic stir bar at room temperature to ensure complete dissolution. To prepare sensing membranes, circular inert porous supports with a 19.1 mm diameter were cut from Fluoropore filters using a

hole punch. Aliquots of 35 μL of the fluoruous solutions with **4** (and optionally **2**) were added onto the inert porous circular supports. This turned the initially solid white Teflon filter pieces transparent, showing that the fluoruous solution had diffused into the pores of the support. In typical measurements, one layer of the Fluoropore support was used for each electrode. For measurements of tetraphenylphosphonium ion (PPh_4^+), tetrabutylammonium ion (NBu_4^+), and tetrapropylammonium ion (NPr_4^+) selectivities, 3 or 4 layers were used instead. This prevents these cations from diffusing through the fluoruous sensing phase to the interface of the sensing membrane and inner filling solution and affecting the phase boundary potential at that interface within the time of the selectivity measurements. Filter disks impregnated with fluoruous solution were mounted between the inner tube and the outer tube of the electrode body. An aqueous solution containing 10 mM K_2HPO_4 , 10 mM KH_2PO_4 , and 10 mM KCl ($\text{pH} = 7.4$) was used as inner filling solution. Note that in typical real-life applications, the sensing membrane is rarely challenged with solutions that result in a potentiometric response dominated by ions other than H^+ . For such applications, one layer of Teflon filter is sufficient. However, membranes with 3 or 4 layers of Teflon filters could be used routinely without any problems.

Electrode Bodies. In conventional ISEs with an inner filling solution, the sensing membrane separates the inner filling solution from the sample. Unlike in the case of plasticized PVC membranes mounted into the well-known Philips-type electrode bodies,¹⁶⁵ sensing membranes supported by a Fluoropore filter cannot be bent into a cone shape by the electrode body, but instead the membrane must remain flat. In our previous design of electrode bodies for fluoruous membranes,⁴⁷ the Fluoropore filter was sandwiched in

between a screw cap and the electrode body. Every so often, the rotating motion in the assembly of the electrode caused an uneven seating of the sensing membrane and, consequently, leaking of the inner filling solutions and sub-Nernstian EMF responses. To eliminate this problem, a new electrode body was designed with an inner and an outer tube as well as a separate screw cap (**Figure 2.3**; see **Figures S2.3–S2.8** of the Supporting Information for further details).

With this new design, the sensing membrane is mounted in between the inner and outer tubes of the electrode body. The inner tube has two lugs that fit into the locking slots of the outer tube, preventing the inner tube from rotating with respect to the outer tube. Therefore, when the cap is screwed onto the outer tube, it exerts pressure onto the inner tube and presses it tightly against the membrane without exertion of rotating forces on the two flat O-rings and the membrane, thus providing a smooth and even seal. Measurements with the new electrode bodies showed much improved reliability. While specifically developed by us for use with fluorinated membranes, we recently also used electrode bodies of this new design to hold rigid nanoporous glass frits, which would have never been possible with Philips-type electrode bodies. This demonstrates the applicability of this new type of electrode body for a wider range of stiff or fragile membrane materials.

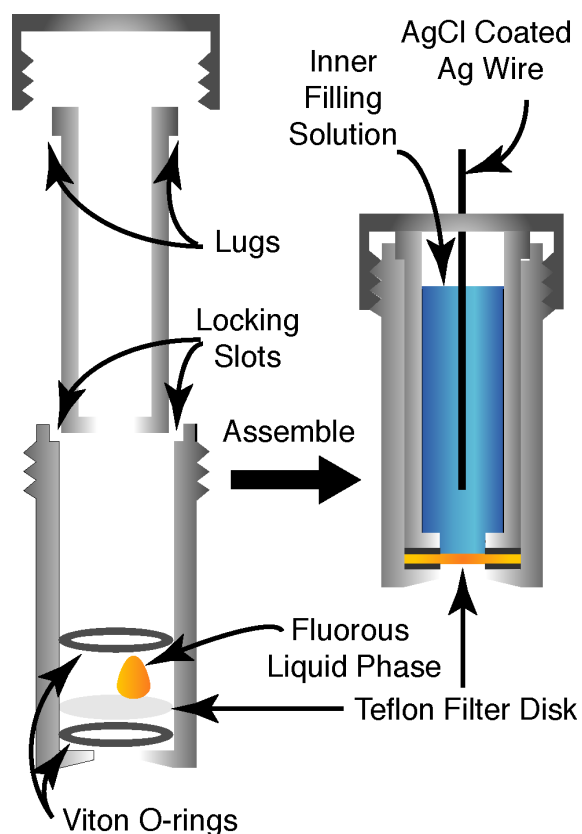


Figure 2.3. Design of an electrode body that avoids exertion of twisting forces on the sensing membrane during electrode assembly.

Preparation of ISEs with plasticized PVC membranes. Solutions to prepare PVC-phase pH membranes were prepared by slowly adding 66 mg PVC into a stirred solution of 132 mg *o*-NPOE in 1.0 mL THF, followed by addition of 13 mmol/kg potassium tetrakis(4-chlorophenyl)borate, and either 52 or 26 mmol/kg tridodecylamine to give an ionophore-to-ionic site ratio of 4:1 or 2:1, respectively (mmol/kg values refer to final concentration in the ISE membrane). Aliquots of these solutions were cast into a glass petri dish of 25 mm diameter, and the solvent was allowed to evaporate over 24 h, giving master

membranes of 200 μm thickness. Smaller circular disks of 7 mm were cut from master membranes and glued onto a Tygon tube using THF.

Potentiometric Measurements. Measurements were performed in stirred solutions with a 16-channel potentiometer (Lawson Labs, Malvern, PA) and a double junction free-flowing free-diffusion reference electrode (DX200, Mettler Toledo, Switzerland; Ag/AgCl as internal reference, AgCl-saturated 3 M KCl as inner solution, and 1M LiOAc as bridge electrolyte). The pH of sample solutions was changed stepwise by adding small aliquots of concentrated KOH or HCl solutions. A half-cell pH glass electrode (InLab 201, Mettler Toledo, Columbus, OH; calibrated with standard NIST pH buffers of pH 4.0, 7.0, 10.0, and 12.0) was used to monitor separately the pH. Selectivity coefficients were determined for K^+ , Na^+ , and Ca^{2+} with the fixed interference method (FIM) and for NPr_4^+ with respect to NBu_4^+ and for NBu_4^+ with respect to PPh_4^+ with the separate solution method (SSM; see the Supporting Information for further details).^{21, 39} Nernstian slopes were confirmed in all cases. All response times in the Nernstian response region were fast (< 5 s). Activities were calculated with a two-parameter Debye–Hückel approximation.¹⁶⁶

Conductivity Measurements. The conductivities of membranes at five different concentrations of ionophore and ionic site were measured using the known shunt method.^{46, 47} An ionophore to ionic site ratio of 4:1 was used for all five concentration levels. The inner filling and measuring solutions contained 10 mM K_2HPO_4 , 10 mM KH_2PO_4 , and 10 mM KCl (pH = 7.4). Conductivity values were calculated based on an estimated cell constant of 0.00924 cm^{-1} .

2.3 Results and Discussion

2.3.1 Response Range of ISEs with the New Ionophore

Calibration curves of fluorous-phase ISEs with the new ionophore were obtained with a constant background consisting of 970 mM KCl and 20 mM phosphate buffer (initially at pH 7.4) by addition of KOH or HCl aliquots. A typical calibration curve in the range between pH 0 and 14 is shown in **Figure 2.4**. As can be seen, even in an electrolyte solution with such a high concentration of a cation with a relatively low hydration energy as K^+ , the new ionophore **2** has a wide working range from pH = 2.2 to pH = 11.2, centered near pH 7 and with a slope of 54.7 ± 0.7 mV/decade ($n = 3$). This fits the need for a single sensor that is capable of measuring a range of biological samples.

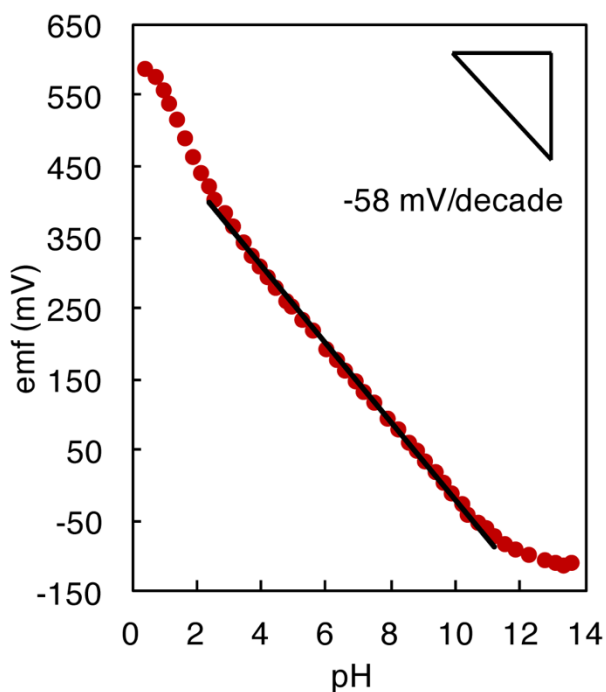


Figure 2.4. Working range of pH ISEs based on ionophore **2**: EMF measurements were started at pH 7.4 (970 mM KCl, 10 mM K₂HPO₄ and 10 mM KH₂PO₄ solution). The pH was increased by adding small aliquots of 10 M KOH solution. Subsequently, starting again at pH 7.4, the pH was decreased by adding aliquots of 1 M HCl solution. See **Figure S2.9** of the Supporting Information for a graph with data for three individual electrodes.

Fluorous-phase ISEs with either one of the structurally close-related fluorophilic trialkylamines **1** or **3** as ionophore were reported previously.⁴⁴ The three C₈F₁₇ chains that all these ionophores share, also referred to as “fluorophilic ponytails,” are necessary to make these ionophores sufficiently soluble in fluorous phases. However, ionophores **1** and **3** differ in the number of -CH₂- groups that separate the nitrogen center from the highly electron withdrawing fluorophilic ponytails. As shown previously in a potentiometric study

that included among other compounds **1** and **3** but not **2**,⁴⁴ the longer the $-(\text{CH}_2)_n-$ spacers are, the better they shield the nitrogen atom from the electron withdrawing effect of the perfluoroalkyl groups, and the more basic the ionophores are. Therefore, variation of the $-(\text{CH}_2)_n-$ spacer is an efficient way to adjust the $\text{p}K_a$ value and, thereby, the selectivity of the ionophore. Gas phase ionization data illustrate this effect. While corresponding data for $\text{N}[(\text{CH}_2)_n\text{R}_{18}]_3$ compounds are not available, the experimental ionization potentials for $\text{P}[(\text{CH}_2)_n\text{R}_{18}]_3$ decrease stepwise by 0.37, 0.26, and 0.1 eV going from $n = 2$ to 3, 4, and 5, respectively.¹⁶⁷ Also, calculated gas phase proton affinities for $\text{NH}_2[(\text{CH}_2)_n\text{CF}_2\text{CF}_3]$ were reported to increase stepwise from $n = 2$ to 3, 4, and 5 by 4.4, 2.0, and 1.7 kcal/mol, respectively.¹⁶³ These data suggest that the $\text{p}K_a$ of **2** similarly lies between the $\text{p}K_a$ values of **1** and **3** but is closer to the $\text{p}K_a$ of **3** than to the $\text{p}K_a$ of **1**.

This is important because the upper and lower detection limits of an ionophore-based pH ISE both depend on the basicity of the ionophore (i.e., the $\text{p}K_a$ of ionophore- H^+ complex). The upper detection limit also depends on the activities and lipophilicities of the counter ions in the sample, and the lower detection limit is also affected by the activities and lipophilicities of interfering ions. However, in the determination of the overall width of the working range, ΔpH , as defined by the difference between the upper and lower detection limits, the K_a terms have been reported to cancel one another.⁵⁹ Bakker et al., who proposed this model, experimentally confirmed its validity for ISEs with plasticized PVC membranes.⁵⁹ Importantly, according to this model, the working range is not expected to depend of the $\text{p}K_a$ of the ionophore. When switching between ionophores differing in

pK_a , both the upper and lower detection limits are expected to shift in the same pH direction, and the overall width of the working range remains unchanged.

In contradiction to these expectations, the working ranges of ISEs based on the fluorophilic ionophores **1** and **3** were reported to be 5 pH units (pH 1.5 to 6.5) and 8 pH units (pH 5.0 to 13.0), respectively.⁴⁴ In both cases, the ionophore to ionic site ratio was 2:1, and the working ranges were determined in the same background, i.e., 1 M KCl with a low concentration of tris(hydroxymethyl)aminomethane as pH buffer to facilitate measurements in the neutral pH range. Since the lower detection limit (at high pH) is determined for both ionophores by the H^+ vs K^+ selectivity, as apparent by the emf leveling off with the 1 M KCl background, the difference in the working ranges of these two ionophores comes from the upper detection limit (that is, low pH). At the upper detection limit, in contrast to a leveling off of the emf response as it is typically expected for the onset of Donnan failure,^{19, 21, 44} super-Nernstian responses were observed. The reason for the super-Nernstian response is not known but may be related to formation of H^+ -ionophore complexes with stoichiometries other than 1:1 as Donnan failure sets in. Note that a similar small super-Nernstian response was also observed for ionophore **2**, but only below pH 2 (see **Figure 2.4**).

For this reason, an ionophore to ionic site ratio of 4:1 was used in this work, ensuring that the formation of complexes of higher stoichiometry would not result in a very low concentration of free ionophore in the bulk of the sensing membrane. In addition, in an attempt to minimize interference from buffer ion interference at low pH, the highly

hydrophilic phosphate was used for the pH buffer rather than the tris(hydroxymethyl)aminomethane used previously.

As **Figure 2.4** shows, the linear response range of the ISE with this new ionophore (pH 2.2 and 11.2) meets the need for a working range centered around pH 7, as desired for most biological samples. It resolves the shortcomings in both of the two previously reported fluorophilic ionophores **1** and **3**. ISEs based on the ionophore **1** evidently fail in the neutral pH region, where most of biological samples fall into, such as blood (pH 7.3–7.4), urine (pH 5.0–8.0) and saliva (pH = 6.4–7.0).¹⁶⁸ ISEs based on ionophore **3** cover a wide pH range from neutral to basic pH but depending on the type of counter ions in the sample are more likely to fail in even moderately acidic solutions. These drawbacks are overcome by the new fluorophilic H⁺ ionophore **2**.

2.3.2 Potentiometric Selectivity

The selectivities of many ionophore-based H⁺ selective electrodes have been reported in the literature, most commonly with respect to K⁺, Na⁺, and Ca²⁺ because of the relevance of these ions for clinical tests. Because sample solutions that contain no H⁺ cannot be prepared, selectivity coefficients for H⁺ selective ISEs are usually determined with the fixed interfering method.^{21, 39} **Figure 2.5** shows for ISEs with **2** as ionophore the pH calibration curves measured in a constant background of K⁺, Na⁺, or Ca²⁺. Corresponding selectivity coefficients are listed in **Table 2.1**, along with selectivities for ISEs based on ionophores **1** and **3**.⁴⁴

As the table and figure show, the new fluoros-phase pH electrode has a high selectivity with respect to all three interfering ions. Even in presence of 1 M K^+ and Na^+ , the electrode starts to respond to interfering ions only at $pH \approx 12$ ($\log K_{H,K}^{pot} = -11.6$, $\log K_{H,Na}^{pot} = -12.4$). Because in the sequence of ionophores **1**, **2**, and **3** the length of the spacers separating the perfluoroalkyl groups from the nitrogen center increases from $-(CH_2)_3-$ to $-(CH_2)_4-$ and $-(CH_2)_5-$, the stability of the H^+ complexes and the selectivities of the corresponding ISEs are expected to increase steadily from **1** to **3**. This expectation is confirmed by the selectivities for H^+ with respect to both Na^+ and K^+ (see **Table 2.1**). Note that Ca^{2+} precipitation prevented the observation of Ca^{2+} interference for ISEs based on ionophore **2**. The electrodes responded perfectly linear all the way to pH 12.2, which permits only specification of an upper limit of the selectivity coefficient ($\log K_{H,Ca}^{pot} < -10.2$).

Table 2.1. Selectivities and Working Ranges of ISEs based on Ionophores 1, 2, and 3.

	Ionophore		
	1 ^a	2 ^b	3 ^a
$\log K_{H,K}^{pot}$	-7.9	-11.6	< -12.8
$\log K_{H,Na}^{pot}$	-9.3	-12.4	< -13.8
$\log K_{H,Ca}^{pot}$	-6.7	< -10.18	< -10.8
Working Range	1.5 – 6.5	2.2 – 11.2	5.0 – 13.0
pK_a	9.8	15.8	15.4

^a See reference 44. ^b This work. Experimentally observed standard deviations: 0.1 in $\log K_{H,K}^{pot}$ and $\log K_{H,Na}^{pot}$; 0.01 in $\log K_{H,Ca}^{pot}$ (n=3).

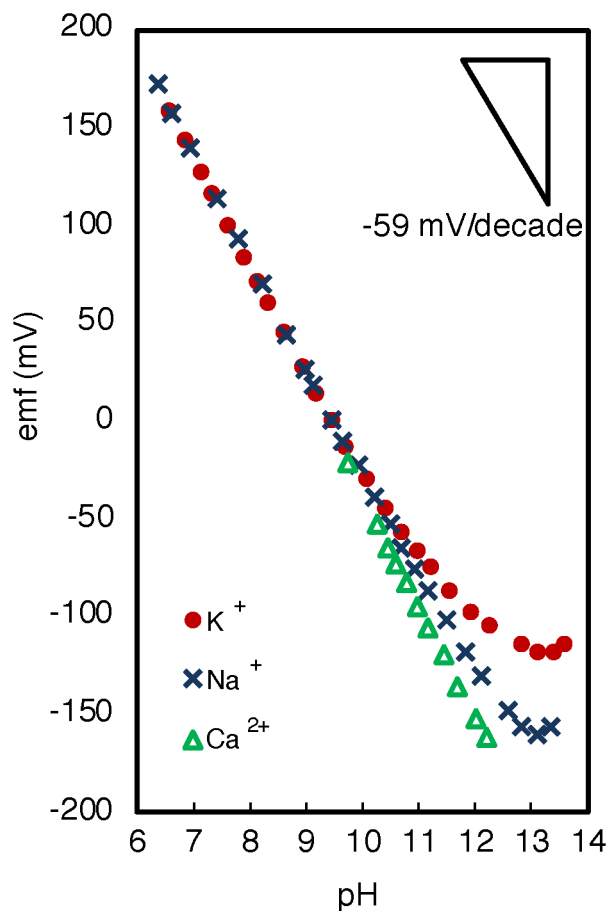


Figure 2.5. EMF response to pH with a constant metal ion concentration, demonstrating the high selectivity of ISEs based on ionophore **2** for H⁺ with respect to K⁺, Na⁺, and Ca²⁺. Selectivities with respect to K⁺ and Na⁺ were measured in a constant 1 M K⁺ and 1 M Na⁺ background, respectively (K⁺ or Na⁺ salts of 10 mM HPO₄²⁻, 10 mM H₂PO₄⁻, and 970 mM Cl⁻). The pH was gradually increased by addition of 10 M KOH or NaOH aliquots. The response to Ca²⁺ was measured with a constant 10 mM Ca²⁺ background; measurements were started with 10 mM Ca(OH)₂, and the pH was gradually decreased by adding aliquots of a solution that contained 3 M HCl and 10 mM CaCl₂.

2.3.3 Basicity of Fluorophilic H⁺ Ionophores

As the basicity of an ionophore dictates to a large extent the selectivity and working range of ionophore-based pH ISEs, it was of interest to determine the effect of the -(CH₂)₄-spacers on the pK_a value of the new fluorophilic pH ionophore **2**. Two common methods to determine the stability of the complexes between ionophores and ions (and, in the case of a H⁺ ionophore, the pK_a of the ionophore–H⁺ complex) are the so-called “sandwich membrane method”¹¹¹⁻¹¹³ and the spectrophotometric method.¹³⁵ Neither of them is suitable for the fluoruous ISE membranes of this work. The former method is not applicable to ISEs with a non-polymeric sensing phase because it requires membranes in which ions diffuse only slowly, and the latter method requires a fluorophilic chromoionophore, which is not currently available. Therefore, the pK_a values of the fluorophilic ionophore **2** was determined here by measurements of the selectivity with respect to an ion that was assumed not to bind to the ionophore.¹⁶⁹⁻¹⁷¹ Specifically, using this approach, the selectivity coefficient of an ionophore-doped membrane for a non-coordinating ion (J⁺) with respect to the primary ion (H⁺), log K_{H,J}^{pot} (L), is compared to the corresponding selectivity coefficient of an ionophore-free ion-exchanger membrane, log K_{H,J}^{pot} (IE). (For a definition of ionophore-free ion-exchanger membranes, see ref. 3, p 1595.) By insertion of these selectivity coefficients, the total ionophore concentration, L_T, and the total ionic site concentration, R_T, into eq 1, the apparent complex conformation constant between the ionophore and the primary ion can be calculated.

$$\beta_{HL} = \frac{K_{H,J}^{\text{pot}}(\text{L})}{K_{H,J}^{\text{pot}}(\text{IE})} \frac{\log K_{H,J}^{\text{pot}}(\text{L}) - \log K_{H,J}^{\text{pot}}(\text{IE})}{[L_T - R_T] \log K_{H,J}^{\text{pot}}(\text{L}) + R_T \log K_{H,J}^{\text{pot}}(\text{IE})} \quad (1)$$

In view of the exceptionally low polarity and polarizability of fluoruous phases, the selectivity coefficients needed to be corrected for ion pair formation, though. The difference between the free H⁺ concentration in the ionophore-doped and ionophore-free membranes is not only caused by the ionophore. There is also a different extent of ion pair formation in the two types of membranes. Specifically, ion pair bonding between the ionic sites and the rather large ionophore–H⁺ complex is expected to be weaker than ion pair bonding between the ionic sites and H⁺, even if the latter is partially hydrated. Ion pair formation constants can be obtained from the conductivity of membranes that contain the ionic site and either H⁺ or ionophore–H⁺ complexes at different concentrations. Fitting the experimentally determined conductivities with the Fuoss–Kraus equation (eq 2) affords the ion pair formation constant.¹⁷²

$$\Lambda = \frac{\Lambda_s^\infty}{c^{1/2} K_{ip}^{1/2}} + \frac{2\Lambda_s^\infty c^{1/2} K_t}{3K_{ip}^{1/2}} \quad (2)$$

Λ and c are the conductivity and salt concentration, respectively, Λ_s^∞ is the limiting molar conductivity of the undissolved salt, and K_{ip} and K_t are the formation constants of the ion pairs and triple ions, respectively. For example, the logarithm of the ion pair formation constant between the ionic site and the complex of ionophore **2** and H⁺, $\log K_{ip,H^+}$, was thus determined to be 12.8 ± 0.1 . Subsequently, selectivity coefficients corrected for ion pairing using eq 3 were inserted into eq 1 to afford pK_a values of ionophore–H⁺ complexes corrected for ion pairing

$$\log K_{H,J}^{\text{pot,corr}}(L) = \log K_{H,J}^{\text{pot}}(L) - (\log K_{ip,J} - \log K_{ip,H^+}) \quad (3)$$

Stabilities of ion pairs between the ionic site and non-coordinating ions J , $K_{ip,J}$, and selectivity coefficients of ionophore-free ion-exchanger membranes were adopted from ref. 46. K^+ was assumed to be a non-coordinating ion. Selectivity coefficients for K^+ with respect to H^+ were directly measured with the fixed interference method.

Correction for ion pair formation gave the pK_a value for ionophore **2** as 15.8 ± 1.2 , which is substantially larger than the previously reported pK_a of 9.8 for ionophore **1** and, therefore, is consistent with the ability of the longer $-(CH_2)_4-$ spacer of **2** to shield the amino center from electronwithdrawing perfluorooctyl groups. However, it is surprising that the pK_a value determined here for ionophore **2** is slightly higher than the previously reported value for ionophore **3**. We suspect that this discrepancy comes from an artifact in the conductivity measurements reported in ref. 44, which resulted in an underestimation of the previously reported pK_a of **3**. The conductivity measurements used to determine the pK_a of ionophores **3** were made at $pH = 3$ with an ionophore to ionic site ratio of 2:1. This is not an ideal pH for ionophore **3**, since ISEs based on this ionophore exhibit a super-Nernstian response at this pH . This adds uncertainty to the ion pair formation constant and, consequently, the determination of the pK_a value. The formation of H^+ -ionophore complexes of 2:1 stoichiometry and ion aggregates larger than triple ions^{173, 174} may also affect the accuracy of pK_a values of ionophores in ISE membranes.

2.3.4 Improved Resistance of Fluorous-Phase Ion-Selective Electrodes to Biofouling

The uniqueness of fluorous-phase ISEs comes from the extremely non-polar nature of their membrane matrixes.^{40, 41} Fluorous matrixes are both hydrophobic and lipophobic, which minimizes the solvation of interfering species, and in particular of lipophilic species from biological samples. To demonstrate the potential of fluorous membranes to resist biofouling, three types of electrodes were calibrated in standard buffer solutions from pH 7 to pH 14, namely, fluorous-phase pH electrodes with an ionophore-to-ionic-site ratio of 4 to 1 as well as pH electrodes with a plasticized PVC membrane doped with an ionophore-to-ionic-site ratio of 4 to 1 or 2 to 1. Then all three types of electrodes were stored in 10% serum solutions for five days (120 h) before they were calibrated again in the same fashion. All three types of electrodes were calibrated, stored, and calibrated again at the same time and in the same container to ensure the rigor of this comparison. The calibration plots of the fluorous-phase pH electrodes with the 4 to 1 ionophore-to-ionic-site ratio and the PVC-phase pH electrodes with the 2 to 1 ionophore-to-ionic-site ratio, each before and after serum exposure, are shown in **Figure 2.6**.

Fluorous-phase pH electrodes maintained their excellent H⁺ selectivity against K⁺ after exposure to 10% serum (selectivity coefficients $\log K_{H,K}^{\text{pot}}$ as determined before and after serum exposure are -11.3 ± 0.4 and -11.4 ± 1.0 , respectively; $n = 3$). In contrast, the selectivity of the PVC-phase pH electrodes with the 4 to 1 ionophore-to-ionic-site ratio worsened slightly from -11.6 ± 0.1 to -11.3 ± 0.1 , and the selectivity of PVC-phase pH electrodes with the 2 to 1 ionophore-to-ionic-site ratio suffered an even larger loss of

selectivity by 0.56 logarithmic units (from -11.1 ± 0.1 to -10.6 ± 0.1 ; $n = 4$). This finding is consistent with an improved resistance to biofouling of fluoruous-phase pH ISEs.

On a side note, we would also like to point out the slightly higher selectivity of the PVC-phase pH electrodes with the 4 to 1 ionophore-to-ionic-site ratio as compared to electrodes with the same membrane matrix but a 2:1 ionophore-to-ionic-site ratio. The ISE literature has typically assumed 1:1 complex formation between H^+ and trialkylamine ionophores. We first started to suspect that trialkylamine ionophore may also form 2:1 complexes when we worked with fluoruous ionophore-doped membranes and noted the superior performance of membranes with the 4 to 1 ionophore-to-ionic-site ratio.¹⁵¹ The data presented here show that the same effect is also occurring for PVC-phase ISEs, resulting in a not insignificant improvement in selectivity. It is conceivable that this same effect may also apply to H^+ ionophores other than trialkylamines, which may also form not only 1:1 but also 2:1 complexes with H^+ .¹⁷⁵

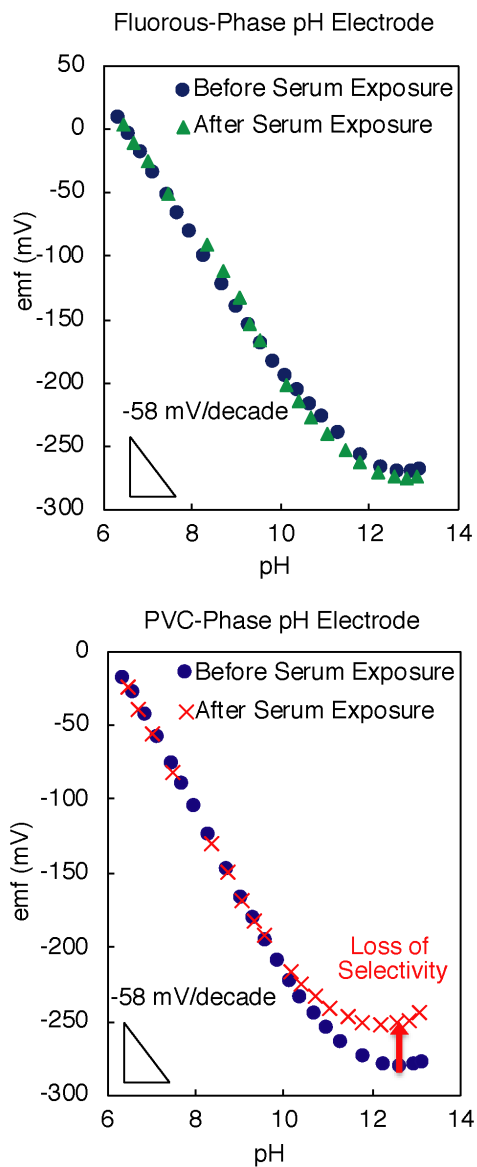


Figure 2.6. Calibration of fluorous-phase pH electrodes with the 4 to 1 ionophore-to-ionic-site ratio and PVC-phase pH electrodes with the 2 to 1 ionophore-to-ionic site ratio, each before and after serum exposure. EMF measurements were started at pH 7.4 (970 mM KCl, 10 mM K_2HPO_4 and 10 mM KH_2PO_4 solution). The pH was increased by adding small aliquots of 10 M KOH solution.

2.4 Conclusions

In previous work, the unique low polarity of fluoruous sensing membranes allowed the preparation of H⁺ selective ISEs based on ionophore **3** with an extremely high selectivity. However, its detection limit at low pH was compromised by too high an affinity of the ionophore for H⁺. In contrast, ISEs based on ionophore **1** exhibited lower selectivities due to a too low H⁺ affinity. In this work, we optimized the affinity of the ionophore for H⁺ and demonstrated that ISEs with the new fluorophilic ionophore **2** have a wide working range centered around the physiologically important pH 7. Measurements in biological samples demonstrated the improved ability of these fluoruous-phase ISEs to maintain a high selectivity after exposure to 10% serum for 5 days. We also found evidence that a 2:1 ionophore-to-ionic-site ratio is too low for the optimum use of trialkylamine ionophores for H⁺, but further study will be needed to establish how matrix-dependent this effect is, and whether this is also true for other H⁺ ionophores.

2.5 Supporting Information

2.5.1. Characterization of the Fluorophilic Ionophore $N[\text{CH}_2\text{CH}_2\text{CH}_2\text{CH}_2\text{R}_{f8}]_3$

(2)

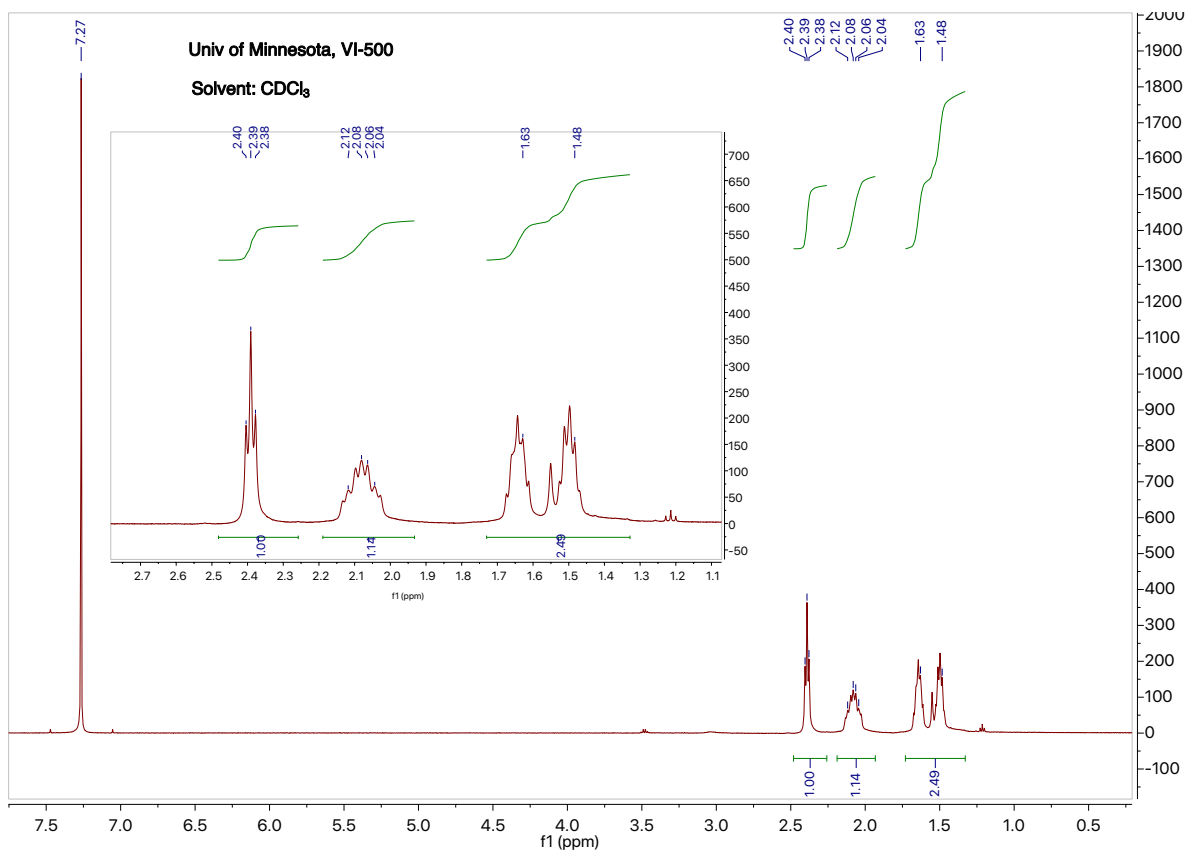


Figure S2.1. ^1H NMR spectrum of the fluorophilic ionophore $N[\text{CH}_2\text{CH}_2\text{CH}_2\text{CH}_2\text{R}_{f8}]_3$ (2).

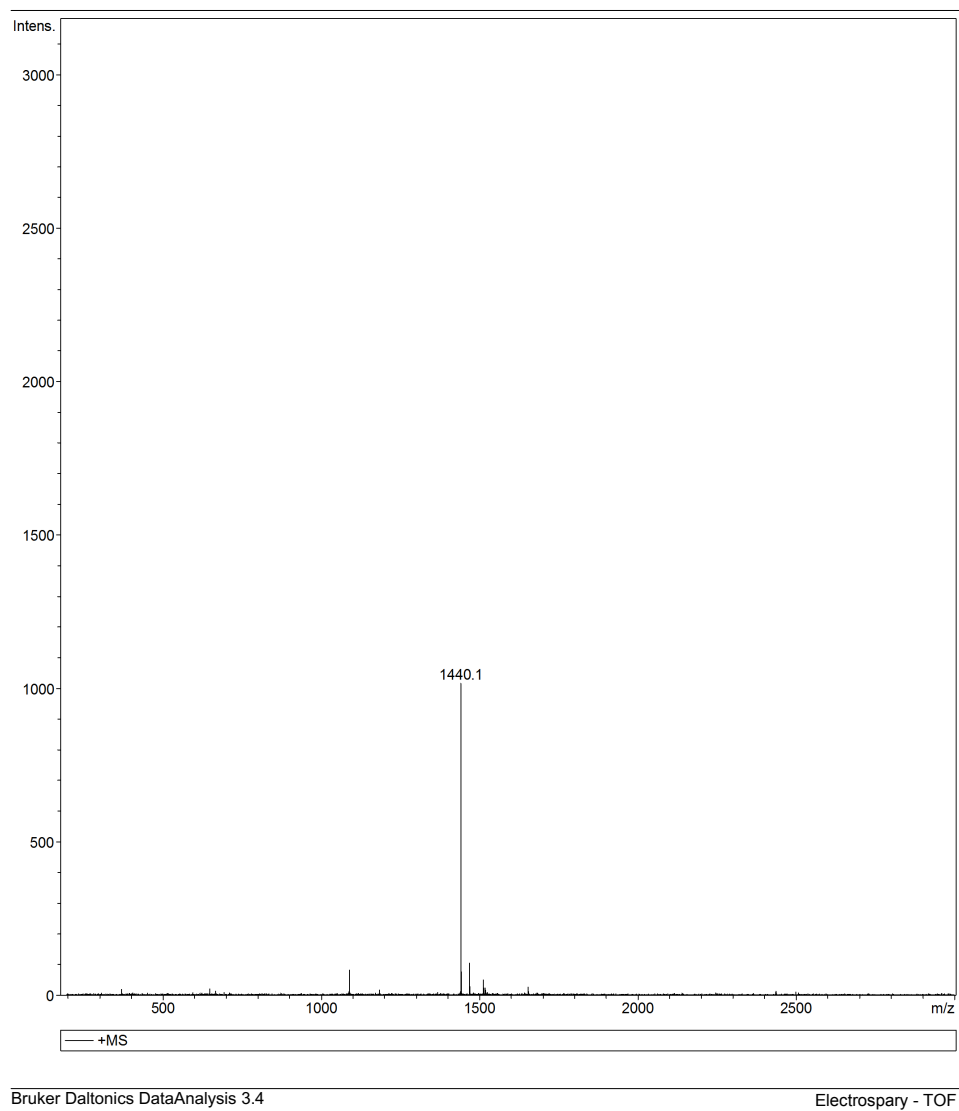


Figure S2.2. Electrospray mass spectrum of fluorophilic ionophore $N[\text{CH}_2\text{CH}_2\text{CH}_2\text{CH}_2\text{R}_{f8}]_3$ (**2**).

2.5.2. Design of Electrode Body

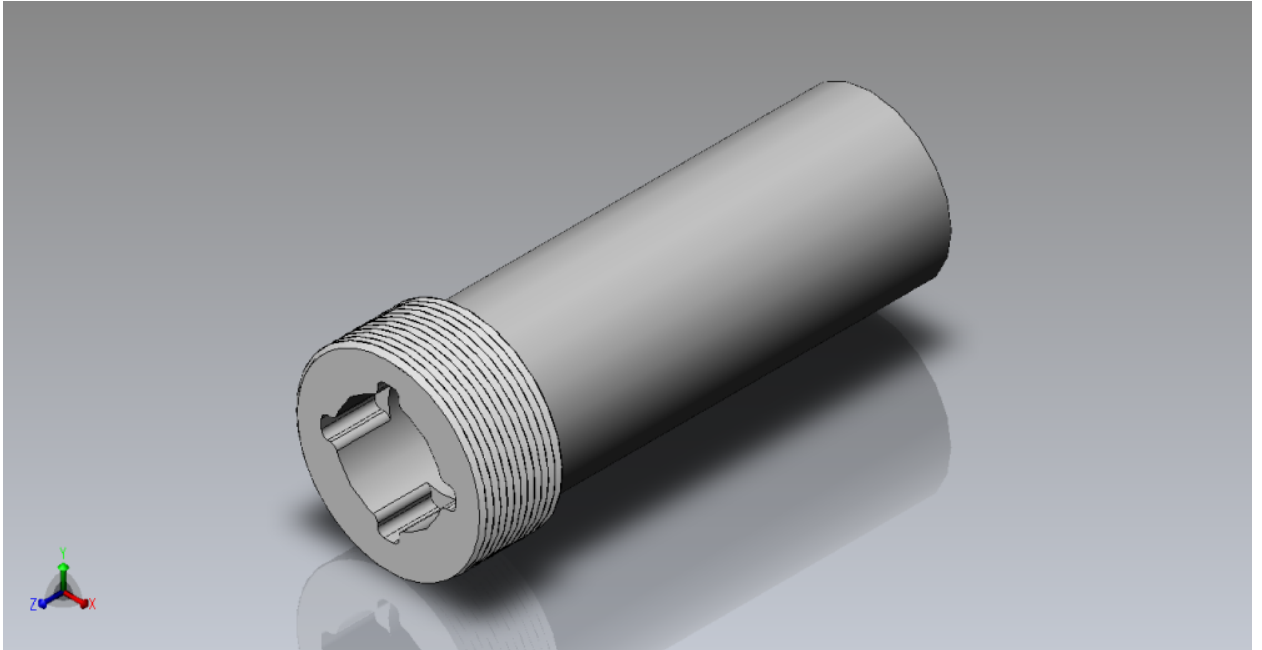


Figure S2.3. 3D view of outer electrode body piece (upper end shown in front). Four locking slots (at 90° to each other) securely hold the lugs of the inner electrode body piece (see **Figures S2.2 and S2.3**), preventing the inner body piece from rotating within the outer electrode body piece when the screw cap is mounted.

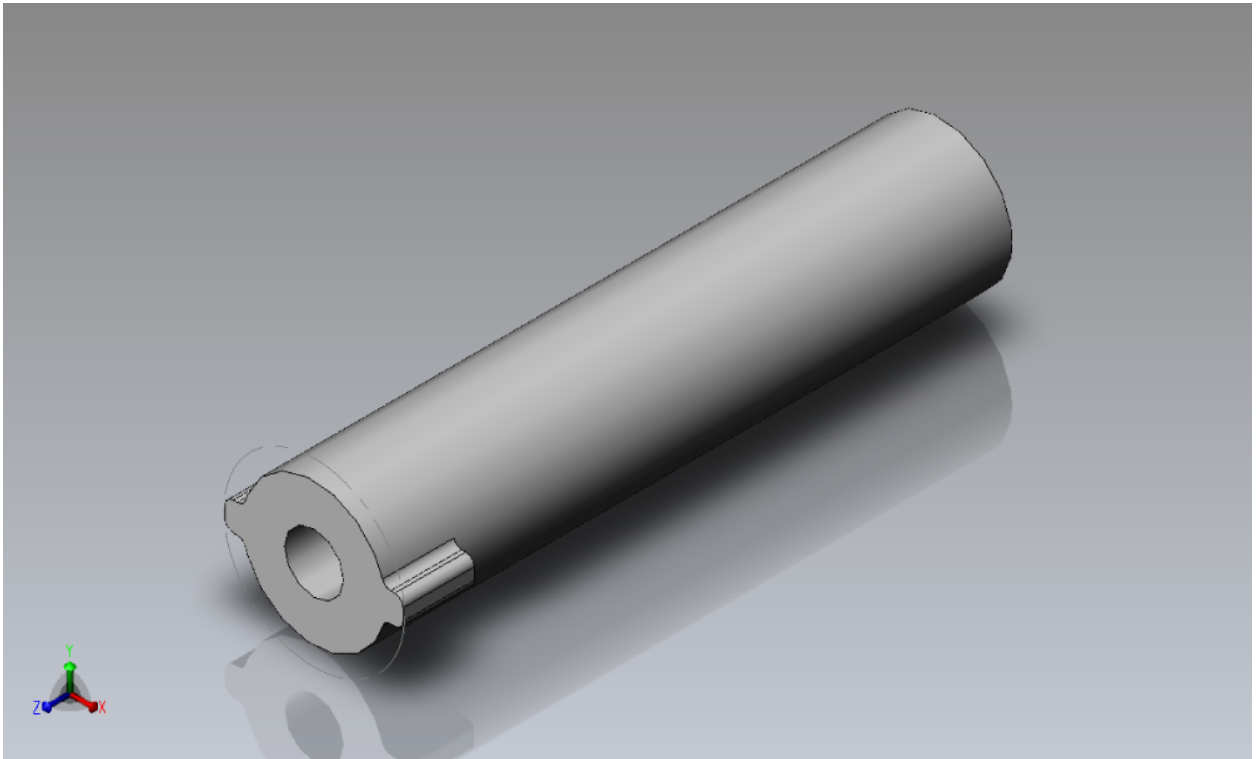


Figure S2.4. 3D view of inner electrode body piece (upper end in front). Two lugs (at 180° to each other) securely fit into locking slots of the inner electrode body piece (see **Figures S2.1** and **S2.3**).

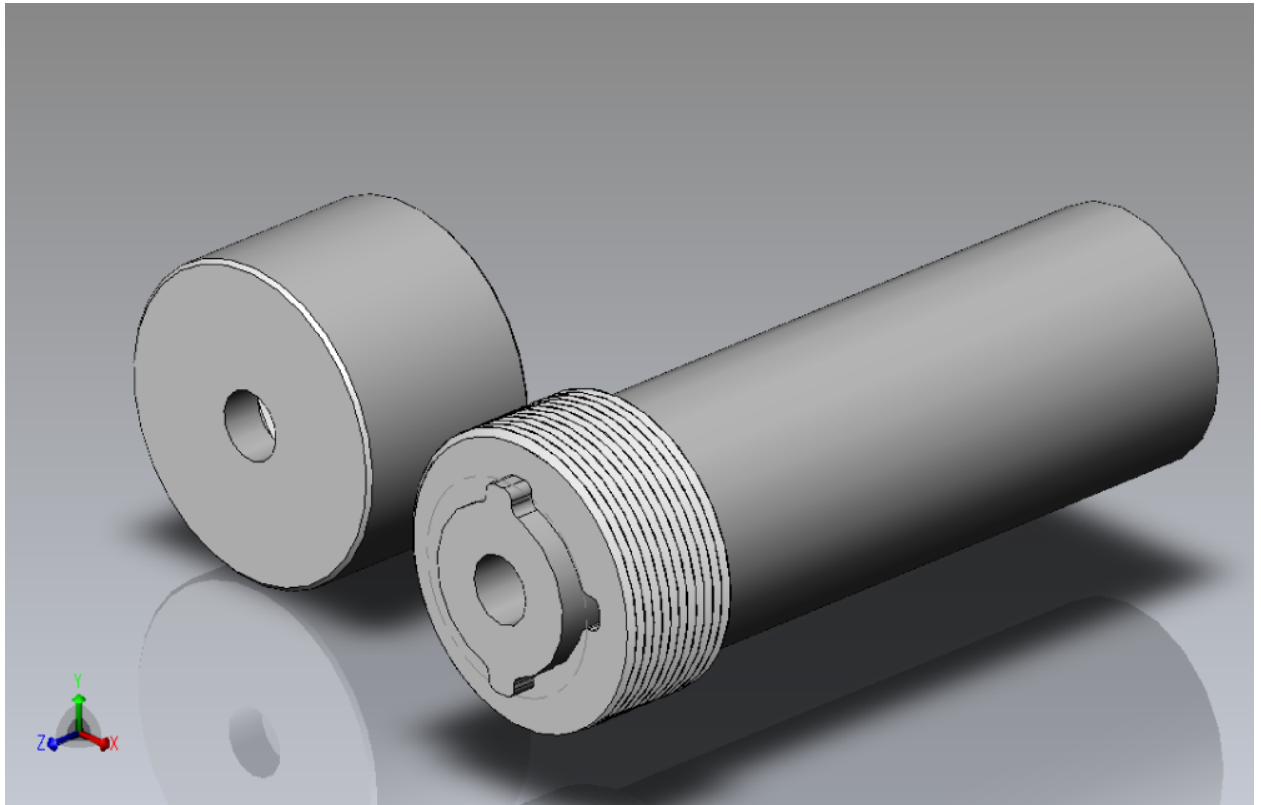


Figure S2.5. 3D view of screw cap (left) and the inner electrode body piece mounted inside the outer electrode body piece (right). The two lugs of the inner electrode body piece fit into the locking slots of the outer body piece. When the cap is screwed onto the outer body piece, it exerts pressure onto the inner body piece, pushing it onto the sensing membrane (located between the inner and outer body pieces) without causing any rotating motion of the membrane. This ensures a tight and smooth mechanical seal of the membrane.

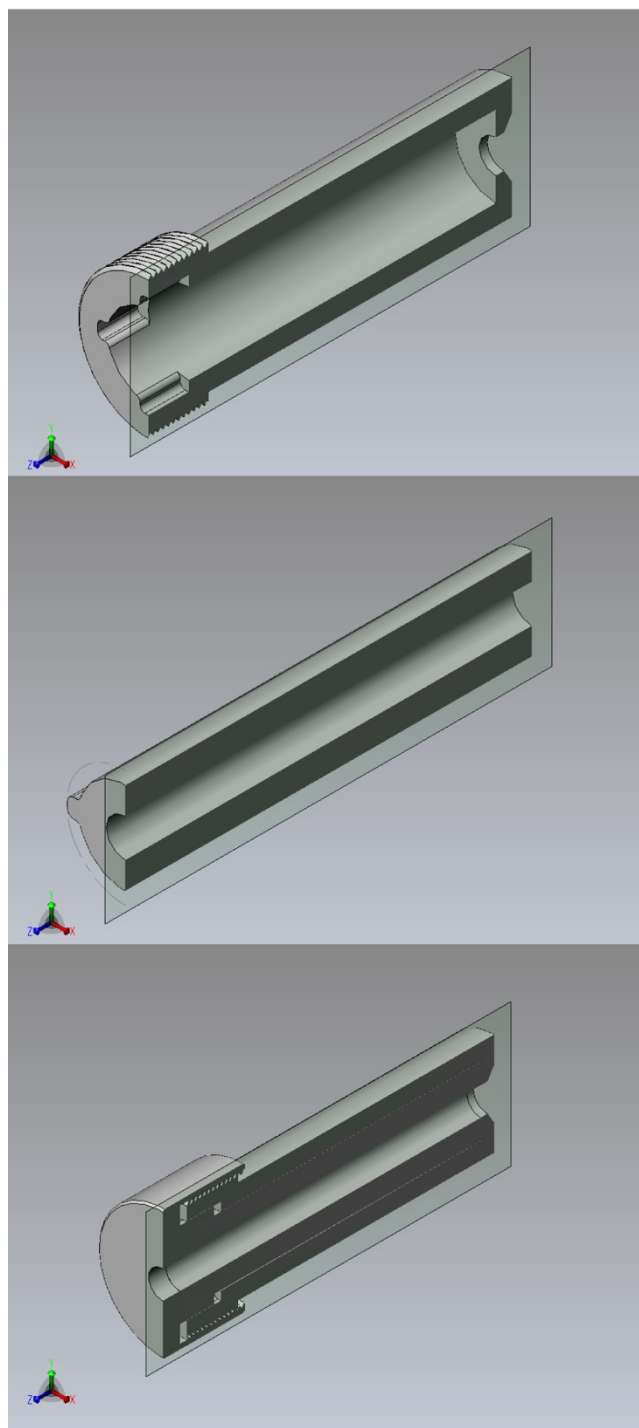


Figure S2.6. 3D views of cross-sections of the outer electrode body piece (top), inner electrode body piece (center), and the whole assembly with the screw cap (bottom).

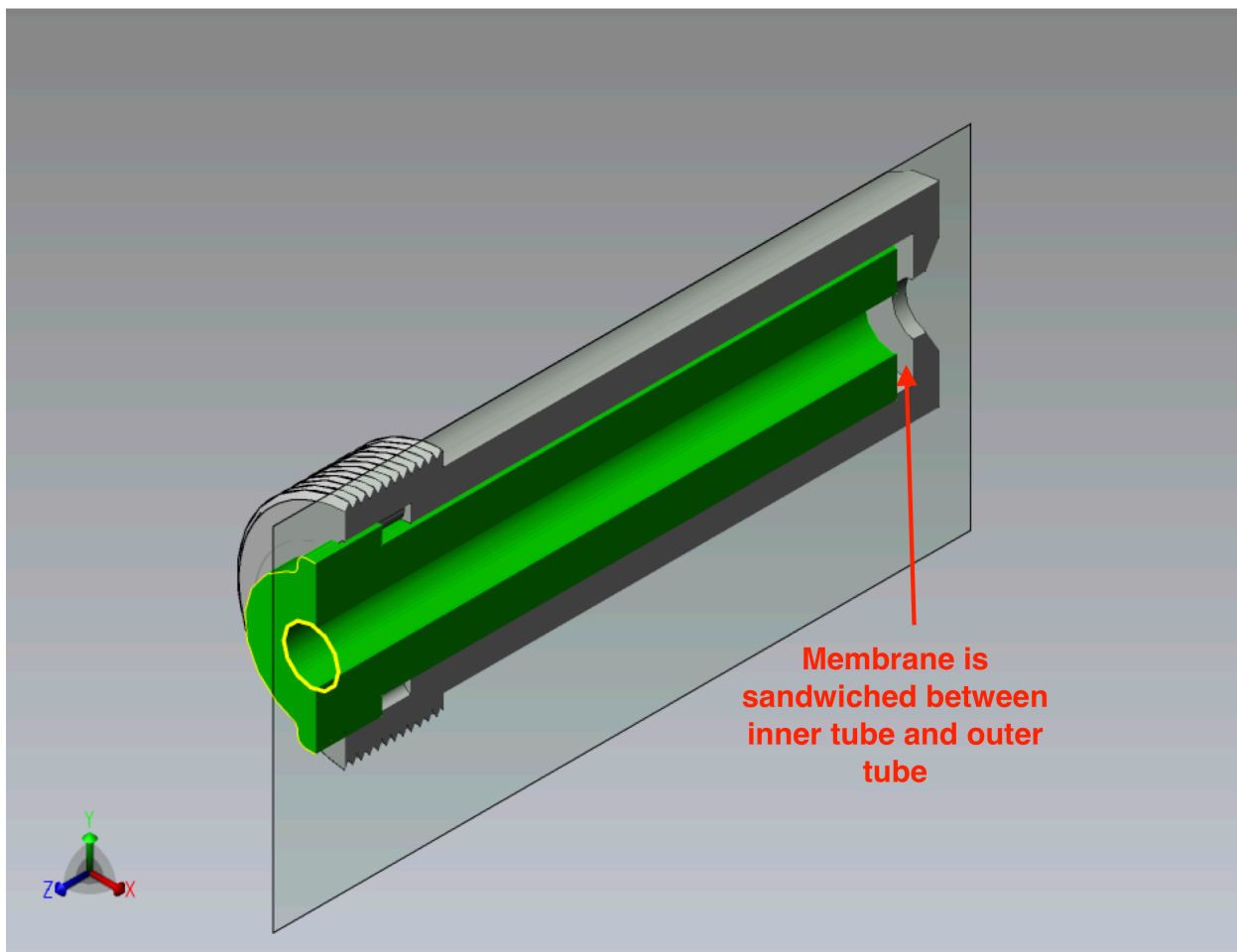


Figure S2.7. 3D view of a cross-section of the inner and outer electrode body pieces, illustrating where the membrane is located.

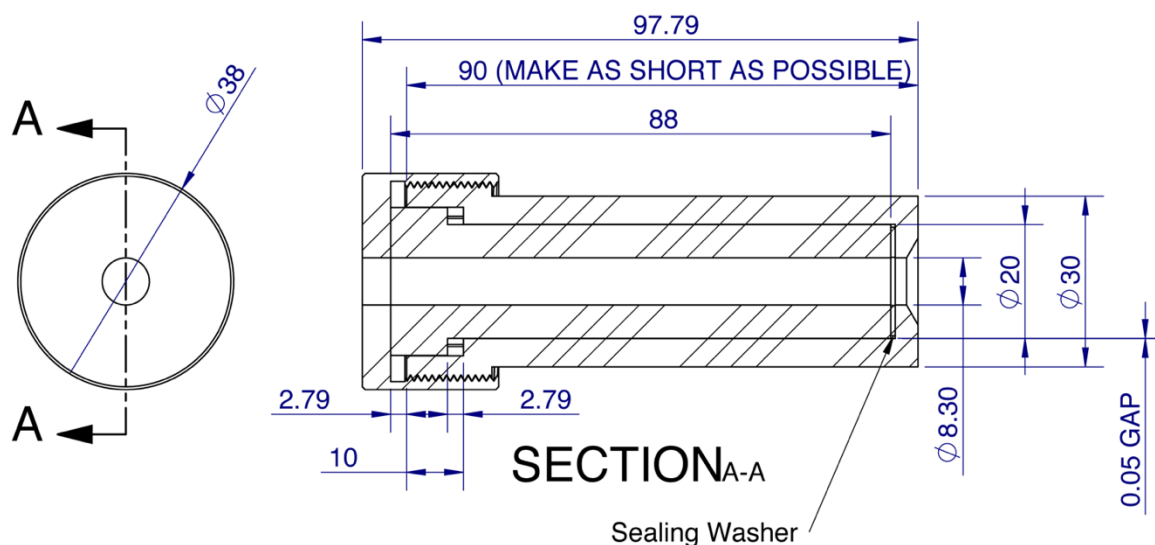


Figure S2.8. Detailed dimensions of the electrode body (unit: mm).

2.5.3. Selectivity Measurements

The non-coordinating reference ion considered initially for the determination of the pK_a of $N[\text{CH}_2\text{CH}_2\text{CH}_2\text{CH}_2\text{R}_{f8}]_3$ in the fluoros phase was the tetraphenylphosphonium ion (PPh_4^+). However, direct measurements of selectivities for PPh_4^+ with respect to H^+ failed because in such experiments PPh_4^+ and H^+ did not give the required Nernstian responses. Therefore, it was also attempted to determine this selectivity coefficient using a “selectivity ladder”, i.e., by measuring the SSM selectivities for NPr_4^+ and NBu_4^+ , which exhibit selectivities intermediate between H^+ and PPh_4^+ . Then, the selectivity for PPh_4^+ with respect to H^+ was computed with eq S1:

$$\log K_{\text{H},\text{PPh}_4}^{\text{pot}} = \log K_{\text{H},\text{NPr}_4}^{\text{pot}} + \log K_{\text{NPr}_4,\text{NBu}_4}^{\text{pot}} + \log K_{\text{NBu}_4,\text{PPh}_4}^{\text{pot}} \quad (\text{S1})$$

The pK_a value determined for ionophore **2** on the basis of $\log K_{\text{H},\text{PPh}_4}^{\text{pot}}$ and eqs 2 and 3 was 16.9 ± 1.2 , which is higher than the value previously reported for ionophore **3** with $-(\text{CH}_2)_5-$

spacers (15.4). This is likely due to errors associated with the indirect measurement of multiple selectivity coefficients using the selectivity ladder approach. In the measurement of each of these selectivity coefficients, intercepts of calibration curves are used to calculate selectivity coefficients. Therefore, errors may come from Nernstian slopes ranging between 56 and 63 mV/decade, which affect intercepts and propagates errors into $\log K_{\text{H,PPH}_4}^{\text{pot}}$.

2.5.4. Working Range of pH ISEs Based on Ionophore 2

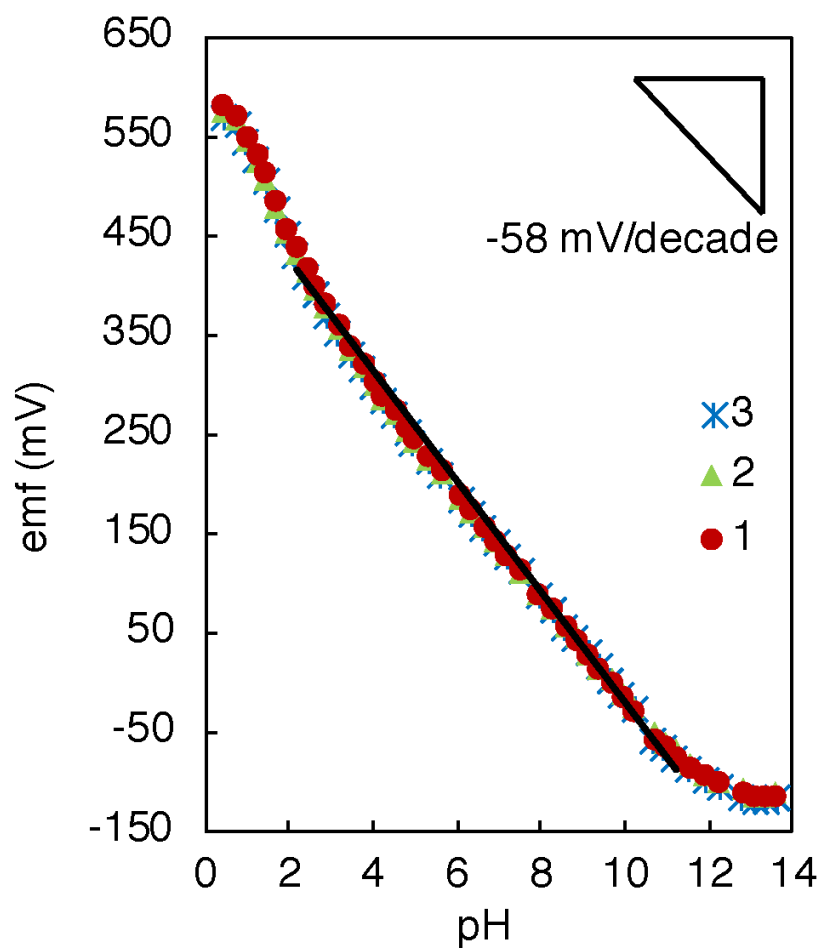


Figure S2.9. Working range of pH ISEs based on ionophore 2: EMF measurements were started at pH 7.4 (970 mM KCl, 10 mM K_2HPO_4 and 10 mM KH_2PO_4 solution). The pH was increased by adding small aliquots of 10 M KOH solution. Subsequently, starting again at pH 7.4, the pH was decreased by adding aliquots of 1 M HCl solution. Three identical electrodes (labeled as 1, 2, and 3) were made and tested together. Linear range: pH 2.2 to 11.2 (Slope: 54.7 ± 0.7 mV/decade; $n = 3$).

**III. Reference Electrodes Based on Ionic Liquid Doped
Reference Membranes with Biocompatible Silicone
Matrixes**

3.1 Introduction

Ion-selective electrodes (ISEs) are of great interest in the context of wearable and implantable sensors for continuous online monitoring of physiologically significant ions, such as K^+ , Na^+ , Cl^- , and pH (H^+). Potentiometric ion-selective sensing systems¹⁻⁶ consist of a working electrode that responds to the ion of interest and a reference electrode that provides an invariant sample-independent reference potential.²¹ To integrate these sensors into wearable and implantable devices, both electrodes have to be miniaturized, and they must be built from biocompatible materials.

Conventional reference electrodes used in potentiometry, such as the well-known Ag/AgCl electrode, contact the sample through a salt bridge that contains nearly equitransferrant cations and anions to provide a sample-independent reference potential.¹⁷⁶ However, salt bridges have drawbacks, such as the need for maintenance and the mutual contamination of the bridge electrolyte and sample solution.¹⁷⁷⁻¹⁷⁹ To address these limitations, reference electrodes that comprise a reference membrane doped with ionic liquids¹⁸⁰⁻¹⁸⁵ or salts of different hydrophilicity¹⁸⁶⁻¹⁸⁹ have been proposed. These devices are designed so that the ionic liquid or salt slowly leaches out of the reference membrane and, thereby, establishes a sample-independent distribution potential at the interface of the reference membrane and the sample.

The polymeric membrane material most commonly used in such reference electrodes is plasticized poly(vinyl chloride) (PVC), which has also been very popular for the fabrication of ISE membranes. Plasticizers lower the glass transition temperature (T_g)

of PVC below room temperature and, thereby, lower the electrical resistance of ion-doped plasticized PVC membranes by many orders of magnitude below that of unplasticized membranes.¹¹ However, these plasticizers may also gradually leach out of reference and ion-selective membrane, which is a concern because many of them are known as endocrine disruptors and inducers of inflammatory reactions.⁶⁴⁻⁶⁷

While much effort has been made to replace ISE membranes made of plasticized PVC with plasticizer-free polymers, such as silicones, polyurethanes, acrylates, and methacrylates,^{87, 106, 190} much less attention has been paid to the membrane matrix of ionic liquid based reference electrodes. The use of plasticizer-free polyurethane¹⁰⁶ and poly(*n*-butyl acrylate)¹⁸⁷ for the preparation of polymeric membrane reference electrodes was reported but in both cases the membranes were doped with a hydrophobic salt rather than an ionic liquid. To date, the only reference electrodes with a plasticizer-free reference membrane doped with an ionic liquid were fabricated with a poly(vinylidene fluoride-*co*-hexafluoropropylene) matrix.¹⁸⁰ Plasticizer-free silicones have not been reported so far as polymer matrixes for reference membranes, but they stand out in several ways as potential materials for this purpose: (i) Silicones are widely used in implantable devices,⁷⁸⁻⁸² and a range of commercially available silicones have been certified as biocompatible or medical grade following manufacturing standards guided by government agencies, such the US Food and Drug Administration.⁶³ (ii) Silicones typically have a very low T_g , which is a prerequisite for use in ISE and reference membranes. (iii) Silicone precursors can be easily dissolved and cast into thin films. (iv) The curing chemistry of silicones offers an

opportunity to covalently attach reference membranes to a range of substrates with surface hydroxyl groups to prevent membrane delamination.^{84, 191, 192}

In the work described here, we used seven commercially available silicone materials and four different ionic liquids to prepare polymeric reference membranes. Excellent potential stability was obtained with a fluorosilicone matrix, using both a conventional electrode setup with an inner filling solution and solid-contact electrodes. Long-term stability tests in artificial blood electrolyte solutions and in 10% animal serum showed low potential drifts. Differential scanning calorimetry (DSC) was used to assess the miscibility of the ionic liquids and the silicones and explain the effect of specific polymers and ionic liquids on the potentiometric performance of the polymeric reference electrodes.

3.2 Experimental Section

Materials. Reagents and materials were obtained from the following sources: Dow RTV 730 fluorosilicone (**Fluorosilicone 1**) and RTV 3140 silicone (**Silicone 1**) from Dow Corning (Midland, MI); NuSil silicones MED-1555 (**Fluorosilicone 2**), MED-2000 (**Silicone 2**), MED-6381 (**Silicone 3**), MED-6385 (**Silicone 4**), and GEL-3500 (**Silicone 5**) from NuSil (Carpinteria, CA); high molecular weight PVC and *o*-nitrophenyl octyl ether (*o*-NPOE) from Fluka (Buchs, Switzerland); the ionic liquids 1-methyl-3-octylimidazolium bis(trifluoromethylsulfonyl)imide ($[\text{C}_8\text{mim}^+][\text{NTf}_2^-]$), 1-methyl-3-decylimidazolium bis(trifluoromethylsulfonyl)imide ($[\text{C}_{10}\text{mim}^+][\text{NTf}_2^-]$), 1-methyl-3-dodecylimidazolium bis(trifluoromethylsulfonyl)imide ($[\text{C}_{12}\text{mim}^+][\text{NTf}_2^-]$), and tributylmethylammonium bis(trifluoromethylsulfonyl)imide ($[\text{NBu}_3\text{Me}^+][\text{NTf}_2^-]$) from Iolitec (Tuscaloosa, AL); valinomycin from Sigma-Aldrich (St. Louis, MO); sodium tetrakis[3,4-bis-(trifluoromethyl)phenyl]borate (NaTFPB) from Dojindo (Kumamoto, Japan). Colloid-imprinted mesoporous (CIM) carbon was prepared as previously reported.¹⁹³ Autonorm freeze-dried animal serum was purchased in powder form from Sero (Billingstad, Norway). All chemicals were used as received. Aqueous solutions were prepared from deionized water treated with a Milli-Q Plus water system (Millipore, Bedford, MA) to give a resistivity of 18.2 M Ω /cm.

Electrode Fabrication. In the case of one-component silicone materials (**Fluorosilicone 1**, **Silicone 1**, **Fluorosilicone 2**, **Silicone 2**), solutions to prepare reference electrode membranes were prepared by dissolving 200 mg of the silicone material and 50 mg ionic liquid in 1.0 mL tetrahydrofuran (THF) and stirring with a magnetic stir bar. Then

the membrane solution was poured into a circular Teflon Petri dish of 25 mm diameter and left to allow for solvent evaporation and silicone curing. In the case of silicone materials with either only a separate catalyst (**Silicone 4**) or both a separate catalyst and a separate crosslinker (**Silicone 3**), a combined amount of 200 mg of the different components in the recommended ratios was used. The base (i.e., the linear polysiloxane) and (if applicable) the crosslinker were dissolved in 1.0 mL THF, followed by stirring, casting of the solution into a Teflon Petri dish of 25 mm diameter, and addition of catalyst into the cast solution right afterwards. In the case of the adjustable two-component **Silicone 5**, a total amount of 200 mg with a 1:1 mass ratio was used. Both components were dissolved in 1.0 mL THF and cast into a Teflon Petri dish of 25 mm diameter. After complete curing of the silicones, small circular disks (7 mm diameter) were cut from the master membranes and mounted into Philips type electrode bodies¹⁶⁵ (Glasbläserei Möller, Zürich, Switzerland; Ag/AgCl internal reference) with a 1.0 mM KCl inner filling solution. The electrodes were conditioned in 1.0 mM KCl for two days prior to use.

For the preparation of solid-contact reference electrodes, gold electrodes (planar circular Au electrodes with a 2 mm diameter, embedded into an inert Kel-F polymer shaft; CH Instruments, Austin, TX) were polished on a polishing cloth, first with 0.5 μm and then with 0.03 μm aqueous aluminum oxide slurry (Buehler, Lake Bluff, IL), and then sonicated first in water and then in ethanol, each for 6 min. A stream of argon was used to dry the electrodes. A CIM carbon suspension solution was prepared by dissolving 47.5 mg CIM carbon and 2.5 mg **Fluorosilicone 1** in 1.0 mL THF followed by sonication for 30 min. Then, 30 μL of this suspension was dropcast onto the gold electrode and left to dry. This

was followed by two aliquots (20 μL followed by 30 μL) of silicone membrane solution dropcast onto the CIM carbon layer. After complete curing of the silicones, the electrodes were conditioned for two days in 1.0 mM KCl solution prior to use. A water layer test using K^+ -selective **Fluorosilicone 1** solid-contact electrodes showed no undesired water layer between **Fluorosilicone 1** and the solid contact material (see the Supporting Information).

Solutions for the preparation of ionic liquid-doped PVC membranes were prepared by dissolving 100 mg high molecular weight PVC, 100 mg of the plasticizer *o*-NPOE, and 50 mg $[\text{C}_8\text{mim}^+][\text{NTf}_2^-]$ in 1.0 mL THF. Solutions for the fabrication of blank plasticized PVC membranes were prepared by dissolving 100 mg high molecular weight PVC and 100 mg of the plasticizer *o*-NPOE in 1.0 mL THF. In both cases, the solutions were stirred until the PVC had completely dissolved and then poured into a glass Petri dish of 22 mm diameter and left to dry over 24 h to give a plasticized PVC membrane.

Electrochemical Measurement. Potentiometric measurements were performed with a 16-channel potentiometer (Lawson Labs, Malvern, PA) controlled by EMF Suite software (Fluorous Innovation, Arden Hills, MN). Potential responses of all polymeric membrane reference electrodes were measured in stirred solutions against a conventional free-flow double-junction reference electrode (DX200, Mettler Toledo, Switzerland; AgCl saturated 3.0 M KCl as inner reference electrolyte and 1.0 M LiOAc as bridge electrolyte). Unless mentioned otherwise, all measurements were performed at room temperature (20 $^{\circ}\text{C}$). For KCl calibrations, measurements began at 1.0 mM KCl, and aliquots of concentrated KCl solutions were added to double the concentration stepwise to 16 mM. All emf values were corrected for the liquid junction potentials of the double-junction

reference electrode.⁵¹ Activity coefficients were calculated based on a two parameter Debye-Hückel approximation.¹⁶⁶ Membrane resistances were measured with the known shunt method.¹²

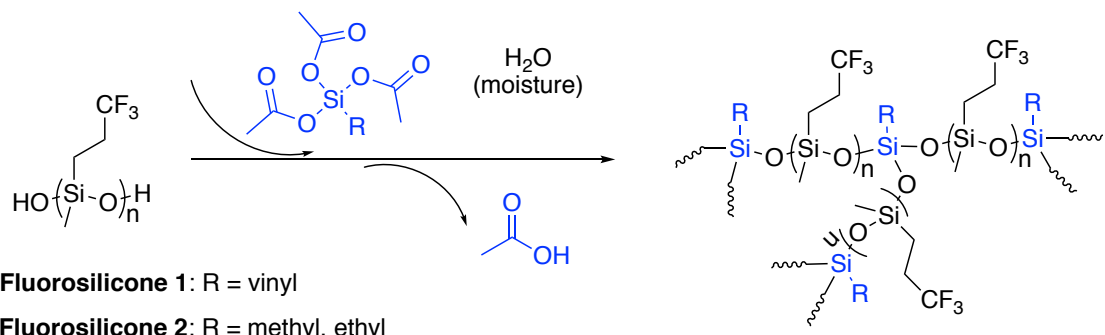
Differential Scanning Calorimetry. Cast membranes were left to dry for at least two weeks prior to DSC experiments to ensure that the membranes were fully cured, and all solvent had evaporated. Experiments were performed with a TA Instrument Q1000 DSC (New Castle, DE) with a liquid nitrogen cooling system. Small pieces of samples were cut from the master membranes and enclosed in a lidded sample pan. They were first thermally equilibrated at 40 °C for one minute. Then the samples were scanned to –180 °C and back to 40 °C, with a consistent 1.0 °C/min heating and cooling rate. Glass transition temperatures were determined as midpoints of transition zones.

3.3 Results and Discussion

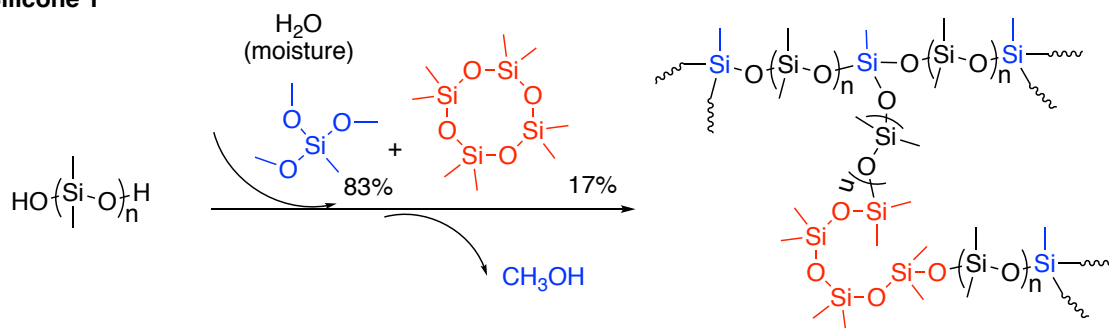
3.3.1 Silicone Materials and Sensor Membrane Fabrication

Seven commercially available silicones were used in this work. **Fluorosilicone 1**, **Fluorosilicone 2**, **Silicone 1**, and **Silicone 2** are so-called one-component silicones. Once exposed to air, they cure upon reaction with water from the atmosphere, releasing either an alcohol or acetic acid as byproduct. Typically, they contain an organotin catalyst to facilitate this reaction (see **Scheme 3.1**). The three other silicone materials used in this work were prepared by mixing multiple components. **Silicone 4** is prepared from two components. One of these components contains a tin catalyst and is used in a few weight percent with respect to the other component, which contains the linear polysiloxane backbone and crosslinker. In the case of **Silicone 3**, the crosslinker is provided separately as a third component. In the case of **Silicone 5**, the two components are added in a 1:1 ratio. Curing occurs upon mixing of the two or three components in a ratio recommended by the manufacturer (see Experimental Section). From a fabrication point of view, one-component silicones are advantageous as their use reduces the number of fabrication steps and eliminates the need to control the ratio of multiple components.

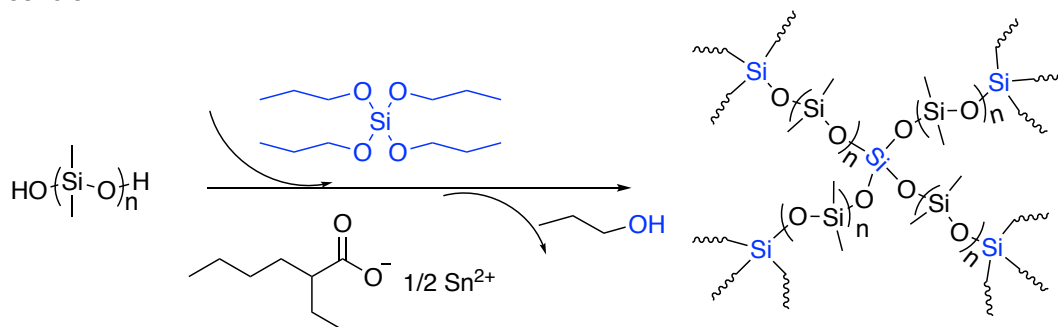
Fluorosilicone 1 and Fluorosilicone 2



Silicone 1



Silicone 3



Scheme 3.1. Curing chemistries of representative fluorosilicones and silicones studied in this work (see also **Table 3.1**).

Even though the exact structures of these silicones differ from each other in a number of ways, their linear backbones are either poly(3,3,3-

trifluoropropylmethylsiloxane) (**Fluorosilicone 1** and **Fluorosilicone 2**, referred to in the following as fluorosilicones) or poly(dimethylsiloxane) (**Silicone 1**, **Silicone 2**; **Silicone 3**, **Silicone 4**, and **Silicone 5**). Many silicone materials also contain fillers such as silica or titanium dioxide to improve their mechanical properties (see **Table 3.1**). Some of these fillers can be removed by centrifugation if that is desired for sensing purposes.⁹²

The electrical resistances of blank silicone membranes that were not doped with an ionic liquid all fall into the relative narrow range of 0.2 to 2.0 GΩ (**Table S3.1**), except for **Silicone 1** (15 GΩ). These resistances are very high, but they are not infinite as it would be expected for an ideal material without ionic impurities. This suggests that the different silicone materials have low levels of intrinsic ionic impurities. Notably, there is no evident correlation between membrane resistances and the type of silicone.

Casting of **Silicone 3** gave self-standing membranes in both its pure form and when doped with 20 wt % [C₈mim⁺][NTf₂⁻]. However, when **Silicone 3** was doped with 20 wt % [C₈mim⁺][NTf₂⁻], clear liquid aggregates with average sizes of 1 to 2 mm diameter macro-phase separated from the polymer, as could be readily detected with the naked eye. In three attempts to cast such membranes, varying patterns and shapes of liquid aggregates appeared. Areas were randomly selected for cutting out smaller circular disks for use in electrodes. Casting of the two-component **Silicone 4** and **Silicone 5** did not give self-standing membranes, independently of whether it was in a pure form or doped with 20 wt % [C₈mim⁺][NTf₂⁻]. Therefore, neither of these two polymers was deemed suitable for electrochemical work.

Table 3.1. Characteristics of Reference Electrode Membranes.

Membrane matrix	Silicone type	Polymer backbone	Biocompatibility	Resistance (doped with [C ₈ mim ⁺][NTf ₂ ⁻]) /MΩ ^a
Fluoro-silicone 1	one-component, acetic acid evolving	poly[(3,3,3-trifluoropropyl)methylsiloxane], OH-terminated ^b	no plasticizer	4.7 ± 4.0
Fluoro-silicone 2	one-component, acetic acid evolving	poly[(3,3,3-trifluoropropyl)methylsiloxane], OH-terminated	medical grade ^c	8.0 ± 2.7
Silicone 1	one-component, alcohol evolving	poly(dimethylsiloxane), OH-terminated	no plasticizer	(7.1±7.9)×10 ³
Silicone 2	one-component, acetic acid evolving	n.a. ^d	medical grade ^c	(4.9±6.5)×10 ³
Silicone 3^e	three-component (base, crosslinker, Sn catalyst)	poly(dimethylsiloxane), OH-terminated	medical grade ^c	160 ± 120
Silicone 4^f	two-component (base, Sn catalyst)	n.a. ^d	medical grade ^c	n.a.
Silicone 5^g	two-component, Pt catalyst	poly[dimethylsiloxane- <i>co</i> -(3,3,3-trifluoropropyl)methylsiloxane], vinyl-terminated	no plasticizer	n.a.

Membrane matrix	Silicone type	Polymer backbone	Biocompatibility	Resistance (doped with [C ₈ mim ⁺][NTf ₂ ⁻]) /MΩ ^a
Plasticized PVC	n.a.	poly(vinyl chloride)	plasticizer required	0.59 ± 0.08 ^h

^a Electrical resistance of membranes doped with 20 wt % [C₈mim⁺][NTf₂⁻] (n = 4). ^b Numerical locants of fluorines inferred from Chemical Abstract number; material data safety sheet only specifies trifluoropropyl. ^c Medical grade for intended use in, on, or in contact with the body, according to regulatory standards: Current Good Manufacturing Practice 21 Code of Federal Regulations §820 (Device) and §210-211 (Drug/Active Pharmaceutical Ingredient) from the US Food and Drug Administration and ISO 9001 from the International Organization for Standardization.¹⁹⁴ ^d Exact structure not available from manufacturer. ^e Membranes doped with 20 wt % [C₈mim⁺][NTf₂⁻] contained liquid aggregates.^f **Silicone 4** Membrane does not form robust self-standing membranes. ^g At the 1:1 component ratio recommended by the manufacturer, **Silicone 5** does not form robust self-standing membranes. ^h From ref. 186 (n = 4).

3.3.2 Responses to KCl of Reference Electrode Membranes Doped with [C₈mim⁺][NTf₂⁻]

The response mechanism of reference electrodes with ionic liquid-doped reference membranes relies on the control of the phase boundary potential at the membrane–sample interface by distribution of the ionic liquid between the two phases.^{180-182, 184} Sample ions most likely to negatively affect the reference potential have a comparatively small hydration energy, which lowers the energy barrier for transfer into the reference membrane.

Considering physiological ion concentrations in human blood serum and typical ion transfer energies, as apparent, e.g., from the selectivity of ionophore-free ion exchanger ISEs,² one of the ions of most concern is potassium, which has a mean concentration of 4.10 mM in human blood serum of healthy adults (95% range: 3.5 to 4.7 mM).¹⁹⁵

In order to assess whether potassium affects the ideally sample-independent response of reference electrodes with ionic liquid doped silicone membranes, the use of these electrodes was tested in the KCl concentration range from 1.0 to 16 mM. As can be seen in **Figure 3.1** and **Table S3.2**, when doped with [C₈mim⁺][NTf₂⁻], only reference electrode membranes based on the **Fluorosilicone 1** matrix provided a sample-independent potential. The other silicone materials (**Silicone 1**, **Fluorosilicone 2**, **Silicone 2**, and **Silicone 3**) did not give reference potentials independent of the KCl concentration. Given the similar polarities of all of these silicone and fluorosilicone matrixes, it appears unlikely that differences in the free energies of transfer of K⁺ or Cl⁻ from aqueous samples into the reference membranes explain these results alone. Indeed, the electrical resistance of the silicones doped with [C₈mim⁺][NTf₂⁻] and the DSC results suggest that the poor miscibility between the ionic liquid and the silicone polymer is the major cause for the poor performance as reference electrode membranes.

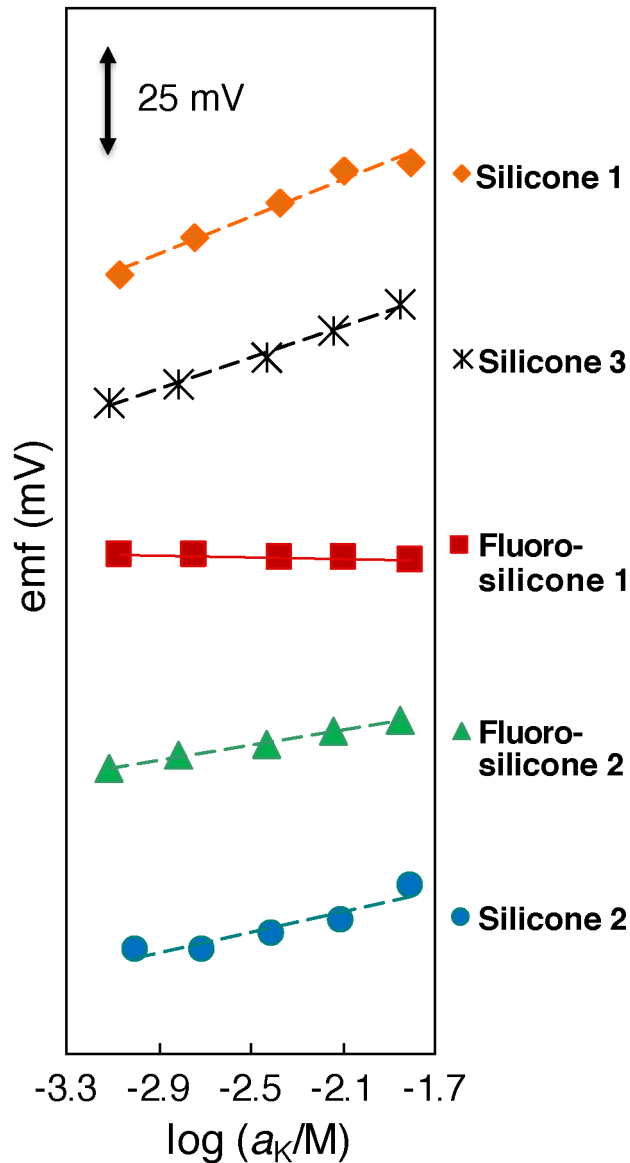


Figure 3.1. Effect of KCl (1.0 to 16 mM) on the potential of reference electrodes with $[\text{C}_8\text{mim}^+][\text{NTf}_2^-]$ -doped silicone membranes (conventional electrode setup with a 1.0 mM KCl inner filling solution), as measured against a free-flow double-junction reference electrode. The average slopes and standard deviations of the linear regressions of each of the five types of membranes are given in **Table S3.2**.

3.3.3 Functionality of Reference Electrodes and Miscibility of Ionic Liquids with Silicone Materials

Because **Fluorosilicone 1** doped with $[\text{C}_8\text{mim}^+][\text{NTf}_2^-]$ emerged as the most successful matrix for reference electrodes, we used DSC to further characterize this material. For comparison, we also used DSC to test the pure ionic liquid as well as undoped and $[\text{C}_8\text{mim}^+][\text{NTf}_2^-]$ -doped membranes with polymer matrixes consisting of **Fluorosilicone 2**, **Silicone 1**, **Silicone 2**, or **Silicone 3**. **Table 3.2** summarizes the glass transition temperatures determined from the DSC traces.

Table 3.2. Glass Transition Temperatures of the Ionic Liquid $[\text{C}_8\text{mim}^+][\text{NTf}_2^-]$, Neat Polymers, and $[\text{C}_8\text{mim}^+][\text{NTf}_2^-]$ -Doped Polymers.

Material	Undoped (°C)	Doped with 10 wt % $[\text{C}_8\text{mim}^+][\text{NTf}_2^-]$ (°C)	Doped with 20 wt % $[\text{C}_8\text{mim}^+][\text{NTf}_2^-]$ ^b (°C)
$[\text{C}_8\text{mim}^+][\text{NTf}_2^-]$	-84 ^a	n.a.	n.a.
Fluorosilicone 1	-67	-66	-66 and -83 ^b
Fluorosilicone 2	-67	-67 and -83 ^b	-67 and -82 ^b
Silicone 1	-117	-117 and -84 ^b	-116 and -84 ^b
Silicone 2	-120	-120 and -82 ^b	-119 and -83 ^b
Silicone 3	-117	-118 and -83 ^b	-121 and -81 ^b
Plasticized PVC	-54	n.a.	-56

^a T_g of pure $[\text{C}_8\text{mim}^+][\text{NTf}_2^-]$. ^bTwo glass transitions observed, one corresponding to pure $[\text{C}_8\text{mim}^+][\text{NTf}_2^-]$.

At 10 wt % doping with $[\text{C}_8\text{mim}^+][\text{NTf}_2^-]$, **Fluorosilicone 1** only shows one T_g at -66 °C, which coincides within error with the T_g of undoped **Fluorosilicone 1** at -67 °C.

This indicates that at this doping level, the ionic liquid and **Fluorosilicone 1** are fully miscible. When the doping level is increased to 20 wt %, an additional T_g consistent with the ionic liquid appears, which is a clear sign for phase separation. This confirms that the miscibility of $[\text{C}_8\text{mim}^+][\text{NTf}_2^-]$ in **Fluorosilicone 1** is at least 10 wt % and is consistent with the electrical resistance of these membranes, which is two orders of magnitude lower than for undoped **Fluorosilicone 1** (see **Table S3.1**).

For all other fluorosilicone and silicone matrixes studied by DSC, even at the low doping level of 10 wt % the DSC trace shows two glass transitions, one corresponding to the T_g of the pure ionic liquid, and the other corresponding to the T_g of the undoped polymer, indicating phase separation. Moreover, addition of $[\text{C}_8\text{mim}^+][\text{NTf}_2^-]$ to these membrane matrixes has within error no effect on the membrane resistance (see **Table S3.1**), except for the case of **Fluorosilicone 2**. Although $[\text{C}_8\text{mim}^+][\text{NTf}_2^-]$ and **Fluorosilicone 2** are not fully miscible at the 10 wt % doping level, the amount of dissolved $[\text{C}_8\text{mim}^+][\text{NTf}_2^-]$ was sufficient to lower the membrane resistance to some extent. All of this is consistent with a poor miscibility between $[\text{C}_8\text{mim}^+][\text{NTf}_2^-]$ and these polymers and the poor performance of these matrixes as reference membranes.

For comparison, DSC tests were also performed with $[\text{C}_8\text{mim}^+][\text{NTf}_2^-]$ -doped PVC membranes plasticized with *o*-NPOE. At the doping level of 20 wt %, which is the weight ratio that was used in prior work,²³ the plasticized PVC membranes exhibited only one T_g . Moreover, doping of the plasticized PVC membrane with $[\text{C}_8\text{mim}^+][\text{NTf}_2^-]$ lowered the membrane resistance to 0.59 M Ω , consistent with a high solubility of the ionic liquid in the plasticized PVC matrix.

Based on these DSC and resistance data, we conclude that the poor performance of many of the **Fluorosilicone 2**, **Silicone 1**, **Silicone 2**, and **Silicone 3** membranes doped with ionic liquid is primarily explained by the low solubility of the ionic liquid in the polymer matrix, which results in a high electrical resistance but may also affect the amount of ionic liquid distributed across the membrane/sample phase boundary.

3.3.4 Effect of Sample Concentration on Solid-Contact Reference Electrodes with Fluorosilicone 1 Membranes

In view of the results obtained with conventional electrode bodies with an inner filling solution as discussed above, only **Fluorosilicone 1** was used for subsequent work with solid-contact reference electrodes. CIM carbon, a hydrophobic, highly pure carbon material with a high surface area (321 m²/g) and a low surface concentration of polar functional groups (0.053 mmol/m² ketone groups; phenol, lactone, lactol, and carboxylic acid group concentrations too low to detect)¹⁹³ was used as transducer layer between the reference membrane and gold as the underlying electron-conducting metal. In the 1.0 mM to 16 mM KCl range, solid-contact **Fluorosilicone 1** reference electrodes showed a sample-independent emf response, with an emf dependence on the logarithm of the K⁺ activity of 0.0 ± 0.7 mV/decade (n = 3; see **Figure S3.1**). The difference between the maximum and minimum potentials over the entire activity range was 2.0 ± 1.4 mV (n = 3). This demonstrates that the good characteristics of **Fluorosilicone 1** reference membranes carry over to the solid-contact setup with CIM carbon as transducer.

To simulate the working environment of wearable or implantable sensors, electrolyte solutions mimicking critical blood parameters in terms of pH and K^+ , Na^+ , Cl^- , and phosphate concentrations were used. Specifically, two such electrolyte solutions, designated below as HIGH and LOW, were prepared (see **Table 3.3** for their composition) to represent unusually high and low blood electrolyte concentrations. **Figure 3.3** confirms that **Fluorosilicone 1** reference electrodes provide the same potential in HIGH and LOW solutions.

Table 3.3. Composition of Artificial Blood Electrolyte Solutions and Potential Stability Characteristics of Reference Electrodes with $[C_8mim^+][NTf_2^-]$ -doped Fluorosilicone 1 Membranes Tested in Artificial Blood Electrolyte Solutions.

Electrolyte	HIGH (mM)	LOW (mM)
KCl	4.7	3.5
NaCl	102.8	96.4
Na_2HPO_4	0.82	0.74
NaH_2PO_4	0.18	0.26
pH	7.45	7.35

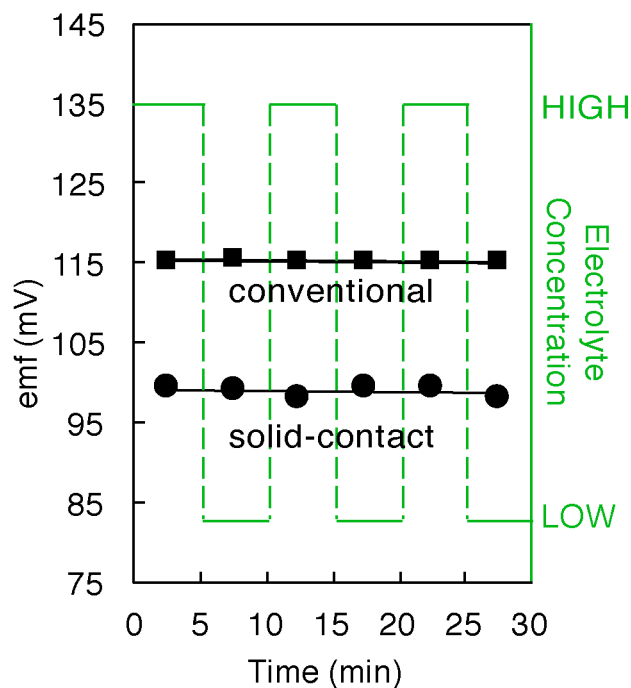


Figure 3.3. Potential responses of $[\text{C}_8\text{mim}^+][\text{NTf}_2^-]$ -doped **Fluorosilicone 1** reference electrodes to artificial blood electrolyte solutions of high and low concentrations (see **Table 3.3** for the composition of test solutions). Solid contact electrodes were prepared with CIM carbon as transducer layer, and conventional electrode bodies contained 1.0 mM KCl inner filling solution. Potentials were measured against a free-flow double-junction reference electrode. The average slopes of conventional electrodes and solid-contact electrodes are $-0.01 \pm 0.00_2$ mV/decade ($n=3$) and -0.1 ± 0.2 mV/decade ($n=3$), respectively.

3.3.5 Long-term Stability in Artificial Blood Electrolyte Solution

To test the long-term stability of reference electrodes with **Fluorosilicone 1** membranes, their emf was tested in a 1:1 mixture of HIGH and LOW solution (see **Table 3.3**) in a temperature-controlled box at 37 °C. The drift over 8 days was only -88 ± 59 $\mu\text{V}/\text{h}$

($n = 3$), with the best performing electrode giving a drift of only $20 \mu\text{V/h}$ (see **Figure 3.4**). The reference electrodes were also tested for long-term stability in tenfold diluted animal serum solution (37°C). Over 5.8 days, a drift of $112 \pm 26 \mu\text{V/h}$ ($n = 3$) was observed, which is within error the same as for measurements in artificial electrolyte solutions. For comparison, **Fluorosilicone 1** reference membranes doped with $[\text{C}_8\text{mim}^+][\text{NTf}_2^-]$ tested with a conventional electrode setup with an inner filling solution gave a drift of $27 \pm 14 \mu\text{V/h}$ ($n = 3$) over 3 days in artificial blood electrolyte solution. This suggests that additional improvements in the fabrication may further reduce the drift of the solid-contact reference electrodes.

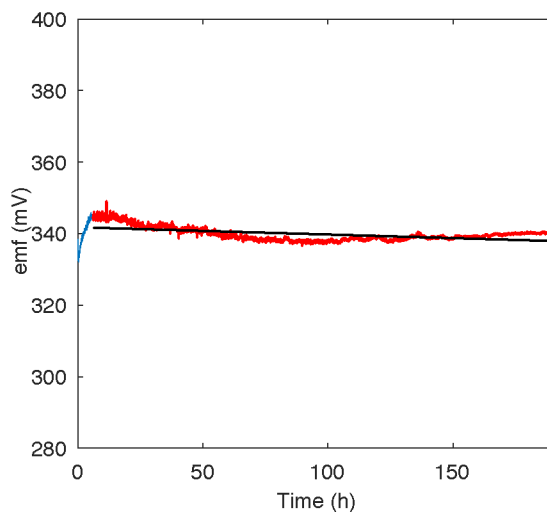


Figure 3.4. Long term emf as observed with a $[\text{C}_8\text{mim}^+][\text{NTf}_2^-]$ -doped **Fluorosilicone 1** solid-contact reference electrode immersed into artificial blood electrolyte solutions (a 1:1 mixture of the HIGH and LOW solutions described by **Table 3.3**) against a free-flow double-junction reference electrode at 37°C . (The data highlighted in red was used for the linear fit shown in black.)

3.3.6 Comparison of Reference Membranes doped with Different Ionic Liquids

In view of possible further improvements in potential stability, we carried out experiments with **Fluorosilicone 1** reference membranes doped with several other ionic liquids. Key requirements to make ionic liquids suitable for use in reference electrodes membranes are a moderate hydrophobicity and chemical stability of both the cation and anion.¹⁹⁶ To this end, three other ionic liquids were chosen for further work: [C₁₀mim⁺][NTf₂⁻] and [C₁₂mim⁺][NTf₂⁻] differ from [C₈mim⁺][NTf₂⁻] only in the length of the alkyl chain of the cation, and [NBu₃Me⁺][NTf₂⁻] shares the same anion with the other ionic liquids but has a tetraalkylammonium instead of a imidazolium cation. To test these **Fluorosilicone 1** reference electrodes, their potential was again determined in the 1.0 to 16 mM KCl range. EMF results are shown in **Figure 3.5** and potential stability characteristics are summarized in **Table 3.4**.

Table 3.4. Effect of KCl on EMF of Reference Electrodes with Fluorosilicone 1 Membranes Doped with Different Ionic Liquids.

Ionic liquid	Slope of linear regression (mV/decade) ^a	Standard ion-transfer potential, $\Delta_{\text{DCE}}^{\text{W}} \phi_i^{\circ}$ (V) ^b	Potential change over the physiological K ⁺ range (mV) ^c
[NBu ₃ Me ⁺][NTf ₂ ⁻]	2.1 ± 0.4	-0.105	0.27
[C ₈ mim ⁺][NTf ₂ ⁻]	-1.5 ± 0.7	-0.113	0.19
[C ₁₀ mim ⁺][NTf ₂ ⁻]	-0.4 ± 0.6	-0.190	0.05
[C ₁₂ mim ⁺][NTf ₂ ⁻]	0.2 ± 0.3	-0.220	0.03

^a Average and standard deviation of the slope of emf responses to KCl in the 1.0 to 16 mM activity range (n = 4, except for n = 3 for [NBu₃Me⁺][NTf₂⁻]). ^b Experimental standard

potential for ion transfer from water to 1,2-dichloroethane.^{197, 198} ^b Physiological K⁺ range: 3.5 to 4.7 mM.¹⁹⁹

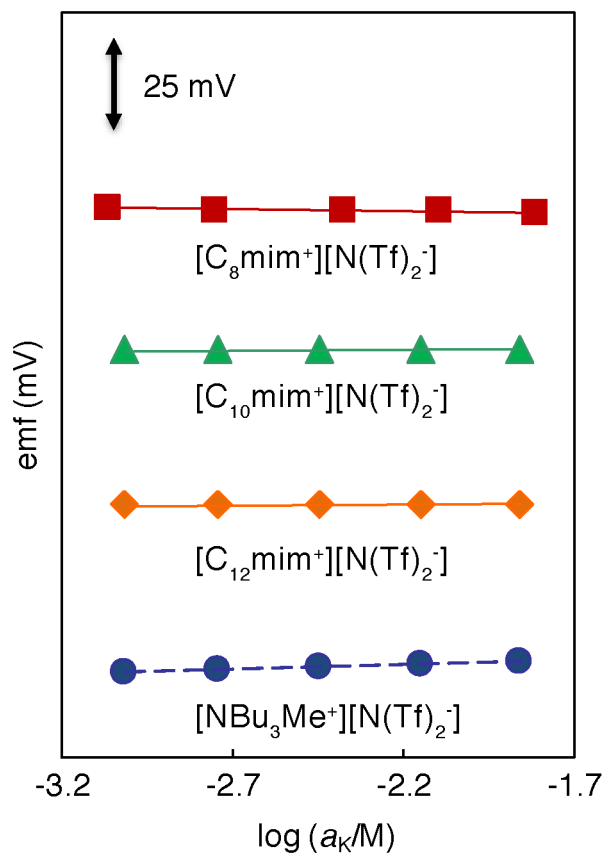


Figure 3.5. Potential responses of reference electrodes with **Fluorosilicone 1** membranes doped with [C₈mim⁺][NTf₂⁻], [C₁₀mim⁺][NTf₂⁻], [C₁₂mim⁺][NTf₂⁻], or [NBu₃Me⁺][NTf₂⁻] in the 1.0 to 16 mM KCl range. Average slopes and standard deviations of linear regressions are shown in **Table 3.4**.

Over the entire tested range of KCl concentrations, the effect of KCl on the reference potential provided by the three types of reference membranes doped with

[C₈mim⁺][NTf₂⁻], [C₁₀mim⁺][NTf₂⁻], and [C₁₂mim⁺][NTf₂⁻] was minimal. It may appear that [C₁₂mim⁺][NTf₂⁻], which has the longest alkyl chain and is the most hydrophobic of these three ionic liquids, afforded the smallest variability of the reference potential, but superiority of the [C₁₂mim⁺][NTf₂⁻]-based over the [C₁₀mim⁺][NTf₂⁻]-based reference electrode cannot be confirmed with statistical significance. This finding is consistent with similar conclusions by Lindner and co-workers for ionic liquid based reference electrodes with membrane matrixes other than silicones.¹⁸⁵

Fluorosilicone 1 reference membranes doped with [C₁₀mim⁺][NTf₂⁻] and [C₁₂mim⁺][NTf₂⁻] were also tested over five days for their long-term stability (data not shown). Similar drifts as for the membranes doped with [C₈mim⁺][NTf₂⁻] were observed, showing here too the differences among the [C₈mim⁺][NTf₂⁻]-, [C₁₀mim⁺][NTf₂⁻]-, and [C₁₂mim⁺][NTf₂⁻]-based reference electrodes to be minimal. This is consistent with the conclusion that the long-term stability may have been less influenced by the ionic liquid but more by other factors, such as the variability of the solid contact, minor fluctuations of the half-cell potential of the free-flow double-junction reference electrode with respect to which these new reference electrodes were tested, or variability in sample flow conditions.¹⁸⁵

While medical grade silicones are used in many medical devices,⁷⁸⁻⁸¹ the ionic liquid too must be considered when assessing the biocompatibility of membrane-based reference electrodes. Unfortunately, toxicology data for ionic liquids are still few, and most available studies focused on cytotoxicity.^{200, 201} In one of the few investigations of the toxicity of ionic liquids for mammals, an acute oral median lethal dose (LD₅₀) of 3150

$\mu\text{mol/kg}$ body weight was reported for 1-butyl-3-methylimidazolium chloride in female rats.²⁰² Considering the typical amount of membrane material used in a reference membrane (e. g., 12 mg silicone polymer and 3 mg ionic liquid) and assuming a worst case scenario in which the ionic liquid of an individual sensor leaches out completely over a short period, a concentration of the ionic liquid of $0.08 \mu\text{mol/kg}$ body weight would be obtained for a human exposed to this sensor. This value appears very low compared to the LD_{50} value for rats, but this is evidently only a very crude assessment. To evaluate the biocompatibility of ionic liquid based silicone reference electrodes for safety and regulatory purposes, detailed toxicology studies will be required.

3.4 Conclusions

Reference electrodes fabricated from biocompatible materials and used in wearable and implantable sensors may serve an important role in clinical diagnostics and health monitoring of the future. This work demonstrates that silicones are suitable matrixes for ionic liquid-doped reference membranes. Silicones are particularly promising for this application because they do not require a plasticizer and are available in a range of biocompatible, commercially available varieties. Use of **Fluorosilicone 1** doped with $[\text{C}_8\text{mim}^+][\text{NTf}_2^-]$, $[\text{C}_{10}\text{mim}^+][\text{NTf}_2^-]$, or $[\text{C}_{12}\text{mim}^+][\text{NTf}_2^-]$ provides stable and sample-independent potentials in solutions that contain electrolytes in concentrations representative for a wide range of blood samples. In long-term stability tests, the electrodes exhibited potential drifts as low as $20 \mu\text{V/h}$ over 8 days in artificial blood electrolyte solution and $112 \mu\text{V/h}$ over 5.8 days in 10% animal serum. Not all tested combinations of ionic liquids and silicone matrixes were successful, though, and resistance measurements and differential scanning calorimetry suggest that the limited solubility of the ionic liquid in the silicone matrix is a main reason for this.

3.5 Supporting Information

3.5.1. Characteristic of Reference Electrode Membranes

Table S3.1. Characteristics of Reference Electrode Membranes.

Membrane material	Resistance of blank membranes/ $G\Omega^a$	Resistance of IL-doped membranes/ $G\Omega^b$	Physical appearance	Fillers
Fluorosilicone 1	0.49 ± 0.85	0.0047 ± 0.0040	solid white	titanium dioxide and silica
Fluorosilicone 2	0.26 ± 0.20	0.0080 ± 0.0027	translucent white	silica
Silicone 1	14.9 ± 9.7	7.1 ± 7.9	translucent white	silica
Silicone 2	2.0 ± 1.3	5.0 ± 6.5	translucent white	silica
Silicone 3^c	0.23 ± 0.31	0.16 ± 0.12	transparent	none
Silicone 4^d	n.a.	n.a.	transparent	silica
Silicone 5^d	n.a.	n.a.	translucent white	none
Plasticized PVC ^e	—	0.00059 ± 0.00008	transparent	none

^a Membranes without IL doping (n = 4). ^b Membranes doped with 20 wt % $[C_8mim^+][NTf_2^-]$ (n = 4). ^c Membranes with a **Silicone 3** matrix and doped with 20 wt % $[C_8mim^+][NTf_2^-]$ contained liquid aggregates clearly visible to the naked eye. ^d At the manufacturer's recommended ratio of the two components (100:0.5 of base/crosslinker to catalyst for **Silicone 4** and 1:1 for **Silicone 5**), films of 200 μm thickness of neither **Silicone 4** or **Silicone 5** were not self-supporting. ^e Resistance value from reference 1 (n = 4).

3.5.2. Sample Dependence of the Potential of Reference Electrodes Based on Different Silicone Materials.

Table S3.2. Sample Dependence of the Potential of Reference Electrodes Based on Different Silicone Materials.

Membrane material	Difference between maximum and minimum potential over full activity range (mV) ^a	Slope of linear regression (mV/decade) ^b
Fluorosilicone 1	-1.9 ± 0.9	-1.5 ± 0.7
Fluorosilicone 2	13.0 ± 8.1	10.1 ± 6.2
Silicone 1	26.6 ± 11.5	20.7 ± 8.9
Silicone 2	8.7 ± 6.5	7.0 ± 5.3
Silicone 3	24.7 ± 16.9	19.4 ± 13.0

^aAverage and standard deviation of the difference between the maximum and minimum potential over the entire activity range (n = 4). ^bAverage and standard deviation of slopes of linear regression of potentials taken at different activities (n = 4).

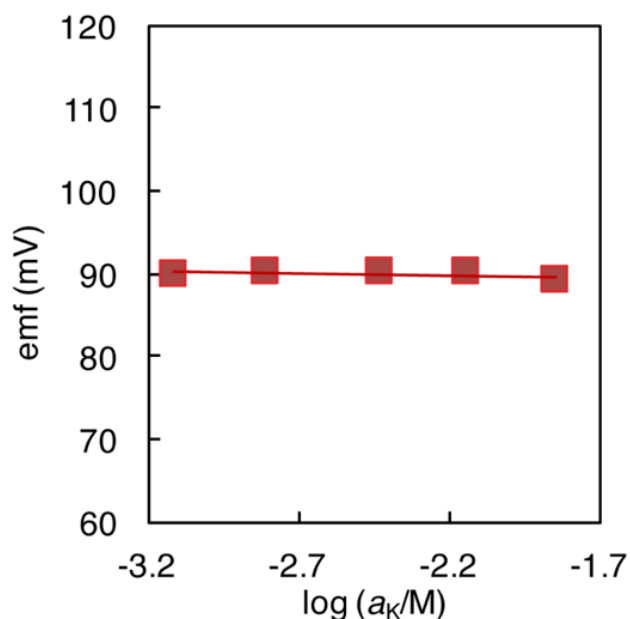


Figure S3.1. Potential stability of **Fluorosilicone 1** solid-contact reference electrodes in the range of 1.0 to 16 mM KCl. Membranes were doped with $[\text{C}_8\text{mim}^+][\text{NTf}_2^-]$, and CIM carbon was used as solid contact between the silicone membrane and conducting substrate. Measurements started in 1.0 mM KCl, and aliquots of concentrated KCl solution were added to sequentially double the KCl concentration. Potentials were measured against a free-flow double-junction reference electrode.

3.5.3 Water Layer Test

In order to be able to perform a water layer test, ionophore-doped solid-contact electrodes were prepared by dissolving 200 mg **Fluorosilicone 1**, 2.0 mg valinomycin, and 1.2 mg NaTFPB (75 mol % with respect to valinomycin) in THF. Electrodes were fabricated in the same fashion as the solid-contact reference electrodes. After complete curing of the membranes, the electrodes were conditioned in 0.1 M KCl for two days before water layer tests were performed.

Formation of an unintentional water layer between the solid-contact material and ion-selective membrane is a common concern for solid-contact ISEs.²⁰³ The presence of an undesirable water layer is evidenced by a positive potential drift when switching from a primary cation solution to an interfering cation solution and a negative potential drift when switching back from the interfering cation solution to the primary ion solution. Here, to assess whether such an undesirable water layer was formed between **Fluorosilicone 1** and the solid contact material used, K⁺-selective **Fluorosilicone 1** membranes were first immersed into 0.1 M KCl solution for 48 h prior to measurements. After the start of emf measurements, at t = 0.4 h, the solution was switched to 0.1 M NaCl. This resulted in an immediate drop of 176 mV in potential, confirming the high selectivity for K⁺. At t = 2.5 h, the solution was switched back to 0.1 M KCl, resulting in an immediate potential increase back to what had been observed previously in 0.1 M KCl. No potential drift was observed during these processes, showing that no undesired water layer was formed between **Fluorosilicone 1** and the solid-contact material used in this study (see **Figure S3.2**).

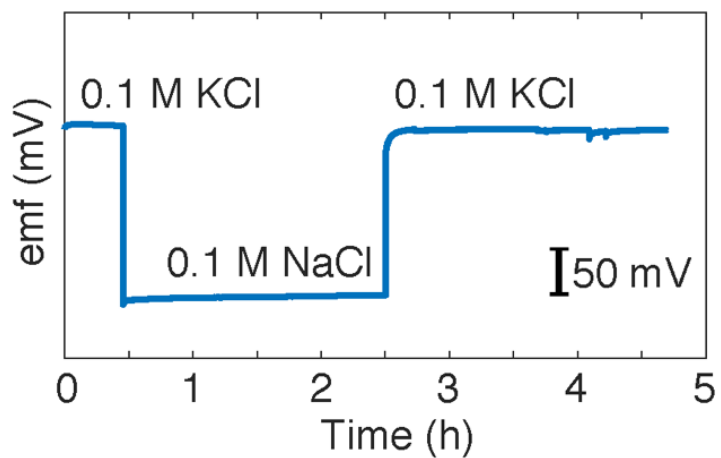


Figure S3.2. Water layer test of a **Fluorosilicone 1** solid-contact electrode. The electrode was conditioned in 0.1 M KCl solution for 48 h prior to measurements. At $t = 0.4$ h, the solution was exchanged for a 0.1 M NaCl solution, and at $t = 2.5$ h, the solution was switched back to 0.1 M KCl.

3.5.4 Differential Scanning Calorimetry Original Traces

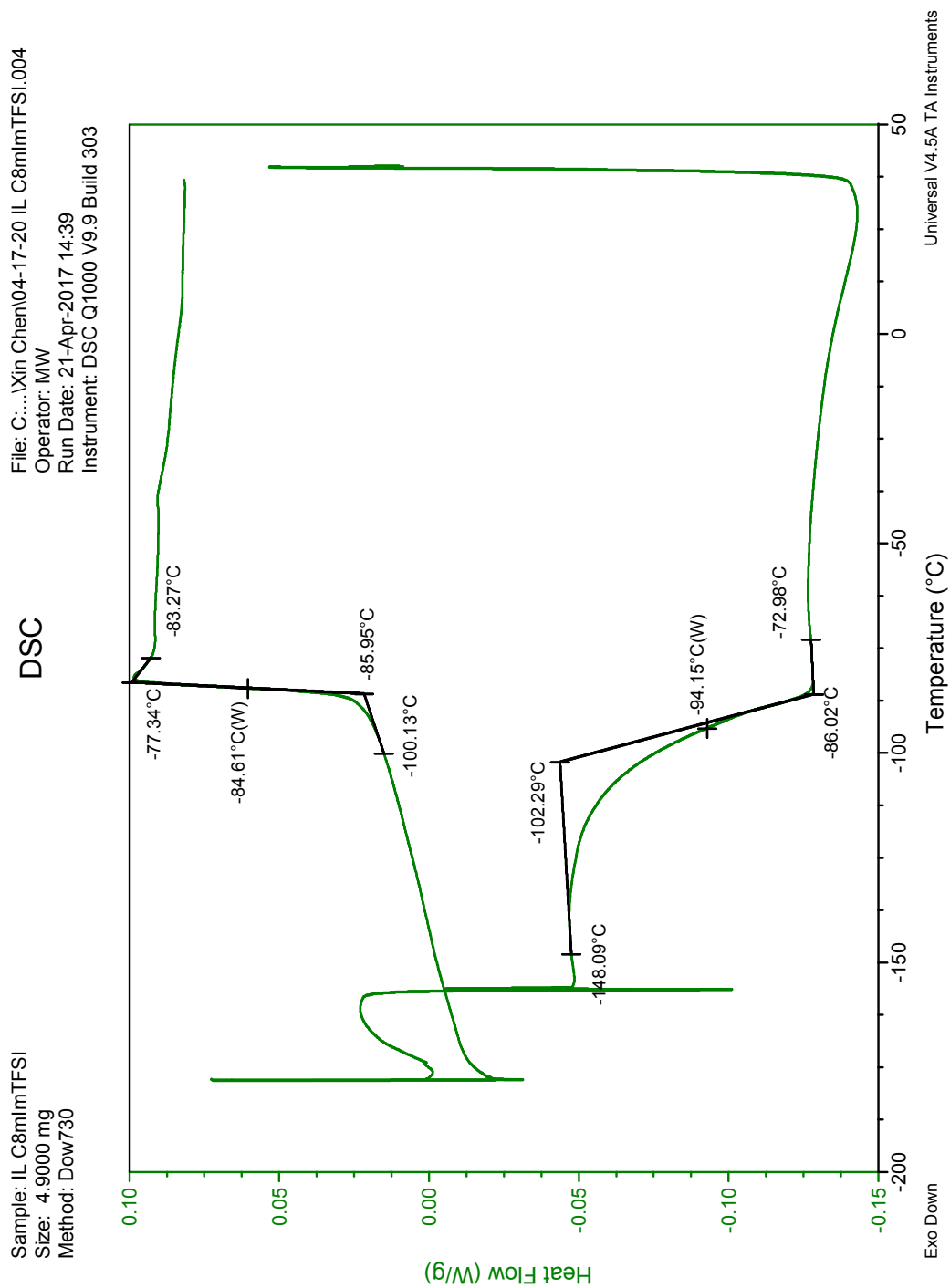


Figure S3.3. DSC trace of ionic liquid $[C_8mim^+][NTf_2^-]$.

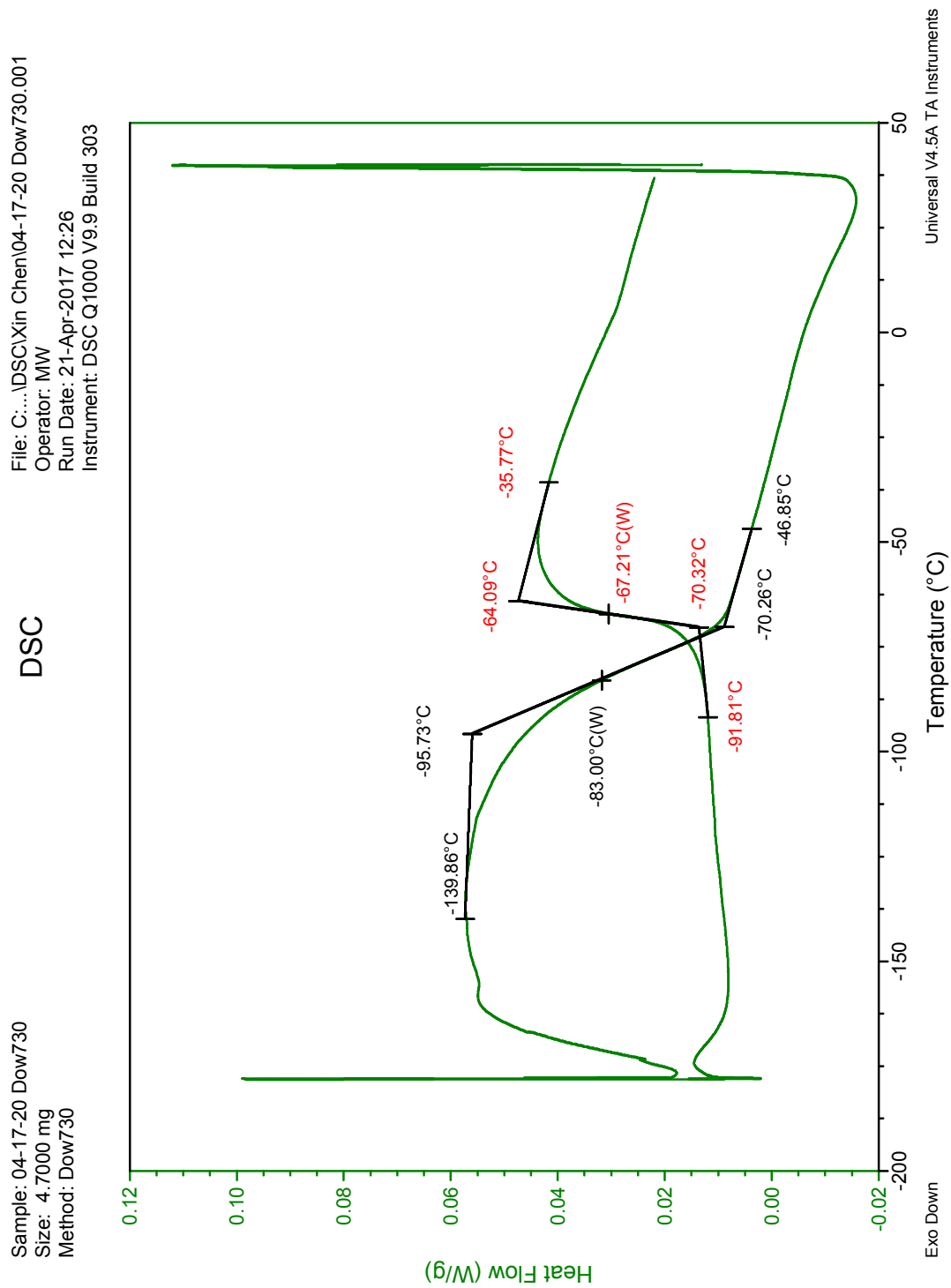


Figure S3.4. DSC trace of neat polymer **Fluorosilicone 1**.

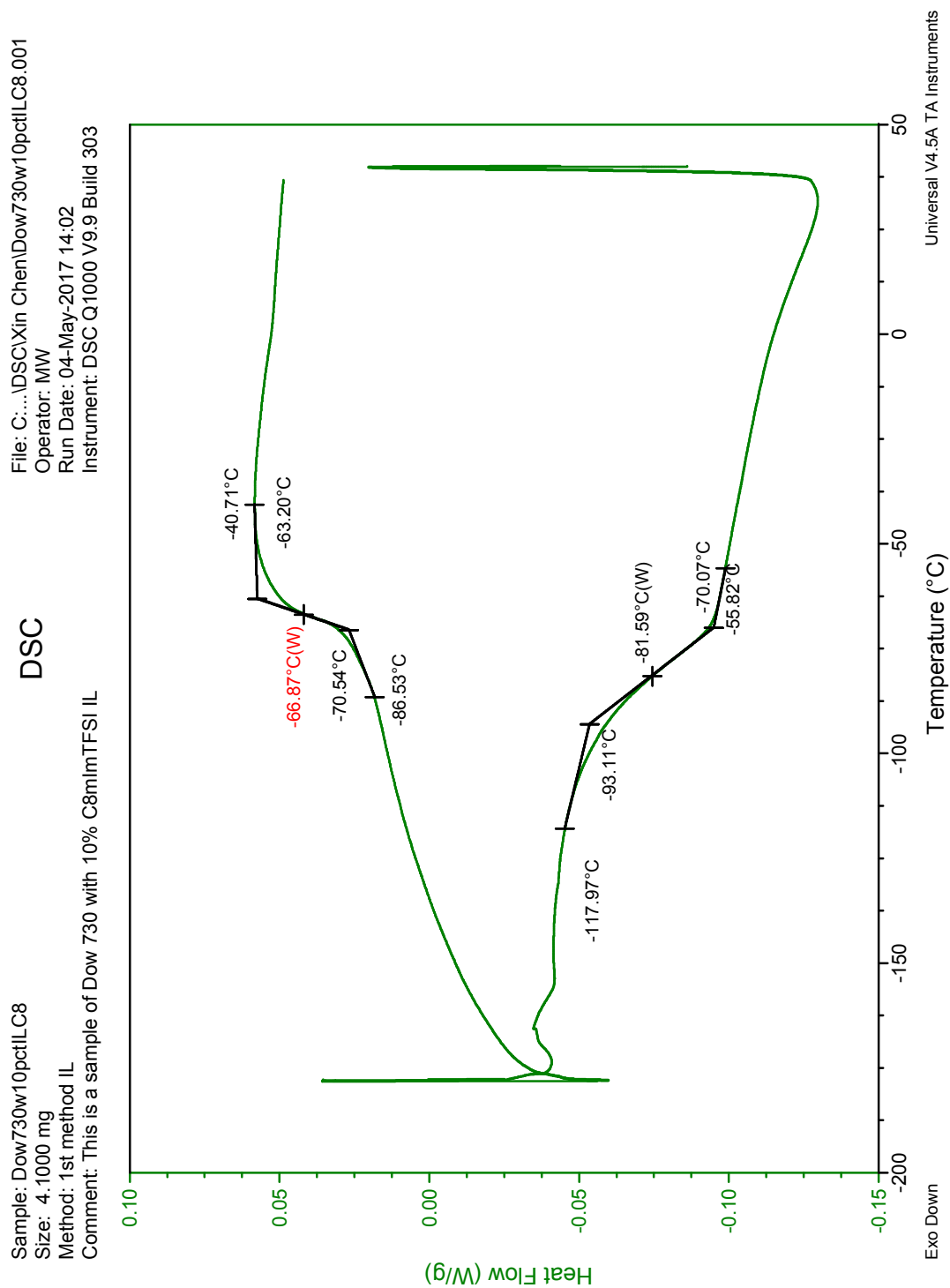


Figure S3.5. DSC trace of **Fluorosilicone 1** membrane doped with 10 wt% $[\text{C}_8\text{mim}^+][\text{NTf}_2^-]$.

File: ...04-17-20 Dow730w20perILC8mlmTFSI.001
Operator: MW
Run Date: 21-Apr-2017 13:16
Instrument: DSC Q1000 V9.9 Build 303

DSC

Sample: 04-17-20 Dow730w20perILC8mlmTFS
Size: 4.3000 mg
Method: Dow730

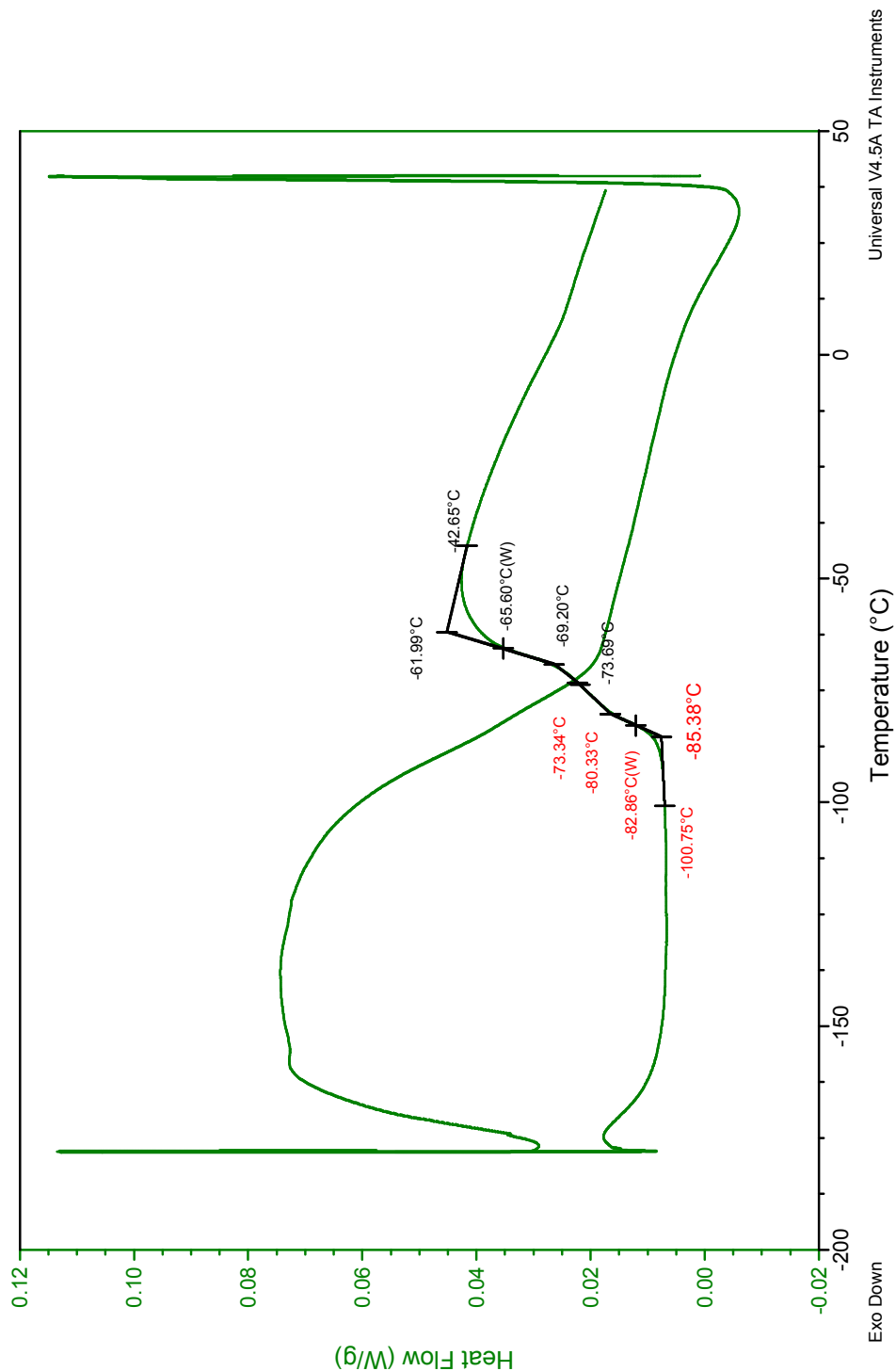


Figure S3.6. DSC trace of **Fluorosilicone 1** membrane doped with 20 wt% $[\text{C}_8\text{mim}^+][\text{NTf}_2^-]$.

File: C:\TA\Data\DSC\Xin Chen\MED1555blank.001
Operator: HC
Run Date: 28-Mar-2019 19:29
Instrument: DSC Q1000 V9.9 Build 303

DSC

Sample: MED1555blank
Size: 6.5000 mg
Method: 1st method IL

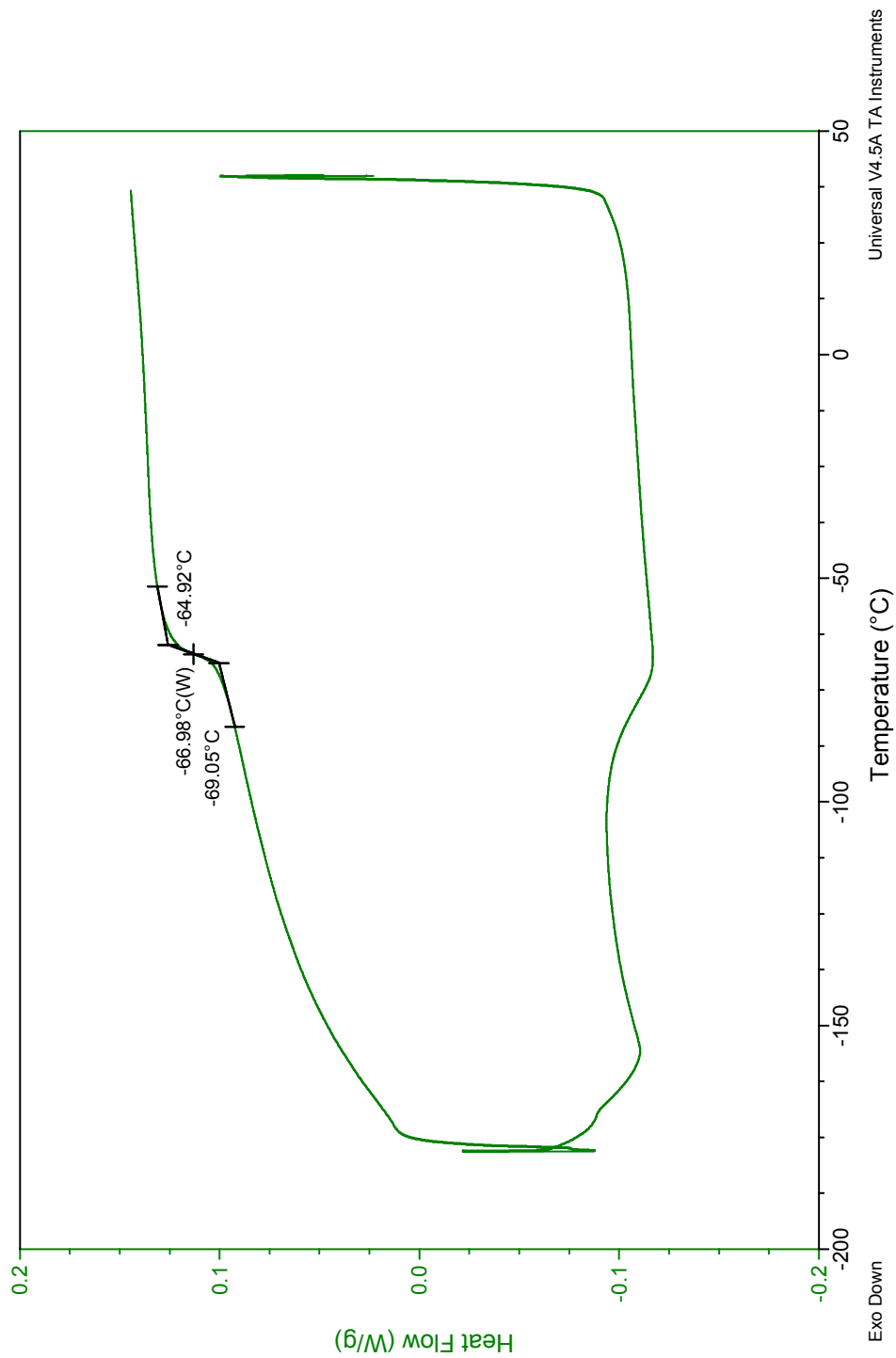


Figure S3.7. DSC trace of neat polymer Fluorosilicone 2.

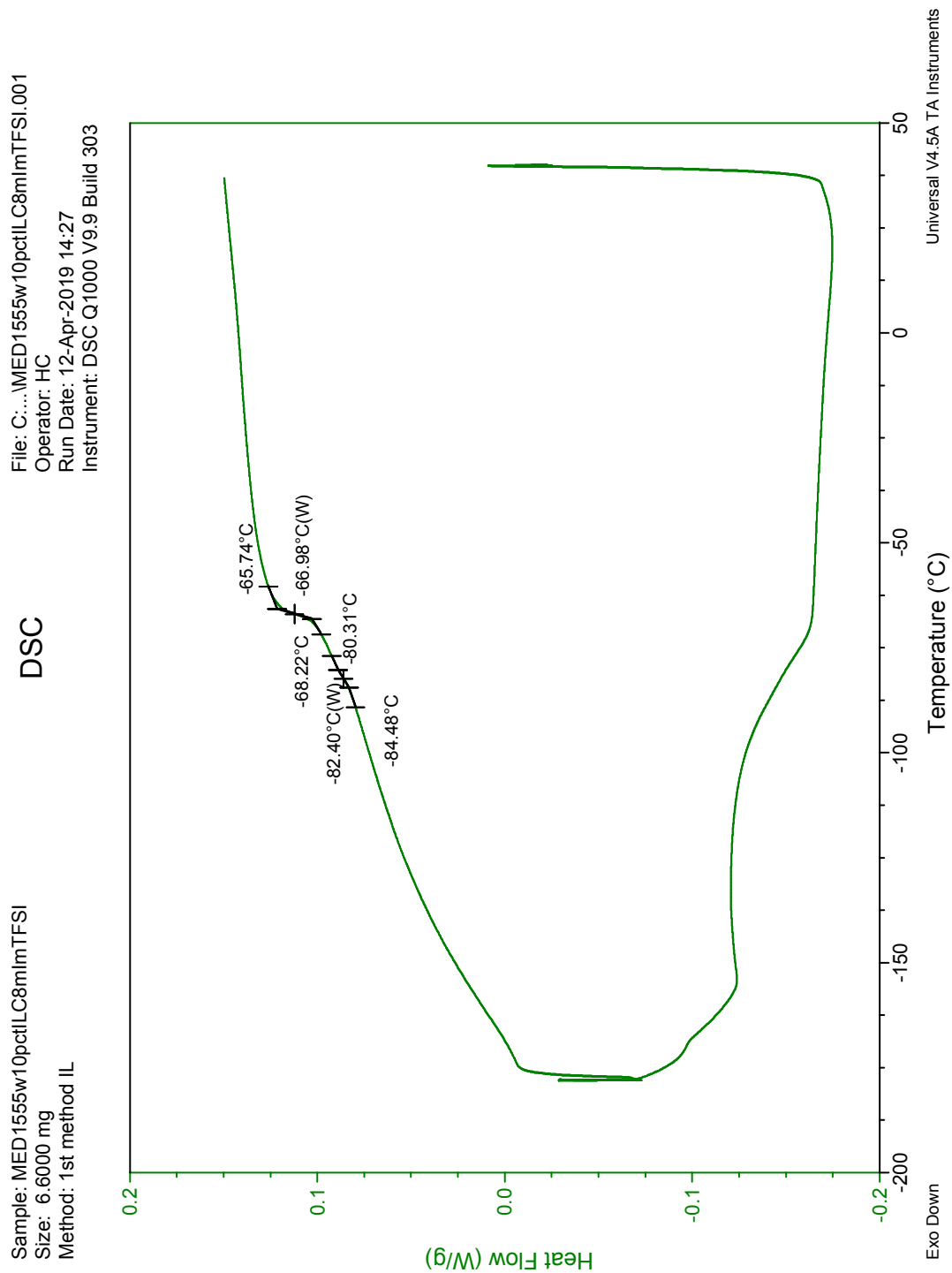


Figure S3.8. DSC trace of **Fluorosilicone 2** membrane doped with 10 wt% $[C_8mim^+][NTf_2^-]$.

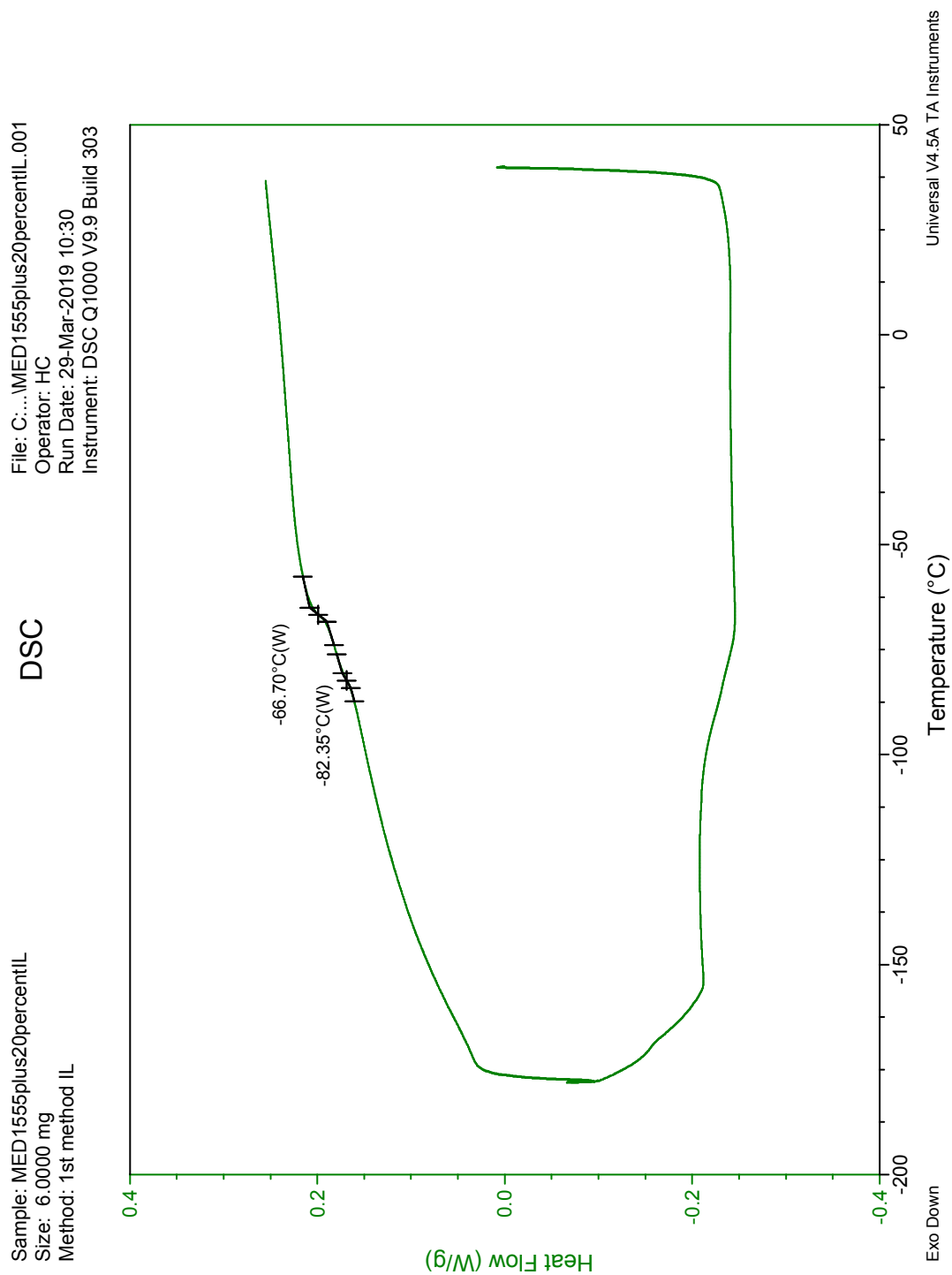


Figure S3.9. DSC trace of **Fluorosilicone 2** membrane doped with 20 wt% $[\text{C}_8\text{mim}^+][\text{NTf}_2^-]$.

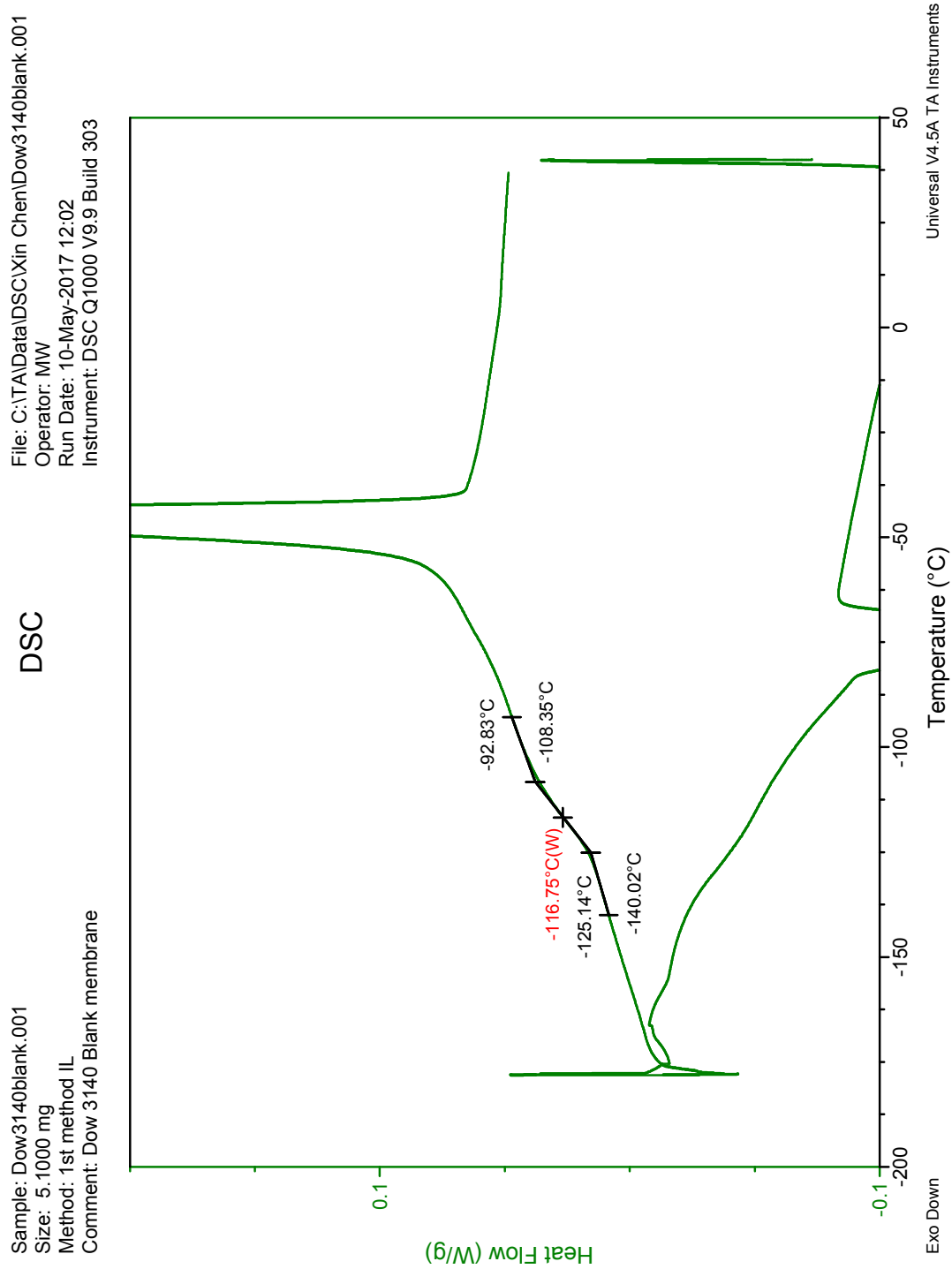


Figure S3.10. DSC trace of neat polymer **Silicone 1**.

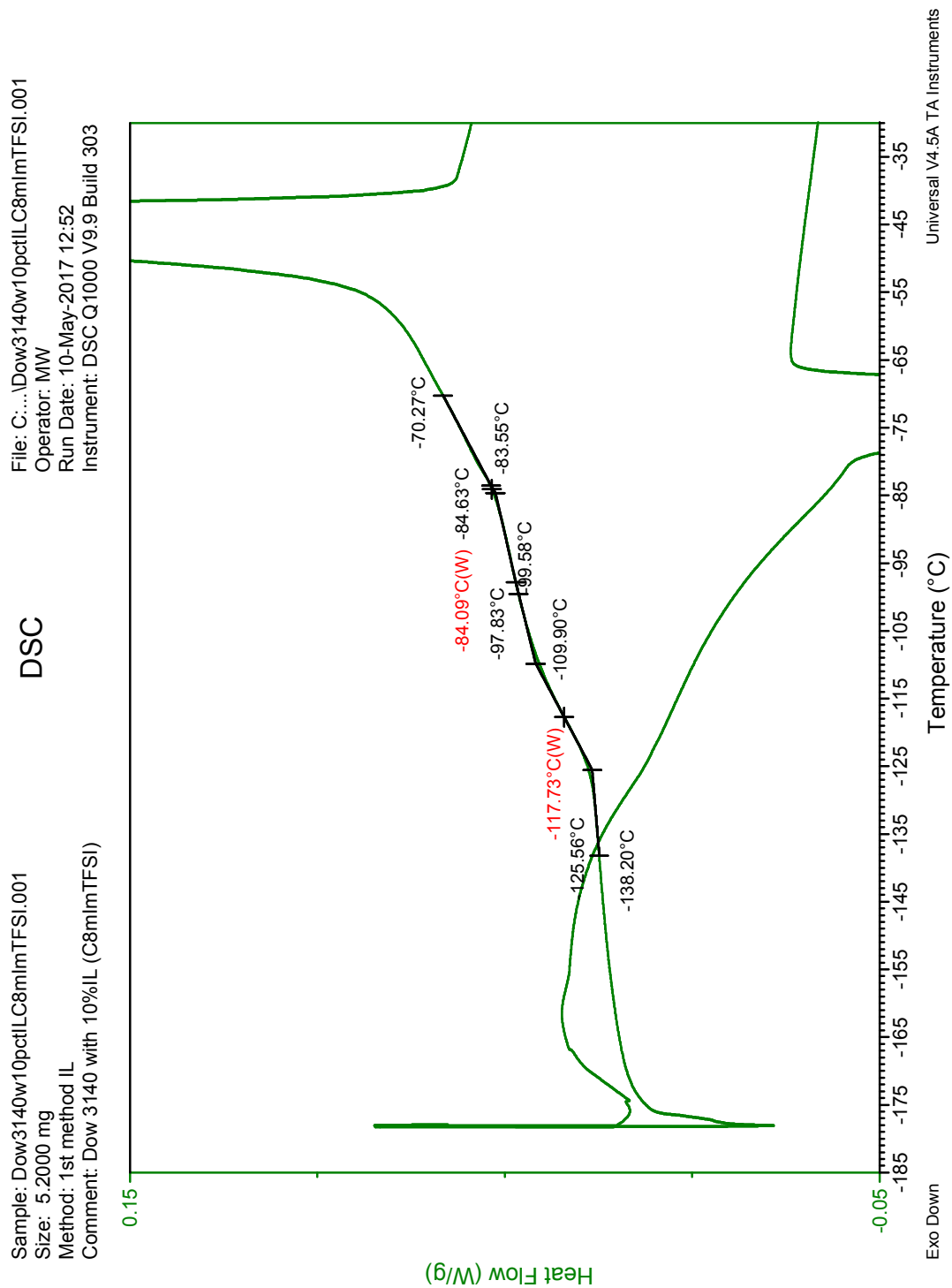


Figure S3.11. DSC trace of **Silicone 1** membrane doped with 10 wt% $[C_8mim^+][NTf_2^-]$.

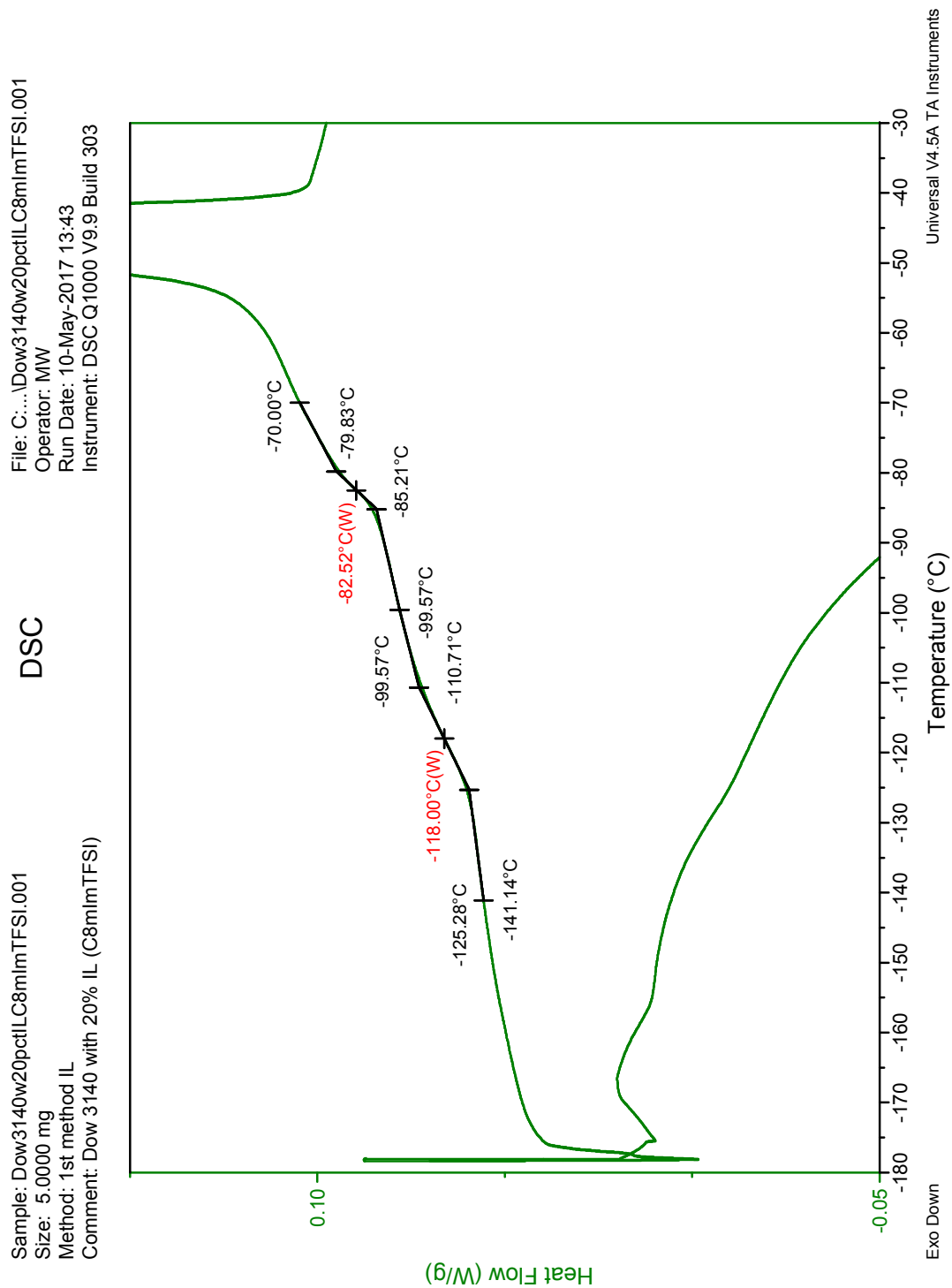


Figure S3.12. DSC trace of **Silicone 1** membrane doped with 20 wt% $[C_8mim^+][NTf_2^-]$.

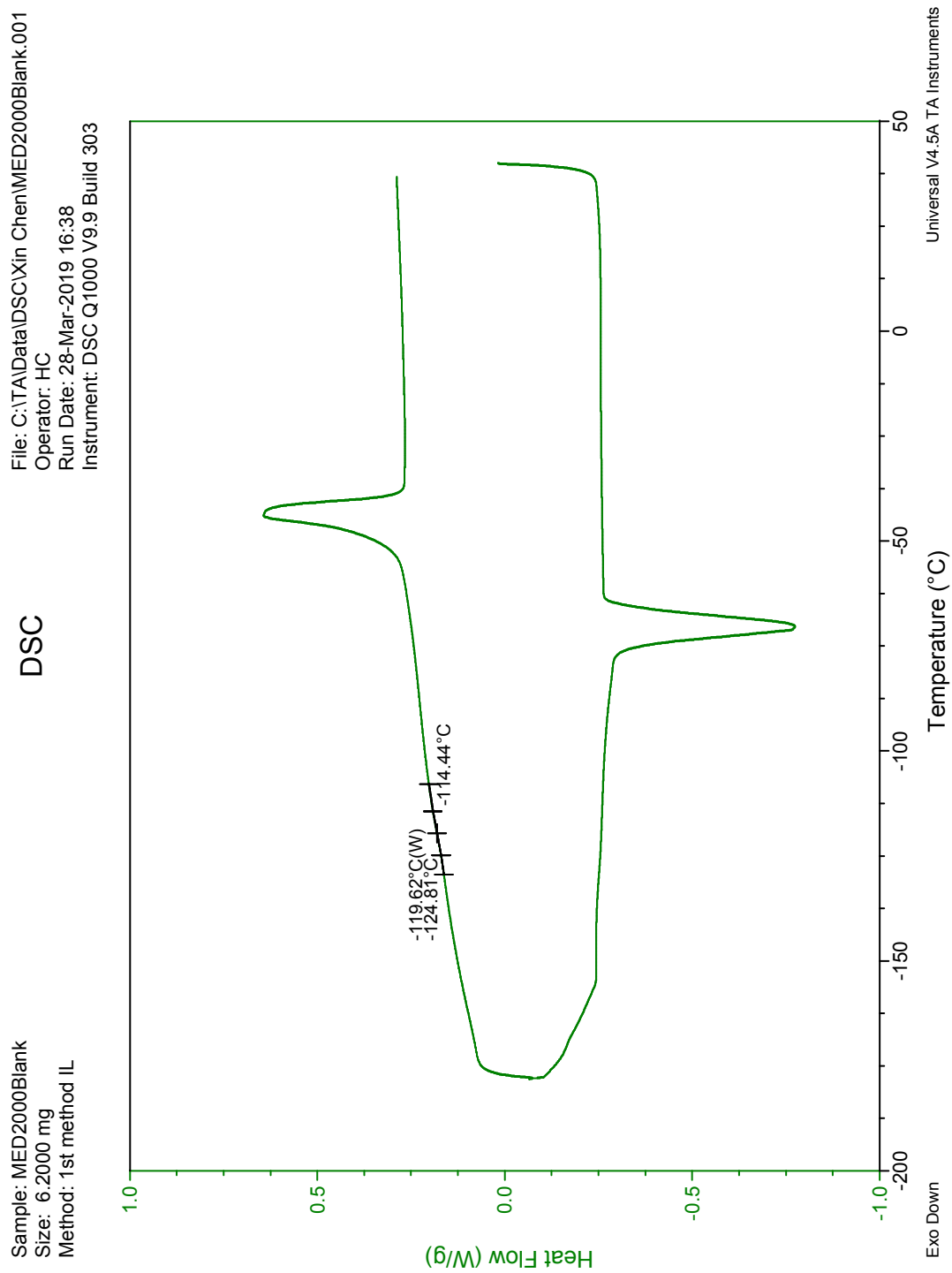


Figure S3.13. DSC trace of neat polymer **Silicone 2**.

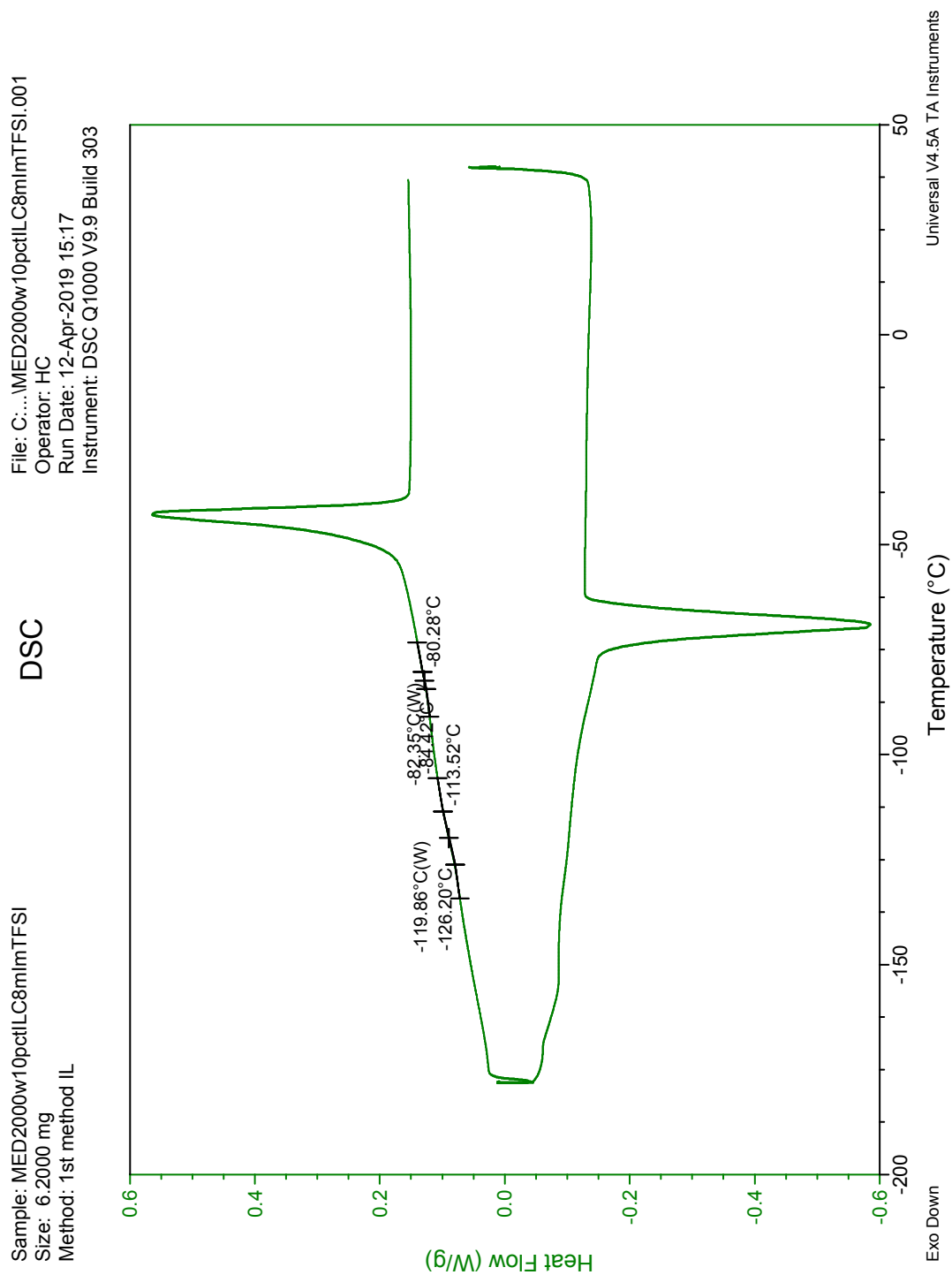


Figure S3.14. DSC trace of **Silicone 2** membrane doped with 10 wt% $[C_8mim^+][NTf_2^-]$.

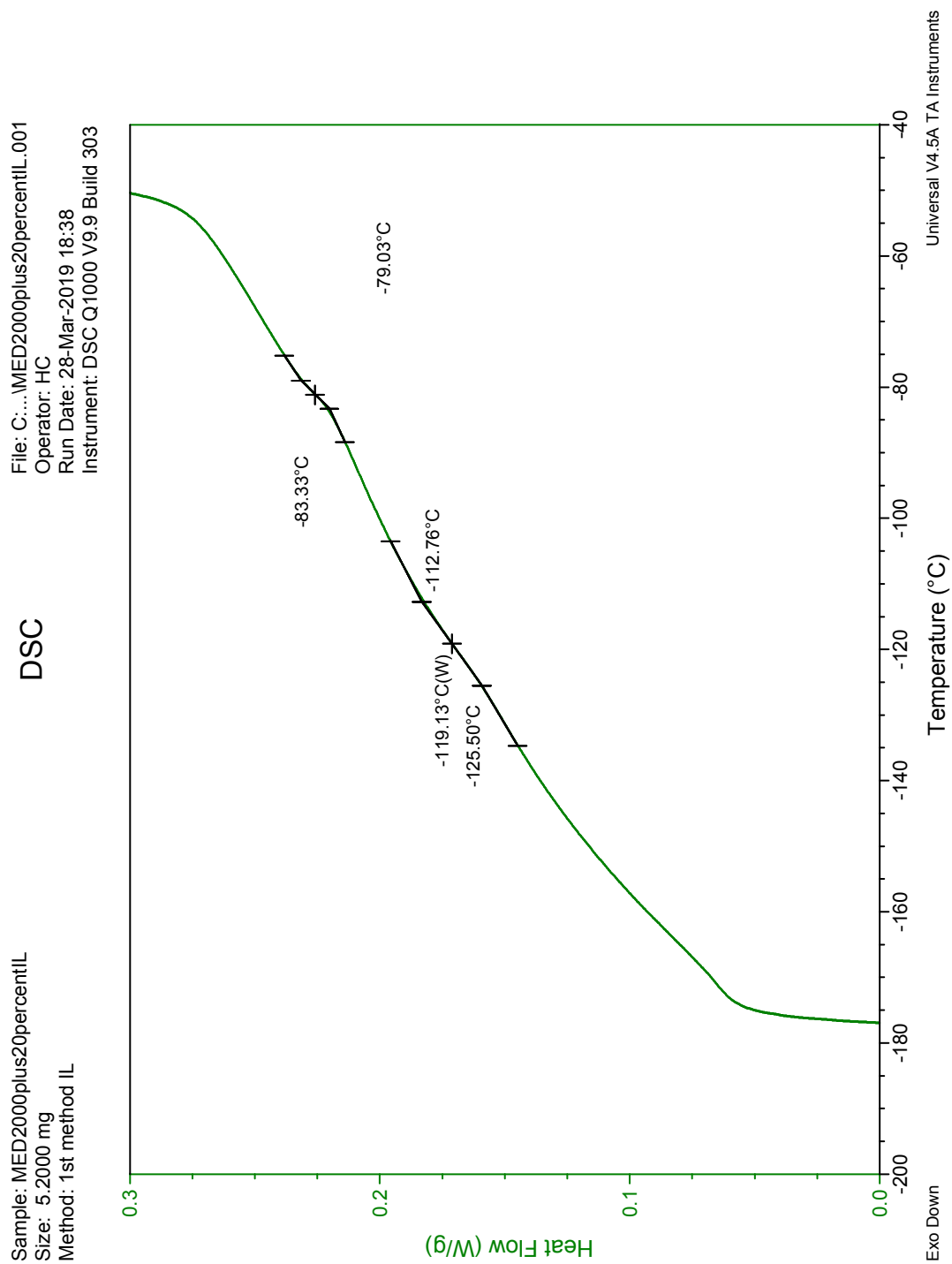


Figure S3.15. DSC trace of **Silicone 2** membrane doped with 20 wt% $[C_8mim^+][NTf_2^-]$.

File: C:\TA\DATA\DSC\Xin Chen\MED6381blank.001
Operator: HC
Run Date: 29-Mar-2019 11:20
Instrument: DSC Q1000 V9.9 Build 303

DSC

Sample: MED6381blank
Size: 5.4000 mg
Method: 1st method IL

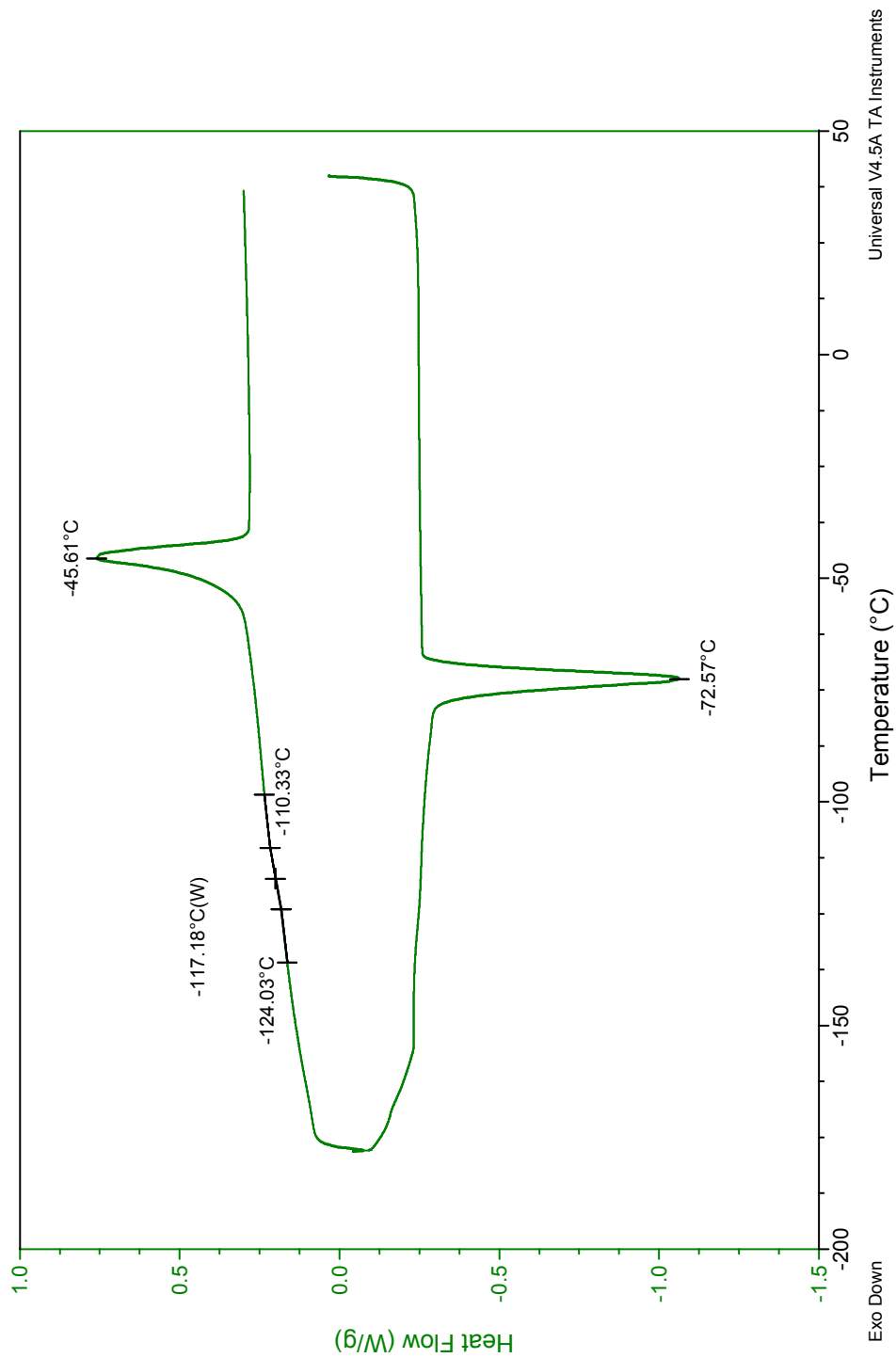


Figure S3.16. DSC trace of neat polymer **Silicone 3**.

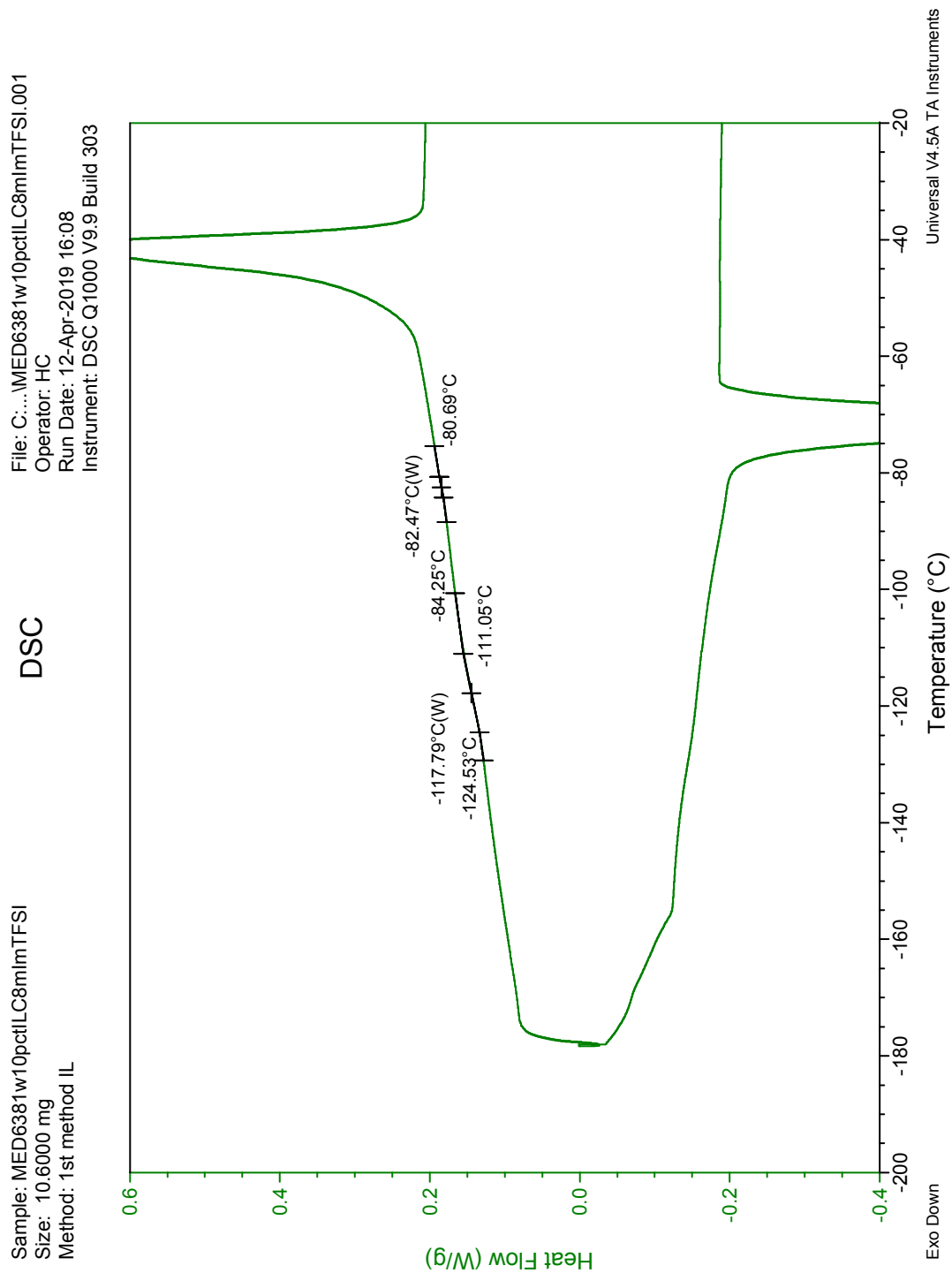


Figure S3.17. DSC trace of **Silicone 3** membrane doped with 10 wt% $[C_8mim^+][NTf_2^-]$.

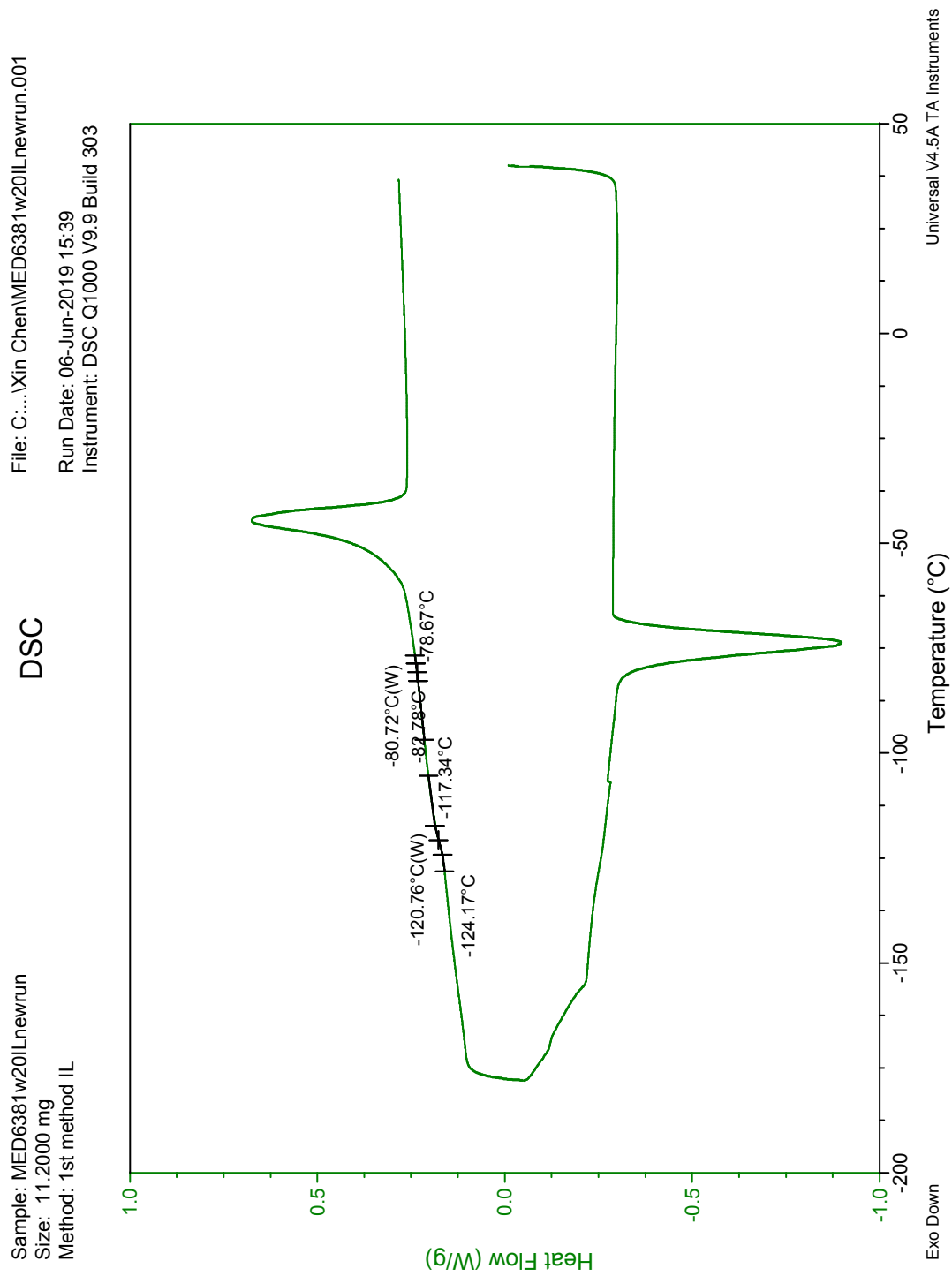


Figure S3.18. DSC trace of **Silicone 3** membrane doped with 20 wt% $[C_8mim^+][NTf_2^-]$.

IV. DEVELOPMENT OF BIOCOMPATIBLE ELECTROCHEMICAL SENSORS FOR POTASSIUM MEASUREMENTS

Brian Spindler made contributions in calibrations of silicone-based ISEs.

4.1 Introduction

The introduction of pacemakers (PMs) and implantable cardioverter defibrillators (ICDs) has enabled automatic detecting and correcting of life-threatening cardiac arrhythmias, such as ventricular fibrillation and non-perfusing tachycardia.²⁰⁴ Sensing data including detected arrhythmias can also be transmitted wireless to physicians.²⁰⁵ This remote monitoring ability allows physicians to take timely and proactive actions,²⁰⁶ improves quality of care and assurance for patients,²⁰⁷ and reduces overall cost of healthcare system.^{208, 209} However, the sensing ability of current PMs and ICDs is limited only to basic information such as electrocardiograms, lead impedance, and device battery voltage. Other critical information, for example, concentrations of key electrolytes, can be extremely beneficial for patients with cardiovascular diseases. Electrolyte disorders, chiefly hyperkalemia in which blood serum potassium (K^+) is severely elevated, can cause life-threatening cardiac arrest.²¹⁰ Implantable ion sensors can be of great assistance to monitoring levels of these important electrolytes in patients.

Potentiometric ion-selective electrodes (ISEs) are widely used in many fields including industrial process, laboratory testing, and environmental monitoring.¹⁻⁶ Notably, ionophore-based ISEs are used in commercial clinical analyzers as they are the recommended method for potassium and sodium (Na^+) measurements in diluted serum, plasma, or whole blood by the International Federation of Clinical Chemistry and Laboratory Medicine (IFCC).^{211, 212} Potassium and sodium ions have normal ranges of 3.4 to 4.7 mM and 125 to 145 mM in blood, respectively.¹⁹⁹ With an accepted measurement error of ± 0.5 mM by federal regulation²⁷, a potentiometric selectivity ($\log K_{K,Na}^{pot}$) of -2.45

on the logarithmic scale is needed for a ± 0.5 mM measurement error of K^+ in the presence of high concentrations of Na^+ (145 mM). A more stringent criterion of no more than 5% error when detecting the least amount of K^+ in the presence of most concentrated Na^+ requires a selectivity of -2.92. Successful K^+ ionophores used in ISEs, such as the valinomycin,²¹³ the bis (crown ether) BME-44,^{214, 215} and the less used hemispherand ionophores⁸⁶ (see **Figure 4.1**) are all able to provide potentiometric selectivity ($\log K_{K,Na}^{pot}$) better (i.e. more negative) than -3.3.³

When designing sensors for human body use, including implantable and wearable devices, in addition to selectivity, considerations should also be given to preventing leaching of any sensor components that may pose potential toxicity. The most commonly used PVC-based membranes contain plasticizers that gradually leach out. This not only reduces selectivity and lifetime but can also cause inflammatory reactions.⁶⁴⁻⁶⁷ Suitable plasticizer-free polymer options with glass transition temperatures below room temperature include silicones, polyurethanes, polyacrylates, and polymethacrylates.^{87, 106,}

190

Besides plasticizers, typical ionophores such as valinomycin can also gradually leach out of the sensing membrane,^{12, 122, 123} and depending on the amount used and specific applications, can be toxic to surrounding cells and tissues.^{66, 216-218} To alleviate these potential toxic effects as well as preserve ISE functionality, efforts have been made to covalently attach ionophores to polymeric membranes. One strategy is to minimally modify existing ionophores with functional groups that can be covalently attached to polymer backbones but at the same time maintain the core structure for selectivity. Such

examples include derivatives of valinomycin,^{124, 125} BME-44,¹²⁶ and hemispherand-21^{84, 86} as covalently attachable K⁺ ionophores, a bis(12-crown-4) ether as covalently attachable Na⁺ ionophore,¹⁰⁴ a derivative of ETH 129 as covalently attachable Ca²⁺ ionophore,¹²⁷ and a calix[4]arene as covalently attachable Na⁺ ionophore^{83, 102, 108} and as Pb²⁺ ionophore.¹²⁸ Others have developed covalently attachable ionophores that are structurally very different from previously reported mobile ionophores. Such examples include mono crown ethers as K⁺,^{107, 109, 129, 130} Na⁺,^{102, 104} and Pb²⁺ ionophores,¹³¹ a cyclic polyamine as dibasic phosphate ionophore,¹³² a derivative of Chromoionophore II as H⁺ ionophore,¹³³ and porphyrins as In³⁺ ionophores.¹³⁴

Here, uses of silicone (polydimethylsiloxane) and fluorosilicone (poly[(3,3,3-trifluoropropyl)methylsiloxane]) materials as ISEs membranes without any added plasticizer are described. Silicone materials have been used widely in medical devices,⁷⁸⁻⁸² and medical grade silicones are also available.⁶³ For the first time, a minimally modified BME-44 with a novel triethoxysilyl functional unit was synthesized that can be covalently attached to silicone during the polysiloxane curing process. Silicone/fluorosilicone-based ISEs with mobile and triethoxysilyl-modified BME-44 were tested. The design of sensors for implantable and wearable devices, fabrication of thin-layer planar electrodes, and leaching of sensor components out of ISE membranes are also discussed.

4.2 Experimental

4.2.1 Materials

Potassium tetrakis(4-chlorophenyl)borate (KTPClPB), BME-44 (Potassium Ionophore III), valinomycin (Potassium Ionophore I), 4'-amino-5'-nitrobenzo-15-crown-5, 1,1'-carbonyldiimidazole (CDI), phosgene solution (15 wt% in toluene) in a sure/seal bottle, 2-(allyloxymethyl)-2-ethyl-1,3-propanediol, triethoxysilane, chloroplatinic acid hydrate (99.995% trace metal basis), anhydrous inhibitor-free tetrahydrofuran (THF), anhydrous toluene, and anhydrous dichloromethane (DCM) were purchased from Sigma Aldrich (St. Louis, MO). Triethylamine was purchased from Fisher Scientific (Fair Lawn, NJ). Dow RTV 730 fluorosilicone (**Fluorosilicone 1**) was purchased from Dow Corning (Midland, MI). The NuSil silicones MED-1555 (**Fluorosilicone 2**) and MED-2000 (**Silicone 1**) were purchased from NuSil (Carpinteria, CA). Anhydrous THF was passed through a column of basic alumina to remove traces of peroxide. Anhydrous DCM was further dried over 4 Å molecular sieves. Colloid-imprinted mesoporous (CIM) carbon was prepared as previously reported.¹⁹³ All aqueous solutions were prepared with deionized and charcoal-treated water (0.182 MΩ cm specific resistance) from a Milli-Q Plus reagent-grade water system (Millipore, Bedford, MA).

4.2.2 Silicone Electrode Fabrication

Removal of fillers: Fillers (trimethylsilylated silica and titanium dioxide) were removed in some cases from **Fluorosilicone 1** before it was used for membrane preparation. To do so, 250 mg pristine **Fluorosilicone 1** was added to 1 mL THF and stirred before it

was centrifuged at 14,000 rpm for 10 min. The upper translucent polymer solution was carefully decanted, leaving solid fillers (18 wt% of pristine **Fluorosilicone 1**) at the bottom of the microcentrifuge tubes.

Electrode preparation: Solutions to prepare K⁺-selective silicone membranes were prepared by adding 1 mL of a THF solution of 200 mg silicone polymer (pristine **Fluorosilicone 1**, centrifuged **Fluorosilicone 1**, **Fluorosilicone 2**, or **Silicone 1**) to 3.0 mg valinomycin and 0.60 mg KTpClPB (45 mol% with respect to valinomycin), 2.8 mg BME-44 and 0.64 mg KTpClPB (45 mol% with respect to BME-44), or 2.65 mg covalently attachable triethoxysilyl-modified BME-44 and 0.65 mg KTpClPB (45 mol% to BME-44). For the conventional electrode setup, after the solution was stirred, it was added into a Teflon Petri dish of 25 mm diameter and left for the solvent to evaporate overnight to give a master membrane of approximately 200 μm thickness. Small circular disks (7 mm diameter) were cut from these master membranes and mounted into Philips type electrode bodies¹⁶⁵ (Glasbläserei Möller, Zürich, Switzerland; Ag/AgCl internal reference) with a 1.0 mM KCl inner filling solution. The electrodes were conditioned in 1.0 mM KCl for two days prior to use.

For the preparation of solid-contact reference electrodes, gold electrodes (planar circular Au electrodes with a 2 mm diameter, embedded into an inert Kel-F polymer shaft; CH Instruments, Austin, TX) were polished on a polishing cloth, first with 0.5 μm and then with 0.03 μm aqueous aluminum oxide slurry (Buehler, Lake Bluff, IL), and then sonicated, first in water and then in ethanol, each for 6 min. A stream of argon was used to dry the electrodes. A CIM carbon suspension solution was prepared by dissolving 47.5 mg CIM

carbon and 2.5 mg pristine **Fluorosilicone 1** in 1.0 mL THF, followed by sonication for 30 min. Then, 30 μL of this suspension was dropcast with a micropipette onto the gold electrode, and the solvent was allowed to evaporate. This was followed by two aliquots (20 μL followed by 30 μL) of silicone membrane solution dropcast with a micropipette onto the CIM carbon layer. After complete curing of the silicones, the electrodes were conditioned for two days in 1.0 mM KCl solution prior to use.

For the preparation of thin-layer spin-coated membranes, CHI gold electrodes were prepared in the same fashion. A 10 μL solution containing 5 μL of polymer solution and 5 μL THF was closely cast onto a spinning CHI gold electrode (500 rpm) with a microsyringe. The THF quickly evaporated, yielding a membrane of approximately 30 μm thickness. For the preparation of dip-coated membranes, thin tip-shaped gold electrodes (14 mm long, 0.6 mm wide, 0.03 mm thick, Medtronic, Mounds View, MN) were first polished on a polishing cloth with 0.3 μm and 0.05 μm aqueous aluminum oxide slurry to remove a polymeric protection layer and then rinsed with THF, acetone, and ethanol. Then the gold surface of the electrodes was briefly submerged (dipped) in the ion-selective membrane solution. After the solvent had evaporated to a large extent (1 to 2 min) and a thin layer membrane had formed, a second dip-coating was performed in the same fashion. After complete curing of the silicones, the electrodes were conditioned overnight in 1.0 mM KCl solution prior to use.

4.2.4 Electrochemical Measurement.

Potentiometric measurements were performed with a 16-channel potentiometer (Lawson Labs, Malvern, PA) controlled by EMF Suite software (Fluorous Innovation, Arden Hills, MN). Potential responses were measured in stirred solutions against a conventional free-flow double-junction reference electrode (DX200, Mettler Toledo, Switzerland; AgCl saturated 3.0 M KCl as inner reference electrolyte and 1.0 M LiOAc as bridge electrolyte). All emf values were corrected for the liquid junction potentials of the double-junction reference electrode.⁵¹ Activity coefficients were calculated based on a two parameter Debye-Hückel approximation.¹⁶⁶ Membrane resistances were measured with the known shunt method.¹²

4.2.5 Synthesis of Covalently Attachable Triethoxysilyl-Modified-BME-44

Synthesis of 4'-isocyanato-5'-nitrobenzo-15-crown-5: Phosgene solution was used in this synthesis. Appropriate personal protective equipment and extreme caution should be used.

The intermediate 4'-isocyanato-5'-nitrobenzo-15-crown-5 was synthesized from the starting material 4'-amino-5'-nitrobenzo-15-crown-5 by converting the amino to an isocyanato group through reaction with phosgene. The method used was modified from a literature, using phosgene solution (15 wt% in toluene) as a safer alternative to phosgene gas.²¹⁹ 200 mg (0.601 mmol) 4'-amino-5'-nitrobenzo-15-crown-5 was added to a round bottom flask, followed by addition of 1 mL chlorobenzene and a magnetic stir bar. The round bottom flask was then connected through a Liebig condenser to the bottom end of a

three-way distillation adaptor. The top opening of the adaptor was sealed with a rubber septum, and the side opening (75°) of the adaptor was connected to a second Liebig condenser. A vacuum distillation distribution adaptor connected the second Liebig condenser to an empty flask as a safety trap to collect any liquid that an unexpected pressure drop might push out from the toluene-filled trap or the reaction flask. The side opening of the adaptor was connected through Teflon tubes to two fritted gas wash bottles in sequence. The first wash bottle contained toluene and KOH pellets and the second wash bottle contained an aqueous KOH solution. The wash bottles served as safety traps to both eliminate any phosgene gas from escaping and prevent backpressure buildup. The exhaust from the second wash bottle was connected through a Teflon tube into the ventilation outlet of the hood. To ensure safety, all Teflon tubes were clamped to the glassware, and all glass joints except the joint between the round bottle reaction flask and the first Liebig condenser were sealed with grease. All glass joints were also secured in place with Keck clamps.

Argon was first used to purge the reaction flask, introduced it into the system through the septum on the three-way distillation adaptor to check for a tight seal of the system as recognizable by formation of bubbles in the wash bottles. Using a long stem cannula inserted through the septum, the adaptor, and the first Liebig condenser and terminating in the round bottom flask, 12 mL phosgene solution (a 25 molar excess with respect to the crown ether) was carefully delivered into the round bottom flask. Then the mixture was stirred and heated slowly to boiling (131 °C). After complete evolution of HCl (~3h), the cooling water running through the first Liebig condenser was turned off to allow removal of solvent (toluene and chlorobenzene) and any remaining phosgene. (A long stem

cannula delivering a gentle stream of argon can be used to flush out gas in the mid-section of the first Liebig condenser that is stuck there due to gas locking, slowing down removal of solvent from the reaction flask.) After the evaporation of the solvent, the content of the round bottom flask was further dried under high vacuum. Thereby, the target compound 4'-isocyanato-5'-nitrobenzo-15-crown-5 was obtained in quantitative yield as yellow solid. ^1H NMR (CDCl_2) δ : 7.58 (s, 1H), 6.51 (s, 1H), 4.07 (m, 4H), 3.77 (m, 4H), 3.58 (m, 8H), 1.25–1.39 (m, 60H, N-CH₂-(CH₂)₁₀-CH₃), 0.87 (m, 9H, N-CH₂-(CH₂)₁₀-CH₃). ESI-MS (methanol): m/z (relative intensity) [4'-methyl-carbamate-5'-nitrobenzo-15-crown-5 + Na⁺] = 409.1, resulting from reaction of the isocyanate group of the target compound with the methanol used to inject the sample into the ESI-MS, forming a methyl carbamate (relative intensity: 100); [4'-amino-5'-nitrobenzo-15-crown-5 + Na⁺] = 351.1 (0.07). For the ^1H NMR and MS spectra, see **Figures S4.1** and **S4.2** in the Supporting Information.

Synthesis of vinyl-modified BME-44: Using a modified literature²²⁰ procedure, a bifunctional diol was used as a linker to connect two mono crown ethers with isocyanate groups, giving a bis(crown ether). 215 mg (0.61 mol) 4'-isocyanato-5'-nitrobenzo-15-crown-5, 52.6 mg (0.31 mmol) 2-(allyloxymethyl)-2-ethyl-1,3-propanediol, and 30 μL triethylamine were added to 5 mL anhydrous dichloromethane to react overnight at room temperature. The reaction mixture was then diluted with 5 mL dichloromethane and washed first with 5 mL 1 N HCl and then 5 mL DI water. The organic phase was dried over sodium sulfate, the solvent was removed with a rotary evaporator, and finally dried on the high vacuum. After the crude product was suspended in ethyl ether, filtered on a Buchner funnel, and the filter cake was washed with a small amount of ethyl ether, it was

then recrystallized from ethyl acetate. ^1H NMR (CDCl_2) δ : 10.10 (s, 2H), 8.04 (s, 2H), 7.55 (s, 2H), 5.80 (m, 1H), 5.24 (m, 1H) 4.15–4.02 (m, 12H), 3.91 (m, 2H), 3.77 (m, 8H), 3.61–3.58 (m, 16H), 3.35 (m, 2H), 1.46 (m, 2H), 0.87 (m, 3H). ESI-MS (methanol): m/z (relative intensity) [vinyl-modified-BME-44 + K^+] = 409.1 (100). For the ^1H NMR and MS spectra, see **Figures S4.3** and **S4.4** of the Supporting Information.

Synthesis of triethoxysilyl-modified-BME-44: The carbon–carbon double bond of the vinyl-modified-BME-44 was converted to a triethoxysilyl group by platinum-catalyzed hydrosilylation using a modified literature procedure.¹⁰² 30.66 mg (0.035 mmol) vinyl-modified BME-44 was added to 1 mL of anhydrous toluene (pre-dried over molecular sieves). 6.6 μL (0.035 mmol) triethoxysilane was added to the mixture, followed by quick addition of an unweighted catalytic amount of very hygroscopic chloroplatinic acid solid. The reaction was heated at 80 °C for 15 h. After the reaction was cooled down, black solids were filtered off with a 0.45 μm PTFE syringe disc filter. Evaporation of the solvent gave the final product. ^1H NMR (CDCl_2) δ : 10.14–10.09 (m, 2H), 8.03–8.02 (m, 2H), 7.57–7.55 (m, 2H), 4.13–4.03 (m, 12H), 3.77 (m, 12H), 3.61–3.58 (m, 18H), 3.32–3.30 (m, 1H), 1.44 (m, 24H), 1.12–1.10 (m, 4H), 0.88–0.87 (m, 3H). The ^1H NMR spectrum may have been affected by trace amounts of the remaining platinum catalyst. ESI-MS: m/z (relative intensity) 881.4 (100); [triethoxysilyl-modified-BME-44 + K^+] = 1085.6 (26.5). For the ^1H NMR and MS spectra, see **Figures S4.5** and **S4.6** of the Supporting Information.

4.3 Results and Discussion

4.3.1 K⁺-Selective ISEs based on Silicone/Fluorosilicone Membranes and Mobile Ionophores

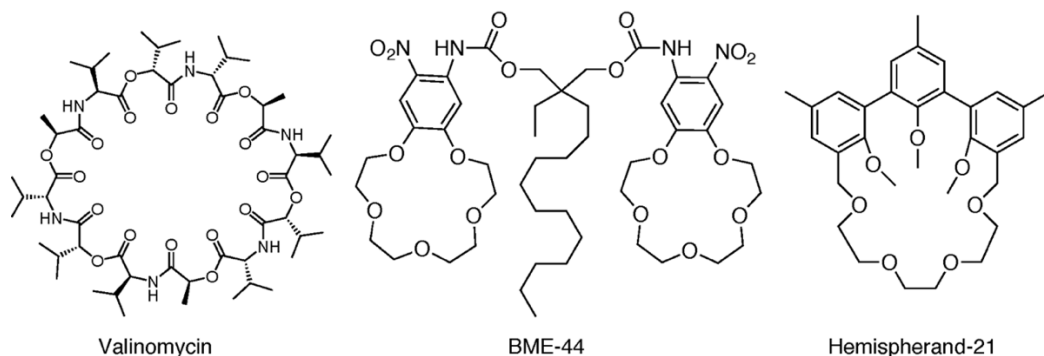


Figure 4.1 Potassium ionophores with good selectivity against sodium.^{86, 213-215}

From among common potassium ionophores (**Figure 4.1**) with good potentiometric selectivities,^{3, 86, 209, 213-215} valinomycin and BME-44 were tested as mobile ionophores with silicone and fluorosilicone matrixes. Valinomycin-doped ISEs membranes based on both pristine and centrifuged **Fluorosilicone 1** in both a conventional electrode setup with an inner filling solution and a solid-contact electrode setup were first calibrated in KCl solutions. Representative calibration curves from these four types of electrodes are shown in **Figure 4.2**. Results show that the solid-contact setup performed better than the conventional setup with closer to Nernstian slopes, regardless of whether solid binders had been removed by centrifugation or not. For the conventional setup, linearity started to deteriorate towards 0.1 M KCl, indicating early onset of Donnan failure.^{19, 20} Since **Fluorosilicone 1** evolves acetic acid during curing,²²¹ we suspect acetate produced during curing maybe weakly binding to the poly[(3,3,3-trifluoropropyl)methylsiloxane] backbone,

making it difficult to remove it from the sensing membrane by exposure to water. It appears that binding is favored by the electron-withdrawing trifluoropropyl side groups (see **Figure 4.3**).^{222, 223} The possible slow release of acetate may have affected the interfacial potential between these ISE membranes and the inner filling solution. For the better-performing solid-contact setup, no significant difference was found between pristine and centrifuged **Fluorosilicone 1** membranes doped with valinomycin as ionophore. There was also no significant difference in resistance of the membranes (average: $27.9 \pm 15.8 \text{ M}\Omega$; n=6). However, pristine **Fluorosilicone 1** has better mechanical properties due to the binders (trimethylsilylated silica and titanium dioxide), with centrifuged **Fluorosilicone 1** being softer than its pristine counterpart.

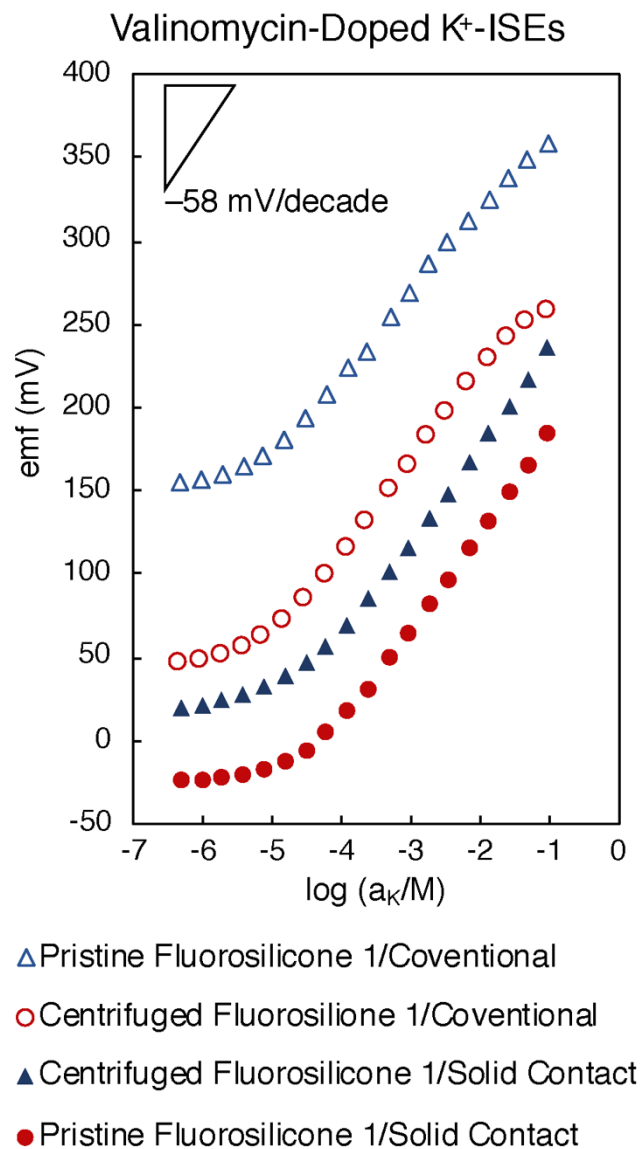


Figure 4.2 KCl response of K⁺-selective ISEs based on mobile valinomycin-doped fluorosilicone matrixes. Measurements were started at $1 \times 10^{-6.3}$ M KCl, and the KCl concentration was gradually increased by adding aliquots of concentrated KCl. Average slopes (mV/decade; n=3): pristine **Fluorosilicone 1** with a conventional ISE setup (51.5 ± 1.5); centrifuged **Fluorosilicone 1** with a conventional ISE setup (51.4 ± 0.9); pristine **Fluorosilicone 1** with a solid-contact ISE setup (57.5 ± 2.4); centrifuged **Fluorosilicone 1** with a solid-contact ISE setup (56.8 ± 2.3 ; n=2).

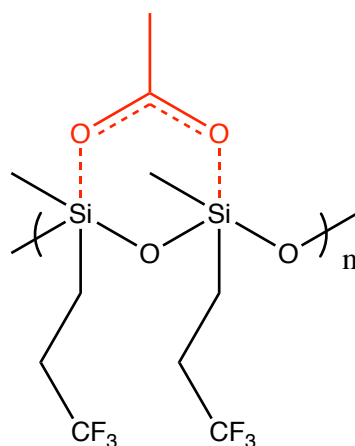


Figure 4.3 Suspected acetate binding to fluorosilicone backbone assisted by electro-withdrawing trifluoropropyl groups.

Following tests of mobile valinomycin-doped ISEs, mobile BME-44—another commonly used potassium ionophore known for its larger hydrophobicity^{214, 215}—was tested with **Fluorosilicone 1**, **Fluorosilicone 2**, and **Silicone 2** as membrane matrixes. Calibrations curves are shown in **Figure 4.4**. As for valinomycin/**Fluorosilicone 1** ISEs, regardless of centrifugation, the solid-contact setup provided Nernstian response slopes, outperforming the conventional setup. When the conventional setup was used with 1 mM KCl as inner filling solution, the electrodes only gave response slopes approximately half of the theoretical value. The use of phosphate-buffered (pH 7.4) solution with 1 mM KCl improved the response slope to around 40 mV/decade, still far lower than what was observed for the solid contact ISE setup. In addition, membranes prepared from another acetic acid-evolving **Fluorosilicone 2** and tested with a conventional ISE setup also gave much lower than-Nernstian response. In contrast, membranes based on the acetic acid-evolving polydimethylsiloxane-based **Silicone 1** resulted in Nernstian response. These

results appear consistent with acetate binding to the poly[(3,3,3-trifluoropropyl)methylsiloxane] backbone, delaying acetic acid release.^{222, 223} Contrary to ISEs with valinomycin-doped membranes, BME-44/**Fluorosilicone 1** ISEs only gave Nernstian responses when filler particles were removed from **Fluorosilicone 1** by centrifugation. This indicates fillers in **Fluorosilicone 1** removed by centrifugation (trimethylsilylated silica and titanium dioxide) may be binding to BME-44, reducing the availability of free BME-44. BME-44-doped **Fluorosilicone 1** and **Silicone 1** have membrane resistances of 57 ± 36 and $450 \text{ M}\Omega$, respectively. Chapter III describes ionic liquid (IL) 1-methyl-3-octylimidazolium bis(trifluoromethylsulfonyl)imide doped reference electrode membranes with **Fluorosilicone 1** and **Silicone 1** as matrix.²²¹ The resistance of BME-44-doped **Fluorosilicone 1** is one order of magnitude higher than its IL- doped counterpart. This is not surprising given the good miscibility of IL and **Fluorosilicone 1** up to 20 wt% IL. In contrast, the resistance of BME-44-doped **Silicone 1** is one order of magnitude smaller than that of ionic liquid-doped **Silicone 1** reference membranes. This suggests that **Silicone 1** has a lower intrinsic concentration of ionic species but that it is not miscible with IL.²²¹ The potentiometric selectivity coefficient of BME-44 doped centrifuged **Fluorosilicone 1** (measured by separate solution method³⁹) was determined to be -3.74 ± 0.38 ($n = 4$), similar to values reported for valinomycin and BME-44.¹²⁴⁻¹²⁶ This good selectivity of **Fluorosilicone 1** membranes shows that **Fluorosilicone 1** is a membrane matrix compatible with BME-44. The experimentally observed selectivity is sufficient for measurements in blood, which requires $\log K_{\text{K,Na}}^{\text{pot}} \geq -2.92$.

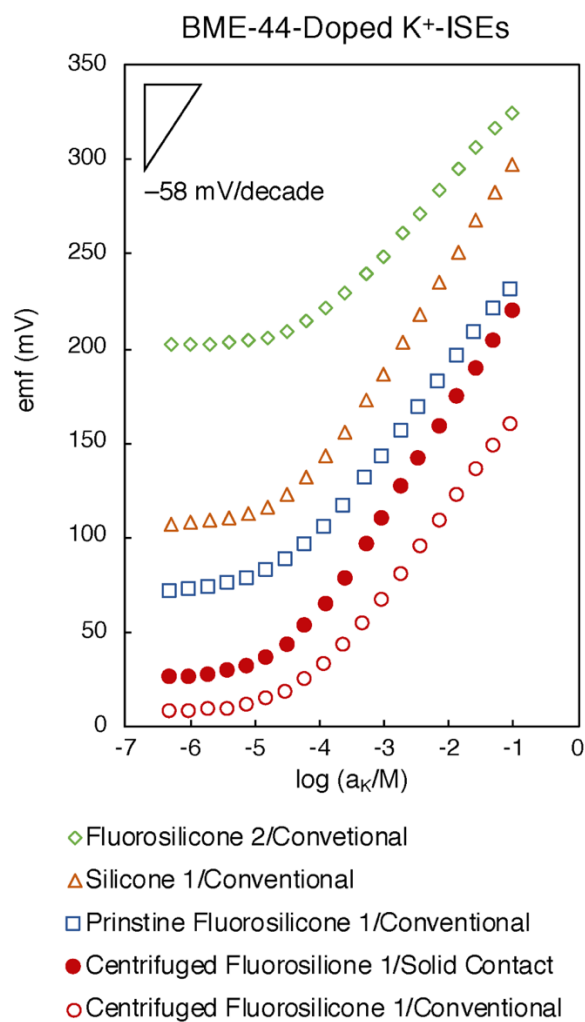


Figure 4.4 KCl response of K⁺-selective ISEs based on mobile BME-44-doped silicone matrixes. Measurements were started at $1 \times 10^{-6.3}$ M KCl, and the KCl concentration was gradually increased by adding aliquots of concentrated KCl. Average slopes (mV/decade; n=3): **Fluorosilicone 2** with a conventional ISE setup (27.4 ± 9.4); **Silicone 2** with a conventional ISE setup (51.6 ± 4.8); pristine **Fluorosilicone 1** with a conventional ISE setup (42.3 ± 1.5); centrifuged **Fluorosilicone 1** with a solid-contact ISE setup (53.1 ± 3.8); centrifuged **Fluorosilicone 1** with a conventional ISE setup (40.4 ± 6.0). Calibrations curves were shifted vertically for clarity.

4.3.2 Planar Electrodes and Micro-Electrodes

In view of developing thin-layer planar electrodes for implantable and wearable devices, ISEs membranes should be preferably thin and electrodes should have small form factors. Spin-coating on conventional bulk gold electrodes and dip-coating on micro-electrodes were evaluated (see **Figure 4.5**). Spin-coated membranes with two-fold diluted membrane solutions provided 30 μm thick membrane, which is one order of magnitude thinner than normal bulk ISE membranes. Two types of dip-coated thin membranes were prepared on tip-shaped micro-electrodes. The first type was prepared by dipping micro-electrodes into a four-fold concentrated valinomycin/pristine **Fluorosilicone 1** membrane solution. Valinomycin was used as a performance reference for BME-44, and the solid white color of pristine **Fluorosilicone 1** can help aid visual confirmation of dip-coating since the dipping solutions tend to drip back. The four-fold concentrated polymer solutions also help reduce dripping back. As a proof of concept, a second type of membrane was prepared by dipping micro-electrodes into a normal concentration BME-44/**Silicone 1** membrane solution. The dip-coated thin membranes have a similar thickness of about 30 μm (measured by a caliper) as compared to spin-coated ones. Solid contact materials were not used in these experiments. All three types of electrodes provided Nernstian responses (see **Figure 4.6**).



Figure 4.5 (a) Top and (b) side views of thick membranes (200 μm thickness) with a CIM carbon solid contact (left) and spin-coated thin-layer membranes (30 μm thickness, translucent yellow) without CIM carbon solid contact (right); (c) dip-coated membrane on a microelectrode, along with microscope views.

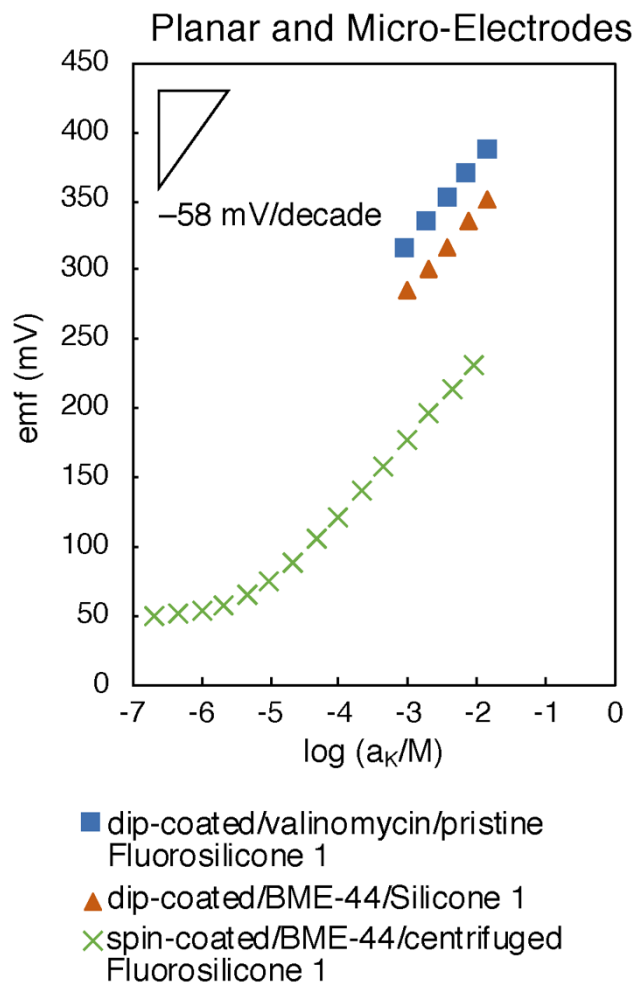


Figure 4.6 KCl response of K^+ -selective ISEs based on dip-coated thin-layer microelectrodes and spin-coated thin-layer electrodes. Measurements of spin-coated thin-layer membranes were started at 1×10^{-7} M KCl. Measurements of dip-coated microelectrodes were started at 1 mM KCl. The KCl concentration was gradually increased by adding aliquots of concentrated KCl. Average slopes (mV/decade; $n=3$): spin-coated BME-44/centrifuged **Fluorosilicone 1** (55.9 ± 0.3); dip-coated valinomycin/pristine **Fluorosilicone 1** (55.9 ± 0.3); dip-coated BME-44/**Silicone 1** (56.9 , $n=1$).

4.3.3 Leaching of Sensor Components and Covalent Attachment of Ionophore.

Leaching of sensing components Sensing components of ISEs, such as ionophores

and ionic sites, are typically freely dissolved in the organic membrane phase. They can slowly leach out due to their partitioning between the organic membrane and the aqueous sample phase. Based on a simple well-developed model,^{12, 122, 123} the leaching rates of both electrically neutral and charged compounds (and, therefore, the sensor lifetime) can be quantitatively related to their partition coefficient (i.e., lipophilicity) between 1-octanol and water. Assuming a regular sensing membrane thickness of 200 μm , a typical diffusion coefficient of sensing components in the aqueous phase of $3 \times 10^{-6} \text{ cm}^2 \text{ s}^{-1}$, a typical Nernst layer of 30 μm , and logarithmic 1-octanol/water partition coefficients on logarithmic scale of 8.6 and 10.0 for valinomycin and BME-44, respectively, 100% valinomycin and 99.99% BME-44—the two most used potassium ionophores—will leach out into serum samples in a span of 14 days. For thin-layer membranes with a 30 μm thickness, 100% valinomycin and 99.99% BME-44 will leach out in just one day. In contrast, due to the large lipophilicity and the pairing with the primary cation–ionophore to form a complex in the membrane,^{111, 135} ionic site salts such as KTpClPB will leach out 0% in 14 days. Therefore, there is a need to covalently attach potassium ionophores when the intended use is in biological samples.

Synthesis of Covalently Attachable Triethoxysilyl-BME-44 Triethoxysilyl-BME-44 was synthesized in three steps by first functionalizing a mono crown ether (Step 1), then connecting two mono crown ether units into a bis (crown ether) compound through formation of two carbamate linkages (Step 2), and finally reacting a vinyl unit of the bis(crown ether) to introduce a covalently attachable triethoxysilyl unit by platinum-catalyzed hydrosilylation (Step 3). The first two steps give a compound with a structure very similar to the bis(crown ether) BME-44.

Reaction with phosgene is a common way to prepare isocyanates and, therefrom, carbamates. However, because of its reactivity and volatility, phosgene is also a very toxic gas that must be handled with precaution. In the research laboratory, phosgene is nowadays often replaced with 1,1'-carbonyldiimidazole (CDI), which is less reactive and is a solid.²²⁴⁻²²⁸ As phosgene too, the symmetrical CDI can react with either an amine or an alcohol to form an imidazole-*N*-carboxamide or imidazole-*N*-carboxylate, respectively, followed by reacting with a second amine or alcohol to form a urea, a carbamate, or a carbonate.²²⁹ Reactions schemes for Route 1 and 2 are shown in **Figure 4.7**.

Initial trials attempting to react CDI with 4'-amino-5'-nitrobenzo-15-crown-5 at room temperature in THF did not yield any products detectable by NMR or MS spectrometry. This is not unexpected due to the para-positioned nitro group that deactivates the amino group, yielding a much lower nucleophilicity. Further attempts were then conducted using the aprotic solvents chlorobenzene or toluene, favoring activation of amino groups at elevated temperature. ¹H NMR spectra showed that the products thus obtained were a mixture of an imidazole-*N*-carboxamide and isocyanate. Methyl carbamate—i.e., the product of either imidazole-*N*-carboxamide or isocyanate with methanol—was detected with MS spectrometry, which also showed the absence of starting material. However, it was difficult to interpret the ¹H NMR spectra due to the side product imidazole. A peak at 2336 cm⁻¹ in IR spectra is close to the literature value for isocyanates (2270 cm⁻¹). The thus obtained reaction mixture was not purified but allowed to react with the diol (i.e., 2-(allyloxymethyl)-2-ethyl-1,3-propanediol) in the presence of a base. Three types of bases were used. Triethylamine and KOH did not yield the desired bis(crown

ether). The stronger base NaH, which quantitatively deprotonates the diol, gave the final product bis(crown ether) (referred to in the following as vinyl-BME-44) in low yield. The separation of the bis(crown ether), unreacted mono crown ether, and imidazole from one another by chromatography was difficult and unsuccessful.

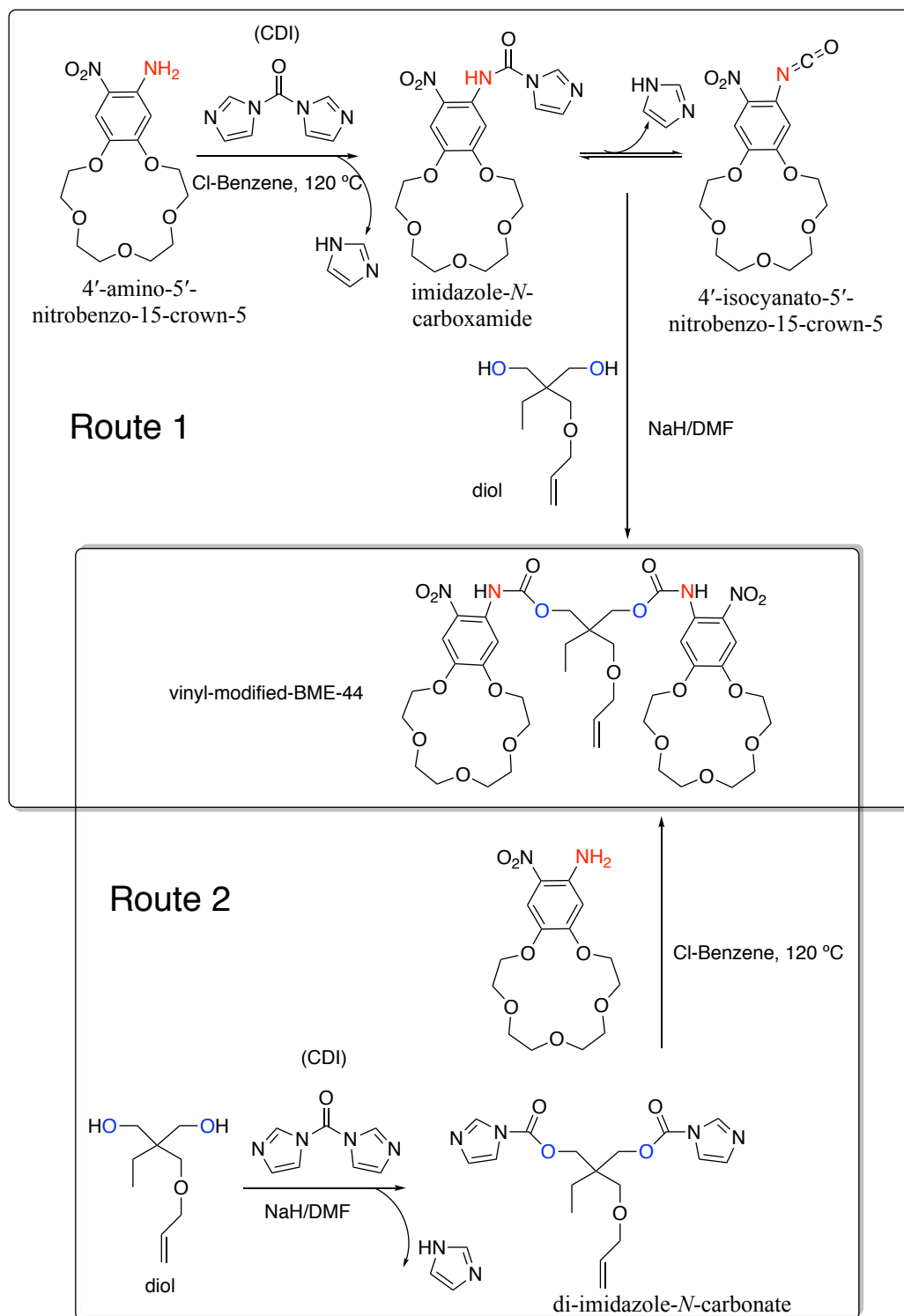


Figure 4.7 Synthesis Route 1 and Route 2 with CDI as reagent.

Efforts were also made on an alternative route (Route 2) that swapped Step 1 and Step 2 by allowing CDI to first react with diol to form a di-imidazole-*N*-carbonate, followed by reaction with 4'-amino-5'-nitrobenzo-15-crown-5 to form the carbamate linkage. Similar to Route 1, the first step in Route 2 was successful, giving the di-imidazole-*N*-carbonate successfully, as confirmed by MS spectrometry. Three equivalents of CDI were used to avoid formation of a cyclic carbonate because the two -OH groups of the diol are separated by only three carbon, making this a likely side reaction²³⁰⁻²³⁴ that could be successfully avoided. However, the second step of Route 2, i.e., the reaction of di-imidazole-*N*-carbonate with 4'-amino-5'-nitrobenzo-15-crown-5, resulting in the replacement of the second imidazole of each initial CDI unit, was unsuccessful.

The results from Route 1 and Route 2 demonstrated the reduced reactivity of CDI as compared to phosgene. Imidazole is not as good a leaving group as chloride, and the separation of the desired product from side products is needed. This is often not a problem in similar reactions²²⁵⁻²²⁸ but a clear hurdle in this case because the deactivating effect of the para-positioned nitro group demands a higher reactivity. Importantly, in both Route 1 and Route 2, the reactivity for the second step is much lower, making both routes difficult. This is consistent with similar claims in the literature.²³⁵

Phosgene is 170 times more reactive than triphosgene, which itself is more reactive than CDI.²³⁶ For safety reasons, in this work 15 wt% phosgene/toluene solution was used because the solution is easier to handle than a phosgene gas cylinder. However, extreme caution should still be used handling phosgene with appropriate personal protective equipment.²³⁶ The reaction Route 3 using phosgene is shown in **Figure 4.8**. Due to the ease

of HCl elimination in the reaction at elevated temperature, pure 4'-isocyanato-5'-nitrobenzo-15-crown-5 was obtained in quantitative yield. The reaction between the resulting isocyanate and the diol in Step 2 of Route 3 happened at room temperature in the presence of triethylamine, without formation of any side product that had to be removed. After purification (see experimental section for details), the vinyl-modified-BME-44 was obtained in good yield. In Step 3 of Route 3, the vinyl bond introduced with the diol was used to introduce a triethoxysilyl group by platinum-catalyzed hydrosilylation. The triethoxysilyl-modified BME-44 can be readily covalently attached to the silicon polymer backbone during silicone curing since this compound and the silicone precursors have exactly the same chemistry.

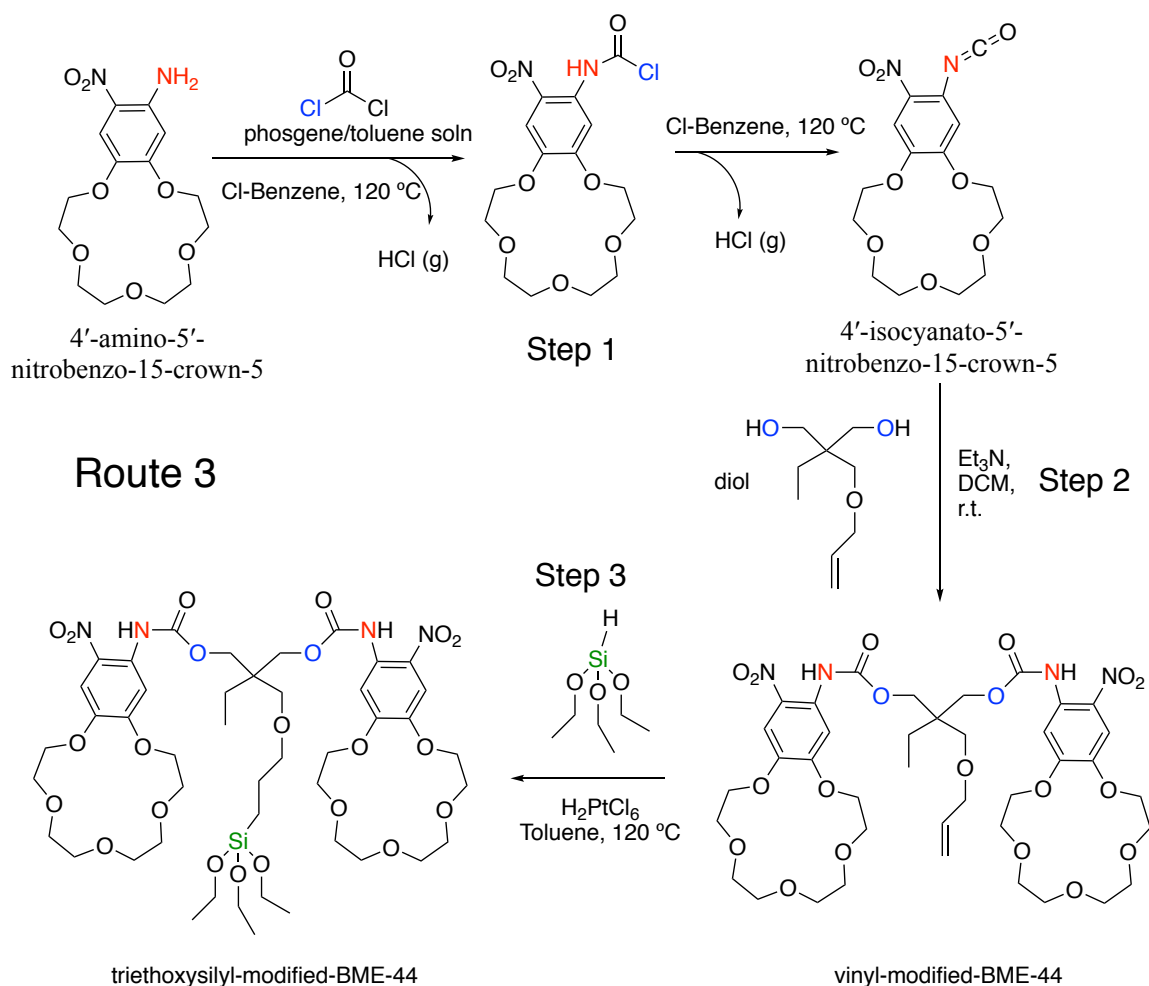


Figure 4.8 Synthesis Route 3 with phosgene as the key reagent.

4.3.4 Evaluation of Covalent Attachment

To verify covalent attachment, qualitative Soxhlet extraction was performed on centrifuged **Fluorosilicone 1** membranes doped with either mobile BME-44 or triethoxysilyl-modified-BME-44 (**Figure 4.9 a**). First, hexane was tested as extraction solvent with centrifuged **Fluorosilicone 1** membranes doped with mobile BME-44. The volume of the Soxhlet extractor used afforded siphoning approximately every 4 minutes. After 16 h extraction (320 times extraction), hexane did not sufficiently extract mobile

BME-44 from the **Fluorosilicone 1** membrane, as indicated by only a minor diminishing of the characteristic yellow color of the membrane. The more polar solvent DCM completely extracted all freely dissolved mobile BME-44 within 20 h (400 extraction steps), making DCM a suitable solvent for Soxhlet extraction tests. In contrast, after 21 h extraction with DCM, membrane doped with the covalently attachable triethoxysilyl-BME-44 still maintained a medium level of its yellow color. A possible explanation for the observed color reduction is that membranes contain some non-crosslinked oligomers due to incomplete curing and that the BME-44 covalently attached to such oligomers may have been leached out together with those oligomers. It is also possible that some triethoxysilyl-modified BME-44 can bond to one another, forming dimers, trimers or tetramers not attached to polymer backbone. Here it is worth pointing out that Soxhlet extraction with DCM is a much more strenuous test than any likely real-life applications of **Fluorosilicone 1** membranes with covalently attached ionophore, most of which are aqueous. This demonstrates that covalent attachment via triethoxysilyl group occurring concurrently during silicone curing is a simple yet effective strategy.

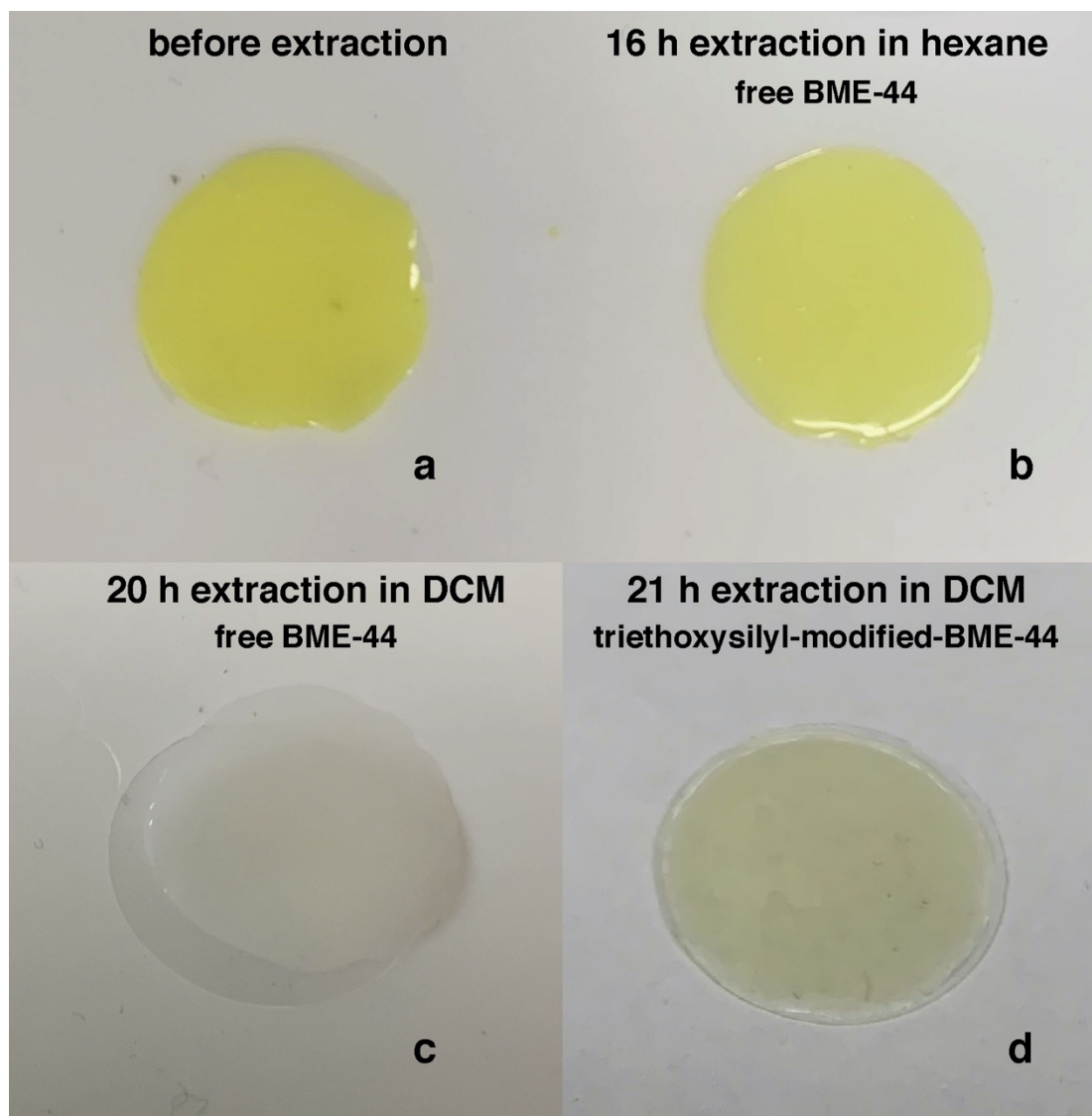


Figure 4.9 Soxhlet extraction of **Fluorosilicone 1** membranes: (a) before extraction; (b) after 16 h extraction with hexane of **Fluorosilicone 1** membranes doped with mobile BME-44; (c) after 20 h extraction with dichloromethane of **Fluorosilicone 1** membranes doped with mobile BME-44; (d) after 21 h extraction with dichloromethane of **Fluorosilicone 1** membranes modified with triethoxysilyl-modified-BME-44.

4.3.5 Performances ISEs Based on Covalently Attached Ionophore

ISEs based on centrifuged **Fluorosilicone 1** membranes doped with triethoxysilyl

modified-BME-44 were tested in the same fashion as membranes with mobile BME-44. Electrodes with a common concentration of 13 mmol/kg of triethoxysilyl-modified-BME-44 gave an average slope of 44.7 ± 1.4 mV/decade ($n = 9$; **Figure 4.10**). In view of improving response slopes, efforts were made with membranes that contained 10 wt% ionophore triethoxysilyl-modified-BME-44 (106 mmol/kg). However, the observed response slope for these membranes was within error the same (44.6 ± 2.1 mV/decade; $n = 9$). At 10 wt%, the membrane solution was significantly more viscous than at the lower ionophore concentrations, which may have affected the process of dropcasting as well as the interface between the ion-selective membrane and the solid contact layer. Resistances of membranes with covalently attached ionophores are 32.8 ± 8.9 M Ω , which is very similar to those of membranes doped with mobile BME-44. This confirms a good and comparable ion mobility as for membranes with the same mobile ionic site and mobile ionophore.

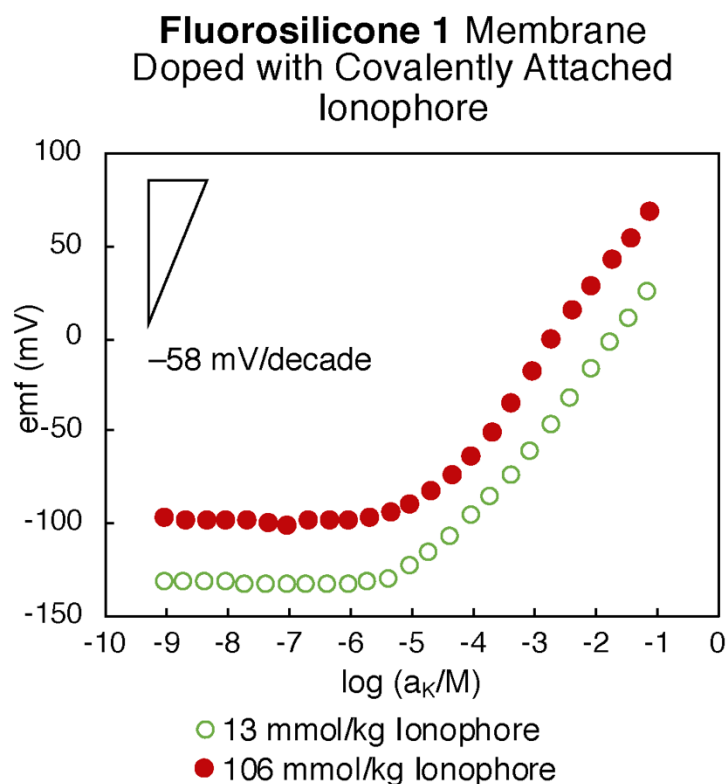


Figure 4.10 KCl response of ISEs based on **Fluorosilicone 1** membrane doped with the covalently attached ionophore triethoxysilyl-modified BME-44. Measurements were started at 1×10^{-9} M KCl and the KCl concentration was gradually increased by adding aliquots of concentrated KCl. Average slopes: **Fluorosilicone 1** doped with 13 mmol/kg triethoxysilyl-modified-BME-44 (44.7 ± 1 mV/decade; $n = 9$); **Fluorosilicone 1** doped with 106 mmol/kg (10 wt%) triethoxysilyl-modified BME-44 (44.6 ± 2.1 mV/decade; $n = 4$).

4.4 Conclusions

This chapter describes the preparation and characterization of plasticizer-free silicone and fluorosilicone materials as ISEs membranes for K^+ -selective sensors. Four types of silicone and fluorosilicone matrixes doped with two types of mobile K^+ ionophore were tested. Nernstian responses to K^+ were obtained with valinomycin-doped **Fluorosilicone 1** membranes as well as BME-44-doped centrifuged **Fluorosilicone 1** and **Silicone 1** membranes. In addition, high K^+ selectivity with respect to Na^+ was confirmed for BME-44-doped centrifuged **Fluorosilicone 1** membranes. The effect of the curing process, namely the formation of acetic acid during curing, on ISEs response was discussed. Acetic acid formation appears to have a major impact on fluorosilicone membranes mounted in convectional ISE electrode bodies. The difference in the performance of silicones with and without trifluoropropyl groups suggests that acetate may be bound to the fluorosilicone backbone, assisted by trifluoropropyl group. Spin-coating and dip-coating were successfully used to fabricate 30 μm thin-layer membranes on conventional bulk gold electrodes and on microelectrodes. Similar Nernstian responses were observed. The synthesis of a triethoxysilyl-modified-BME-44 that can be covalently attached to the fluorosilicone backbone is reported here for the first time. Soxhlet extraction confirmed the covalent attachment of ionophore to membrane backbone but also showed that some of the ionophore may be bound to oligomers that are not bound to the rest of the polymer, emphasizing the need for efficient silicone curing. ISEs based on covalently attached ionophore provided near Nernstian responses and optimization of ionophore concentration in the membranes to improve the responses is underway.

4.5 Supporting Information

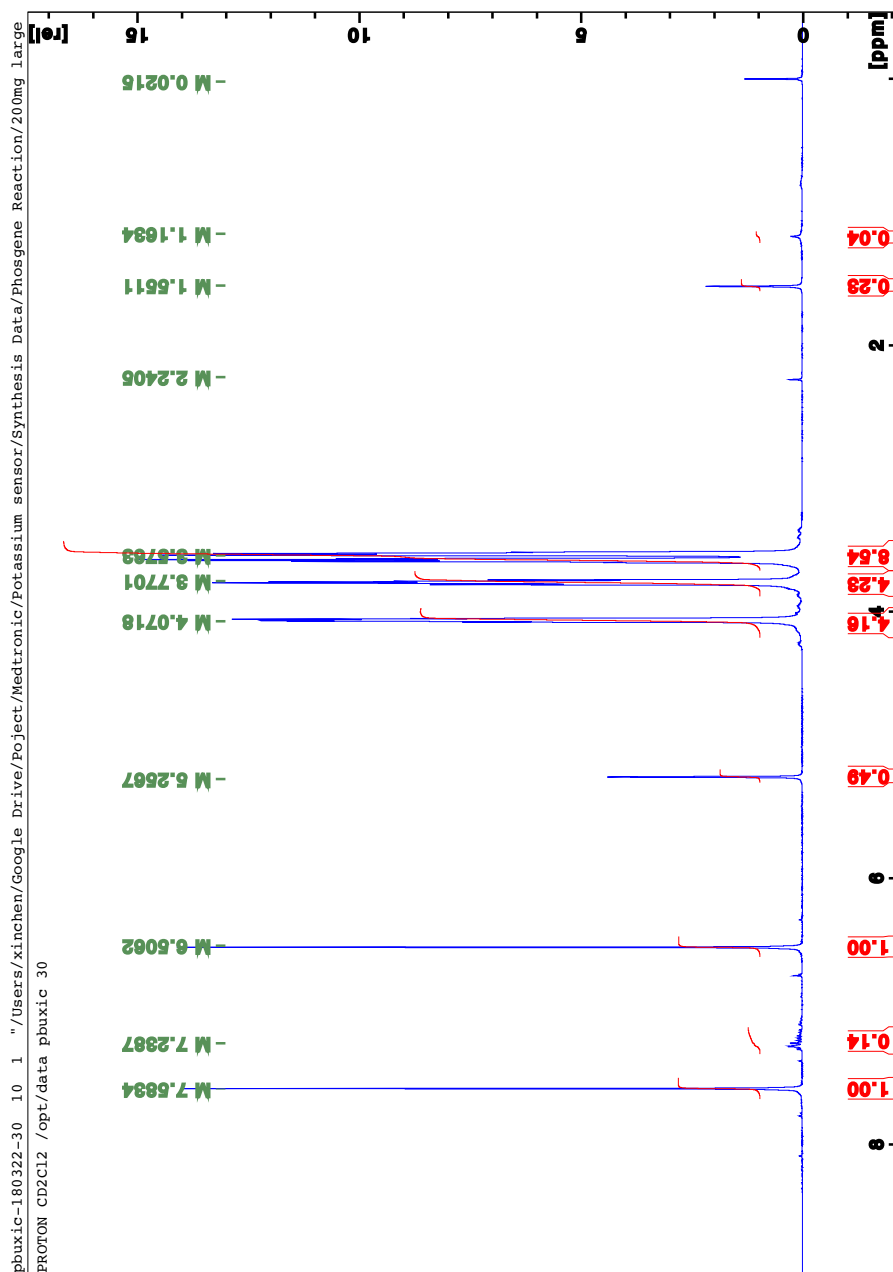


Figure S4.1 ^1H NMR (CDCl_2) spectrum of 4'-isocyanato-5'-nitrobenzo-15-crown-5.

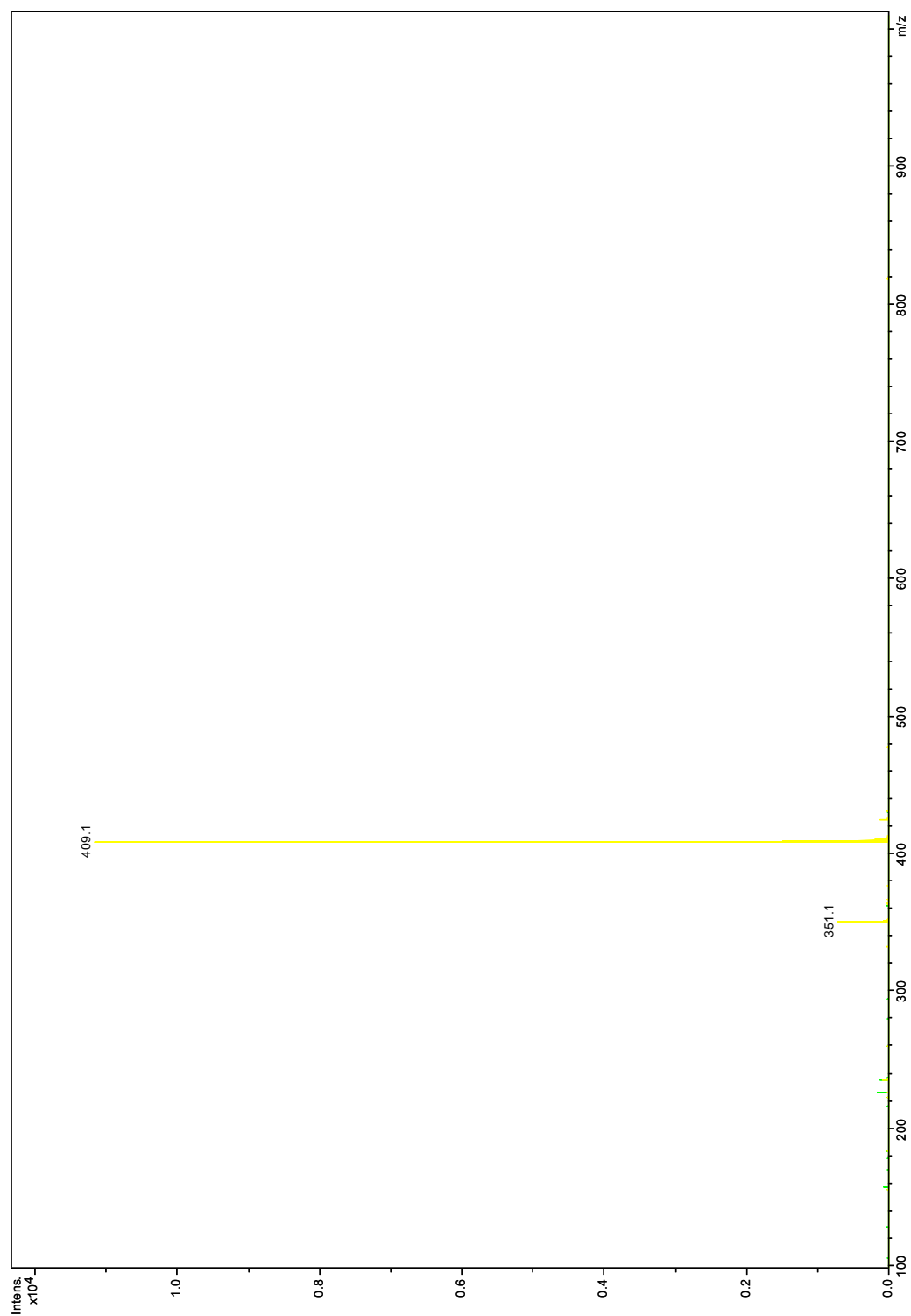


Figure S4.2 ESI-MS spectrum of purified 4'-isocyanato-5'-nitrobenzo-15-crown-5.

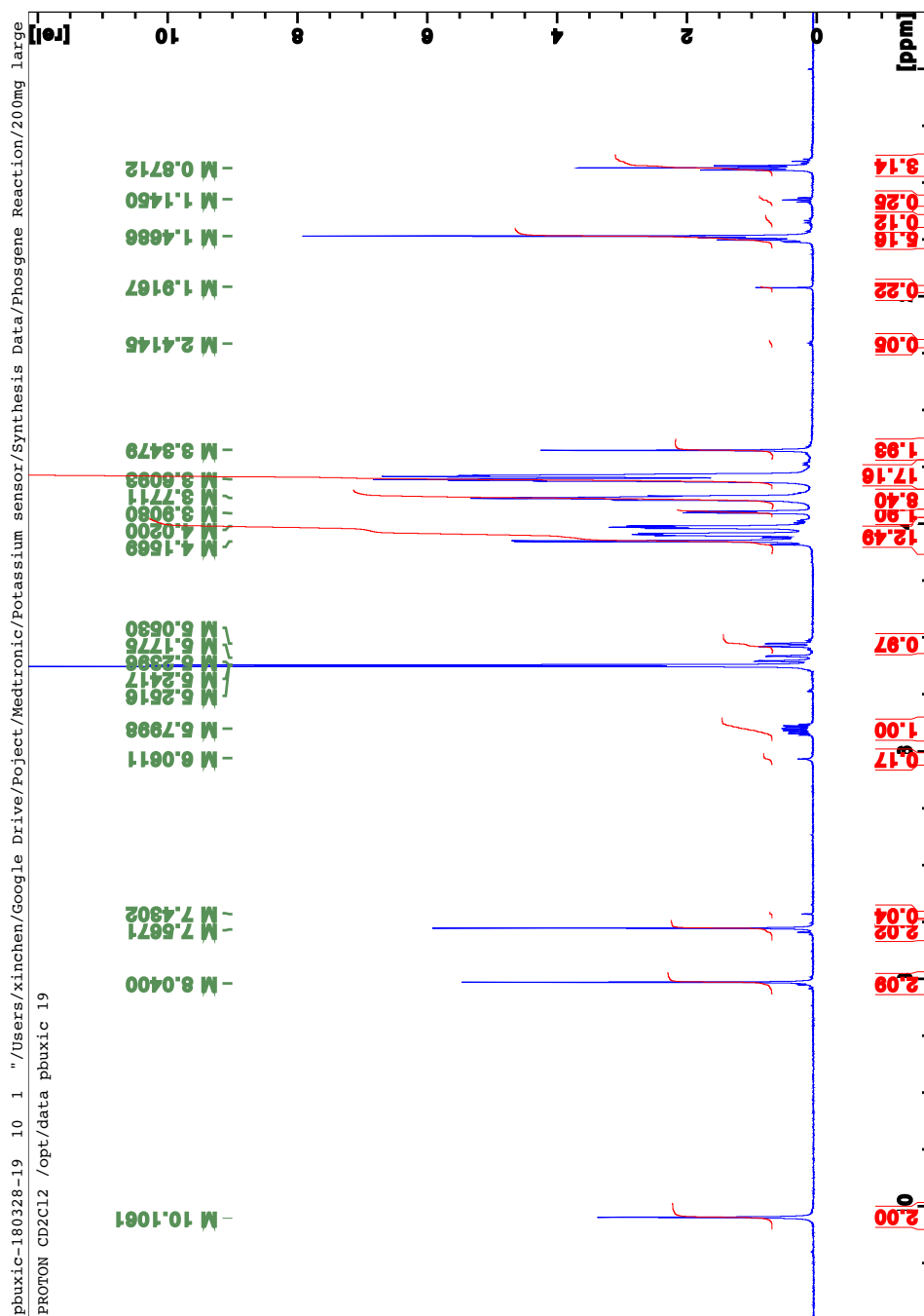


Figure S4.3 ¹H-NMR (CDCl₂) spectrum of vinyl-modified-BME-44.

Mass Spectrum Molecular Formula Report

Analysis Info

Method pos_highmass_010616.tofpar
Sample Name vinyl_BME_44_after_recristalization
Comment

Acquisition Date 3/31/2018 3:11:16 PM

Operator operator name
Instrument BioTOF II

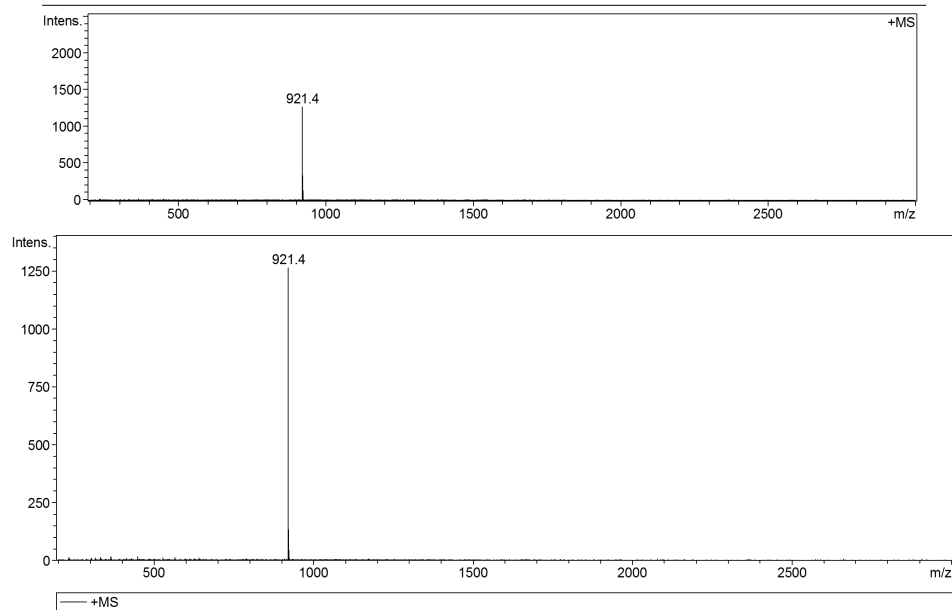


Table 'GenFormulaResults' could not be found in this analysis

Figure S4.4 ESI-MS spectrum of vinyl-modified-BME-44.

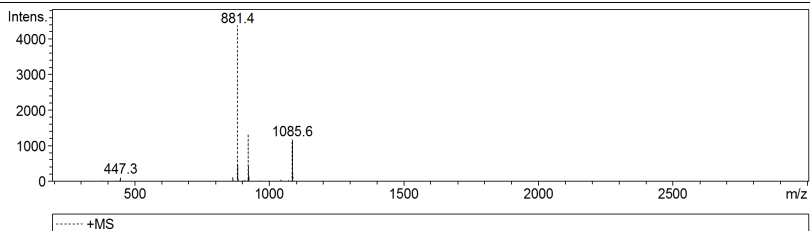
Mass Spectrum List Report

Analysis Info

Analysis Name 2smpl_MeOH Acquisition Date 3/31/2018 3:17:08 PM
Method pos_highmass_010616.tofpar Operator operator name
Sample Name triethoxysilyl_BME_44_rxn_12h_no_filtration Instrument BioTOF II
This is the rxn betw vinylBME44 andHSi(OEt)3 after 12h no filtration Free format comments

Acquisition Parameter

n/a n/a n/a n/a detbias 1750 V
EndP -4000 V n/a n/a n/a



#	m/z	I
1	447.3	105
2	865.4	115
3	881.4	4360
4	882.4	1367
5	883.4	462
6	923.5	1328
7	924.5	439
8	925.5	143
9	1085.6	1157
10	1086.6	518
11	1087.6	208

Figure S4.6 ESI-MS spectrum of covalently attachable triethoxysilyl-modified-BME-44.

**V. DEVELOPMENT OF POLY(METHACRYLATE)-
BASED PH SENSORS WITH ALL SENSOR
COMPONENTS COVALENTLY ATTACHED**

Kwangrok Choi made contributions in calibrations of poly(methacrylate)-based ISEs and elemental analysis.

5.1 Introduction

Glass electrodes with a solid-state glass membrane are the standard sensors for pH measurements recommended by International Federation of Clinical Chemistry (IFCC) and by IUPAC with a wide working range and high selectivity.^{237, 238} However, glass membranes have intrinsic disadvantages. Many types of glass membranes contain lead.²³⁹ The fragility of glass is challenging in application areas such as food processing and implantable or wearable sensing. The fouling by protein adsorption onto the pH sensitive glass bulb also requires frequent cleaning and maintenance.¹⁵⁹ Glass electrodes are also difficult to miniaturize due to the high resistivity of glass.¹⁵⁸

Polymeric membranes are an alternative to solve some of the aforementioned challenges. Plasticized PVC membranes have become the conventional type of polymeric membrane ISEs with a wide range of pH ionophores developed successfully.^{2, 3} These ionophores have functional groups that can be protonated such as in the case of amine^{160, 161} and pyridine^{122, 162} derivatives. However, the plasticizers used in PVC-based membrane can leach out over time. This gradual loss of plasticizer not only undermines the functionality and selectivity of the selective membrane,²⁴⁰⁻²⁴³ but can also cause inflammatory reactions,⁶⁴⁻⁶⁷ making plasticized polymers undesirable for use in areas such as long-term monitoring, the food and pharmaceutical industry, and implantable and wearable sensing applications.

To avoid a plasticizer, the polymer itself needs to be “self-plasticized”. In term of polymeric membranes for ISEs, the polymers need to have a glass transition temperature (T_g) below the temperature of intended use so that the membranes have a “rubber-like”

nature so that sensing components such as the ionophore and ionic sites can diffuse freely within them. A common standard is a T_g below room temperature for most routine measurements. Unique application areas can require the T_g to be below $-10\text{ }^\circ\text{C}$, such as for certain industrial process control uses, or to be just below body temperature ($37\text{ }^\circ\text{C}$) for implantable sensors. Common plasticizer-free polymers suitable for ISEs fall into three major categories: polyurethane, silicone, and poly(methacrylate)- and poly(acrylate)-based polymers.^{87, 106, 190} Poly(methacrylate)- and poly(acrylate)-based polymers have the distinct advantages that the T_g of these polymers can be adjusted by carefully varying the ratio of the monomer(s) of the alkyl methacrylate or alkyl acrylate.

In view of developing sensors capable of long-term use and monitoring, it is beneficial to covalently attach critical sensors components to the membrane backbone to avoid the gradual loss of these components by leaching into samples. The aforementioned methacrylate and acrylate polymerization chemistry opens the opportunity of covalently attaching components such as ionophores, ionic sites, ionic liquids, and salts to the backbone of the membrane polymer. Based on a well-known theoretical model, when freely dissolved in a membrane, pH ionophores such as tridodecylamine, 4-nonadecylpyridine (ETH 1907), or octadecyl isonicotinate (ETH1778) will leach out over 180 days into serum samples to an extent of 100%, 6.5%, and 92.3%, respectively.^{12, 122, 123} For certain applications, covalent attachment of sensor components is also attractive for ISEs used at higher temperatures. However, past work on covalently attaching sensor components are limited, with only a few studies covalently attaching K^+ or Na^+ ionophores or tetraphenylborate-based ionic site to a polymer backbone.^{84, 86, 102, 104, 127, 244}

In this chapter, a methacrylate-based alkyl sulfonate as a covalently attached ionic site for crosslinked poly(methacrylate) membranes is described. The methacrylate unit ensures a precise reactivity match to the methacrylate monomer and methacrylate crosslinker for optimal covalently attachment. To the best of our knowledge, this is the first time a methacrylate-based alkyl sulfonate is used successfully as a covalently attached ionic site with Nernstian response. In addition, two types of methacrylate-based amines were used for the first time as covalently attached ionophore and provided Nernstian responses comparable to conventional ISE membranes doped with the free pH ionophore tridodecylamine. However, when both of the ionophore and ionic site are covalently attached to the membrane polymer, only one electrode gave a satisfactory response so far. Elemental analysis was used to confirm the covalent attachment. The concept of poly(methacrylate)-based solid-state ISEs can also be easily expanded to measurements other than pH, with a change of the pH ionophore to appropriate ionophores for other ions.

5.2 Experimental

5.2.1 Materials

Potassium tetrakis(4-chlorophenyl)borate (KpCIPB), decyl methacrylate (DMA), lauryl methacrylate (LMA), methyl methacrylate (MMA), 2,2'-azobis(2-methylpropionitrile) (AIBN), 2,2-dimethoxy-2-phenylacetophenone (DMPP), hexanediol dimethacrylate, 2-(dimethylamino)ethyl methacrylate, 2-(diisopropylamino)ethyl methacrylate, and 3-sulfonylpropyl methacrylate potassium salt were purchased from Sigma Aldrich (St. Louis, MO). Tridodecylamine (TDDA) was purchased from Sigma (St. Louis, MO). High molecular weight PVC and *o*-nitrophenyl octyl ether (*o*-NPOE) were purchased from Fluka (Buchs, Switzerland). Nanographite powder (GS-4827, BET surface area of 250 m²/g, particle size distribution from 0.10 μm to 10 μm) and fine extruded graphite rod (0.25-inch outer diameter) were purchased from graphitestore.com (Northbrook, IL). Fullerene powder (mixed, typically 98% C₆₀ and 2% C₇₀) and potassium tetrakis(pentafluorophenyl)borate (KTPFB) were purchased from Alfa Aesar (Tewksbury, MA). Anhydrous ethyl acetate was further dried over activated 4 Å molecular sieves overnight prior to use. Anhydrous inhibitor-free THF was passed through a column of basic alumina to remove traces of peroxide. Colloid-imprinted mesoporous (CIM) carbon was prepared as previously reported.¹⁹³ All aqueous solutions were prepared with deionized and charcoal-treated water (0.182 MΩ cm specific resistance) using a Milli-Q Plus reagent-grade water system (Millipore, Bedford, MA).

5.2.2 Purification of pH Ionophore Tridodecylamine

Solids were found at the bottom of a bottle of tridodecylamine. To purify this compound, 1 g of tridodecylamine was dissolved in 15 mL diethyl ether and washed with 1 mM aqueous potassium hydroxide solution (15 mL x 3) and then with water (10 mL). Then the organic phase was collected and dried with magnesium sulfate. After removal of the magnesium sulfate by filtration, the organic solvent was removed under vacuum. ^1H NMR spectroscopy, MS, and elemental analysis showed that the thus-purified and the unpurified tridodecylamine were within error identical. ^1H NMR (CDCl_3 , δ): 2.33 [t, 6H, N- $\underline{\text{CH}_2}$ -(CH_2) $_{10}$ - CH_3], 1.25–1.39 [m, 60H, N- CH_2 -($\underline{\text{CH}_2}$) $_{10}$ - CH_3], 0.87 [m, 9H, N- CH_2 -(CH_2) $_{10}$ - $\underline{\text{CH}_3}$]. ESI-MS: [Tridodecylamine-H] $^+$ = 521.7; [Didodecylamine-H] $^+$ = 354.5. Elemental Analysis (Atlantic Microlab, Norcross, GA): Found: 83.04% C, 14.42% H, 2.48% N (Theoretical: 82.83% C, 14.48% H, 2.68% N). For ^1H NMR and MS spectra of purified and unpurified tridodecylamine, see the **Figures S5.1 to S5.4** in the Supporting Information.

5.2.3 PVC Membrane Preparation

Solutions to prepare pH-selective PVC membranes were prepared by slowly adding 66 mg PVC into a stirred solution of 132 mg *o*-NPOE and 1 mL THF, followed by addition of 39 mmol/kg tridodecylamine and potassium tetrakis(4-chlorophenyl)borate to give an ionophore-to-ionic site ratio of 3 to 1 or 1.5 to 1 (giving 13 or 26 mmol/kg as the final concentration of ionic site in the ISE membrane, respectively). Solutions were stirred until the PVC had completely dissolved and then poured into a glass Petri dish of 25 mm diameter and left to dry over 24 h to give a plasticized PVC master membrane. Smaller

circular disks of 7 mm were cut from master membranes and glued onto a Tygon tube with THF.

5.2.4 Synthesis of Poly(MMA-co-LMA) Copolymer and Membrane Preparation

Removal of inhibitor in monomers: To remove the inhibitor 4-methoxyphenol, 5 mL MMA or DMA was washed with aqueous solutions containing 5 g NaOH/100 mL water and 20 g NaCl/100 mL water three times (15 mL x 3), then with water until the pH of resulting aqueous phase was neutral. The organic liquids were collected, dried over sodium sulfate, and the drying agent was removed by filtration prior to use.

Synthesis of poly(MMA-co-LMA) copolymers: The synthesis method was adapted from a previously reported procedure.²⁴⁵ 1.06 g MMA and 3.94 g LMA (**Type I**, 25 wt% MMA and 75 wt% LMA) or 1.50 g MMA and 1.50 g LMA (**Type II**, 50 wt% MMA and 50 wt% LMA) were dissolved in 3 mL anhydrous ethyl acetate and added to a two-neck round bottom flask and purged three times with argon. Then 1 mL anhydrous ethyl acetate solution of 10.54 mg AIBN was added with a syringe. To ensure the correct ratio of MMA and LMA, sealing of the reaction flask is critical given the low vapor pressure of MMA. After the reaction was refluxed under argon for 18 h, solvent evaporation yielded a light-yellow viscous liquid which was then re-dissolved in 20 mL dioxane. Then the dioxane solution was added dropwise through a dropping funnel to a beaker of 800 mL vigorously stirred DI water, resulting in the formation of a very sticky white precipitate. The water phase was discarded, and the white precipitate was re-dissolved in 100 mL dichloromethane and dried over sodium sulfate. Removal of the

drying agent by filtration and evaporation of the solvent gave 2.03 g of the final product (yield: 40.6%).

Membrane preparation: Cocktail solutions for pH-selective poly(MMA-*co*-LMA) membranes were prepared by adding 13.34 mg TDDA and 3.59 mg KTpCIPB (giving a 3 to 1 ratio of ionophore to ionic site) to a 6 mL stirred THF solution of 1.041 g copolymer.

For electrodes with a conventional setup with an inner filling solution, an amount of cocktail solution with copolymer equivalent to 200 mg was then added into a Teflon Petri dish of 25 mm diameter and left to dry overnight to give a master membrane. Smaller circular disks of 19 mm were cut from these master membranes and mounted in custom-made electrode bodies (See Chapter II, **Figure 2.3**).²⁵ An aqueous solution containing 10 mM NaCl, 10 mM Na₂HPO₄, and 10 mM NaH₂PO₄ solution (pH = 7.4) was used as inner filling solution. Prior to use, the electrodes were conditioned overnight in solutions with the same composition as the inner filling solution.

For electrodes in solid contact setup, gold electrodes (planar circular Au electrodes with a 2 mm diameter, embedded into an inert Kel-F polymer shaft; CH Instruments, Austin, TX) were polished on a polishing cloth, first with 0.5 μm and then with 0.03 μm aqueous aluminum oxide slurry (Buehler, Lake Bluff, IL), and then sonicated first in water and then in ethanol, each for 6 min. A stream of argon was used to dry the electrodes. A CIM carbon suspension solution was prepared by dissolving 50 mg CIM carbon in 1.0 mL THF. Then, 30 μL of this suspension was dropcast onto the gold electrode and left to dry. This was followed by two aliquots (20 μL followed by 30 μL) of copolymer membrane solution dropcast onto the CIM carbon layer. After letting the solvent evaporate overnight,

the electrodes were conditioned in 10 mM NaCl, 10 mM Na₂HPO₄, and 10 mM NaH₂PO₄ solution (pH = 7.4) prior to use.

5.2.5 Synthesis of Crosslinked Poly(Decyl Methacrylate) and Membrane Preparation

To remove the inhibitor hydroquinone, DMA and hexanediol dimethacrylate were passed through a column of basic alumina. For blank polymer membranes without added sensor components, a total of 600 mg polymer matrix was prepared. 1.5 wt% photoinitiator DMPP was weighted in a vial. Then crosslinker hexanediol dimethacrylate of 2, 3, and 5 wt% and monomer decyl methacrylate of 96.5, 95.5, and 94.5 wt%, respectively, were converted to volume and added to DMPP via micropipette. The solution was stirred to completely dissolve the initiator. For membranes doped with free ionic sites, 13 mmol/kg potassium tetrakis(pentafluorophenyl)borate and 40 mmol/kg ionophore tridodecylamine, or 2-(dimethylamino)ethyl methacrylate, or 2-(diisopropylamino)ethyl methacrylate were added to the membrane matrix mixture. For membranes doped with covalently attached ionic sites, see the Results and Discussion for specific concentrations.

For conventional self-standing membranes, solutions of membranes were placed in between two UV transparent quartz glass separated by a pair of Feeler gauges of 0.25 mm thickness. A sealed box was purged with argon for 10 min. With the argon flow continuing, a UV lamp with peak output at 365 nm was used for 20 min (too short or too long may result in incomplete polymerization or carbonization of the membrane, respectively) to yield a crosslinked polymethacrylate membrane by polymerization. Smaller circular disks of 19 mm were cut from master membranes and mounted into custom-made electrode

bodies (See Chapter II, **Figure 2.3**).²⁵ An aqueous solution containing 10 mM NaCl, 10 mM Na₂HPO₄, and 10 mM NaH₂PO₄ (pH = 7.4) was used as inner filling solution. Prior to use, the electrodes were conditioned overnight in solutions with the same composition as the inner filling solutions.

For electrodes with nanographite or fullerene as solid contact, gold electrodes were cleaned and prepared in the same fashion as described in Section 5.2.4. A carbon suspension solution of either nanographite or fullerene was prepared by dissolving 50 mg carbon in 1.0 mL THF, followed by sonication for 30 min. Then, 2 μ L of this suspension was dropcast with a microsyringe to form a disk that was large enough to cover the gold surface entirely but smaller than necessary to fully cover the inert Kel-F enclosing the gold electrode. This was followed by carefully adding 5 μ L membrane solution using a microsyringe from the edge of the electrode surface to allow gradual flow of the membrane solution onto the previously deposited carbon layer. This way the carbon layer was not disturbed by the addition of polymer solution. For electrodes with the solid contact setup comprising a graphite rod, graphite rods were polished with sandpaper (100 grit size followed by 600 grit size) to give a flat surface. Two aliquots (5 μ L followed by 30 μ L) of polymer membrane solution were dropcast onto the rod surface.

After the addition of membrane solutions, the electrodes were placed into a well-sealed box covered by a UV transparent quartz glass plate. The box was purged with argon for 10 min, then with the same argon flow continuing, membranes were polymerized under UV irradiation (peak output: 365 nm) for 20 min. The oxygen-free environment provided

by with the sealed box and the argon flow were found to be critical. Without a well-sealed setup and the argon flow, partial or complete lack of polymerization was observed.

In the case of electrodes with a graphite rod as solid contact, an external custom-made electrode body case was used to carefully and fully enclose the carbon rod, and a copper wire was used to connect the carbon rod to the potentiostat. Caution should be used to cause as little rotating motion as possible when assembling the electrode body. No unnecessarily excessive mechanical pressure should be used so that the edge of the electrode body interfacing the sensing membrane does not cut or damage the poly(methacrylate) membrane. All electrodes were conditioned in 10 mM NaCl, 10 mM Na₂HPO₄, and 10 mM NaH₂PO₄ solution (pH = 7.4) prior to use.

5.2.6 Synthesis of the Covalently Attachable Ionic Site 3-Sulfonylpropyl Methacrylate Tridodecylammonium Salt

512.12 mg 3-sulfonylpropyl methacrylate potassium salt (4 eq) was dissolved in 7 mL aqueous 1 M HCl solution, and 271.80 mg TDDA (1 eq) was dissolved in 33 mL diethyl ether. The two solutions were carefully equilibrated with one another in a separatory funnel. The ether phase was then collected and dried over magnesium sulfate. Removal of the drying agent and evaporation of the solvent yielded the final product (367.97 mg total, 75 mol% 3-sulfonylpropyl methacrylate tridodecylammonium salt and 25 mol% TDDA). See **Figure S5.5** for the ¹H-NMR spectrum of the final product and **Figure S5.6** for the ¹H-NMR spectrum of the 3-sulfonylpropyl methacrylate potassium salt.

5.2.7 Synthesis of 3-Sulfonylpropyl Methacrylate *N*-Isopropyl-*N*-(2-(Methacryloyloxy)-ethyl)propan-2-ammonium Salt

Five gram strongly acidic cation-exchanger resin was packed in a column and washed with 150 mL 1 M HCl. Then the resin was washed with DI water until the pH was neutral. 0.30 g 3-sulfonylpropyl methacrylate potassium salt (1 eq) was dissolved in a small amount of water and added to the column. Acidic fractions from the column were collected and 0.26 g 2-(diisopropylamino)ethyl methacrylate was added to the aqueous solution. The solution was allowed to freeze in a freezer at -80 °C over a period of 2 h before it was placed in a high vacuum freeze-dryer (0.124 mbar) for one day. Removal of water yielded a viscous colorless liquid as final product (see **Figure S5.5.7** for the ¹H-NMR spectrum).

5.2.8 Potentiometry

Potentiometric measurements were performed in stirred solutions with a 16-channel potentiometer (Lawson Labs, Malvern, PA) and a free-flowing free-diffusion double-junction reference electrode (DX200, Mettler Toledo, Switzerland; Ag/AgCl as internal reference, AgCl-saturated 3.0 M KCl as inner solution, and 1.0 M LiOAc as bridge electrolyte). The pH of sample solutions was changed stepwise by adding small aliquots of concentrated NaOH or HCl solutions. A half-cell pH glass electrode (InLab 201, Mettler Toledo, Columbus, OH; calibrated with standard NIST pH buffers of pH 4.0, 7.0, 10.0, and 12.0) was used to monitor separately the pH. Selectivity coefficients were determined for Na⁺ with the fixed interference method (FIM).^{21, 39} Nernstian slopes were confirmed in all

cases. All response times in the Nernstian response region were fast (< 5 s). Activities were calculated with a two-parameter Debye–Hückel approximation.¹⁶⁶

5.3 Results and Discussion

5.3.1 Optimal Ratio of Ionophore and Ionic sites

Tridodecylamine (**Figure 5.1**) is a well-known pH ionophore that is commercially available as Hydrogen Ionophore I. Its large hydrophobicity affords it the tendency to remain in organic membrane phases, providing it a good resistance to the gradual loss of ionophore into sample solutions.

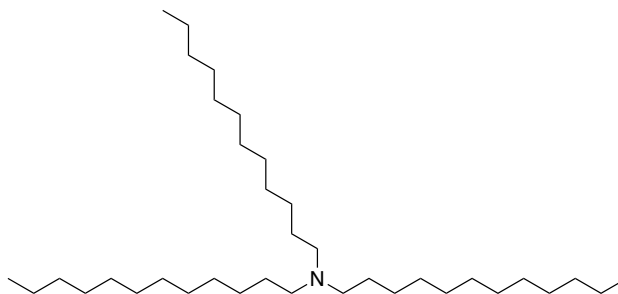


Figure 5.1 Structure of tridodecylamine

Plasticized PVC membranes made with two different ionophore-to-ionic site ratios—namely, 3 to 1 and 1.5 to 1—were investigated to establish the optimal ratio (see **Figure 5.2**). ISE membranes with a 3 to 1 ratio resulted in higher and closer-to-theoretical Nernstian response slopes (-57.7 ± 0.5 mV/decade, $n=7$) compared to membranes with a 1.5 to 1 ratio (-51.6 ± 1.1 mV/decade, $n=7$). Membranes with the 3 to 1 ionophore-to-ionic site ratio are also more selective with respect to interfering Na^+ , with a potentiometric selectivity coefficient ($\log K_{\text{H,Na}}^{\text{pot}}$) of -10.0 ± 0.7 ($n=3$), which is two

orders of magnitude higher than that of ISE membranes with a 1.5 to 1 ionophore-to-ionic site ratio ($\log K_{\text{H,Na}}^{\text{pot}}: -7.7 \pm 0.1, n=6$).

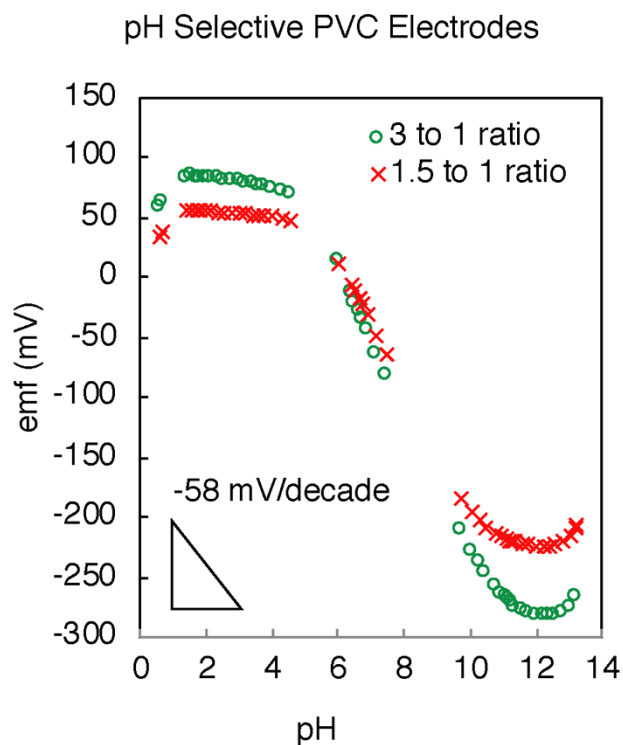


Figure 5.2 pH response of PVC-phase pH-selective electrodes with two different ionophore-to-ionic site ratios (3 to 1 and 1.5 to 1). EMF measurements were started at pH 7.4 (10 mM NaCl, 10 mM Na₂HPO₄, and 10 mM NaH₂PO₄ solution). The pH was increased by adding small aliquots of 6 M NaOH solution. Subsequently, starting again at pH 7.4, the pH was decreased by adding aliquots of 1 M HCl solution. Linear range: pH 4.1 to 12.0. Slope: -57.7 ± 0.5 mV/decade for the 3 to 1 ionophore-to-ionic site ratio ($n = 7$) and -51.6 ± 1.1 mV/decade for the 1.5 to 1 ionophore-to-ionic site ratio ($n = 7$).

The higher slope and better selectivity in ISE membranes with the 3 to 1 ionophore-to-ionic site ratio strongly suggests that contrary to the conventionally assumed 1:1 binding ratio between common pH ionophores and H^+ as primary ion, the ionophore tridodecylamine studied here and H^+ form concurrently also a 2:1 complex in addition to the 1:1 complex. This can explain the under-performance of membranes with the 1.5 to 1 ionophore-to-ionic ratio, in which due to the formation of 2:1 ionophore- H^+ complexes, there is not enough free ionophore. Free ionophore not bound to the primary ion is a prerequisite for high potentiometric selectivity (see Chapter I). Nonpolar fluoruous-phase ISEs were also shown to exhibit superior performance when prepared with a 4 to 1 ionophore-to-ionic-site ratio.¹⁵¹ It appears likely that 2:1 complexes can also be formed between H^+ and other trialkylamine ionophores.¹⁷⁵

5.3.2 ISEs with Poly(MMA-*co*-LMA) Copolymers Membrane

Two types of pH selective poly(MMA-*co*-LMA) copolymer membranes were prepared with the synthesis scheme shown in **Figure 5.3**. Sealing of the reaction system against ambient air is critical to ensure the desired ratio of monomers given the low vapor pressure of and the potential loss of MMA during the course of the reflux reaction. **Type I** copolymer, which has 25 wt% MMA and 75 wt% LMA with a Fox-equation-calculated glass transition temperature of $-35\text{ }^{\circ}\text{C}$, did not give self-standing membranes. The copolymer at this ratio turned out to be soft, hard to peel off even from the Teflon substrate, and when in contact with water, it swelled easily and turned gel-like. **Type II** copolymer prepared from 50 wt% MMA and 50 wt % LMA with a Fox-equation-calculated glass

transition temperature of $-5\text{ }^{\circ}\text{C}$ is self-supporting (see **Figure 5.4**). Since **Type I** membranes are not self-supporting, solid-contact electrodes with a carbon interlayer were fabricated to characterize their pH response. **Type II** membranes were tested with a conventional setup with an inner filling solution. Response curves of **Type I** and **Type II** membranes to pH are shown in **Figure 5.5** and **Figure 5.6**, respectively. Electrodes made with both types of poly(MMA-*co*-LMA) membranes gave within error the same linear range (pH 4.1 to 12.4) and slopes (**Type I**: 54.8 ± 1.1 , $n = 5$; **Type II**: 53.8 ± 1.8 ; mV/decade, $n = 3$) of the pH response as well as selectivity against Na^+ (selectivity coefficient $\log K_{\text{H,Na}}^{\text{pot}} = -10.9$, $n = 5$ and 3). The linear range, slope, and selectivity of pH selective poly(MMA-*co*-LMA)-based ISEs are also the same as for PVC based ISEs with the same ionophore-to-ionic site ratio (as shown in earlier sections in this chapter). It can be safely concluded that the change of membrane matrix from plasticized PVC phase to poly(MMA-*co*-LMA) had no impact on the ISE response to pH. This demonstrates that copolymers with MMA/LMA ratios ranging from 25/75 wt% to 50/50 wt% have a very similar membrane polarity to PVC plasticized with *o*-NPOE and that poly(MMA-*co*-LMA) is a suitable membrane matrix option for developing plasticizer-free pH ISEs.

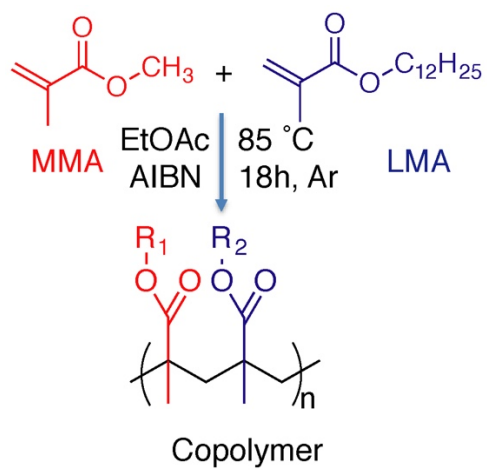


Figure 5.3 Formation of poly(MMA-*co*-LMA) by copolymerization.



Figure 5.4 Type II poly(MMA-*co*-LMA) copolymer membrane.

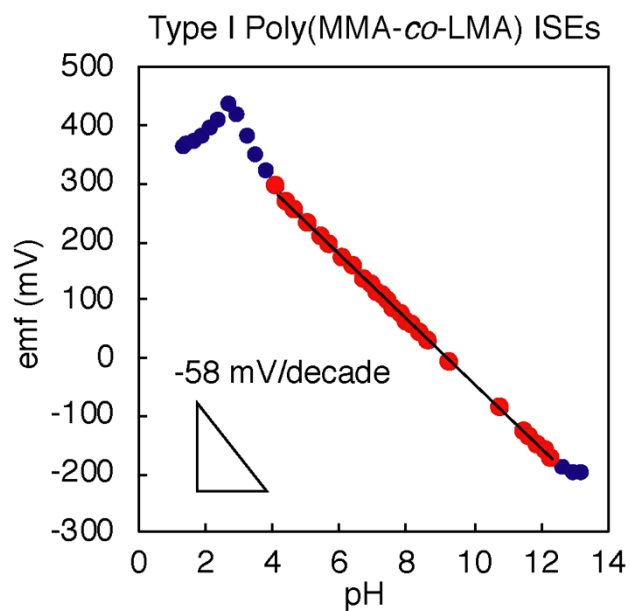


Figure 5.5 pH response of a solid-contact **Type I** poly(MMA-*co*-LMA) copolymer membrane. EMF measurements were started at pH 7.4 (10 mM NaCl, Na₂HPO₄, and 10 mM NaH₂PO₄ solution). The pH was increased by adding small aliquots of 6 M NaOH solution. Subsequently, starting again at pH 7.4, the pH was decreased by adding aliquots of 1 M HCl solution. Linear range: pH 4.1 to 12.4 (slope: -54.8 ± 1.1 mV/decade; $n = 5$).

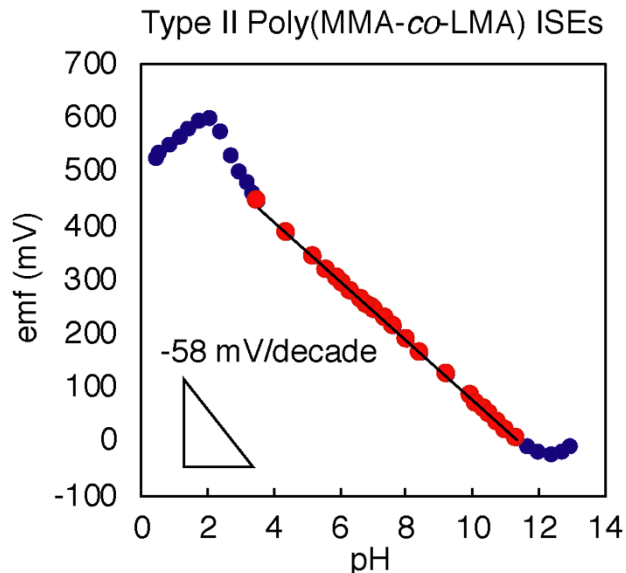


Figure 5.6 pH response of a **Type II** poly(MMA-co-LMA) copolymer membrane mounted in a conventional electrode body with inner filling solution (10 mM NaCl, Na₂HPO₄, and 10 mM NaH₂PO₄ solution). EMF measurements were started at pH 7.4 (10 mM NaCl, Na₂HPO₄, and 10 mM NaH₂PO₄ solution) solution. The pH was increased by adding small aliquots of 6 M NaOH solution. Subsequently, starting again at pH 7.4, the pH was decreased by adding aliquots of 1 M HCl solution. Linear range: pH 4.1 to 12.4 (Slope: -53.8 ± 1.8 mV/decade; n = 3).

5.3.3 UV-polymerized Crosslinked Poly(Decyl Methacrylate) Membranes

In view of developing plasticizer-free poly(methacrylate)-based membranes that can be prepared faster and in a more straightforward manner, UV polymerization was examined, as described in this section. With appropriate photoinitiators, UV polymerization can produce membranes suitable for use in ISEs within a few minutes, as compared to the much longer time (>18 h) needed for thermal polymerization. This also is

beneficial when ISEs with membranes comprise ionophores, ionic sites, ionic liquids, or salts that are unstable at higher temperature. The use of crosslinked membranes also opens the opportunity for covalently attaching sensor components that have a similar functional unit as the monomers used to prepare the membrane matrix—ideally methacrylate units for precise matching of reactivity. Chemical bonding of sensor components such as ionophores and ionic sites can prevent leaching of these components into samples. This is especially important for the development of sensors for long-term use and in special applications that involve high temperatures or high pressures.

This section describes the development of blank membranes without any sensor components from decyl methacrylate monomers by UV-polymerization with different weight percentages of bifunctional crosslinker hexanediol dimethacrylate to investigate the effect of different concentrations of crosslinker on the physical properties of the membrane matrix. The reaction scheme is shown in **Figure 5.7**, and a comparison of the physical appearances of the resulting membranes is presented in **Figure 5.8**. With a 2 wt% crosslinking level, membranes are soft, sticky, and very hard to remove from the underlying substrate. With a 3 wt% crosslinking level, the membranes are less sticky and easier to remove from the substrate. With a 5 wt% crosslinking level, membranes are not sticky and are very easy to be remove from the underlying substrate. The substrate tested here was glass. Teflon would be an ideal substrate; however, Teflon is soft and not flat, leading to either unsealed conditioned or incomplete polymerization. In the case where the entire Teflon substrate is placed in a well-sealed box, liquid membrane solutions may leach out from under the Teflon ring that makes up the dish.

For crosslinked poly(methacrylates) that are intended for long-term use, it is important to understand their physical properties and any change induced by exposure to water. To this end, contact angle measurements on methacrylate membranes with different levels of crosslinking before and after water exposure are currently underway.

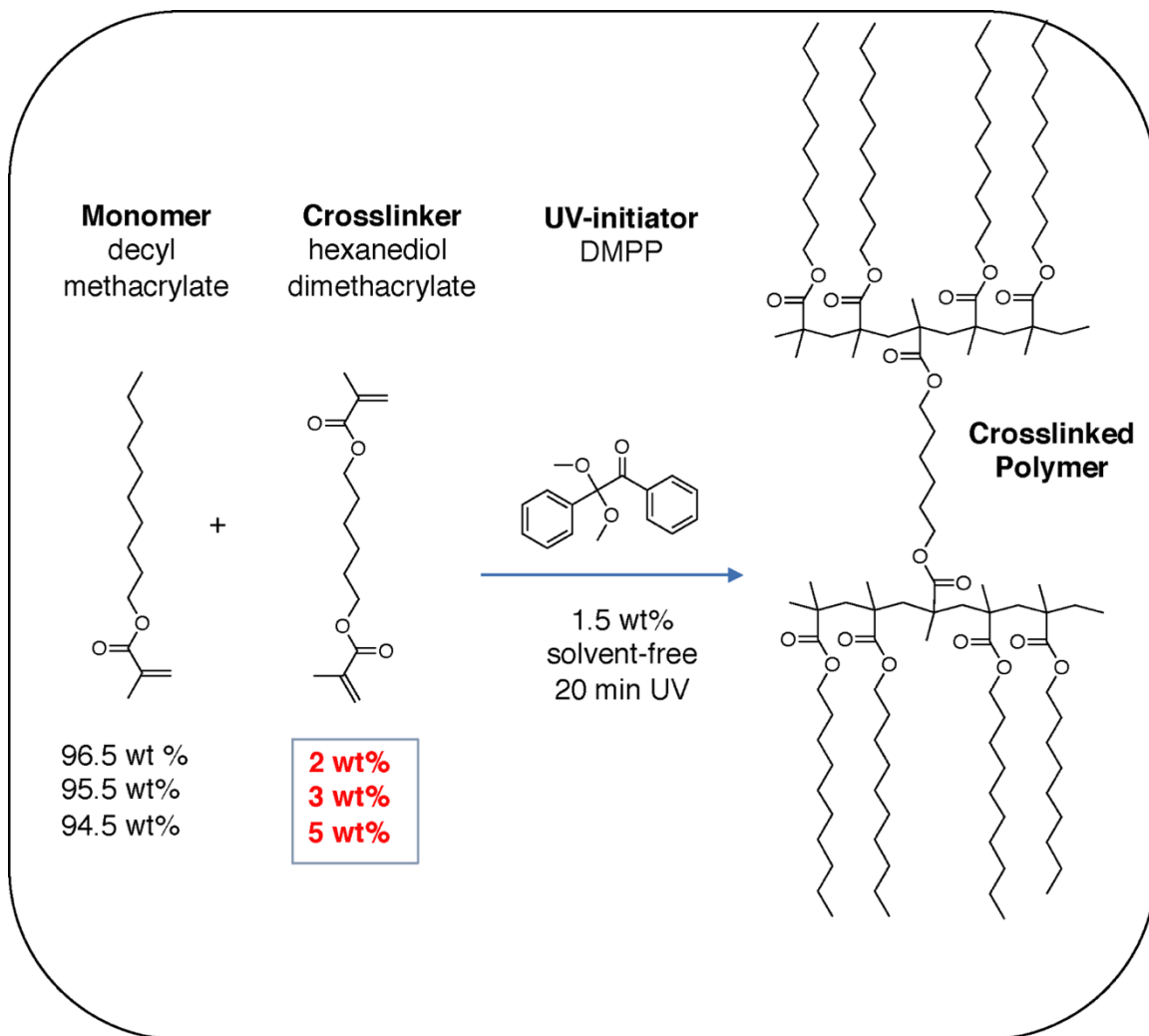


Figure 5.7 Reaction scheme for the preparation of crosslinked poly(decyl methacrylate) membranes.

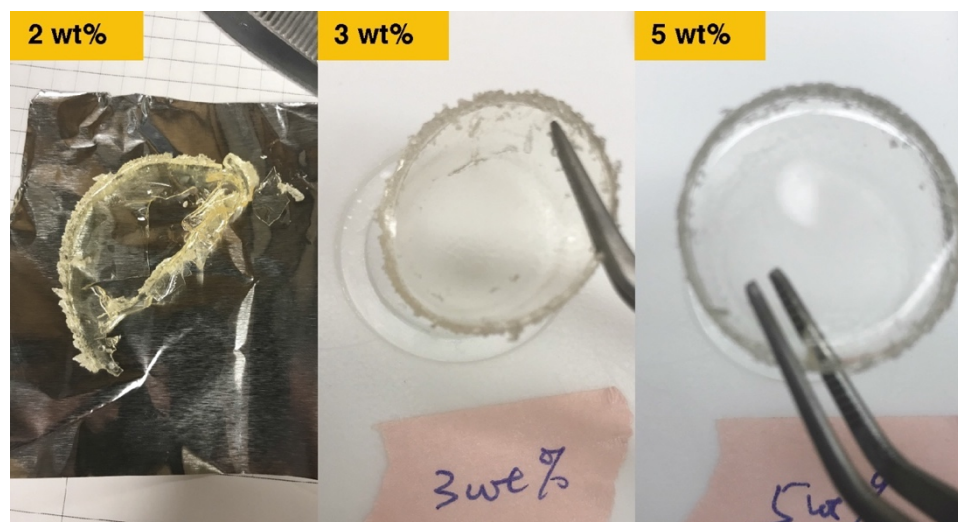


Figure 5.8 Physical appearance of poly(decyl methacrylate) membranes with different weight percentages of crosslinker.

5.3.4 ISEs with Crosslinked Poly(Decyl Methacrylate) Membranes

Three identical electrodes with pH-selective crosslinked poly(decyl methacrylate) membranes and a 3 to 1 ionophore-to-ionic site ratio were tested for their pH response. Two of the electrodes gradually developed pinholes in the membrane during conditioning and, therefore, failed due to the complete leaking of inner filling solution, losing electric contact between Ag/AgCl wire and ISE membrane, resulting in an open circuit. The remaining electrode gave within errors the same linear range (pH 4.1 to 12.4) and slope (54.9 mV/decade) in pH response as well as selectivity against Na^+ (selectivity coefficient $\log K_{\text{H,Na}}^{\text{pot}} = -10.9$; **Figure 5.9**) as pH-selective ISEs based on poly(MMA-co-LMA) and the PVC-based ISE membranes with the same ionophore to ionic site ratio, as shown in earlier sections in this chapter. We conclude here that these three membrane matrixes—

plasticized PVC, poly(MMA-*co*-LMA), and crosslinked poly(decyl methacrylate)—have a similar matrix polarity. This also demonstrates that crosslinked poly(decyl methacrylate) is a suitable membrane matrix for developing plasticizer-free pH ISEs, with the advantages of fast UV-polymerization and a methacrylate chemistry that permits the covalent attachment of sensors components such as ionophore, ionic site, ionic liquid, or salt to the polymer backbone.

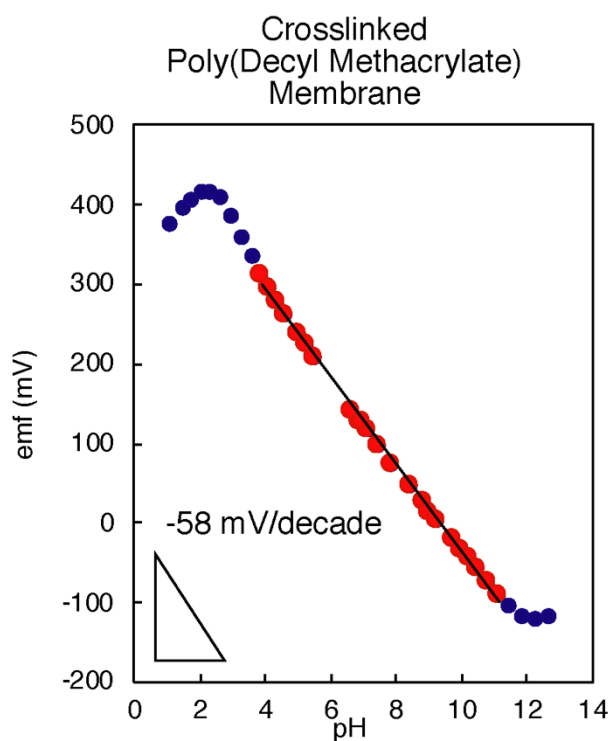


Figure 5.9 pH response of crosslinked poly(decyl methacrylate) membranes mounted in conventional ISE bodies with an inner filling solution (10 mM NaCl, Na₂HPO₄, and 10 mM NaH₂PO₄ solution). EMF measurements were started at pH 7.4 (10 mM NaCl, Na₂HPO₄, and 10 mM NaH₂PO₄ solution) solution. The pH was increased by adding small aliquots of 6 M NaOH solution. Subsequently, starting again at pH 7.4, the pH was decreased by adding aliquots of 1 M HCl solution. Linear range: pH 4.1 to 12.4 (slope: – 54.9 mV/decade; n = 1).

5.3.5 Effect of Heat Exposure on ISEs with Crosslinked Poly(methacrylate) Membranes

The effect of heat exposure was investigated for crosslinked poly(methacrylate) membranes following the measurement of their pH response. The electrode was placed in water at 90 °C for 30 min, followed by reconditioning for 1 h at room temperature and retesting of their pH response. A comparison of the pH response before and after heat exposure is shown in **Figure 5.10**, and a comparison of their potential–time profile is shown in **Figure 5.11**. The electrodes maintained their linear Nernstian responses, resistance, and selectivity against Na⁺ (before: slope: 51.3 mV/decade, resistance: 590 MΩ, and selectivity coefficient $\log K_{\text{H,Na}}^{\text{pot}} = -10.9$; after: slope: 52.8 mV/decade, resistance: 450 MΩ, and selectivity coefficient $\log K_{\text{H,Na}}^{\text{pot}} = -10.9$). This demonstrates the heat exposure at 90 °C does not compromise their excellent pH characteristics. However, the electrodes had an approximately one order of magnitude slower response (**Figure 5.11**). The response time to reach 95% of the final response after a pH change (t_{95}) increased from 5 s to 50 s after heat exposure. To understand and prevent this slower response, further investigation of membranes with increased crosslinking levels and covalently attached ionophore and ionic site is currently under way.

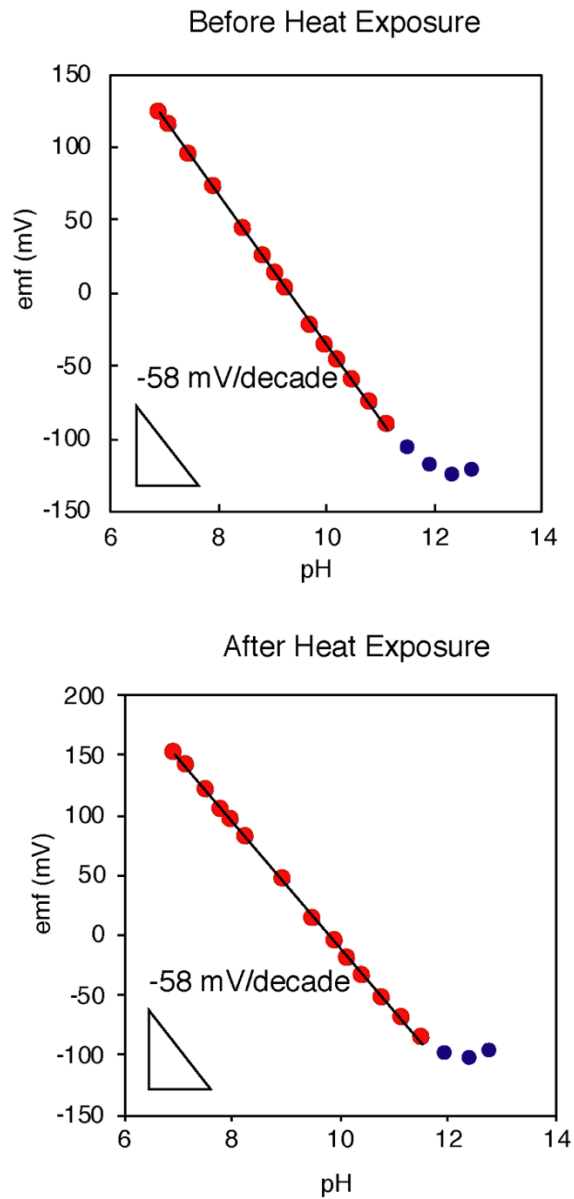


Figure 5.10 pH response of a crosslinked poly(decyl methacrylate) membrane in a conventional electrode setup with an inner filling solution (10 mM NaCl, Na₂HPO₄, and 10 mM NaH₂PO₄ solution). EMF measurements were started at pH 7.4 (10 mM NaCl, Na₂HPO₄, and 10 mM NaH₂PO₄ solution) solution. The pH was increased by adding small aliquots of 6 M NaOH solution.

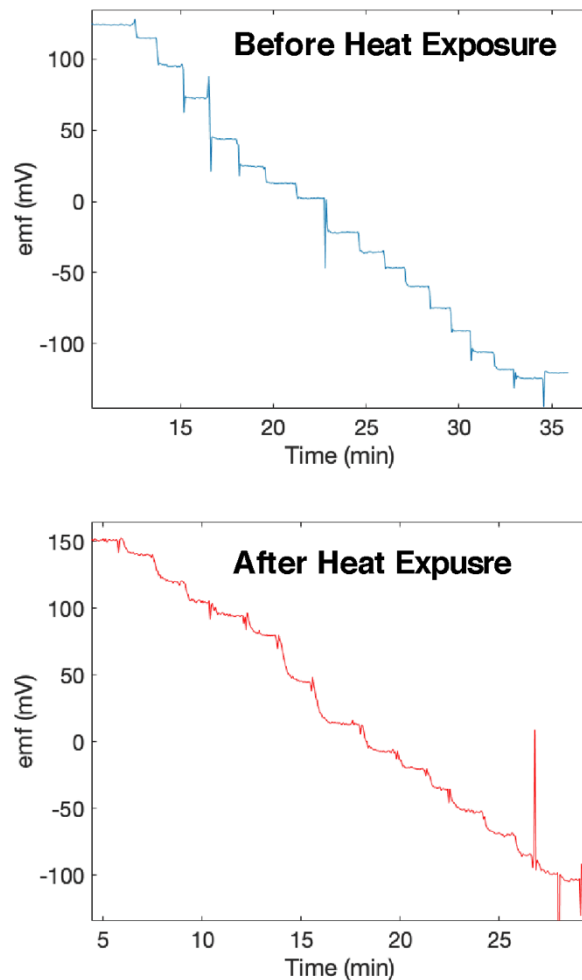


Figure 5.11 Time profile of the pH response of a crosslinked poly(decyl methacrylate) membrane in a conventional electrode setup with an inner filling solution (10 mM NaCl, Na_2HPO_4 , and 10 mM NaH_2PO_4 solution). EMF measurements were started at pH 7.4 (10 mM NaCl, Na_2HPO_4 , and 10 mM NaH_2PO_4 solution). The pH was increased by adding small aliquots of 6 M NaOH solution.

5.3.6 Solid-Contact ISEs with Crosslinked Poly(Decyl Methacrylate) Membranes Containing Free Ionophore and Ionic Sites

Optimization of the UV-polymerization of pencil-shaped solid-contact electrodes with crosslinked poly(methacrylate) membranes. Methacrylate membranes on top of fullerene solid contacts failed to polymerize because the methacrylate cocktail remained liquid after UV irradiation. It is likely due to dissolution of the fullerene into the methacrylate solution, impeding UV polymerization by absorption of the UV light by the fullerene. In initial experiments, methacrylate membranes on top of nanographite solid contacts polymerized; however, the polymerization conditions also resulted in severe cracking and disruption of the carbon layer. Optimization of this process was performed by reduction of the size of the carbon disk so that it was only slightly larger than the gold surface but smaller than the inert Kel-F polymer surrounding the gold disk. Then methacrylate membranes were cast to cover the entire front face of the Kel-F body, thus enclosing the smaller carbon disk entirely. UV polymerization in this setup proved to be reliable and did not cause any cracking problems.

In addition, an improved well-sealed box for the polymerization with continuous argon purging during the polymerization also proved to be very critical. Without an argon atmosphere, a lower polymerization efficiency or even at times no polymerization was observed. With the new membrane/carbon layer structure and improved oxygen- and water-free environment, UV polymerization of methacrylate membranes with nanographite carbon solid contacts is reliable. An electrode made with this procedure is shown in **Figure 5.12**.

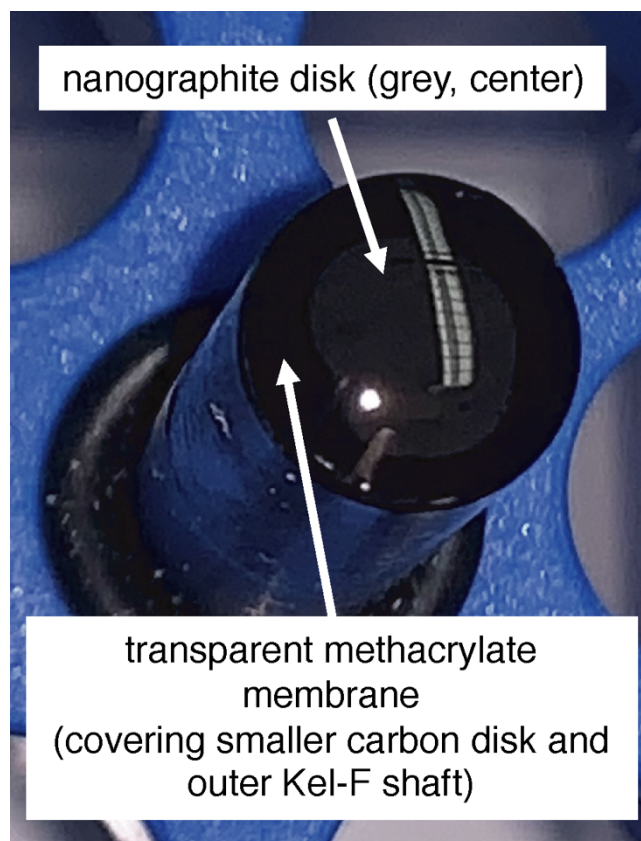


Figure 5.12 Crosslinked polymethacrylate membrane UV-polymerized on top of nanographite carbon as solid-contact material. With the improved setup and oxygen- and water-free conditions, membranes can be efficiently and reliably polymerized without any cracks in the carbon solid contact.

ISE pH response and reversibility. pH-selective crosslinked poly(methacrylate) membranes were tested for the response reversibility in the range of their linear (Nernstian) response (pH 4 to 11). Two types of crosslinked poly(methacrylate) membranes (1.5 wt% and 4 wt% crosslinker concentrations) and two types of solid contact materials (nanographite and graphite rods) were used in all possible combination, giving four different configurations. Three identical electrodes were made for each of these four

configurations. Reversibility was assessed by comparing the slope and intercept of two subsequent calibrations for each electrode: first a response curve from pH 4 to pH 11, and then a response curve from pH 11 back to pH 4. The complete set of slope, intercept, and resistance values is shown in **Table 5.1**, with calibration curves of Electrodes 1, 6, 9, and 10 shown in **Figure 5.13** as representatives of each of the four configurations.

When nanographite was used as solid-contact, both 1.5 and 4 wt% crosslinked poly(methacrylate) membranes gave good Nernstian and reversible pH responses, with the 1.5 wt% crosslinked membranes having slightly better reversibility. When a graphite rod was used as solid contact, both 1.5 and 4 wt% crosslinked poly(methacrylate) membranes gave good Nernstian and reversible pH responses, with 4 wt% membranes having slightly better reversibility.

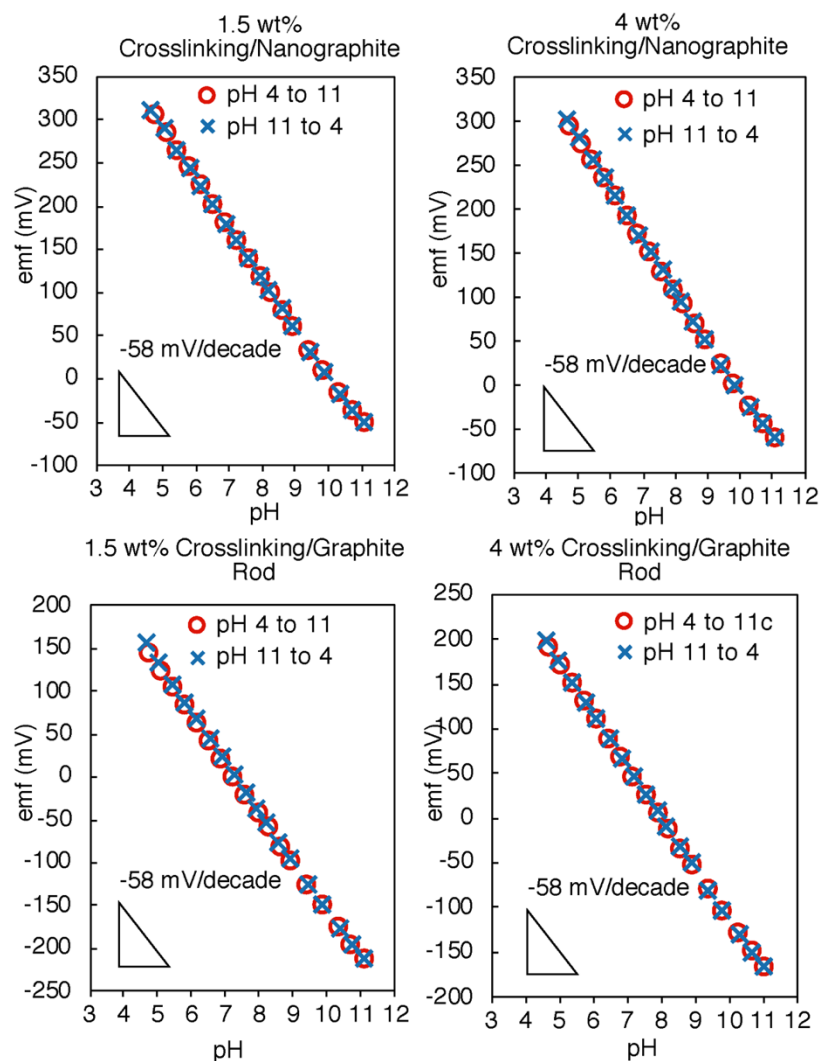


Figure 5.13 pH response and reversibility of crosslinked poly(decyl methacrylate) membranes in a solid-contact electrode set up. Top left and right: 1.5 wt% and 4 wt% crosslinked poly(methacrylate) membranes with nanographite as solid contact. Bottom left and right: 1.5 wt% and 4 wt% crosslinked poly(methacrylate) membranes with a graphite rod as solid contact. EMF measurements were started at pH 4.7 (10 mM NaCl and 10 mM NaH_2PO_4 solution) solution. The pH was increased by adding small aliquots of 6 M NaOH solution. Subsequently the pH was lowered by adding small aliquots of 1 M HCl solution.

Table 5.1. pH Response and Reversibility of Solid-Contact ISEs with Crosslinked Poly(methacrylate) Membranes.

Membrane Crosslinking	Nanographite solid contact					
	pH calibration direction	Slope/mV/decade		Intercept/mV		R/M Ω
		4→11	11→4	4→11	11→4	
1.5 wt%	Electrodes No.	Individual electrode				
	1	-57.3	-57.2	574.1	573.7	30
	2	-57.3	-57.2	577.9	578.0	17
	3	-57.2	-58.2	551.8	563.2	38
4 wt%	Electrodes No.	Individual electrode				
	4	-57.0	-57.8	546.6	557.1	35
	5	-56.9	-58.0	551.4	564.7	34
	6	-56.9	-57.2	561.9	565.4	11
Membrane Crosslinking	Graphite rod solid contact					
	pH calibration direction	Slope/mV/decade		Intercept/mV		R/M Ω
		4→11	11→4	4→11	11→4	
1.5 wt%	Electrodes No.	Individual electrode				
	7	-56.9	-57.8	422.5	432.9	420
	8	-50.9	-51.3	445.3	440.2	4
	9	-57.1	-57.8	414.0	422.4	331
4 wt%	Electrodes No.	Individual electrode				
	10	-57.0	-57.2	459.4	461.6	100-7
	11	-55.7	-56.0	437.5	440.6	730
	12	-52.7	-52.9	431.9	428.6	33

Water leaking and shorting of graphite-rod solid-contact electrodes. Electrodes 8 and 12, both with a graphite rod as solid contact enclosed within an external electrode body, exhibited a more than two orders of magnitude lower resistance. This is clear evidence of water entering the electrode body, resulting in shorting with the conductive carbon. This is a problem with the external electrode body design. An illustration of the electrode body design with a carbon shorting pathway is given in **Figure 5.14** (left). A fundamentally different way to avoid this problem is to covalently attach the sensing membranes to the external body (in **Figure 5.14**, right). Suitable materials for such as tube-shape electrode body include glycol-modified polyethylene terephthalate (PET-G) which through surface modification can yield functional methacrylate units that can allow attachment of poly(methacrylate)-based membranes to avoid any water shorting problems.²⁴⁶ This is a promising direction since for many applications pencil shape electrodes are desirable, and membrane delamination from substrate is a frequent problem.^{84, 191, 192} Work to develop the covalent attachment of sensing membranes to PET-G electrode bodies is currently underway.

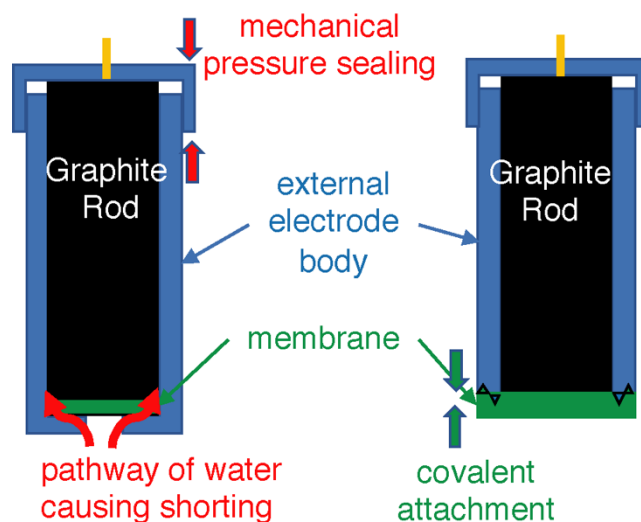


Figure 5.14 Illustration of common electrode body design that can lead to water bypassing the sensing membrane and shorting problems (left), and a design with polymeric membranes covalently attached to the external electrode body, avoiding such shorting (right).

5.3.7 ISEs with Crosslinked Poly(Decyl Methacrylate) Membranes and Covalently Attached Ionophore

Poly(methacrylate) ISEs membranes doped with covalently attached ionophore were made by copolymerization with an amine that has a methacrylate group, i.e., 2-(dimethylamino)ethyl methacrylate or 2-(diisopropylamino)ethyl methacrylate (see **Figure 5.13** for the reaction scheme). Since this ionophore has exactly the same functional methacrylate unit as the monomer of the polymer matrix, it is covalently attached during polymerization to the matrix polymer backbone. This approach avoids loss of ionophore during exposure of the sensor to samples and is expected to result in improved sensor lifetimes as compared to ISEs membranes doped with an ionophore not covalently attached to the polymer matrix.

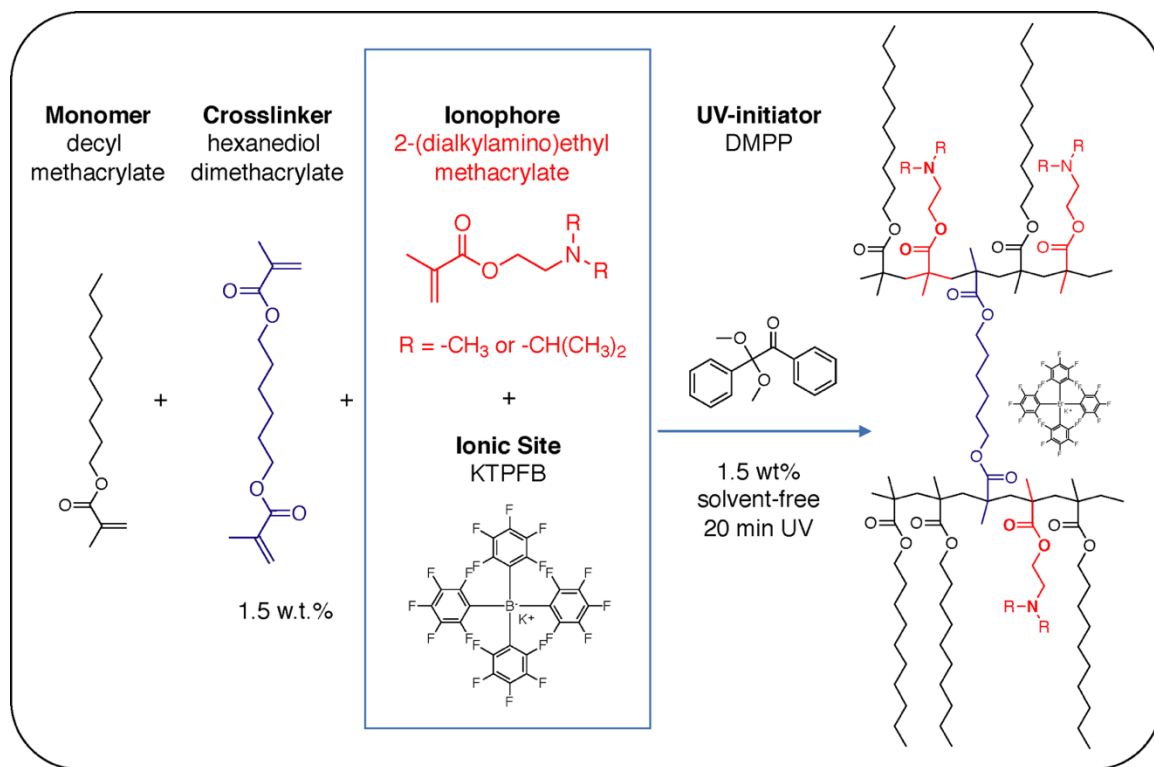


Figure 5.15 Reaction scheme for the preparation of crosslinked poly(methacrylate) membranes doped with a covalently attached pH ionophore.

The calibration of electrodes with covalently attached ionophore gave Nernstian and reversible responses (**Figure 5.16**). The linear range, from pH 1.9 to pH 9.2, is approximately two pH units shifted to the acidic direction as compared to ISEs with membranes doped with mobile tridodecylamine as ionophore. This is expected based on a well-developed theory⁵⁹ given that 2-(dimethylamino)ethyl methacrylate is a structurally less basic amine than tridodecylamine. The pK_a value of 2-(dimethylamino)ethyl methacrylate and tridodecylamine were calculated to be 8.18 and 9.84 using Advanced Chemistry Development (ACD).²⁴⁷⁻²⁴⁹ The difference between their pK_a is 1.66 in logarithmic scale, very close to their working range shift of 2 pH units. The resistance was

measured to be 300 M Ω , which is the same order of magnitude as for the same membrane matrix with the mobile ionophore tridodecylamine. This is not a surprise given that the ionic site is the same and not covalently attached to the polymer backbone. Among six identical electrodes, three gave an average slope of 55.7 ± 1.0 mV/decade while three others gave slopes below 50 mV/decade.

Follow-up experiments with a covalently attachable ionophore 2-(diisopropylamino)ethyl methacrylate are under way. With two isopropyl groups replacing the two methyl groups on the center nitrogen, the new ionophore is more basic (pK_a : 9.33 calculated by ACD) and is expected to give a pH range closer to that of tridodecylamine. (For the theory of ionophore-based pH ISEs, see Chapter I.)⁵⁹

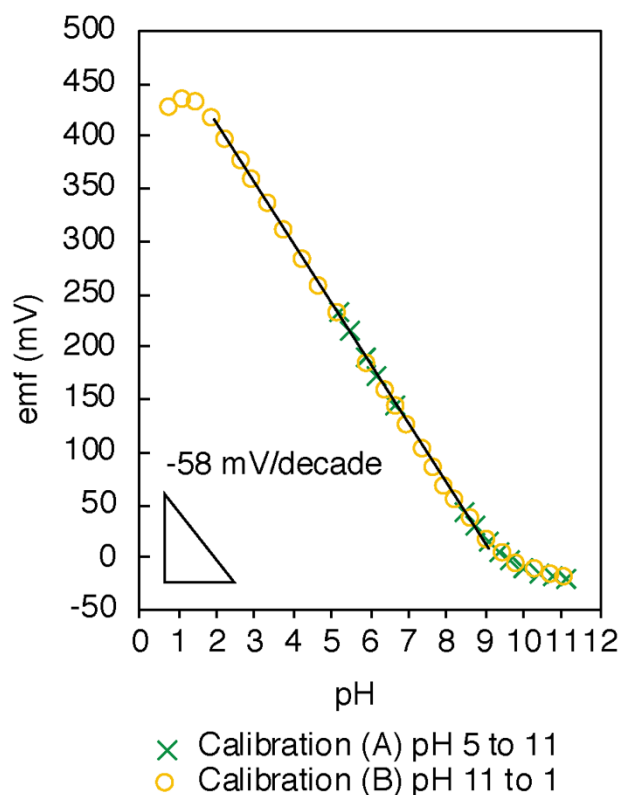


Figure 5.16 pH response and reversibility of crosslinked poly(decyl methacrylate) membranes in a solid contact ISE set up with a covalently attached ionophore. EMF measurements were started at pH 4.7 (10 mM NaCl and 10 mM NaH₂PO₄ solution) solution. The pH was increased by adding small aliquots of 6 M NaOH solution. Subsequently the pH was lowered by adding small aliquots of 1 M HCl solution. Average slope: -55.7 ± 1.0 mV/decade (n=3).

5.3.8 ISEs with Crosslinked Poly(Decyl Methacrylate) Membranes and Covalently Attached Ionic Sites

Covalently attachable ionic sites. The mobile ionic sites most frequently used for the fabrication of ISEs are highly hydrophobic tetraphenylborate modified on all four of

their aromatic rings with groups, such as 4-Cl-, 2,3,4,5,6-pentafluoro-, or 3,5-trifluoromethyl-phenyl groups. Note that these electron-withdrawing groups not only increase the hydrophobicity but also improve chemical stability.² Ionic sites for covalently attachment that have been reported in the literature previously are tetraphenylborates modified with a methacryloylmethyl unit,⁸⁴ a methacryloylethyl unit,⁸³ a triethoxysilylpropoxy unit,^{102, 103, 136} or an allyloxy unit.^{103, 136} A sulfonated PVC polymer (sulfonate as ionic sites) has also been reported.¹³⁷ The first three in this list are not commercially available and only one of their four phenyl rings was modified with a covalently attachable unit. The remaining three phenyl rings were left unmodified, which may be a disadvantage in terms of chemical stability. The latter, i.e., the sulfonated PVC polymer, cannot be readily used with non-PVC polymeric membranes. Styrene sulfonate, which has not been used previously for ISE membrane purposes but is often used to prepare other types of membranes with ion exchange properties, has a carbon-carbon double bond, but because it is not methacrylate its reactivity is not well matched for use in polymethacrylate membranes.

In the research described here, for the first time, an alkyl sulfonate with a methacrylate unit was used to match the reactivity in the polymerization precisely with that of the methacrylate matrix monomer. For pH measurements, one pre-requisite is that the ionic site has a pK_a low enough that in all relevant applications, the ionic site remains dissociated from H^+ and negatively charged. The pK_a values for the sulfonate salt used in this study has not been reported previously. For approximation and comparison, however, the pK_a of benzenesulfonic acid and methanesulfonic acid in water are -2.8 and -1.9,²⁵⁰

respectively, both of which are sufficiently low for the vast majority of applications.

However, a commercially available alkyl sulfonate with a methacrylate unit, the 3-sulfopropyl methacrylate potassium salt, is not sufficiently soluble in decyl methacrylate. To increase its solubility, the potassium ion was exchanged for the tridodecylammonium ion, the protonated form of the ionophore tridodecylamine by equilibration of an acidic aqueous solution with an ether solution of the ionophore in the presence of the sulfonate. Other (inert) hydrophobic cations such as tetraalkylammonium ions have been used to pair with ionic sites to increase the solubility of ionic site salt in monomer solutions used for the polymerization of ISE ion exchanger membranes. However, it is disadvantageous to use such inert ions because they need to be replaced by ion exchange with H^+ for membranes that are selective for pH (H^+). The use of protonated form of tridodecylamine as the cation eliminates the subsequent need for ion exchange and can, therefore, significantly simplify the conditioning of ISE membranes.

After equilibration of an acidic aqueous solution with an ether solution of tridodecylamine in the presence of the sulfonate, 1H -NMR spectra (see **Figure S5.5**) confirmed that the product contained 75 mol% 3-sulfopropyl methacrylate tridodecylammonium salt and 25 mol% excess of neutral tridodecylamine. The product is fully soluble in the decyl methacrylate monomer. The excess tridodecylamine was not removed since in ISE membranes ionophores are used in greater amount than ionic site (for example 3 to 1 ionophore-to-ionic site ratio used here) and have to be added anyway to the solution needed for the polymerization. The polymerization scheme for the preparation of membranes doped with covalently attached alkyl sulfonate ionic sites is shown in **Figure**

5.17.

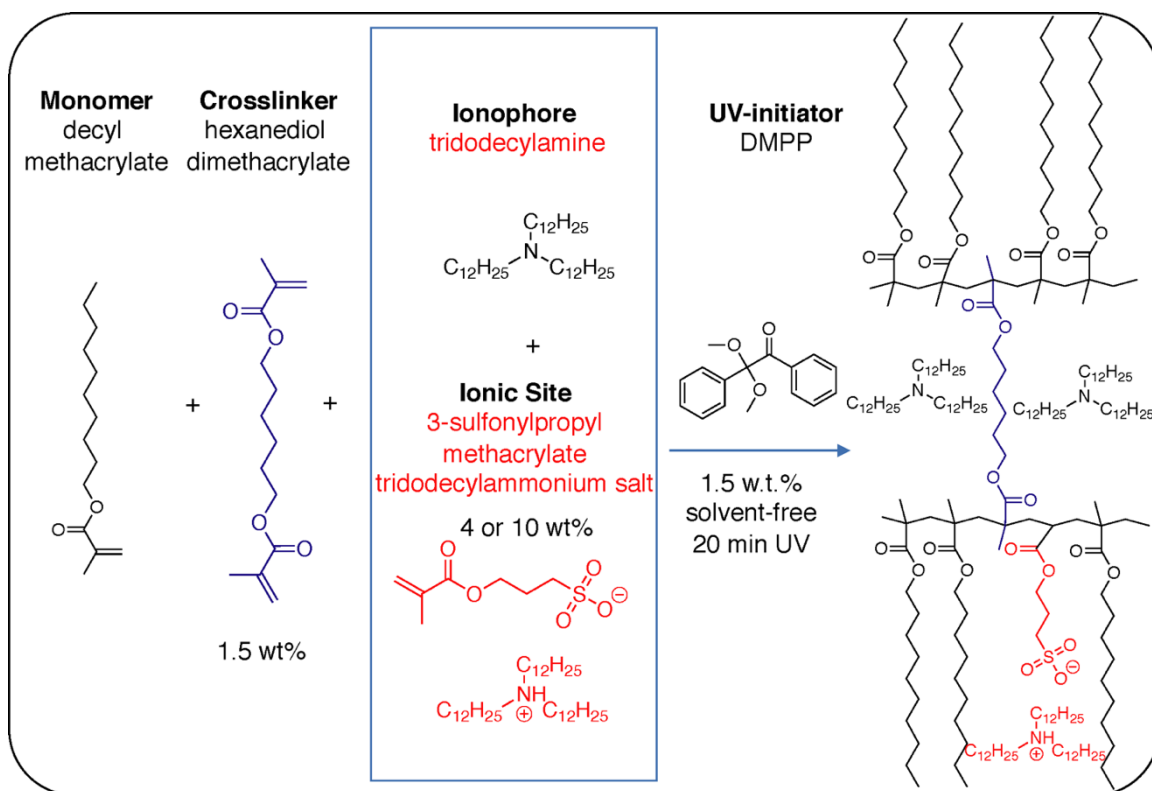


Figure 5.17 Reaction scheme for crosslinked poly(methacrylate) membranes doped with covalently attached ionic site.

pH response of membranes doped with covalently attached ionic sites. Two types of poly(decyl methacrylate) membranes—doped with either 4 or 10 wt% covalently attached ionic site and the (mobile) ionophore tridodecylamine—were prepared and tested for pH response. The membrane solution with 4 w.t.% covalently attachable ionic site was clear whereas the membrane solution with 10 w.t.% covalently attachable ionic site was homogeneously translucent. Calibration curves for ISEs with membranes that have 4 and 10 wt% covalently attached ionic sites show similar linear ranges of the pH response as

membranes doped with mobile ionic sites (pH 4 to 12). Among six identical electrodes with membranes doped with 4 wt% ionic site, one electrode gave a very close to theoretical Nernstian response slope of 56.0 mV/decade, with 23 G Ω membrane resistance. Another three electrodes gave an average slope of 48.3 ± 1.7 mV/decade (average resistance: 18 G Ω) and the other two electrodes did not give a satisfactory pH response. This demonstrates that ISEs with a covalently attached ionic site can give Nernstian responses but have an almost two orders of magnitude higher resistance than ISE membranes doped with free ionic site (with either free or covalently attached ionophore). These electrodes were made with 4 wt% ionic sites (corresponding to 54 mmol/kg concentration in membrane) which is already higher than the normal concentration of mobile ionic sites used for the work described in previous sections of this chapter (13 mmol/kg).

With the goal of improving reproducibility and reducing membrane resistance, membranes doped with 10 wt% covalently attached ionic sites were tested. Results showed similar Nernstian pH response with improved reproducibility (-51.9 ± 2.1 mV/decade, n=5). Albeit higher ionic site concentration of 10 wt% (135 mmol/kg), the resistance ranged from 4 to 30 G Ω , slightly lower than that of 4 wt% ionic sites. This indicates that the maximum solubility of covalently attachable ionic site 3-sulfonylpropyl methacrylate tridodecylammonium salt is between 4 and 10 wt% and likely closer to 4 wt% in decyl methacrylate since the increase of wt% did not significantly reduce resistance.

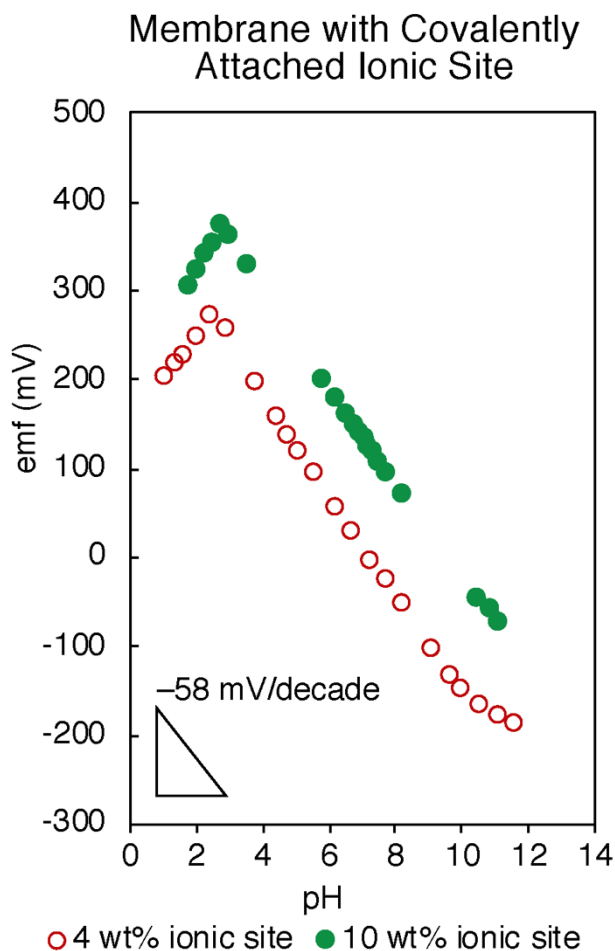


Figure 5.18 pH response of crosslinked poly(decyl methacrylate) membranes in a solid contact ISE set up with a covalently attached ionic site (4 or 10 wt%). EMF measurements were started at pH 12.0 (10 mM NaCl and 10 mM NaH₂PO₄ solution adjusted to pH 12). The pH was lowered by adding small aliquots of 1 M HCl solution. Average slope (mV/decade): 4 wt%, -56.0 (n=1); 10 wt%, -51.9 ± 2.1 (n=5).

The covalent attachment of ionic site was confirmed by elemental analysis (Atlantic Microlab, GA). Two conditions of poly(decyl methacrylate) membranes doped with 10 wt% covalently attached ionic site 3-sulfonylpropyl methacrylate tridodecylammonium and two additional mol equivalent tridodecylamine were sent for elemental analysis, i.e., pristine

membranes as polymerized, and that had exposed vigorously to stirred water for 24 h. Membranes in both conditions were dried prior to analysis under vacuum for 24 h. Results showed that before and after water exposure, the membranes contained 0.36 and 0.28 wt% sulfur, respectively. Comparison of these values to the theoretically expected sulfur content of 0.35 wt% shows that the water exposure only reduced the sulfur content slightly, still maintaining sufficient existence in the poly(methacrylate) membrane.

5.3.9 ISEs with Crosslinked Poly(Decyl Methacrylate) Membranes and Both Ionic Site and Ionophore Covalently Attached

Salt with covalently attachable ionophore and ionic site. Pairing 3-sulfonylpropyl methacrylate with 2-(diisopropylamino)ethyl methacrylate gives an ammonium-sulfonate salt that has the protonated ionophore (2-(diisopropylamino)ethyl methacrylate) as the cation and the ionic site (3-sulfonylpropyl methacrylate) as anion, i.e. 3-sulfonylpropyl methacrylate *N*-isopropyl-*N*-(2-(methacryloyloxy)ethyl)propan-2-ammonium. In this way both the ionophore and ionic site can be covalently attached to the membrane since both contain exactly the same methacrylate functional unit and together this ammonium-sulfonate salt is sufficiently soluble in the methacrylate matrix.

Initial attempts to synthesize the 3-sulfonylpropyl methacrylate *N*-isopropyl-*N*-(2-(methacryloyloxy)ethyl)propan-2-ammonium salt through water/ether extraction gave <1% yield due to the large hydrophilicity of both the cation and anion. The subsequent use of water/ethyl acetate extraction did not give the desired compound either, possibly due to side reactions resulting from the elevated temperature required for the evaporation of the

ethyl acetate solvent. To prepare the desired salt, the 3-sulfonylpropyl methacrylate potassium salt was instead first passed through a strongly acidic cation exchanger column to yield the protonated 3-sulfonylpropyl methacrylate (i.e., the sulfonic acid) as an aqueous solution. Then it was added 2-(diisopropylamino)ethyl methacrylate to form a solution of the ammonium salt, from which the water was removed by freeze-drying to give the final product a viscous colorless liquid (see the supporting information **Figure S5.7** for the ^1H -NMR spectrum). The polymerization scheme for membranes with both the ionophore and ionic site covalently attached to the polymeric membrane matrix is shown in **Figure 5.19**.

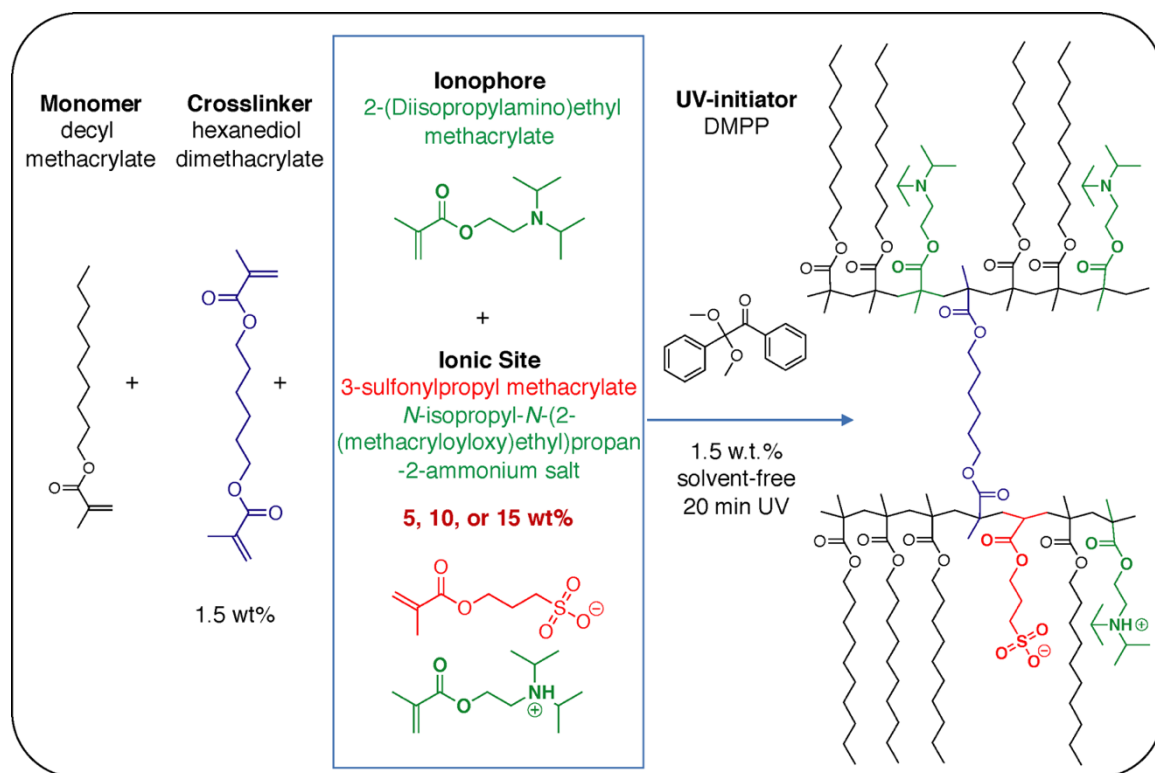


Figure 5.19 Reaction scheme for the preparation of crosslinked poly(decyl methacrylate) membranes with both ionophore and ionic site covalently attached to the polymer backbone.

pH response of membranes with ionophore and ionic site both covalently attached. Membranes with ionophore and ionic site both covalently attached were prepared in three different concentrations: 5, 10, or 15 wt% covalently attachable salt. At every concentration level, two additional mol equivalent (2 eq) covalently attachable ionophore was also added (giving, in total, a 3:1 ionophore-to-ionic-site ratio). Prior to polymerization, membrane solutions with 5 wt% covalently attachable salt were clear, whereas solutions with 10 and 15 wt% salt showed cloudiness with precipitates. This suggests that the maximum solubility of this covalently attachable salt in decyl methacrylate is between 5 and 10 wt%.

Initial calibrations of ISEs with membranes that contain 4 wt% covalently attached salt did not give satisfactory Nernstian responses. Among six identical electrodes made, one electrode gave a slope of -27.6 mV/decade in the range from pH 4.6 to pH 8.2. The other five electrodes gave little to no response to pH in the range in which electrodes with this ionophore are expected to respond. Four of the electrodes gave membrane resistances of 1.4, 1.6, 6.0, and 210 G Ω while the other two electrodes had membrane resistances that were too high to be measured with the shunt method (for the shunt method, see Chapter D).^{46, 47} ISE membranes with 15 wt% covalently attached salt gave random responses to pH with membrane resistances too high to be measured with the known shunt method as well.

In a third attempt, ISE membranes with 10 wt% covalently attached salt exhibited improved electrode responses. Among five identical electrodes, one provided a Nernstian response to pH (-54.6 mV/decade, **Figure 5.20**) with a similar linear range (pH 4 to 12) as

ISE membranes with either the ionophore or ionic site mobile and ISE membranes with both ionophore and ionic site mobile. The other four electrodes gave response slopes of –48.8, –34.2, –19.4, and –9.0 mV/decade. The average membrane resistance was measured to be $11.4 \pm 5.7 \text{ G}\Omega$ ($n=3$), similar to that of membranes with only ionic site attached, but the later provided reproducibly Nernstian responses. The resistances of both types of membranes are more than one order of magnitude higher than the resistance of membranes doped with a mobile tetraphenylborate derivative-based ionic site (with either mobile or attached ionophore). This suggests that the high resistance, i.e., low membrane ion mobility, is a result of either the covalent attachment of ionic site or the use of a sulfonate-based ionic site, or the combination of both, in contrast to a mobile tetraphenylborate derivative-based ionic site,. The octanol/water partition coefficient, $\log P$, an indicator of hydrophobicity, calculated by ChemDraw for the covalently attachable ionic site 3-(methacryloyloxy)propane-1-sulfonate (i.e., 3-sulfopropyl methacrylate anion), covalently attachable ionophore *N*-isopropyl-*N*-(2-(methacryloyloxy)ethyl)propan-2-ammonium, tridodecylammonium, mobile ionic site tetrakis(pentafluoro)borate, and potassium cation are –3.6, 3.25, 17.9, 9.6, and –1.3, respectively. By simple addition of $\log P$ for its cation and anion, the total partition coefficient of a salt can be calculated ($\log P_{AC} = \log(P_{C^+} + P_{A^-}) = \log P_{C^+} + \log P_{A^-}$). The $\log P$ for the 3-sulfopropyl methacrylate tridodecylammonium salt and potassium tetrakis(pentafluoro)borate are 14.3 and 8.3, respectively. The higher $\log P$ suggests that a higher solubility of 3-sulfopropyl methacrylate tridodecylammonium salt might be expected, although it must be recalled that solubilities and hydrophobicity are not directly correlated. Therefore, it may be that the

higher resistance is the result of the covalent attachment. Further work will have to be performed to confirm this.

On the other hand, the salt consisting of a cation that is the covalently attachable ionophore in its protonated form and an anion that is a covalently attachable ionic site (i.e., 3-sulfopropyl methacrylate *N*-isopropyl-*N*-(2-(methacryloyloxy)ethyl)propan-2-ammonium) has only a small logP value of -0.35 , which is an indicator for a relatively low hydrophilicity and, therefore, a limited solubility in the decyl methacrylate, which has a rather low polarity. This is reflected by the results from the elemental analysis of polymerized membranes. Unlike membranes doped with covalently attached sulfonate-based ionic site and mobile ionophore that showed sulfur content in elemental analysis both before and after water exposure, membrane doped with both ionophore and ionic site attached (both at 10 and 15 wt%) did not show any sulfur content in elemental analysis, neither before nor after water exposure. This is in direct disagreement with potentiometric results of membranes doped with 10 wt% covalently attached ionophore and ionic site, where the resistance was not infinite (i.e., some ionic species existed in membrane) and one electrode gave a Nernstian response. It appears likely that due to a limited solubility of the salt in the decyl methacrylate liquid phase used for the polymerization (resulting in cloudiness and precipitate formation, i.e., inhomogeneity), the sulfur (which is an indicator for the presence of ionic sites) varied from electrode to electrode depending on which portion of the master membrane was used for a given electrode membrane.

Other approaches to boost ion mobility may be the addition to the sensing membrane of a mobile ionophore in a low concentration (e.g., equivalent to 10 mol % of

the covalently attached ionophore) or by using an additional very hydrophobic salt such as ETH 500 (tetradodecylammonium tetrakis(4-chlorophenyl)borate) as electrolyte.

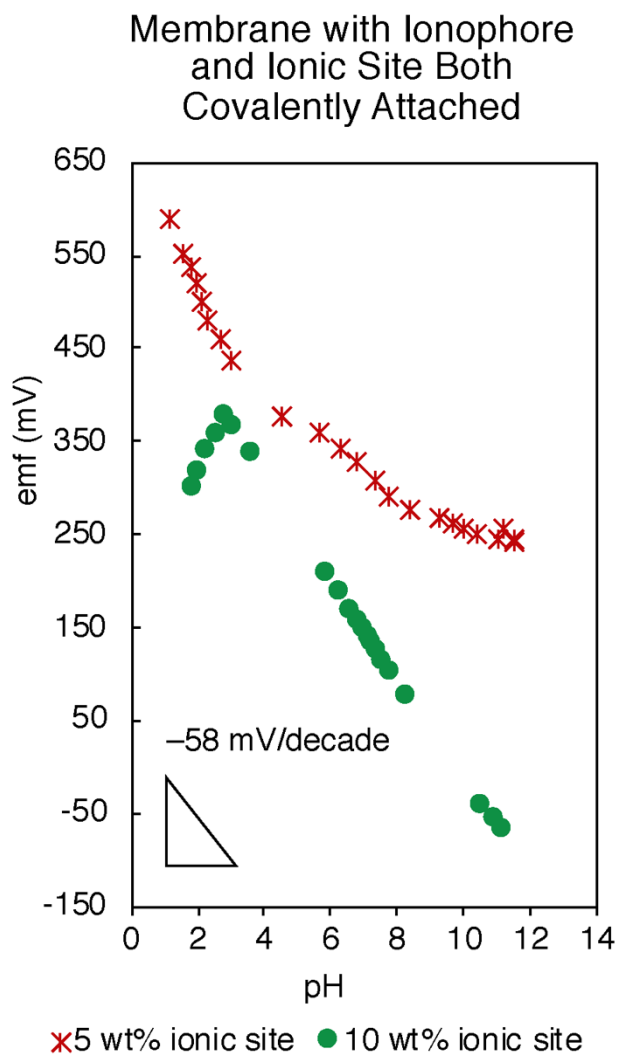


Figure 5.20 pH response of crosslinked poly(decyl methacrylate) membranes in a solid contact ISE set up with both ionophore and ionic sites covalently attached at two different concentrations (5 or 10 wt%). EMF measurements were started at pH 12.0 (10 mM NaCl and 10 mM NaH₂PO₄ solution adjusted to pH 12). The pH was lowered by adding small aliquots of 1 M HCl solution. Average slope (mV/decade): 10 wt%, -54.6 (n=1), 5 wt%, -10.5 ± 12.3 (n=6).

5.4 Conclusion

An optimal 3 to 1 ionophore-to-ionic site ratio was established by using PVC phase membranes. This finding points to the possible formation of 2:1 ionophore- H^+ complexes of trialkylamine ionophores, contrary to the long-held assumption of the formation of 1:1 ionophore- H^+ complexes. Non-crosslinked methacrylate copolymers and crosslinked methacrylate homopolymers were found to be suitable plasticizer-free membrane matrix options that provide comparable pH response characteristics as conventional plasticized PVC membranes. Crosslinked poly(decyl methacrylate) membranes have advantages over non-crosslinked copolymeric membranes that lie in their improved mechanical robustness and the faster UV polymerization synthesis. In view of long-term uses and special applications, we for the first time reported the successful use of a methacrylate-based sulfonate as covalently ionic site and of a methacrylate-based amine as covalently attached ionophore. We demonstrated that crosslinked poly(methacrylate) with either an attached ionophore or ionic site gave comparable and reproducible Nernstian responses. However, when both the ionophore and ionic site were attached, only one electrode provided Nernstian response and elemental analysis has not yet been successfully used to confirm the covalent attachment. Work aiming to enable ion hopping in membranes with both the ionic site and ionophore covalently attached is currently underway. Using different ionophores, the concept of poly(methacrylate)-based solid-state ISEs with covalently attached sensor components can be easily expanded to measurements of analytes other than pH.

5.5 Supporting Information

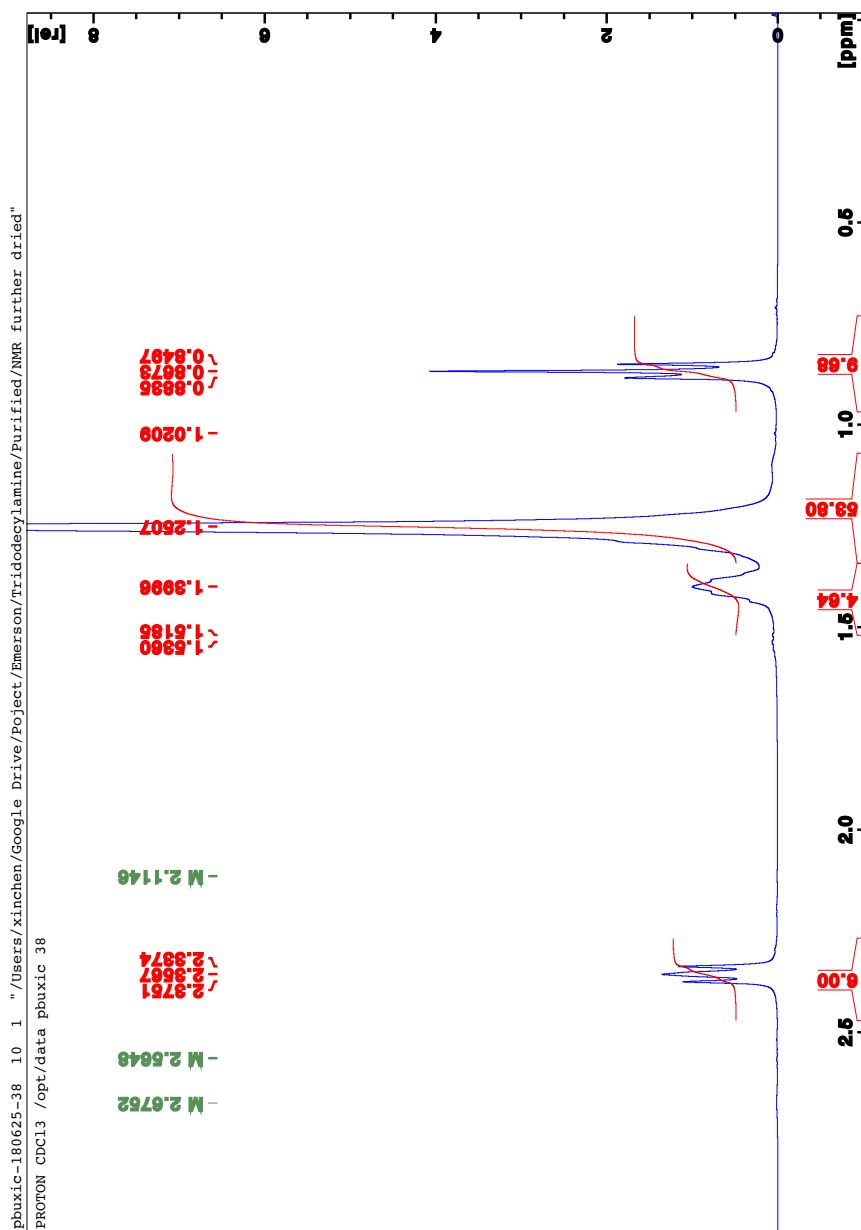


Figure S5.1 $^1\text{H-NMR}$ (CDCl_3) spectrum of purified tridodecylamine.

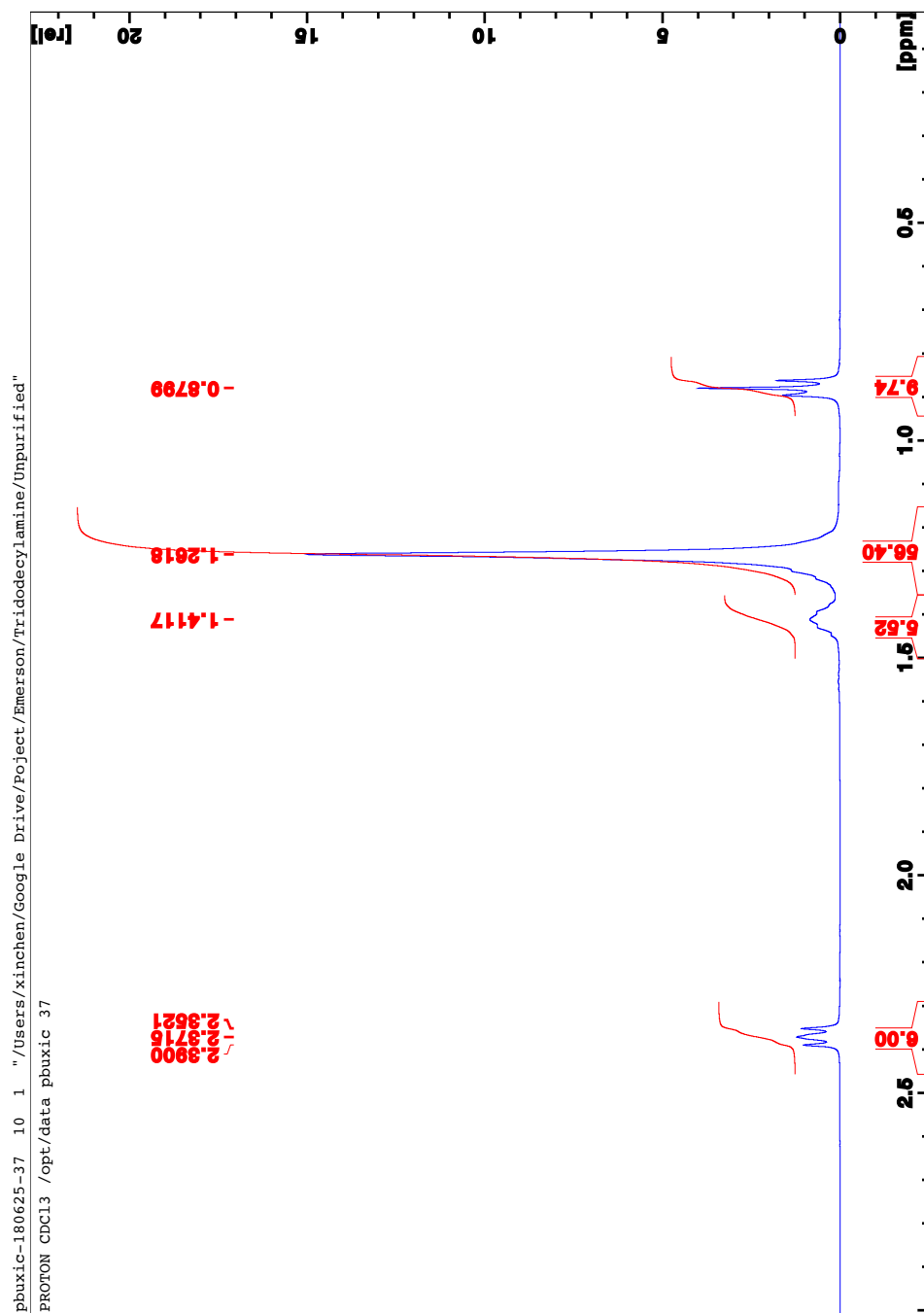


Figure S5.2 $^1\text{H-NMR}$ (CDCl_3) spectrum of unpurified tridodecylamine.

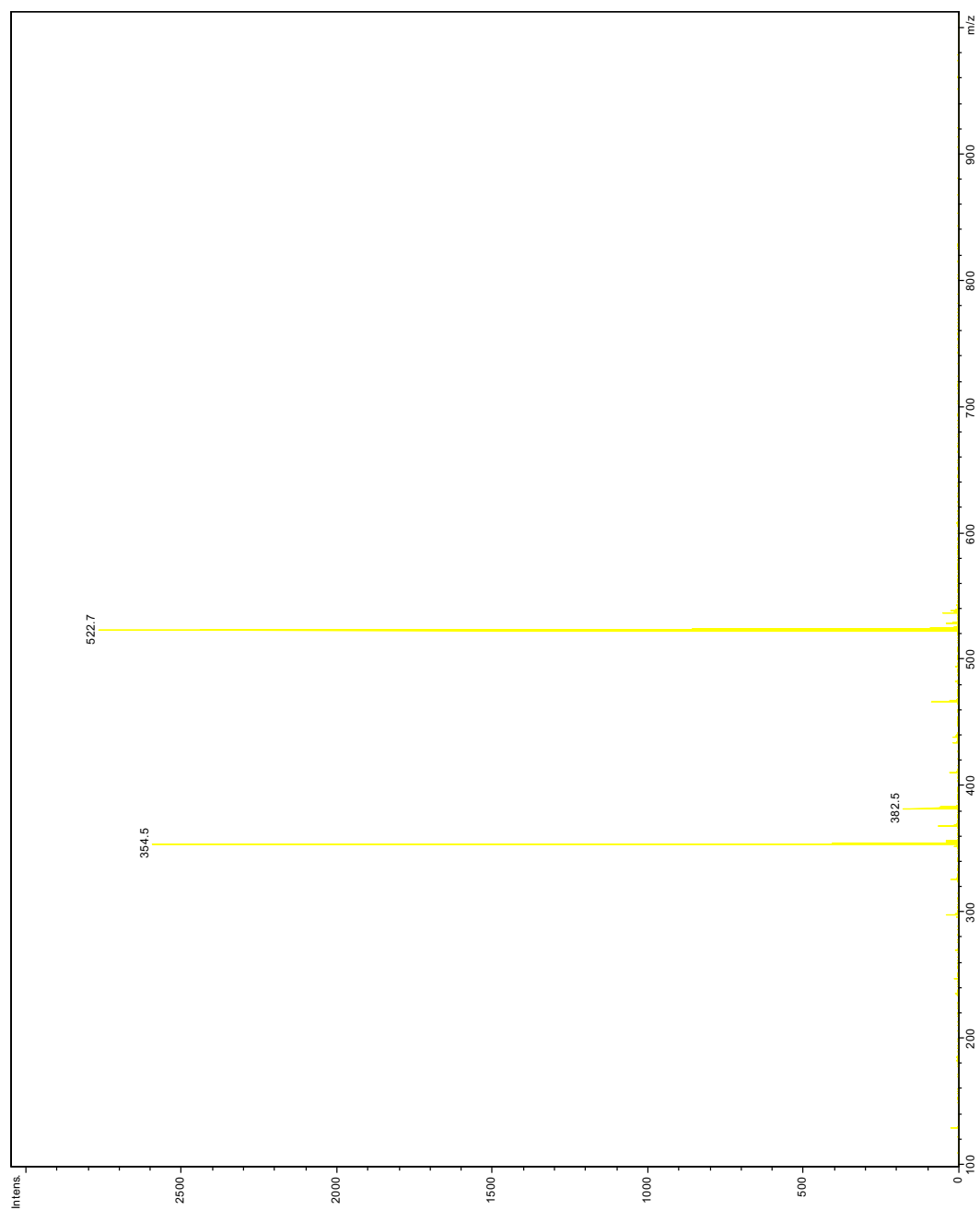


Figure S5.3 ESI-MS spectrum of purified tridodecylamine.

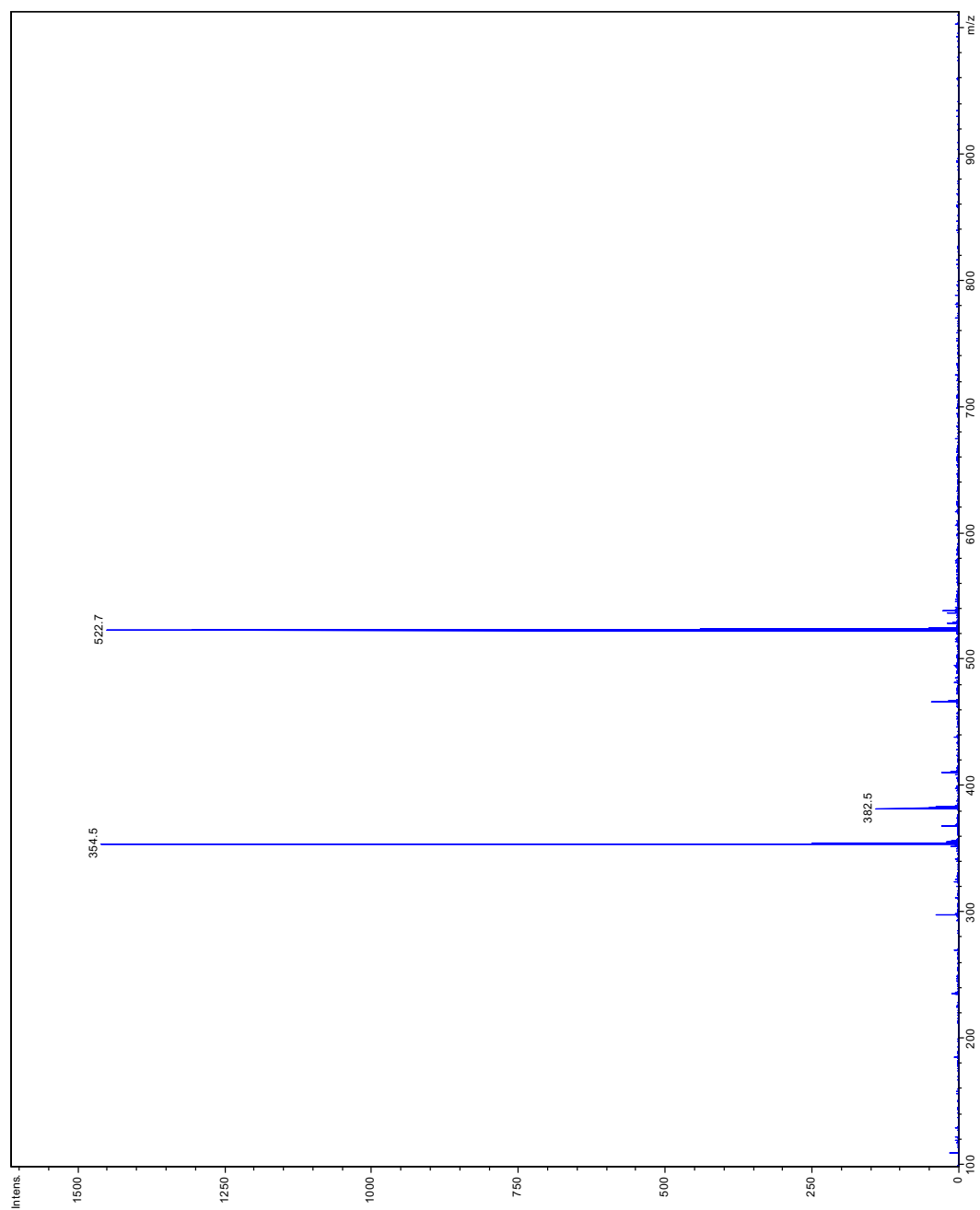


Figure S5.4 ESI-MS spectrum of unpurified tridodecylamine.

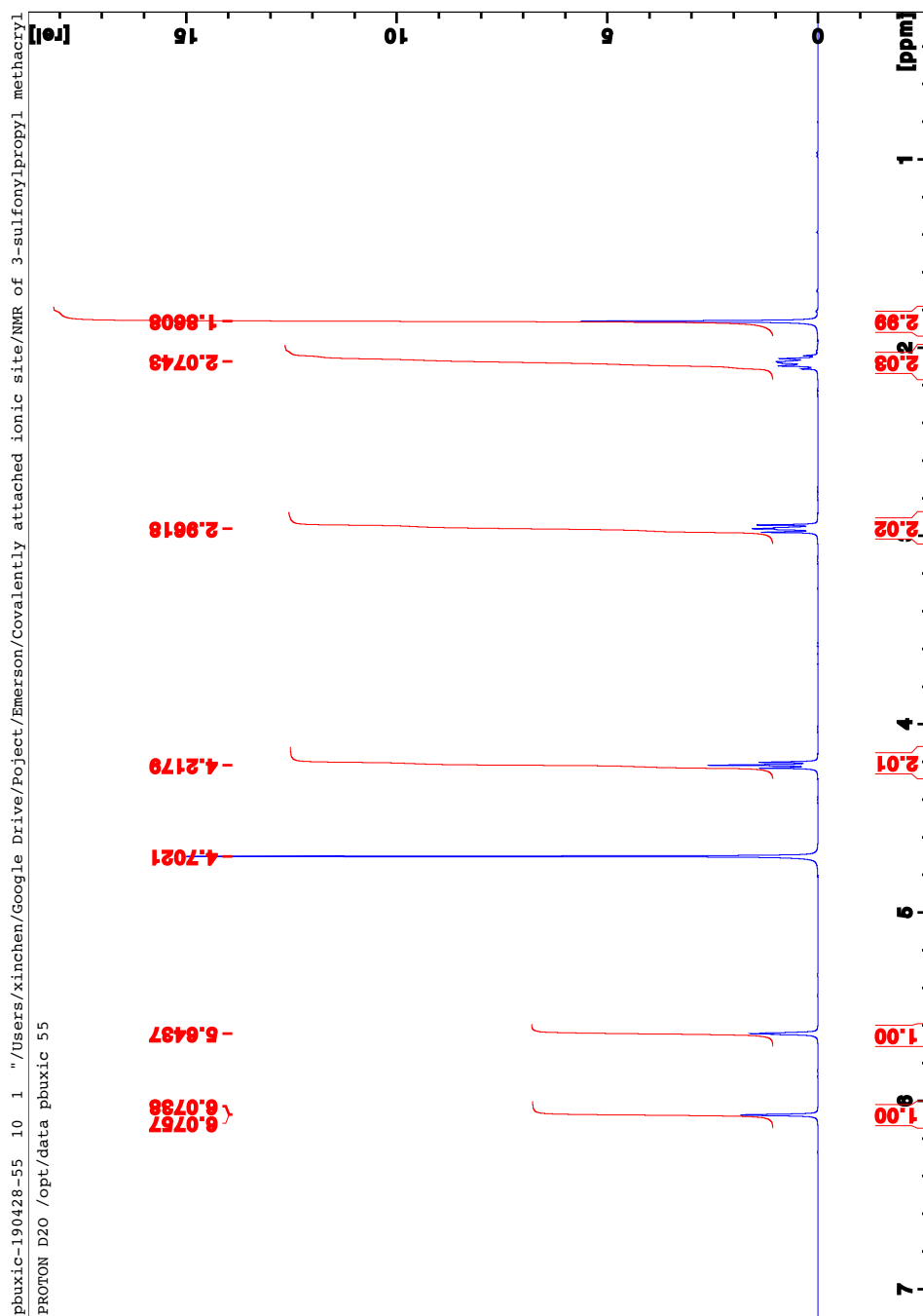


Figure S5.6 $^1\text{H-NMR}$ (D_2O) spectrum of 3-sulfonylpropyl methacrylate potassium salt.

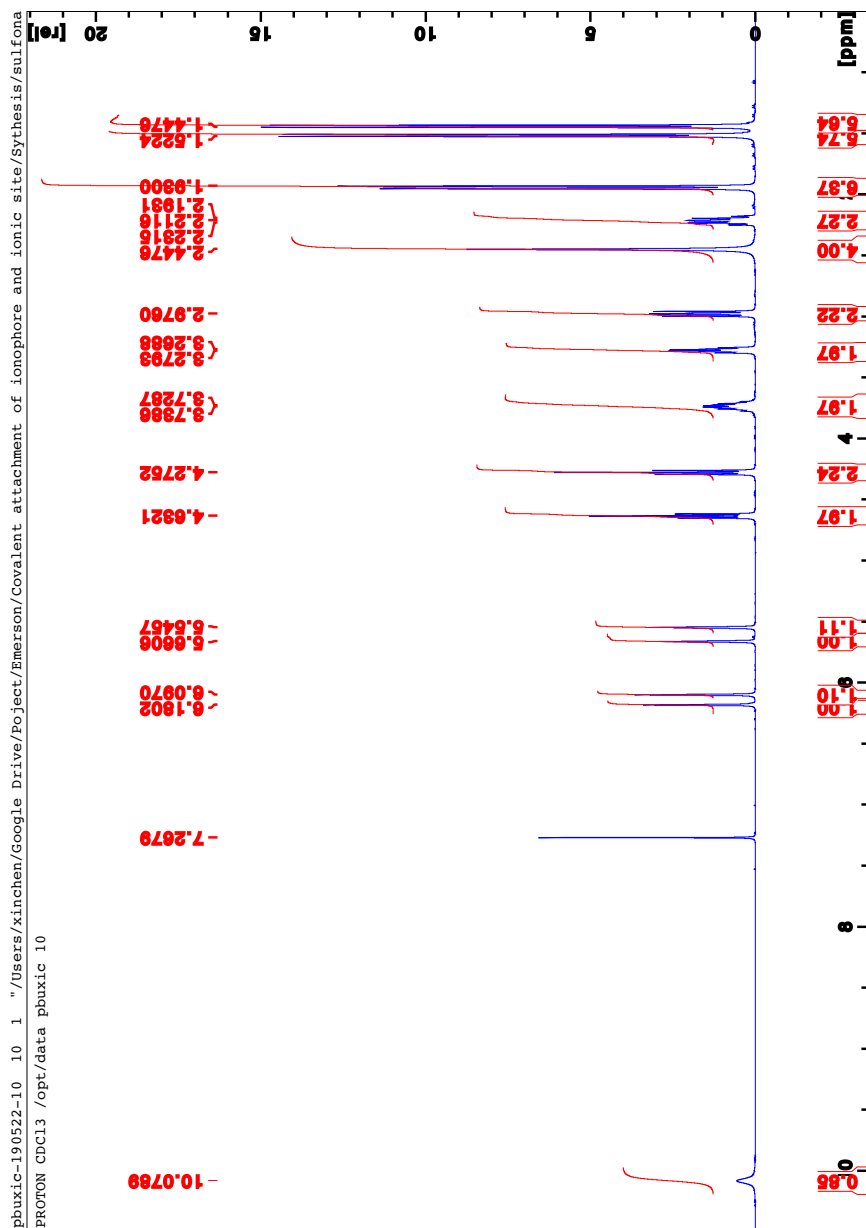


Figure S5.7 $^1\text{H-NMR}$ (CDCl_3) spectrum of 3-sulfonylpropyl methacrylate *N*-isopropyl-*N*-(2-(methacryloyloxy)ethyl)propan-2-ammonium.

VI. CONCLUSIONS AND OUTLOOK

6.1 Summary of Results

The first goal of the research reported in this dissertation was to develop robust electrochemical sensors with improved selectivity and reduced biofouling. Fluorous-phase ion-selective electrodes with a newly synthesized fluorophilic H^+ ionophore were developed and were characterized for pH sensing. Due to the nonpolar nature of the fluoruous matrix, the solvation of both interfering cations such as K^+ , Na^+ , and Ca^{2+} and counter anions was significantly reduced, thus expanding both the lower and upper detection limits of pH sensing. The new fluorophilic amine-based H^+ ionophore was optimized to have four $-(\text{CH}_2)-$ spacers between its nitrogen center and electron-withdrawing fluoruous ponytails, yielding a basicity of this ionophore suitable for a neutral pH-centered working range. The reliability of this sensor was also improved by introducing a new design of electrode body that eliminates rotating motions exerted on the sensing membrane when electrodes are being assembled. This ensures a smooth and tight sealing of the fluoruous membrane in the electrode body. Since the fluoruous phase is nonpolar to the degree that it is both hydrophobic and lipophobic, fluoruous-phase ISEs are ideal for reduced biofouling. To demonstrate this, both fluoruous-phase and PVC-phase ISEs were exposed to serum solutions for a prolonged period of five days. Results showed fluoruous-phase ISEs to retain their excellent pre-exposure selectivity, whereas PVC-phase ISEs lost selectivity. It was also found that the previously often used ionophore-to-ionic site ratio of 2:1 is not optimal for use of tridodecylamine as pH ionophore in PVC-phase ISEs. It appears very likely that the same is also true for a number of other H^+ ionophores.

The second goal of the research described in this dissertation was to develop ISEs with improved biocompatibility for use in implantable and wearable devices. Several silicone polymers were evaluated as membrane materials because of their previously reported biocompatibility and their low glass transition temperature that eliminates the need for plasticizers, some of which have known inflammatory effects. Reference electrodes based on ionic liquid-doped silicone membranes provided sample-independent half-cell potentials in artificial blood electrolyte solutions and long-term stabilities with a small drift of 112 $\mu\text{V}/\text{h}$ in serum solutions. Resistance measurement and differential scanning calorimetry revealed differences in the miscibility of ionic liquids and different silicone materials. Silicones miscible with ionic liquids without phase separation were observed to provide functional and sample-independent potentials, whereas silicone materials that phase-separated from ionic liquids did not provide sample-independent potentials. This suggests that a limited solubility of the ionic liquid is a key cause preventing the control of the phase boundary potential at the membrane/sample interface, as it is required for an ionic liquid-based reference electrode. The miscibility of the silicone matrix and ionic liquid serves as guidance to predict what combinations of ionic liquids and polymers are suitable for ionic liquid-doped polymeric reference electrodes.

K^+ -selective electrodes based on two types of silicones—**Fluorosilicone 1** and **Silicone 1**—doped with two mobile ionophores—valinomycin and BME-44—provided Nernstian responses and good selectivities with respect to Na^+ that meet minimum requirements stipulated by federal regulations. To prevent leaching of the ionophore out of silicone membranes into the samples phase, an analog of the ionophore BME-44 with a

triethoxysilyl unit was synthesized and covalently attached to a silicone matrix in the course of the silicone curing process. The attachment was successful, as confirmed by Soxhlet extraction. Membranes with covalently attached BME-44 showed close to Nernstian responses. Solid-state ISEs were successful using a gold microelectrode platform on a polyimide substrate.

Plasticizer-free poly(methacrylate) membranes were also developed for pH sensing. Both non-crosslinked poly(methyl methacrylate-*co*-lauryl methacrylate) and crosslinked poly(decyl methacrylate) showed Nernstian pH responses and good selectivities, with the latter being more mechanically robust due to crosslinking. To improve the biocompatibility of poly(methacrylate)-based ISEs for applications such as in the food industry, two amine-based ionophores and a sulfonate-based ionic site—all containing methacrylate units—were covalently attached to poly(methacrylate) membranes. When either the ionophore or the ionic site was covalently attached to the ISE membrane polymer, ISEs showed the same good characteristics as ISEs with mobile sensing components, and the covalent attachment was confirmed by elemental analysis. However, when both the ionophore and the ionic site were covalently attached to the sensor membrane polymer, Nernstian responses were not consistently observed.

6.2 Future Work

For fluororous-phase ISEs, future work should be focused on understanding and expanding their utility for measurements in biological samples. Early generation fluororous-phase ISEs have been shown to have a stir-rate dependence when used in biological samples.^{251, 252} It has been suspected that the observed rate dependence can be explained by albumin facilitating the transfer of ionophore out of the ISE membrane into sample solution in a carrier-like fashion. Fluororous-phase ISEs doped with the newly synthesized fluorophilic ionophore with four $-(CH_2)-$ spacers should be tested for a possible stir-rate dependence of their response. Furthermore, to verify the role of albumin, future work should be performed with pure albumin samples. If albumin is not the cause, selective filtration of serum samples could be used to determine which species of serum cause a stir rate dependence of the ISEs responses of fluororous-phase ISEs. Similar efforts could be expanded to other biological samples such as urine or sweat. To reduce the stir-rate dependence, as an alternative to using more fluorophilic ionophores and ionic sites, a hydrophilic cellulose filter paper or glass microfiber filter with a pore size smaller than albumin but large enough to allow sufficient diffusion of small ions could be stacked on the fluororous-phase ISEs as a strategy to reducing albumin interference.

For ionic liquid-doped silicone reference electrodes, since only one of five tested silicones provided sample-independent potentials (**Fluorosilicone 1**), expanding to other types of silicones (such as addition-type silicones) or synthesizing silicones from siloxanes could be important in cases where the current silicone does not meet other requirements for implantable or wearable devices. For both reference and ion-selective electrodes, the

binding of acetic acid released as a byproduct during **Fluorosilicone 1** curing may have contributed to increased potential drifts as compared to PVC-phase electrodes. Use of silicones that do not evolve acetic acid during curing, such as an alcohol-evolving silicone or addition-type silicones that do not release any side product, may help further to reduce long-term potential drifts. Furthermore, silicone materials can be covalently attached to underlying solid-contact materials and substrate (for example, the polyimide substrate of the microelectrodes used for some of this work) to reduce device failure by formation of a water layer at the substrate–membrane interface. For K^+ -selective silicone electrodes with a covalently attached ionophore, to improve the response slope, the concentration of ionophore should be optimized. Alternatively, a different silicone matrix could be used. The performance of ISEs with covalently attached ionophores after exposure to biological samples should be evaluated and compared to the corresponding performance of ISEs with mobile ionophores.

For poly(methacrylate) based ISEs with both ionophore and ionic site covalently attached, since the response characteristics were not consistent, differential scanning calorimetry may be used to study the effect of membrane heterogeneity on the sensor performance. With such additional insight, a fundamental question—i.e., whether a sensor can function satisfactorily if all sensing components are covalently attached—could be given a final answer. If the answer is no, doping of such sensing membranes with a small percentage of free ionophore or a lipophilic salt alongside with the covalently attached ionophore and ionic site could help boost ion hopping, resulting in the desired Nernstian responses and lower membrane resistance. In addition, one type of solid contact material—

i.e., graphite rods—could not be used in combination with an electrode body to provide consistently favorable ISE responses. This was likely caused by damage of the sensing membrane by tightening of the electrode body to prevent electrical leakage. Covalent attachment of poly(methacrylate) membranes to underlying electrode bodies could be a novel and different way to solve this problem. Furthermore, to demonstrate the usefulness of crosslinked poly(methacrylate)-based ISEs, such sensors should also be tested after exposure to heating and high pressure.

VII. REFERENCES

1. Bühlmann, P.; Chen, L. D., Ion-Selective Electrodes with Ionophore-Doped Sensing Membranes. In *Supramolecular Chemistry: From Molecules to Nanomaterials*, Jonathan, W.; Steed, P. A. G., Eds. John Wiley & Sons, Ltd: New York, NY, 2012; Vol. 5, pp 2539-2580.
2. Bakker, E.; Bühlmann, P.; Pretsch, E., Carrier-Based Ion-Selective Electrodes and Bulk Optodes. 1. General Characteristics. *Chem. Rev.* **1997**, *97*, 3083-3132.
3. Bühlmann, P.; Pretsch, E.; Bakker, E., Carrier-Based Ion-Selective Electrodes and Bulk Optodes. 2. Ionophores for Potentiometric and Optical Sensors. *Chem. Rev.* **1998**, *98*, 1593-1688.
4. Johnson, R. D.; Bachas, L. G., Ionophore-Based Ion-Selective Potentiometric and Optical Sensors. *Anal. Bioanal. Chem.* **2003**, *376*, 328-341.
5. Amemiya, S., Potentiometric Ion-Selective Electrodes. In *Handbook of Electrochemistry*, Zoski, C., G, Ed. Elsevier: 2007; pp 261-294.
6. Bobacka, J.; Ivaska, A.; Lewenstam, A., Potentiometric Ion Sensors. *Chem. Rev.* **2008**, *108*, 329-351.
7. Morf, W. E., The Principle of Ion-Selective Electrodes and of Membrane Transport. **1981**.
8. Henderson, L. J., Blood as a Physicochemical System. *J. Biol. Chem.* **1921**, *46*, 411-419.
9. Bakker, E.; Nägele, M.; Schaller, U.; Pretsch, E., Applicability of the Phase Boundary Potential Model to the Mechanistic Understanding of Solvent Polymeric Membrane-Based Ion-Selective Electrodes. *Electroanalysis* **1995**, *7*, 817-822.
10. Fiedler, U.; Departtnetlt, C., Selectrode - the Universak Ion-Selective Electrode. *Anal. Chim. Acta* **1973**, *67*, 179-193.
11. Simon, M. A.; Kusy, R. P., The Molecular, Physical and Mechanical Properties of Highly Plasticized Poly(Vinyl Chloride) Membranes. *Polymer* **1993**, *34*, 5106-5115.

12. Oesch, U.; Simon, W., Life Time of Neutral Carrier Based Ion-Selective Liquid-Membrane Electrodes. *Anal. Chem.* **1980**, *52* (4), 692-700.
13. Büchi, R.; Pretsch, E.; Simon, W., C-13-NMR - Studies on Ion-Selective Liquid Membranes. *Helv. Chim. Acta* **1976**, *59* (7), 2327-2334.
14. Chan, A. D. C.; Harrison, D. J., Carbon-13 Spin—Lattice Relaxation Studies of the Effect of Water on Ion-Selective Electrode Membranes. *Talanta* **1994**, *41* (6), 849-856.
15. Ammann, D.; Bissig, R.; Güggi, M.; Pretsch, E.; Simon, W.; Borowitz, I. J.; Weiss, L., Preparation of Neutral Ionophores for Alkali and Alkaline Earth Metal Cations and Their Application in Ion Selective Membrane Electrodes. *Helv. Chim. Acta* **1975**, *58* (6), 1535-1548.
16. Anker, P.; Wieland, E.; Ammann, D.; Dohner, R. E.; Asper, R.; Simon, W., Neutral Carrier Based Ion-Selective Electrode for the Determination of Total Calcium in Blood Serum. *Anal. Chem.* **1981**, *53* (13), 1970-1974.
17. Morf, W.; Simon, W., Evaluation of Alkali and Alkaline Earth Ion Selectivity of Electrically Neutral Carrier Antibiotics and Model Compounds. *Helv. Chim. Acta* **1971**, *54* (8), 2683-2704.
18. Simon, A., Structure and Bonding of Alkali Metal Suboxides. In *Inorganic Chemistry and Spectroscopy*, Springer: 1979; pp 81-127.
19. Bühlmann, P.; Amemiya, S.; Yajima, S.; Umezawa, Y., Co-Ion Interference for Ion-Selective Electrodes Based on Charged and Neutral Ionophores: A Comparison. *Anal. Chem.* **1998**, *70* (20), 4291-4303.
20. Ogawara, S.; Carey, J. L.; Zou, X. U.; Bühlmann, P., Donnan Failure of Ion-Selective Electrodes with Hydrophilic High-Capacity Ion-Exchanger Membranes. *ACS Sens.* **2016**, *1* (1), 95-101.
21. Buck, R. P.; Lindner, E., Recommendations for Nomenclature of Ion-Selective Electrodes - (IUPAC Recommendations 1994). *Pure Appl. Chem.* **1994**, *66* (12), 2527-2536.

22. Bühlmann, P.; Yajima, S.; Tohda, K.; Umezawa, K.; Nishizawa, S.; Umezawa, Y., Studies on the Phase Boundaries and the Significance of Ionic Sites of Liquid Membrane Ion-Selective Electrodes. *Electroanalysis* **1995**, *7*, 811-816.
23. Bühlmann, P.; Yajima, S.; Tohda, K.; Umezawa, Y., EMF Response of Neutral-Carrier Based Ion-Sensitive Field Effect Transistors with Membranes Free of Ionic Sites. *Electrochim. Acta* **1995**, *40*, 3021-3027.
24. Amemiya, S.; Bühlmann, P.; Pretsch, E.; Rusterholz, B.; Umezawa, Y., Cationic or Anionic Sites? Selectivity Optimization of Ion-Selective Electrodes Based on Charged Ionophores. *Anal. Chem.* **2000**, *72*, 1618-1631.
25. Fluorous-Phase Ion-Selective Ph Electrodes for Measurements in Biological Samples. **2019**, *submitted for publication*.
26. Oesch, U.; Ammann, D.; Simon, W., Ion-Selective Membrane Electrodes for Clinical Use. *Clin. Chem.* **1986**, *32*, 1448-1459.
27. Laboratory Requirement. In *42, Laboratory Requirement Code of Federal Regulations: 2018; Vol. Part 493.931*.
28. Schaller, U.; Bakker, E.; Spichiger, U. E.; Pretsch, E., Nitrite-Selective Microelectrodes. *Talanta* **1994**, *41* (6), 1001-1005.
29. Vanysek, P., Ed., *Electrochemistry on Liquid/Liquid Interfaces*. Springer Science & Business Media: 2012; Vol. 39.
30. Hofmeister, F., Concerning Regularities in the Protein-Precipitating Effects of Salts and the Relationship of These Effects to the Physiological Behaviour of Salts. *Arch. Exp. Pathol. Pharmacol* **1888**, *24*, 247-260.
31. Marcus, Y., A Simple Empirical Model Describing the Thermodynamics of Hydration of Ions of Widely Varying Charges, Sizes, and Shapes. *Biophys. Chem.* **1994**, *51* (2), 111-127.
32. Umezawa, Y., Ed., *Crc Handbook of Ion-Selective Electrodes: Selectivity Coefficients*. CRC press Boca Raton, FL: 1990.
33. Eisenman, G.; Rudin, D. O.; Casby, J. U., Glass Electrode for Measuring Sodium Ion. *Science* **1957**, *126*, 831-834.

34. Ross, J. W., Calcium-Selective Electrode with Liquid Ion Exchanger. *Science* **1967**, *156*, 1378-1379.
35. Bakker, E.; Meruva, R. K.; Pretsch, E.; Meyerhoff, M. E., Selectivity of Polymer Membrane-Based Ion-Selective Electrodes: Self-Consistent Model Describing the Potentiometric Response in Mixed Ion Solutions of Different Charge. *Anal. Chem.* **1994**, *66* (19), 3021-3030.
36. Eugster, R.; Spichiger, U. E.; Simon, W., Membrane Model for Neutral-Carrier-Based Membrane Electrodes Containing Ionic Sites. *Anal. Chem.* **1993**, *65* (6), 689-695.
37. Horvai, G., The Selectivity of Polymer Membrane Ion-Selective Electrodes Obeying the Ion Exchanger Model. *TrAC, Trends Anal. Chem.* **1997**, *16* (5), 260-266.
38. Umezawa, Y.; Umezawa, K.; Sato, H., Selectivity Coefficients for Ion-Selective Electrodes: Recommended Methods for Reporting $K_{a,B}^{\text{pot}}$ Values (Technical Report). *Pure Appl. Chem.* **1995**, *67*, 507-518.
39. Bakker, E.; Pretsch, E.; Bühlmann, P., Selectivity of Potentiometric Ion Sensors. *Anal. Chem.* **2000**, *72* (6), 1127-1133.
40. Horváth, I. T.; Rábai, J., Facile Catalyst Separation without Water: Fluorous Biphasic Hydroformylation of Olefins. *Science* **1994**, *266* (5182), 72-75.
41. Gladysz, J. A.; Curran, D. P.; Horváth, I. T., Ed., *Handbook of Fluorous Chemistry*. Wiley & Sons: New York, 2005.
42. Gladysz, J. A., Fluorous to the Core. *Science* **2006**, *313*, 1249-1250.
43. Horvath, I., Ed., *Fluorous Chemistry*. 2012; Vol. 308, p 1-411.
44. Boswell, P. G.; Szíjjártó, C.; Jurisch, M.; Gladysz, J. A.; Rábai, J.; Bühlmann, P., Fluorophilic Ionophores for Potentiometric pH Determinations with Fluorous Membranes of Exceptional Selectivity. *Anal. Chem.* **2008**, *80*, 2084-2090.
45. Brady, J. E.; Carr, P. W., Perfluorinated Solvents as Nonpolar Test Systems for Generalized Models of Solvatochromic Measures of Solvent Strength. *Anal. Chem.* **1982**, *54*, 1751-1757.

46. Boswell, P. G.; Bühlmann, P., Fluorous Bulk Membranes for Potentiometric Sensors with Wide Selectivity Ranges: Observation of Exceptionally Strong Ion Pair Formation. *J. Am. Chem. Soc.* **2005**, *127* (25), 8958-8959.
47. Boswell, P. G.; Lugert, E. C.; Rábai, J.; Amin, E. A.; Bühlmann, P., Coordinative Properties of Highly Fluorinated Solvents with Amino and Ether Groups. *J. Am. Chem. Soc.* **2005**, *127*, 16976-16984.
48. Lai, C. Z.; Fierke, M. A.; da Costa, R. C.; Gladysz, J. A.; Stein, A.; Bühlmann, P., Highly Selective Detection of Silver in the Low ppt Range with Ion-Selective Electrodes Based on Ionophore-Doped Fluorous Membranes. *Anal. Chem.* **2010**, *82* (18), 7634-7640.
49. Chen, L. D.; Mandal, D.; Pozzi, G.; Gladysz, J. A.; Bühlmann, P., Potentiometric Sensors Based on Fluorous Membranes Doped with Highly Selective Ionophores for Carbonate. *J. Am. Chem. Soc.* **2011**, *133*, 20869-20877.
50. Boswell, P. G.; Anfang, A. C.; Bühlmann, P., Preparation of a Highly Fluorophilic Phosphonium Salt and Its Use in a Fluorous Anion-Exchanger Membrane with High Selectivity for Perfluorinated Acids. *J. Fluor. Chem.* **2008**, *129* (10), 961-967.
51. Bard, A. J.; Faulkner, L. R., Ed., *Electrochemical Methods: Fundamentals and Applications*. 2nd ed.; Wiley: New York, 2000.
52. Koryta, J.; Stulík, K., Ed., *Ion-Selective Electrodes*. 2nd ed.; Cambridge University Press: Cambridge, 2009.
53. Dole, M., Ed., *The Glass Electrode: Methods, Applications, and Theory*. John Wiley & Sons: New York, 1941.
54. Eisenman, G., Ed., *Glass Electrodes for Hydrogen and Other Cations: Principles and Practice*. Marcel Dekker: New York, 1967.
55. Bates, R. G., *Determination of pH, Theory and Practice*. 2nd ed.; John Wiley & Sons: New York, 1973.
56. Durst, R. A., *Ion-Selective Electrodes*. National Bureau of Standards Special Publication 314 U.S. Government Printing Office Washington 1969

57. Morf, W. E.; Kahr, G.; Simon, W., Reduction of the Anion Interference in Neutral Carrier Liquid-Membrane Electrodes Responsive to Cations. *Anal. Lett.* **1974**, *7*, 9-22.
58. Bakker, E.; Lerchi, M.; Rosatzin, T.; Rusterholz, B.; Simon, W., Synthesis and Characterization of Neutral Hydrogen Ion-Selective Chromoionophores for Use in Bulk Optodes. *Anal. Chim. Acta* **1993**, *278*, 211-225.
59. Bakker, E.; Xu, A. P.; Pretsch, E., Optimum Composition of Neutral Carrier Based Ph Electrodes. *Anal. Chim. Acta* **1994**, *295* (3), 253-262.
60. Lim, C.; Slack, S.; Ufer, S.; Lindner, E., Protein Adsorption to Planar Electrochemical Sensors and Sensor Materials. *Pure Appl. Chem.* **2004**, *76*, 753-763.
61. Black, J., Ed., *Biological Performance of Materials: Fundamentals of Biocompatibility, Fourth Edition*. 4th ed.; CRC Press: Boca Raton, FL, 2005.
62. Vert, M.; Doi, Y.; Hellwich, K. H.; Hess, M.; Hodge, P.; Kubisa, P.; Rinaudo, M.; Schue, F., Terminology for Biorelated Polymers and Applications (IUPAC Recommendations 2012). *Pure Appl. Chem.* **2012**, *84* (2), 377-408.
63. Use of International Standard Iso 10993-1, "Biological Evaluation of Medical Devices - Part 1: Evaluation and Testing within a Risk Management Process" U.S. Department of Health and Human Services, Food and Drug Administration, Center for Devices and Radiological Health, U.S. Government Printing Office Washington, DC 2016
64. Cosofret, V. V.; Erdösy, M.; Buck, R. P.; Kao, W. J.; Anderson, J. M.; Lindner, E.; Neuman, M. R., Electroanalytical and Biocompatibility Studies on Carboxylated Poly(Vinyl Chloride) Membranes for Microfabricated Array Sensors. *Analyst* **1994**, *119*, 2283-2292.
65. Lindner, E.; Cosofret, V. V.; Ufer, S.; Buck, R. P.; Kao, W. J.; Neuman, M. R.; Anderson, J. M., Ion-Selective Membranes with Low Plasticizer Content: Electroanalytical Characterization and Biocompatibility Studies. *Journal of Biomedical Materials Research* **1994**, *28*, 591-601.

66. Lindner, E.; Cosofret, V. V.; Buck, R. P.; Johnson, T. A.; Ash, R. B.; Neuman, M. R.; Kao, W. J.; Anderson, J. M., Electroanalytical and Biocompatibility Studies on Microfabricated Array Sensors. *Electroanalysis* **1995**, *7*, 864-870.
67. Gourlay, T.; Samartzis, I.; Stefanou, D.; Taylor, K., Inflammatory Response of Rat and Human Neutrophils Exposed to Di-(2-Ethyl-Hexyl)-Phthalate-Plasticized Polyvinyl Chloride. *Artif. Organs* **2003**, *27*, 256-260.
68. Pawlenko, S., Ed., *Organosilicon Chemistry*. Walter de Gruyter: Berlin and New York, 1986.
69. Cervantes, J.; Zárraga, R.; Salazar - Hernández, C., Organotin Catalysts in Organosilicon Chemistry. *Appl. Organomet. Chem.* **2012**, *26* (4), 157-163.
70. Bogdan Marciniak; Hieronim Maciejewski; Cezary Pietraszuk; Pawluć, P., Marciniak, B., Ed., *Hydrosilylation: A Comprehensive Review on Recent Advances*. Springer Science+Business Media: 2009; Vol. I.
71. Plueddemann, E. P., Ed., *Silane Coupling Agents*. 2nd ed.; Springer Science+Business Media: New York, 1991.
72. Colas, A.; Curtis, J., Silicones. In *Biomaterials Science : An Introduction to Materials in Medicine*, Ratner, B. D.; Hoffman, A. S.; Schoen, F. J.; Lemons, J. E., Eds. Elsevier Academic Press: Oxford, 2004.
73. Melody, D. P., Advances in Room-Temperature Curing Adhesives and Sealants - a Review. *British Polymer Journal* **1989**, *21* (2), 175-179.
74. van Der Weij, F. W., The Action of Tin Compounds in Condensation - Type RTV Silicone Rubbers. *Die Makromolekulare Chemie: Macromolecular Chemistry and Physics* **1980**, *181* (12), 2541-2548.
75. Institute of Medicine Committee on the Safety of Silicone Breast, I., The National Academies Collection: Reports Funded by National Institutes of Health. In *Safety of Silicone Breast Implants*, Bondurant, S.; Ernster, V.; Herdman, R., Eds. National Academies Press (US): Washington (DC), 1999.
76. Waters, M. G. J.; Jaggert, R. G.; Winter, R. W., Water Absorption of (RTV) Silicone Denture Soft Lining Material. *J. Dent.* **1996**, *24* (1), 105-108.

77. Rahimi, A.; Mashak, A., Review on Rubbers in Medicine: Natural, Silicone and Polyurethane Rubbers. *Plastics, Rubber and Composites* **2013**, *42* (6), 223-230.
78. Letechipia, J. E.; Peckham, P. H.; Gazdik, M.; Smith, B., In-Line Lead Connector for Use with Implanted Neuroprosthesis. *IEEE Trans. Biomed. Eng.* **1991**, *38* (7), 707-709.
79. Kock, H. J.; Pietsch, M.; Krause, U.; Wilke, H.; Eigler, F. W., Implantable Vascular Access Systems: Experience in 1500 Patients with Totally Implanted Central Venous Port Systems. *World J. Surg.* **1998**, *22* (1), 12-16.
80. Jarvis, J. C.; Salmons, S., The Application and Technology of Implantable Neuromuscular Stimulators: An Introduction and Overview. *Med. Eng. Phys.* **2001**, *23* (1), 3-7.
81. Steiert, A. E.; Boyce, M.; Sorg, H., Capsular Contracture by Silicone Breast Implants: Possible Causes, Biocompatibility, and Prophylactic Strategies. *Medical Devices (Auckland, N.Z.)* **2013**, *6*, 211-8.
82. Boock, R. J.; Swinney, M. R. Silicone Based Membranes for Use in Implantable Glucose Sensors. U.S. Patent 2018/04253A1, February 15, 2018.
83. Brunink, J. A. J.; Lugtenberg, R. J. W.; Brzozka, Z.; Engbersen, J. F. J.; Reinhoudt, D. N., The Design of Durable Na⁺-Selective Chemfets Based on Polysiloxane Membranes. *J. Electroanal. Chem.* **1994**, *378* (1), 185-200.
84. Reinhoudt, D. N.; Engbersen, J. F. J.; Brzozka, Z.; Vandenvlekkert, H. H.; Honig, G. W. N.; Holterman, H. A. J.; Verkerk, U. H., Development of Durable K⁺-Selective Chemically Modified Field Effect Transistors with Functionalized Polysiloxane Membranes. *Anal. Chem.* **1994**, *66* (21), 3618-3623.
85. van der Wal, P. D.; Sudhölter, E. J. R.; Reinhoudt, D. N., Design and Properties of a Flow-Injection Analysis Cell Using Potassium-Selective Ion-Sensitive Field-Effect Transistors as Detection Elements. *Anal. Chim. Acta* **1991**, *245*, 159-166.
86. van der Wal, P. D.; Sudhölter, E. J. R.; Boukamp, B. A.; Bouwmeester, H. J. M.; Reinhoudt, D. N., Impedance Spectroscopy and Surface Study of Potassium-

Selective Silicone Rubber Membranes. *Journal of Electroanalytical Chemistry and Interfacial Electrochemistry* **1991**, 317 (1), 153-168.

87. Cha, G. S.; Liu, D.; Meyerhoff, M. E.; Cantor, H. C.; Rees, A. M.; Goldberg, H. D.; Brown, R. B., Electrochemical Performance, Biocompatibility, and Adhesion of New Polymer Matrices for Solid-State Ion Sensors. *Anal. Chem.* **1991**, 63, 1666-1672.

88. Knoll, M.; Cammann, K.; Dumschat, C.; Sundermeier, C.; Eshold, J., Potentiometric Silicon Microsensor for Nitrate and Ammonium. *Sensors and Actuators B: Chemical* **1994**, 18 (1), 51-55.

89. Malinowska, E.; Oklejas, V.; Hower, R. W.; Brown, R. B.; Meyerhoff, M. E., Enhanced Electrochemical Performance of Solid-State Ion Sensors Based on Silicone Rubber Membranes. *Sensors and Actuators B: Chemical* **1996**, 33 (1), 161-167.

90. van der Wal, P. D.; Skowronska-Ptasinska, M.; van den Berg, A.; Bergveld, P.; Sudhölter, E. J. R.; Reinhoudt, D. N., New Membrane Materials for Potassium-Selective Ion-Sensitive Field-Effect Transistors. *Anal. Chim. Acta* **1990**, 231, 41-52.

91. Dumschat, C.; Alazard, S.; Adam, S.; Knoll, M.; Cammann, K., Filled Fluorosilicone as Matrix Material for Ion-Selective Membranes. *Analyst* **1996**, 121 (4), 527-529.

92. Högg, G.; Lutze, O.; Cammann, K., Novel Membrane Material for Ion-Selective Field-Effect Transistors with Extended Lifetime and Improved Selectivity. *Anal. Chim. Acta* **1996**, 335 (1), 103-109.

93. Lindfors, T.; Szücs, J.; Sundfors, F.; Gyuresányi, R. E., Polyaniline Nanoparticle-Based Solid-Contact Silicone Rubber Ion-Selective Electrodes for Ultratrace Measurements. *Anal. Chem.* **2010**, 82 (22), 9425-9432.

94. Upreti, P.; Metzger, L. E.; Bühlmann, P., Glass and Polymeric Membrane Electrodes for the Measurement of pH in Milk and Cheese. *Talanta* **2004**, 63 (1), 139-148.

95. Pick, J.; Tóth, K.; Pungor, E.; Vasák, M.; Simson, W., A Potassium-Selective Silicone-Rubber Membrane Electrode Based on a Neutral Carrier. *Anal. Chim. Acta* **1973**, 64 (3), 477-480.

96. Spichiger, U. E.; Aiping, X.; Citterio, D.; Bühler, H.; Chaniotakis, N.; Rusterholz, B.; Simon, W., From Molecular Recognition to Analytical Information Using Chemical Sensors: Development of a Combined Catheter Gastric pH - Probe. *Electroanalysis* **1995**, *7* (9), 859-863.
97. Mostert, I. A.; Anker, P.; Jenny, H. B.; Oesch, U.; Morf, W. E.; Ammann, D.; Simon, W., Neutral Carrier Based Silicone Rubber Membranes for H_3O^+ , K^+ , NH_4^+ and Ca^{2+} Selective Electrodes. *Microchimica Acta* **1985**, *85* (1), 33-38.
98. Kimura, K.; Matsuba, T.; Tsujimura, Y.; Yokoyama, M., Unsymmetrical Calix[4]Arene Ionophore/Silicone Rubber Composite Membranes for High-Performance Sodium Ion-Sensitive Field-Effect Transistors. *Anal. Chem.* **1992**, *64* (21), 2508-2511.
99. Tsujimura, Y.; Yokoyama, M.; Kimura, K., Oligosiloxane - Modified Calix [4] Arene Ionophores for Silicone - Rubber - Membrane Sodium Ion - Sensitive Field - Effect Transistors. *Electroanalysis* **1993**, *5* (9 - 10), 803-807.
100. Tsujimura, Y.; Yokoyama, M.; Kimura, K., Comparison between Silicone-Rubber Membranes and Plasticized Poly(Vinyl Chloride) Membranes Containing Calix[4]Arene Ionophores for Sodium Ion-Sensitive Field-Effect Transistors in Applicability to Sodium Assay in Human Body Fluids. *Sensors and Actuators B: Chemical* **1994**, *22* (3), 195-199.
101. Tsujimura, Y.; Yokoyama, M.; Kimura, K., Practical Applicability of Silicone Rubber Membrane Sodium-Selective Electrode Based on Oligosiloxane-Modified Calix[4]Arene Neutral Carrier. *Anal. Chem.* **1995**, *67* (14), 2401-2404.
102. Tsujimura, Y.; Sunagawa, T.; Yokoyama, M.; Kimura, K., Sodium Ion-Selective Electrodes Based on Silicone-Rubber Membranes Covalently Incorporating Neutral Carriers. *Analyst* **1996**, *121* (11), 1705-1709.
103. Kimura, K.; Sunagawa, T.; Yokoyama, M., Chemical Modification of Sol-Gel-Derived Glass by a Neutral Carrier for Ion Sensors. *Chem. Commun.* **1996**, (6), 745-746.
104. Kimura, K.; Sunagawa, T.; Yajima, S.; Miyake, S.; Yokoyama, M., Neutral Carrier-Type Ion Sensors Based on Sol-Gel-Derived Membranes Incorporating a

Bis(Crown Ether) Derivative by Covalent Bonding. *Anal. Chem.* **1998**, *70* (20), 4309-4313.

105. Heng, L. Y.; Hall, E. A. H., Methacrylic–Acrylic Polymers in Ion-Selective Membranes: Achieving the Right Polymer Recipe. *Anal. Chim. Acta* **2000**, *403* (1), 77-89.

106. Heng, L. Y.; Hall, E. A. H., Producing “Self-Plasticizing” Ion-Selective Membranes. *Anal. Chem.* **2000**, *72*, 42-51.

107. Heng, L. Y.; Hall, E. A., One - Step Synthesis of K^+ - Selective Methacrylic - Acrylic Copolymers Containing Grafted Ionophore and Requiring No Plasticizer. *Electroanalysis* **2000**, *12* (3), 178-186.

108. Malinowska, E.; Gawart, L.; Parzuchowski, P.; Rokicki, G.; Brzózka, Z., Novel Approach of Immobilization of Calix[4]Arene Type Ionophore in ‘Self-Plasticized’ Polymeric Membrane. *Anal. Chim. Acta* **2000**, *421* (1), 93-101.

109. Heng, L. Y.; Hall, E. A. H., Assessing a Photocured Self-Plasticised Acrylic Membrane Recipe for Na^+ and K^+ Ion Selective Electrodes. *Anal. Chim. Acta* **2001**, *443* (1), 25-40.

110. Qin, Y.; Peper, S.; Bakker, E., Plasticizer - Free Polymer Membrane Ion - Selective Electrodes Containing a Methacrylic Copolymer Matrix. *Electroanalysis* **2002**, *14* (19 - 20), 1375-1381.

111. Mi, Y. M.; Bakker, E., Determination of Complex Formation Constants of Lipophilic Neutral Ionophores in Solvent Polymeric Membranes with Segmented Sandwich Membranes. *Anal. Chem.* **1999**, *71* (23), 5279-5287.

112. Qin, Y.; Mi, Y. M.; Bakker, E., Determination of Complex Formation Constants of 18 Neutral Alkali and Alkaline Earth Metal Ionophores in Poly(Vinyl Chloride) Sensing Membranes Plasticized with Bis(2-Ethylhexyl)Sebacate and *o*-Nitrophenyloctylether. *Anal. Chim. Acta* **2000**, *421* (2), 207-220.

113. Shultz, M. M.; Stefanova, O. K.; Mokrov, S. S.; Mikhelson, K. N., Potentiometric Estimation of the Stability Constants of Ion-Ionophore Complexes in Ion-

- Selective Membranes by the Sandwich Membrane Method: Theory, Advantages, and Limitations. *Anal. Chem.* **2002**, *74* (3), 510-517.
114. Sutter, J.; Radu, A.; Peper, S.; Bakker, E.; Pretsch, E., Solid-Contact Polymeric Membrane Electrodes with Detection Limits in the Subnanomolar Range. *Anal. Chim. Acta* **2004**, *523* (1), 53-59.
115. Chumbimuni-Torres, K. Y.; Rubinova, N.; Radu, A.; Kubota, L. T.; Bakker, E., Solid Contact Potentiometric Sensors for Trace Level Measurements. *Anal. Chem.* **2006**, *78* (4), 1318-1322.
116. Wang, W.; Wang, C., Polyurethane for Biomedical Applications: A Review of Recent Developments. In *The Design and Manufacture of Medical Devices*, Davim, J. P., Ed. Woodhead Publishing: 2012; pp 115-151.
117. Pinchuk, L., A Review of the Biostability and Carcinogenicity of Polyurethanes in Medicine and the New Generation of 'Biostable' Polyurethanes. *J. Biomater. Sci. Polym. Ed.* **1995**, *6* (3), 225-267.
118. Akindoyo, J. O.; Beg, M.; Ghazali, S.; Islam, M.; Jeyaratnam, N.; Yuvaraj, A., Polyurethane Types, Synthesis and Applications—A Review. *RSC Adv.* **2016**, *6* (115), 114453-114482.
119. Zdrahala, R. J.; Zdrahala, I. J., Biomedical Applications of Polyurethanes: A Review of Past Promises, Present Realities, and a Vibrant Future. *J. Biomater. Appl.* **1999**, *14* (1), 67-90.
120. Lamba, N. K., Ed., *Polyurethanes in Biomedical Applications*. Routledge: 2017.
121. Yun, S. Y.; Hong, Y. K.; Oh, B. K.; Cha, G. S.; Nam, H.; Lee, S. B.; Jin, J.-I., Potentiometric Properties of Ion-Selective Electrode Membranes Based on Segmented Polyether Urethane Matrices. *Anal. Chem.* **1997**, *69* (5), 868-873.
122. Dinten, O.; Spichiger, U. E.; Chaniotakis, N.; Gehrig, P.; Rusterholz, B.; Morf, W. E.; Simon, W., Lifetime of Neutral-Carrier-Based Liquid Membranes in Aqueous Samples and Blood and the Lipophilicity of Membrane-Components. *Anal. Chem.* **1991**, *63* (6), 596-603.

123. Bakker, E.; Pretsch, E., Lipophilicity of Tetraphenylborate Derivatives as Anionic Sites in Neutral Carrier-Based Solvent Polymeric Membranes and Lifetime of Corresponding Ion-Selective Electrochemical and Optical Sensors. *Anal. Chim. Acta* **1995**, *309*, 7-17.
124. Ross, P.; Johnston, A. J.; Judd, A. K. Immobilized Valinomycin Molecule for K⁺ Sensor. U.S. Patent 4,973,394, November 27, 1990.
125. Raguse, B.; Pace, R. J.; King, L. G.; Braach-Makavytie, V. L.; Cornell, B. Method of Producing a First Layer Electrode Membrane for a Biosensor. U.S. Patent 5,879,878, March 9, 1999.
126. Bereczki, R.; Gyurcsányi, R. E.; Ágai, B.; Tóth, K., Synthesis and Characterization of Covalently Immobilized Bis-Crown Ether Based Potassium Ionophore. *Analyst* **2005**, *130* (1), 63-70.
127. Qin, Y.; Peper, S.; Radu, A.; Ceresa, A.; Bakker, E., Plasticizer-Free Polymer Containing a Covalently Immobilized Ca²⁺-Selective Ionophore for Potentiometric and Optical Sensors. *Anal. Chem.* **2003**, *75* (13), 3038-3045.
128. Püntener, M.; Vigassy, T.; Baier, E.; Ceresa, A.; Pretsch, E., Improving the Lower Detection Limit of Potentiometric Sensors by Covalently Binding the Ionophore to a Polymer Backbone. *Anal. Chim. Acta* **2004**, *503* (2), 187-194.
129. Cross, G. G.; Fyles, T. M.; Suresh, V. V., Coated-Wire Electrodes Containing Polymer Immobilized Ionophores Blended with Poly(Vinyl Chloride). *Talanta* **1994**, *41* (9), 1589-1596.
130. Liu, Y.; Xue, Y.; Tang, H.; Wang, M.; Qin, Y., Click-Immobilized K⁺-Selective Ionophore for Potentiometric and Optical Sensors. *Sensors and Actuators B: Chemical* **2012**, *171-172*, 556-562.
131. Parra, E. J.; Blondeau, P.; Crespo, G. A.; Rius, F. X., An Effective Nanostructured Assembly for Ion-Selective Electrodes. An Ionophore Covalently Linked to Carbon Nanotubes for Pb²⁺ Determination. *Chem. Commun.* **2011**, *47* (8), 2438-2440.

132. Le Goff, T.; Braven, J.; Ebdon, L.; Scholefield, D., Phosphate-Selective Electrodes Containing Immobilised Ionophores. *Anal. Chim. Acta* **2004**, *510* (2), 175-182.
133. Puntener, M.; Fibbioli, M.; Bakker, E.; Pretsch, E., Response and Diffusion Behavior of Mobile and Covalently Immobilized H⁺-Ionophores in Polymeric Membrane Ion-Selective Electrodes. *Electroanalysis* **2002**, *14* (19-20), 1329-1338.
134. Qin, Y.; Bakker, E., Elimination of Dimer Formation in In^{III}porphyrin-Based Anion-Selective Membranes by Covalent Attachment of the Ionophore. *Anal. Chem.* **2004**, *76* (15), 4379-4386.
135. Bakker, E.; Willer, M.; Lerchi, M.; Seiler, K.; Pretsch, E., Determination of Complex-Formation Constants of Neutral Cation-Selective Ionophores in Solvent Polymeric Membranes. *Anal. Chem.* **1994**, *66* (4), 516-521.
136. Kimura, K. Y., Satoru; Hayashi, Akio Preparation of Alkoxysilyl-Containing Borate Derivatives and Their Use as Anion Excluders for Sol-Gel-Derived Membrane Ion Sensors. Japan Patent 2000119291, April 25, 2000.
137. Rosatzin, T.; Bakker, E.; Suzuki, K.; Simon, W., Lipophilic and Immobilized Anionic Additives in Solvent Polymeric Membranes of Cation-Selective Chemical Sensors. *Anal. Chim. Acta* **1993**, *280* (2), 197-208.
138. Kaneko, N.; Shinohara, N.; Nezu, H., Extraction and Spectrophotometric Determination of Crown Ether in Electrodeposited Tin Using Tetrabromophenolphthalein Ethyl Ester. *Bunseki Kagaku* **1993**, *42*, 299-299.
139. Andrade, J. D.; Hlady, V., Protein Adsorption and Materials Biocompatibility - a Tutorial Review and Suggested Hypotheses. *Adv. Polym. Sci.* **1986**, *79*, 1-63.
140. Huglin, M., N.A. Peppas, Ed., *Hydrogels in Medicine and Pharmacy* CRC Press Inc.: Boca Raton, FL, 1986.
141. Marchant, R.; Hiltner, A.; Hamlin, C.; Rabinovitch, A.; Slobodkin, R.; Anderson, J. M., In Vivo Biocompatibility Studies. I. The Cage Implant System and a Biodegradable Hydrogel. *J. Biomed. Mater. Res.* **1983**, *17* (2), 301-325.

142. Michalska, A., All-Solid-State Ion Selective and All-Solid-State Reference Electrodes. *Electroanalysis* **2012**, *24* (6), 1253-1265.
143. Crespo, G. A.; Bakker, E., Dynamic Electrochemistry with Ionophore Based Ion-Selective Membranes. *RSC Adv.* **2013**, *3*, 25461-25474.
144. Yin, T. J.; Qin, W., Applications of Nanomaterials in Potentiometric Sensors. *Trends Analyt. Chem.* **2013**, *51*, 79-86.
145. Bakker, E., Potentiometric Sensors. In *Environmental Analysis by Electrochemical Sensors and Biosensors: Fundamentals*, Moretto, L. M.; Kalcher, K., Eds. Springer: New York, NY, 2014; pp 193-238.
146. Xie, X.; Bakker, E., Ion Selective Optodes: From the Bulk to the Nanoscale. *Anal. Bioanal. Chem.* **2015**, *407*, 3899-3910.
147. Qin, W.; Zwickl, T.; Pretsch, E., Improved Detection Limits and Unbiased Selectivity Coefficients Obtained by Using Ion-Exchange Resins in the Inner Reference Solution of Ion Selective Polymeric Membrane Electrodes. *Anal. Chem.* **2000**, *72* (14), 3236-3240.
148. Bakker, E.; Pretsch, E., Potentiometry at Trace Levels. *Trends Analyt. Chem.* **2001**, *20* (1), 11-19.
149. Malon, A.; Vigassy, T.; Bakker, E.; Pretsch, E., Potentiometry at Trace Levels in Confined Samples: Ion-Selective Electrodes with Subfemtomole Detection Limits. *J. Am. Chem. Soc.* **2006**, *128* (25), 8154-8155.
150. Zou, X. U.; Cheong, J. H.; Taitt, B. J.; Bühlmann, P., Solid Contact Ion-Selective Electrodes with a Well-Controlled Co(II)/Co(III) Redox Buffer Layer. *Anal. Chem.* **2013**, *85* (19), 9350-9355.
151. Lugert-Thom, E. C.; Gladysz, J. A.; Rabai, J.; Bühlmann, P., Cleaning of pH Selective Electrodes with Ionophore-Doped Fluorous Membranes in NaOH Solution at 90 Degrees C. *Electroanalysis* **2018**, *30* (4), 611-618.
152. Lai, C.-Z.; Koseoglu, S. S.; Lugert, E. C.; Boswell, P. G.; Rábai, J.; Lodge, T. P.; Bühlmann, P., Fluorous Polymeric Membranes for Ionophore-Based Ion-Selective Potentiometry: How Inert Is Teflon AF? *J. Am. Chem. Soc.* **2009**, *131* (4), 1598-1606.

153. Carey, J. L.; Hirao, A.; Sugiyama, K.; Bühlmann, P., Semifluorinated Polymers as Ion-Selective Electrode Membrane Matrixes. *Electroanalysis* **2017**, *29* (3), 739-747.
154. Gunsolus, I. L.; Mousavi, M. P. S.; Hussein, K.; Bühlmann, P.; Haynes, C. L., Effects of Humic and Fulvic Acids on Silver Nanoparticle Stability, Dissolution, and Toxicity. *Environ. Sci. Technol.* **2015**, *49* (13), 8078-86.
155. Mousavi, M. P. S.; Gunsolus, I. L.; Pérez De Jesús, C. E.; Lancaster, M.; Hussein, K.; Haynes, C. L.; Bühlmann, P., Dynamic Silver Speciation as Studied with Fluorous-Phase Ion-Selective Electrodes: Effect of Natural Organic Matter on the Toxicity and Speciation of Silver. *Sci. Total Environ.* **2015**, *537*, 453-461.
156. Chen, L. D.; Lai, C. Z.; Granda, L. P.; Fierke, M. A.; Mandal, D.; Stein, A.; Gladysz, J. A.; Bühlmann, P., Fluorous Membrane Ion-Selective Electrodes for Perfluorinated Surfactants: Trace-Level Detection and in Situ Monitoring of Adsorption. *Anal. Chem.* **2013**, *85* (15), 7471-7477.
157. Maurer-Jones, M. A.; Mousavi, M. P. S.; Chen, L. D.; Bühlmann, P.; Haynes, C. L., Characterization of Silver Ion Dissolution from Silver Nanoparticles Using Fluorous-Phase Ion-Selective Electrodes and Assessment of Resultant Toxicity to *Shewanella Oneidensis*. *Chemical Science* **2013**, *4* (6), 2564-2572.
158. Ammann, D., Ed., *Ion-Selective Microelectrodes: Principles, Design and Application*. Springer Science & Business Media: 1986; Vol. 50.
159. Simon, W.; Ammann, D.; Anker, P.; Oesch, U.; Band, D. M., Ion-Selective Electrodes and Their Clinical-Application in the Continuous Ion Monitoring. *Ann. N.Y. Acad. Sci.* **1984**, *428* (JUN), 279-285.
160. Anker, P.; Ammann, D.; Simon, W., Blood-pH Measurement with a Solvent Polymeric Membrane-Electrode in Comparison with a Glass-Electrode. *Mikrochim. Acta* **1983**, *1* (3-4), 237-242.
161. EspadasTorre, C.; Bakker, E.; Barker, S.; Meyerhoff, M. E., Influence of Nonionic Surfactants on the Potentiometric Response of Hydrogen Ion-Selective Polymeric Membrane Electrodes. *Anal. Chem.* **1996**, *68* (9), 1623-1631.

162. Chao, P.; Ammann, D.; Oesch, U.; Simon, W.; Lang, F., Extracellular and Intracellular Hydrogen Ion-Selective Microelectrode Based on Neutral Carriers with Extended pH Response Range in Acid-Media. *Pflügers Arch.* **1988**, *411* (2), 216-219.
163. Szlavik, Z.; Tarkanyi, G.; Gomory, A.; Tarczay, G.; Rabai, J., Convenient Syntheses and Characterization of Fluorophilic Perfluorooctyl-Propyl Amines and Ab Initio Calculations of Proton Affinities of Related Model Compounds. *J. Fluorine Chem.* **2001**, *108* (1), 7-14.
164. Rocaboy, C.; Bauer, W.; Gladysz, J. A., Convenient Syntheses of a Family of Easily Recoverable Fluorous Primary, Secondary, and Tertiary Aliphatic Amines $\text{NH}_3 \cdot x[(\text{CH}_2)_M(\text{CF}_2)_7\text{CF}_3]_x$ ($M = 3-5$; $X = 1-3$) - Fine Tuning of Basicities and Fluorous Phase Affinities. *Eur. J. Org. Chem.* **2000**, 2621-2628.
165. Simon, W.; Wuhrmann, H. R.; Vasak, M.; Pioda, L. A. R.; Dohner, R.; Stefanac, Z., Ion-Selective Sensors. *Angew. Chem. Int. Ed.* **1970**, *9* (6), 445-&.
166. Meier, P. C., Two-Parameter Debye-Huckel Approximation for the Evaluation of Mean Activity-Coefficients of 109 Electrolytes. *Anal. Chim. Acta* **1982**, *136* (APR), 363-368.
167. Jiao, H.; Le Stang, S.; Soós, T.; Meier, R.; Kowski, K.; Rademacher, P.; Jafarpour, L.; Hamard, J.-B.; Nolan, S. P.; Gladysz, J. A., How to Insulate a Reactive Site from a Perfluoroalkyl Group: Photoelectron Spectroscopy, Calorimetric, and Computational Studies of Long-Range Electronic Effects in Fluorous Phosphines $\text{P}((\text{CH}_2)_M(\text{CF}_2)_7\text{CF}_3)_3$. *J. Am. Chem. Soc.* **2002**, *124*, 1516-1523.
168. Pratt, C. W., Ed., *Essential Biochemistry*. Third ed.; New York, NY, 2014.
169. Bakker, E.; Pretsch, E., Potentiometric Determination of Effective Complex Formation Constants of Lipophilic Ion Carriers within Ion-Selective Electrode Membranes. *J. Electrochem. Soc.* **1997**, *144* (5), L125-L127.
170. Bakker, E.; Pretsch, E., Ion-Selective Electrodes Based on Two Competitive Ionophores for Determining Effective Stability Constants of Ion-Carrier Complexes in Solvent Polymer Membranes. *Anal. Chem.* **1998**, *70* (2), 295-302.

171. Ceresa, A.; Pretsch, E., Determination of Formal Complex Formation Constants of Various Pb^{2+} Ionophores in the Sensor Membrane Phase. *Anal. Chim. Acta* **1999**, *395* (1-2), 41-52.
172. Kraus, C. A.; Fuoss, R. M., Properties of Electrolytic Solutions. I. Conductance as Influenced by the Dielectric Constant of the Solvent Medium. *J. Am. Chem. Soc.* **1933**, *55*, 21-36.
173. Anderson, E. L.; Gingery, N. M.; Boswell, P. G.; Chen, X. V.; Rábai, J.; Bühlmann, P., Ion Aggregation and $\text{R}_3\text{N}^+-\text{C}(\text{R})-\text{H}\cdots\text{NR}_3$ Hydrogen Bonding in a Fluorous Phase. *J. Phys. Chem. B* **2016**, *120* (43), 11239-11246.
174. Rubinson, K. A.; Bühlmann, P.; Allison, T. C.; Krueger, S.; Moyer, J. J.; Orts, W. J.; Stevenazzi, A., One-Dimensional Ionic Self-Assembly in a Fluorous Solution: The Structure of Tetra-N-Butylammonium Tetrakis 3,5-Bis(Perfluorohexyl)Phenyl Borate in Perfluoromethylcyclohexane by Small-Angle Neutron Scattering (SANS). *Phys. Chem. Chem. Phys.* **2016**, *18* (14), 9470-9475.
175. Yilmaz, I.; Chen, L. D.; Chen, X. V.; Anderson, E. L.; da Costa, R. C.; Gladysz, J. A.; Bühlmann, P., Potentiometric Selectivities of Ionophore-Doped Ion-Selective Membranes: Concurrent Presence of Primary Ion or Interfering Ion Complexes of Multiple Stoichiometries. *Anal. Chem.* **2019**, *91* (3), 2409-2417.
176. Dohner, R. E.; Wegmann, D.; Morf, W. E.; Simon, W., Reference Electrode with Free-Flowing Free-Diffusion Liquid Junction. *Anal. Chem.* **1986**, *58* (12), 2585-2589.
177. D'Orazio, P.; Verghese, D., Hypertonic Versus Isotonic Salt Bridges in Ion-Selective Electrode Based Clinical Analysers. *Ann. Clin. Biochem.* **1991**, *28*, 628-629.
178. Payne, R. B.; Buckley, B. M.; Rawson, K. M., Protein Interference with Ion-Selective Electrode Measurement Depends on Reference Electrode Composition and Design. *Ann. Clin. Biochem.* **1991**, *28*, 68-72.
179. Kakiuchi, T., Salt Bridge in Electroanalytical Chemistry: Past, Present, and Future. *J. Solid State Electrochem.* **2011**, *15* (7-8), 1661-1671.

180. Kakiuchi, T.; Yoshimatsu, T.; Nishi, N., New Class of Ag/AgCl Electrodes Based on Hydrophobic Ionic Liquid Saturated with AgCl. *Anal. Chem.* **2007**, *79*, 7187-7191.
181. Yoshimatsu, T.; Kakiuchi, T., Ionic Liquid Salt Bridge in Dilute Aqueous Solutions. *Anal. Sci.* **2007**, *23*.
182. Shibata, M.; Yamanuki, M.; Iwamoto, Y.; Nomura, S.; Kakiuchi, T., Stability of a Ag/AgCl Reference Electrode Equipped with an Ionic Liquid Salt Bridge Composed of 1-Methyl-3-octylimidazolium Bis(trifluoromethanesulfonyl)- Amide in Potentiometry of pH Standard Buffers. *Anal. Sci.* **2010**, *26*, 1203-1206.
183. Shibata, M.; Sakaida, H.; Kakiuchi, T., Determination of the Activity of Hydrogen Ions in Dilute Sulfuric Acids by Use of an Ionic Liquid Salt Bridge Sandwiched by Two Hydrogen Electrodes. *Anal. Chem.* **2011**, *83*, 164-168.
184. Zhang, T.; Lai, C. Z.; Fierke, M. A.; Stein, A.; Bühlmann, P., Advantages and Limitations of Reference Electrodes with an Ionic Liquid Junction and Three-Dimensionally Ordered Macroporous Carbon as Solid Contact. *Anal. Chem.* **2012**, *84*, 7771-7778.
185. Lindner, E.; Guzinski, M.; Khan, T. A.; Pendley, B. D., Reference Electrodes with Ionic Liquid Salt Bridge: When Will These Innovative Novel Reference Electrodes Gain Broad Acceptance? *ACS Sens.* **2019**, *4* (3), 549-561.
186. Kisiel, A.; Michalska, A.; Maksymiuk, K., Plastic Reference Electrodes and Plastic Potentiometric Cells with Dispersion Cast Poly(3,4-Ethylenedioxythiophene) and Poly(Vinyl Chloride) Based Membranes. *Bioelectrochemistry* **2007**, *71*, 75-80.
187. Kisiel, A.; Michalska, A.; Maksymiuk, K.; Hall, E. A. H., All-Solid-State Reference Electrodes with Poly(N-Butyl Acrylate) Based Membranes. *Electroanalysis* **2008**, *20* (3), 318-323.
188. Mattinen, U.; Bobacka, J.; Lewenstam, A., Solid-Contact Reference Electrodes Based on Lipophilic Salts. *Electroanalysis* **2009**, *21* (17-18), 1955-1960.
189. Rius-Ruiz, F. X.; Kisiel, A.; Michalska, A.; Maksymiuk, K.; Riu, J.; Rius, F. X., Solid-State Reference Electrodes Based on Carbon Nanotubes and Polyacrylate Membranes. *Anal. Bioanal. Chem.* **2011**, *339*, 3613-3622.

190. Lee, H. J.; Hong, U. S.; Lee, D. K.; Shin, J. H.; Nam, H.; Cha, G. S., Solvent-Processible Polymer Membrane-Based Liquid Junction-Free Reference Electrode. *Anal. Chem.* **1998**, *70*, 3377-3383.
191. Sudholter, E. J. R.; Vanderwal, P. D.; Skowronskaptasinska, M.; Vandenberg, A.; Bergveld, P.; Reinhoudt, D. N., Modification of ISFETS by Covalent Anchoring of Poly(Hydroxyethyl Methacrylate) Hydrogel. Introduction of a Thermodynamically Defined Semiconductor-Sensing Membrane Interface. *Anal. Chim. Acta* **1990**, *230* (1), 59-65.
192. Sudholter, E. J. R.; Vanderwal, P. D.; Skowronskaptasinska, M.; Vandenberg, A.; Reinhoudt, D. N., Ion-Sensing Using Chemically-Modified ISFETS. *Sensors and Actuators* **1989**, *17* (1-2), 189-194.
193. Hu, J.; Zou, X. U.; Stein, A.; Bühlmann, P., Ion-Selective Electrodes with Colloid-Imprinted Mesoporous Carbon as Solid Contact. *Anal. Chem.* **2014**, *86* (14), 7111-8.
194. What Is Medical Grade? <https://nusil.com/en/Content-Library/MedicalGrade> (accessed December 12, 2018).
195. Glover, J., Retinol-Binding Proteins. In *Vitam. Horm.*, Harris, R. S.; Diczfalusy, E.; Munson, P. L.; Glover, J.; Thimann, K. V.; Wool, I. G.; Lorawe, J. A., Eds. Academic Press: 1974; Vol. 31, pp 1-42.
196. Kakiuchi, T., Ionic Liquid Salt Bridge. In *Handbook of Reference Electrodes*, Inzelt, G.; Lewenstam, A.; Scholz, F., Eds. Springer-Verlag: Berlin Heidelberg, 2013; pp 57 - 76.
197. Quinn, B. M.; Ding, Z. F.; Moulton, R.; Bard, A. J., Novel Electrochemical Studies of Ionic Liquids. *Langmuir* **2002**, *18* (5), 1734-1742.
198. Fitchett, B. D.; Rollins, J. B.; Conboy, J. C., 1-Alkyl-3-Methylimidazolium Bis(Perfluoroalkylsulfonyl)Imide Water-Immiscible Ionic Liquids. *J. Electrochem. Soc.* **2005**, *152* (8), E251-E258.
199. Patrick, J. M., Geigy Scientific Tables, 8th Edition, Vol 1, 1981, Vol 2, 1982, Vol 3, 1984 - Ciba-Geigy. *Ergonomics* **1986**, *29* (1), 173-174.

200. Egorova, K. S.; Ananikov, V. P., Toxicity of Ionic Liquids: Eco(Cyto)Activity as Complicated, but Unavoidable Parameter for Task-Specific Optimization. *Chemsuschem* **2014**, *7* (2), 336-360.
201. Egorova, K. S.; Gordeev, E. G.; Ananikov, V. P., Biological Activity of Ionic Liquids and Their Application in Pharmaceuticals and Medicine. *Chem. Rev.* **2017**, *117* (10), 7132-7189.
202. Landry, T. D.; Brooks, K.; Poche, D.; Woolhiser, M., Acute Toxicity Profile of 1-Butyl-3-Methylimidazolium Chloride. *Bull. Environ. Contam. Toxicol.* **2005**, *74* (3), 559-565.
203. Fibbioli, M.; Morf, W. E.; Badertscher, M.; De Rooij, N. F.; Pretsch, E., Potential Drifts of Solid-Contacted Ion-Selective Electrodes Due to Zero-Current Ion Fluxes through the Sensor Membrane. *Electroanalysis* **2000**, *12*, 1286-1292.
204. DiMarco, J. P., Implantable Cardioverter–Defibrillators. *N. Engl. J. Med.* **2003**, *349*, 1836-1847.
205. Jung, W.; Rillig, A.; Birkemeyer, R.; Miljak, T.; Meyerfeldt, U., Advances in Remote Monitoring of Implantable Pacemakers, Cardioverter Defibrillators and Cardiac Resynchronization Therapy Systems. *J. Interv. Card. Electrophysiol.* **2008**, *23*, 73-85.
206. Crossley G.H.; Boyle A.; Vitense H.; Chang Y.; R.H., M., The CONNECT (Clinical Evaluation of Remote Notification to Reduce Time to Clinical Decision) Trial: The Value of Wireless Remote Monitoring with Automatic Clinician Alerts. *J. Am. Coll. Cardiol.* **2011**, *57*, 1181-1189.
207. Petersen, H. H.; Larsen, M. C. J.; Nielsen, O. W.; Kensing, F.; Svendsen, J. H., Patient Satisfaction and Suggestions for Improvement of Remote ICD Monitoring. *J. Interv. Card. Electrophysiol.* **2012**, *34*, 317-324.
208. Landolina, M.; Perego, G. B.; Lunati, M.; Curnis, A.; Guenzati, G.; Vicentini, A.; Parati, G.; Borghi, G.; Zanaboni, P.; Valsecchi, S.; Marzegalli, M., Remote Monitoring Reduces Healthcare Use and Improves Quality of Care in Heart Failure Patients with Implantable Defibrillators: The Evolution of Management Strategies of

- Heart Failure Patients with Implantable Defibrillators (Evolvo) Study. *Circulation* **2012**, *125*, 2985-92.
209. Ricci, R. P.; Vicentini, A.; D'Onofrio, A.; Sagone, A.; Vincenti, A.; Padeletti, L.; Morichelli, L.; Fusco, A.; Vecchione, F.; Lo Presti, F.; Denaro, A.; Pollastrelli, A.; Santini, M., Impact of in-Clinic Follow-up Visits in Patients with Implantable Cardioverter Defibrillators: Demographic and Socioeconomic Analysis of the Tariff Study Population. *J. Interv. Card. Electrophysiol.* **2013**, *38*, 101-106.
210. Soar, J.; Perkins, G. D.; Abbas, G.; Alfonzo, A.; Barelli, A.; Bierens, J. J. L. M.; Brugger, H.; Deakin, C. D.; Dunning, J.; Georgiou, M.; Handley, A. J.; Lockey, D. J.; Paal, P.; Sandroni, C.; Thies, K.-C.; Zideman, D. A.; Nolan, J. P., European Resuscitation Council Guidelines for Resuscitation 2010 Section 8 . Cardiac Arrest in Special Circumstances : Electrolyte Abnormalities , Poisoning , Drowning , Accidental Hypothermia , Hyperthermia , Asthma , Anaphylaxis , Cardiac Surgery , Trau. *Resuscitation* **2010**, *81*, 1400-1433.
211. Burnett, R. W.; Covington, A. K.; Fogh-Andersen, N.; Kulpmann, W. R.; Lewenstam, A.; Maas, A. H.; Muller-Plathe, O.; Sachs, C.; Siggaard-Andersen, O.; VanKessel, A. L.; Zijlstra, W. G., Recommendations for Measurement of and Conventions for Reporting Sodium and Potassium by Ion-Selective Electrodes in Undiluted Serum, Plasma or Whole Blood. International Federation of Clinical Chemistry and Laboratory Medicine (IFCC). Ifcc Scientific Division Working Group on Selective Electrodes. *Clin. Chem. Lab. Med.* **2000**, *38* (10), 1065-71.
212. Burnett, R. W.; Covington, A. K.; Fogh-Andersen, N.; Kulpmann, W. R.; Lewenstam, A.; Maas, A. H.; Muller-Plathe, O.; VanKessel, A. L.; Zijlstra, W. G., Use of Ion-Selective Electrodes for Blood-Electrolyte Analysis. Recommendations for Nomenclature, Definitions and Conventions. International Federation of Clinical Chemistry and Laboratory Medicine (IFCC). Scientific Division Working Group on Selective Electrodes. *Clin. Chem. Lab. Med.* **2000**, *38* (4), 363-70.
213. Pioda, L. A.; Stankova, V.; Simon, W., Highly Selective Potassium Ion Responsive Liquid-Membrane Electrode. *Anal. Lett.* **1969**, *2* (12), 665-674.

214. Tarcali, J.; Nagy, G.; Tóth, K.; Pungor, E.; Juhasz, G.; Kukorelli, T., In Vivo Measurements with a Potassium Ion-Selective Microelectrode Based on a New Bis (Crown Ether). *Anal. Chim. Acta* **1985**, *178*, 231-237.
215. Lindner, E.; Tóth, K.; Jeney, J.; Horváth, M.; Pungor, E.; Bitter, I.; Ágai, B.; Tőke, L., Novel Bis (Crown Ether)-Based Potassium Sensor for Biological Applications. *Microchimica Acta* **1990**, *100* (3-4), 157-168.
216. Parrilla, M.; Cuartero, M.; Padrell Sánchez, S.; Rajabi, M.; Roxhed, N.; Niklaus, F.; Crespo, G. A., Wearable All-Solid-State Potentiometric Microneedle Patch for Intradermal Potassium Detection. *Anal. Chem.* **2019**, *91* (2), 1578-1586.
217. Teplova, V. V.; Mikkola, R.; Tonshin, A. A.; Saris, N.-E. L.; Salkinoja-Salonen, M. S., The Higher Toxicity of Cereulide Relative to Valinomycin Is Due to Its Higher Affinity for Potassium at Physiological Plasma Concentration. *Toxicol. Appl. Pharmacol.* **2006**, *210* (1), 39-46.
218. Abraham, V. C.; Towne, D. L.; Waring, J. F.; Warrior, U.; Burns, D. J., Application of a High-Content Multiparameter Cytotoxicity Assay to Prioritize Compounds Based on Toxicity Potential in Humans. *Journal of Biomolecular Screening* **2008**, *13* (6), 527-537.
219. Tőke, L.; Bitter, I. n.; Ágai, B.; Csongor, É.; Tóth, K.; Lindner, E.; Horváth, M.; Harfouch, S.; Pungor, E., Benzocrown Derivatives as Ionophores for Alkali Cations, I Synthesis of Urethane - and Urea - Linked Mono - and Bis - Crown Ethers. *Liebigs Ann. Chem.* **1988**, *1988* (4), 349-353.
220. Bereczki, R.; Ágai, B.; Bitter, I., Synthesis and Alkali Cation Extraction Ability of New Mono and Bis(Benzocrown Ether)S with Terminal Alkenyl Groups. *J. Incl. Phenom. Macrocycl. Chem.* **2003**, *47* (1), 53-58.
221. Reference Electrodes Based on Ionic Liquid Doped Reference Membranes with Biocompatible Silicone Matrixes. **2019**, *submitted for publication*.
222. Corcé, V.; Chamoreau, L. M.; Derat, E.; Goddard, J. P.; Ollivier, C.; Fensterbank, L., Silicates as Latent Alkyl Radical Precursors: Visible - Light

- Photocatalytic Oxidation of Hypervalent Bis - Catecholato Silicon Compounds. *Angew. Chem. Int. Ed.* **2015**, *54* (39), 11414-11418.
223. Alcock, N. W.; Tracy, V. M.; Waddington, T. C., Acetates and Acetate-Complexes. Part 1. Preparation of Acetato-Complexes and Conductimetric Studies in the Acetic Anhydride Solvent System. *J. Chem. Soc., Dalton Trans.* **1976**, (21), 2238-2242.
224. Staab, H. A., New Methods of Preparative Organic Chemistry IV. Syntheses Using Heterocyclic Amides (Azolides). *Angewandte Chemie International Edition in English* **1962**, *1* (7), 351-367.
225. Rannard, S. P.; Davis, N. J., Controlled Synthesis of Asymmetric Dialkyl and Cyclic Carbonates Using the Highly Selective Reactions of Imidazole Carboxylic Esters. *Org. Lett.* **1999**, *1* (6), 933-936.
226. Trost, B. M.; Xu, J.; Schmidt, T., Palladium-Catalyzed Decarboxylative Asymmetric Allylic Alkylation of Enol Carbonates. *J. Am. Chem. Soc.* **2009**, *131* (51), 18343-18357.
227. Duspara, P. A.; Islam, M. S.; Lough, A. J.; Batey, R. A., Synthesis and Reactivity of N-Alkyl Carbamoylimidazoles: Development of N-Methyl Carbamoylimidazole as a Methyl Isocyanate Equivalent. *The Journal of Organic Chemistry* **2012**, *77* (22), 10362-10368.
228. Davis, T. A.; Vilgelm, A. E.; Richmond, A.; Johnston, J. N., Preparation of (-)-Nutlin-3 Using Enantioselective Organocatalysis at Decagram Scale. *The Journal of Organic Chemistry* **2013**, *78* (21), 10605-10616.
229. Armstrong, A.; Li, W., *N,N'* - Carbonyldiimidazole. In *Encyclopedia of Reagents for Organic Synthesis*, John Wiley & Sons, Ltd: 2007.
230. Mindemark, J.; Bowden, T., Synthesis and Polymerization of Alkyl Halide-Functional Cyclic Carbonates. *Polymer* **2011**, *52* (25), 5716-5722.
231. Ajiro, H.; Takahashi, Y.; Akashi, M., Thermosensitive Biodegradable Homopolymer of Trimethylene Carbonate Derivative at Body Temperature. *Macromolecules* **2012**, *45* (6), 2668-2674.

232. Olsson, J. V.; Hult, D.; Cai, Y.; García-Gallego, S.; Malkoch, M., Reactive Imidazole Intermediates: Simplified Synthetic Approach to Functional Aliphatic Cyclic Carbonates. *Polymer Chemistry* **2014**, *5* (23), 6651-6655.
233. Mindemark, J.; Imholt, L.; Brandell, D., Synthesis of High Molecular Flexibility Polycarbonates for Solid Polymer Electrolytes. *Electrochim. Acta* **2015**, *175*, 247-253.
234. Mindemark, J.; Imholt, L.; Montero, J.; Brandell, D., Allyl Ethers as Combined Plasticizing and Crosslinkable Side Groups in Polycarbonate - Based Polymer Electrolytes for Solid - State Li Batteries. *J. Polym. Sci., Part A: Polym. Chem.* **2016**, *54* (14), 2128-2135.
235. Padiya, K. J.; Gavade, S.; Kardile, B.; Tiwari, M.; Bajare, S.; Mane, M.; Gaware, V.; Varghese, S.; Harel, D.; Kurhade, S., Unprecedented “in Water” Imidazole Carbonylation: Paradigm Shift for Preparation of Urea and Carbamate. *Org. Lett.* **2012**, *14* (11), 2814-2817.
236. Cotarca, L.; Eckert, H., Ed., *Phosgenations - A Handbook*. Wiley - VCH Verlag GmbH & Co. KGaA: Weinheim, 2003.
237. Maas, A. H.; Weisberg, H. F.; Burnett, R. W.; Muller-Plathe, O.; Wimberley, P. D.; Zijlstra, W. G.; Durst, R. A.; Siggaard-Andersen, O., Approved Ifcc Methods. Reference Method (1986) for pH Measurement in Blood. International Federation of Clinical Chemistry (IFCC), Expert Panel on Ph, Blood Gases and Electrolytes. *J. Clin. Chem. Clin. Biochem.* **1987**, *25* (4), 281-289.
238. Siggaard-Andersen, O.; Durst, R. A.; Maas, A. H., International Federation of Clinical Chemistry, Scientific Committee, Analytical Section: And Approved Recommendation (1984) on Physico-Chemical Quantities and Units in Clinical Chemistry with Special Emphasis on Activities and Activity Coefficients. *J. Clin. Chem. Clin. Biochem.* **1987**, *25* (6), 369-91.
239. Inorganic and Organic Lead Compounds. Iarc Working Group on the Evaluation of Carcinogenic Risks to Humans. In *Iarc Monogr. Eval. Carcinog. Risks Hum.*, Lyon, France, 2006; Vol. 87.

240. Bedlechowicz, I.; Maj-Żurawska, M.; Sokalski, T.; Hulanicki, A., Effect of a Plasticizer on the Detection Limit of Calcium-Selective Electrodes. *J. Electroanal. Chem.* **2002**, *537* (1), 111-118.
241. Paczosa-Bator, B.; Piech, R.; Lewenstam, A., Determination of the Leaching of Polymeric Ion-Selective Membrane Components by Stripping Voltammetry. *Talanta* **2010**, *81* (3), 1003-9.
242. Radu, A.; Anastasova-Ivanova, S.; Paczosa-Bator, B.; Danielewski, M.; Bobacka, J.; Lewenstam, A.; Diamond, D., Diagnostic of Functionality of Polymer Membrane – Based Ion Selective Electrodes by Impedance Spectroscopy. *Analytical Methods* **2010**, *2* (10), 1490-1498.
243. Zahran, E. M.; New, A.; Gavalas, V.; Bachas, L. G., Polymeric Plasticizer Extends the Lifetime of PVC-Membrane Ion-Selective Electrodes. *Analyst* **2014**, *139* (4), 757-63.
244. Daunert, S.; Bachas, L. G., Ion-Selective Electrodes Using an Ionophore Covalently Attached to Carboxylated Poly(Vinyl Chloride). *Anal. Chem.* **1990**, *62* (14), 1428-1431.
245. Peper, S.; Ceresa, A.; Qin, Y.; Bakker, E., Plasticizer-Free Microspheres for Ionophore-Based Sensing and Extraction Based on a Methyl Methacrylate-Decyl Methacrylate Copolymer Matrix. *Anal. Chim. Acta* **2003**, *500* (1), 127-136.
246. Anderson, E. L. Development of Improved Ion-Selective and Reference Electrodes for in Situ Monitoring of Ion Concentrations. Ph.D. Dissertation, University of Minnesota, Minneapolis MN, 2019.
247. Meloun, M.; Bordovska, S., Benchmarking and Validating Algorithms That Estimate pK_a Values of Drugs Based on Their Molecular Structures. *Anal. Bioanal. Chem.* **2007**, *389* (4), 1267-81.
248. Acid Dissociation (pK_a) Calculation with Acd/Pka. Advanced Chemistry Development. <https://www.acdlabs.com/products/percepta/predictors/pka/#features> (accessed June 30, 2019).
249. Scifinder, C. A. S. <http://www.cas.org/SCIFINDER> (accessed June 30, 2019).

250. Guthrie, J. P., Hydrolysis of Esters of Oxy Acids: pK_a Values for Strong Acids; Brønsted Relationship for Attack of Water at Methyl; Free Energies of Hydrolysis of Esters of Oxy Acids; and a Linear Relationship between Free Energy of Hydrolysis and pK_a Holding over a Range of 20 pK Units. *Can. J. Chem.* **1978**, *56* (17), 2342-2354.
251. Dittmer, A. Ph.D. Dissertation, University of Minnesota, Minneapolis MN, 2019.
252. Dittmer, A., Biofouling of Ion-Selective Electrode Membranes: The Role of Ionic Site Leaching into Biological Samples. In *Pittsburgh Conference of Analytical Chemistry*, Chicago, 2014.